# CONSERVED AND UNCONVENTIONAL RESPONSES TO DNA DAMAGE IN TETRAHYMENA

A Dissertation

by

PAMELA YOHANNA DE LOURDES SANDOVAL OPORTO

Submitted to the Office of Graduate Studies of
Texas A&M University
in partial fulfillment of the requirements for the degree of

DOCTOR OF PHILOSOPHY

May 2011

Major Subject: Genetics

Conserved and Unconventional Responses to

DNA Damage in Tetrahymena

# CONSERVED AND UNCONVENTIONAL RESPONSES TO DNA DAMAGE IN TETRAHYMENA

A Dissertation

by

PAMELA YOHANNA DE LOURDES SANDOVAL OPORTO

Submitted to the Office of Graduate Studies of
Texas A&M University
in partial fulfillment of the requirements for the degree of

DOCTOR OF PHILOSOPHY

Approved by:

| | |
|---|---|
| Chair of Committee, | Geoffrey M. Kapler |
| Committee Members, | Keith A. Maggert |
| | Michael Polymenis |
| | Van G. Wilson |
| Intercollegiate Faculty Chair, | Craig J. Coates |

May 2011

Major Subject: Genetics

# ABSTRACT

Conserved and Unconventional Responses to

DNA Damage in Tetrahymena. (May 2011)

Pamela Yohanna de Lourdes Sandoval Oporto, B.S., Universidad Austral de Chile

Chair of Advisory Committee: Dr. Geoffrey M. Kapler

Here the ciliate protozoa *Tetrahymena thermophila* was used as a model system to study the DNA damage response. *Tetrahymena* enclose nuclear dimorphism, a polyploid somatic macronucleus (MAC), which is transcriptionally active and maintains vegetative growth, and a diploid germline micronucleus (MIC) responsible for the transmition of genetic information during conjugation. Previous studies have identified Tif1p, a novel protein involved in the regulation of rDNA replication in *Tetrahymena*. TIF1 hypomorphic strains acquire spontaneous DNA damage during vegetative cell cycle and are hypersensitive to DNA damaging agents. TIF1-deficient strains acquire DNA damage in both nuclear compartments, suggesting a global role of Tif1p in the maintenance of genomic stability.

In my dissertation research, I studied the role of Tif1p during the cell cycle progression. To this end, I generated tagged-Tif1p strains, which revealed that the subcellular localization of Tif1p is dynamic throughout the cell cycle. However, the addition of epitope tag to this protein generated phenotypes analogous to ones observed in a TIF1-deficient strain. This suggested that the addition of epitope tag to Tif1p

severely affects the properties of Tif1p and hence the overall integrity of the cell. To overcome these limitations, a peptide antibody specific to Tif1p was generated to study the endogenous protein. This work revealed that the abundance of Tif1p protein is not cell cycle regulated and that Tif1p is absent in starved cells. Furthermore, the specific binding of TIf1p to rDNA minichromosome was studied during vegetative cell cycles. Chromatin immunoprecipitation studies revealed that the specific binding of Tif1p extends beyond the cis-acting determinant of replication present at the rDNA origin and promoter. This suggests that coding regions may be targeted for the binding of Tif1p to previously uncharacterized sequences, and that Tif1p preferentially localizes on the rDNA minichromosome.

I also studied the induction of DNA damage response, demonstrating that *Tetrahymena* activates a checkpoint response mediated by an ATR-like pathway. Studies with a hypomorphic TIF1 strain revealed that Tif1p mediates proper activation of the DNA damage response. Further characterization of the response to genotoxic agents showed that *Tetrahymena* is able to activate a $G_1$/S and intra-S phase DNA damage response. The results presented here suggest that a caffeine-dependent checkpoint activator protein modulates the response to DNA damage. In addition, a subunit of the replicative helicase, Mcm6p, is directly affected by the induction of DNA damage. This suggests that *Tetrahymena* uses a novel mechanism to halt the progression of DNA replication forks during genotoxic stress through degradation of Mcm6p.

## DEDICATION

This work is dedicated to my family for their love and support throughout all these years.

## ACKNOWLEDGEMENTS

I would like to thank my committee chair, Dr. Kaper, and my committee members, Dr. Wilson, Dr. Polymenis and Dr. Maggert, for their guidance and support throughout the course of this research.

Thanks also to my friends, colleagues and the faculty and staff of the Department of Molecular and cellular Medicine at HSC for making my time at Texas A&M University a great experience.

Finally, I would like to specially thank my family for their unconditional love, encouragement and understanding.

# TABLE OF CONTENTS

CHAPTER Page

CHAPTER Page

# LIST OF FIGURES

FIGURE Page

FIGURE Page

# LIST OF TABLES

# CHAPTER I

# INTRODUCTION

This work addresses several mechanisms common to the control of eukaryotic DNA replication. To provide a framework for my research, a general overview of the cell cycle will be presented first. A detailed description of the checkpoint pathways that are activated following DNA damage and initial steps in replication will be provided. Finally, I will discus unconventional cell cycles, since they are integral part of the life cycle of the eukaryotic model I have been working with, *Tetrahymena thermophila*.

## Cell cycle and DNA damage response

Classical studies where synchronized cells in different stages of the cell cycle were fused revealed that cell cycle progression is tightly regulated. Heterophasic $S/G_2$ cells divide earlier than homophasic S/S cells, indicating that factors presents in $G_2$ cells were able to promote early entry of S phase nuclei to mitosis. However, in heterophasic $G_1/ G_2$ cells the $G_1$ nuclei was not affected in their progression through S phase or mitosis (Rao & Johnson, 1970). Research over the past 30 years has elucidated regulatory factors that are responsible for restricting entry or exit from a given stage of the cell cycle (Figure 1.1), these factor are organized in several biochemical mechanisms that we recognize as checkpoints (Hartwell & Weinert, 1989).

---

This dissertation follows the style of *The EMBO Journal*.

**Cell cycle regulation**

In unperturbed cells, the transition between different phases of the cell cycle is mainly controlled by the cyclin dependent kinases (CDK) that phosphorylate downstream effector proteins to promote cell cycle progression. CDK catalytic activity and substrate selection depends on its capacity to form a complex with cyclins, which act as a regulatory subunit. CDK-cyclin complexes are responsible for activation of transcription, control cell morphogenesis, promote the initiation of DNA replication, prevent DNA re-replication, support accurate chromosome segregation, control the exit from mitosis, and regulate DNA damage checkpoint activation and DNA repair (Enserink & Kolodner, 2010).

Several CDKs have been described in *S cerevisiae*, however a single CDK (Cdk1) is necessary and sufficient to control cell cycle progression (Figure 1.1A). Cln1, Cln2 and Cln3 are $G_1$ cyclins, the protein level of Cln3 is the first to increase in middle $G_1$ phase (Figure 1.1A). Cdk1-Cln3 promotes transcription of multiple factors involved in DNA metabolism, including the expression of Cln1, Cln2 during late $G_1$ phase (Dirick et al., 1995; Spellman et al., 1998; Tyers & Futcher, 1993). Furthermore, $G_1$ cyclins promote efficient initiation of DNA replication, but the entry to S phase is marked by the increase abundance of early expressed B-type cyclins (Figure 1.1A).

B-type cyclins (Clb1-6) are necessary for S phase and mitotic progression. Cdk1-Clb5 and Cdk-Clb6, promote DNA replication and are the most active complex in regulating DNA synthesis, their levels are highly maintained until the end of the cell

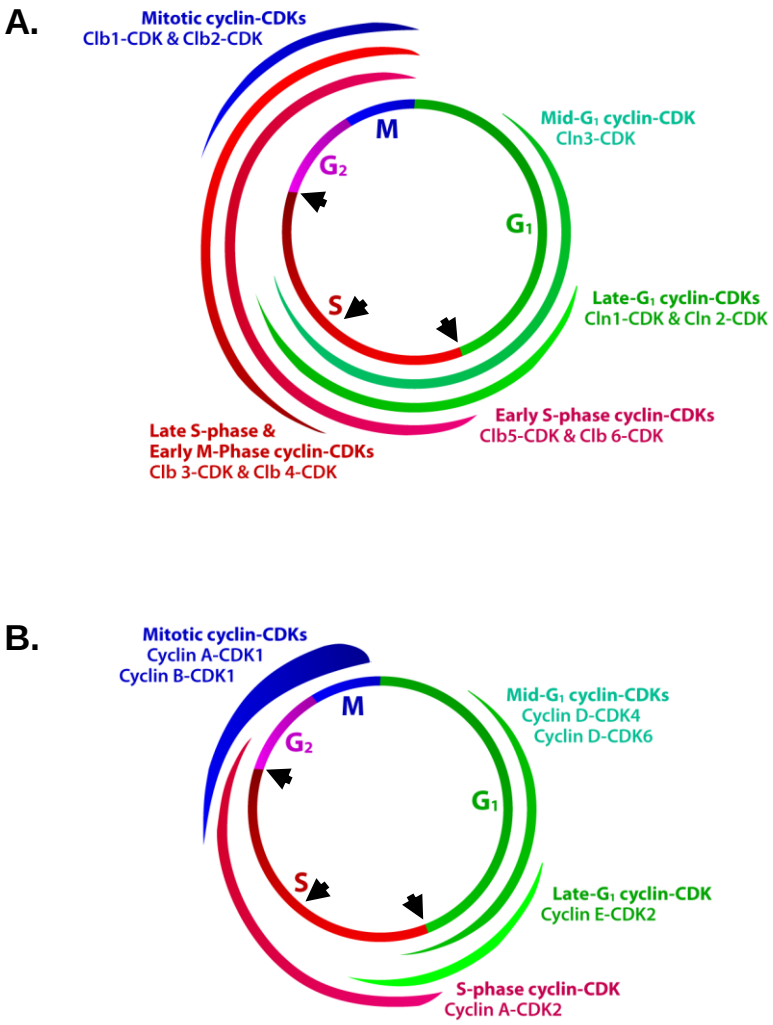


Figure 1.1 Cyclin-CDK regulation of the cell cycle. Cell cycle progression in eukaryotic model systems consists in four faces. The DNA synthesis (S) phase and mitotic (M) phase, separated by two gap phases (G1 and G2). The abundance of cyclin-CDK complexes in relationship to the cell cycle progression is showed. Black arrows indicate checkpoints. A. In yeast B. In mammals. Diagram modified from http://studentreader.com.

cycle (Mendenhall & Hodge, 1998; Schwob & Nasmyth, 1993). Clb3 and Clb4 abundance increases late in S phase and are maintained until anaphase; they are responsible for progression of DNA replication and for the $G_2$/M transition (Richardson et al., 1992). Clb1 and Clb2 are the mitotic cyclins. Their increased abundance marks the entry into $G_2$ phase, and, they are responsible for promoting mitosis by regulating chromosome segregation (Enserink & Kolodner, 2010).

Prior to triggering a cell cycle transition, CDK is accumulated in an inactive state. The synthesis of cyclins is cell cycle regulated, and all are degraded by ubiquitylation during anaphase, providing an effective mechanism to regulate CDK activity (Amon et al., 1994). Furthermore, the presence of specifics CDK-inhibitors, such Sic1 and Far1 during $G_1$ phase, promote the accumulation of high levels of inactive CDK prior to triggering a cellular transition and offers an aditionalregulation of CDK (Alberghina et al., 2004; Schwob et al., 1994). These inhibitors are degraded as soon S phase starts but their abundance increases in anaphase to prepare the cell for a new cycle. During the $G_2$/M transition phosphorylation of CDK by Cdk-inhibitory kinases, such a Swe1p and Mih1p, also contribute to the inactivation of CDK (Russell et al., 1989).

To ensure cell cycle transitions, the Cdc25 phosphatase is responsible for removing inhibitory phosphorylations in cyclin-CDK complexes. CDK is also activated by the phosphorylation induced by CAK (CDK activating kinase), and its activity is maintained high until anaphase (Diffley, 2004; Mandal et al., 1998).

In metazoans at least four CDKs (Cdk1-4) have been described as necessary to maintain normal cell cycle progression (Nurse, 2000). However, Santamaria and

colleagues showed that Cdk1 was sufficient to promote normal cell cycle in a triple knockout in mice suggesting functional redundancy in higher eukaryotes (Santamaria et al., 2007). Nevertheless, four classes of cyclins (A, B, C, D) are required to drive cell cycle progression (Figure 1.1B)(Malumbres, 2005).

Cyclin D in association with Cdk4 or Cdk6 (Figure 1.1B) regulates events in $G_1$ phase, such as phosphorylation of Rb (retinoblastoma) proteins which leads to derepression and activation of E2F target genes that includes E-type cyclins (Kozar & Sicinski, 2005). Through this mechanism cyclin D-CDK complex is able to promote the transition to S phase. Cyclin E-Cdk2 is essential for the irreversible transition to S phase by directly affecting DNA replication, histone biosynthesis and control of centrosome duplication (Hinchcliffe & Sluder, 2002; Sclafani & Holzen, 2007). Cyclin E levels are cell cycle regulated and cyclin E is degraded shortly after the initiation of S phase(Hwang & Clurman, 2005). Cyclin A is responsible for the progression of replication, completion of S phase and entry to $G_2$ (Suryadinata et al., 2010). Cyclin B is the mitotic cyclin and along with cyclin A promotes the entry into mitosis and regulate the segregation of chromosomes (Figure 1.1B)(Jackman et al., 2003). Here, to facilitate the general description in common mechanisms of eukaryotes, those cyclin-CDK complexes that are actively controlling S phase are collectively called S phase specific CDKs (S-CDK), as was previously used in Masumoto et al., 2002 (Masumoto et al., 2002).

Similar to the regulation of CDK in yeast, CDK in mammals can be targeted for degradation by ubiquitin-mediated proteolysis, specific inhibitors may regulate their

abundance and be targeted by inhibitory phosphorylation (Peters, 2006). Animals contain three isoforms of Cdc25 (A, B and C). Cdc25a is responsible for activation of both S-CDK during $G_1$/S transition and CDK1-cyclinB in mitosis (Karlsson-Rosenthal & Millar, 2006).

**Activation of DNA damage checkpoint and DNA repair pathways**

Intracellular metabolic processes (stalled replication fork or reactive oxygen species) and exogenous insults (UV, ionizing radiation (IR) or other genotoxic agents) can induce DNA damage. In order to prevent loss or instability of the genetic material, these lesions need to be repaired. The phase in the cell cycle when the lesion occurred and the type of damage trigger specific checkpoint responses and determine which repair mechanism will be utilized (Figure 1.2).

DNA lesions include double-stranded breaks (DSBs), single-stranded breaks (SSBs), formations of DNA adduct by intra and inter-strand crosslink, and DNA mismatches. Once the lesion is detected, transducers amplify and transmit the checkpoint signal to downstream targets through a phsphorylation cascade (Abraham, 2001). The downstream effectors are responsible for the regulation of cell cycle progression, this can be modulated by the activation of the $G_1$/S checkpoint that blocks entry into S phase, triggering of the intra-S checkpoint that promote a delay in S phase progression; or activation of a $G_2$/M checkpoint to prevent mitotic entry (Bolderson et al., 2009b).

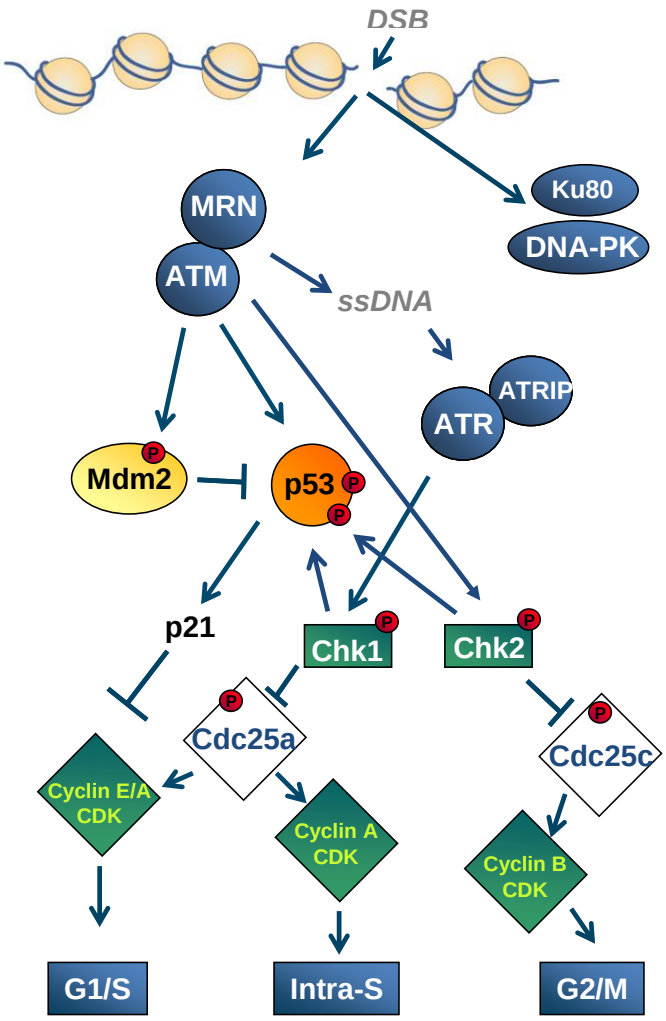


Figure 1.2 Mechanism for checkpoints activation. Showing a DSB (double strands break) as initial lesion that is initially recognized and resolved in ssDNA (single stranded DNA). Factors involved in the recognition, transduction and activation of the checkpoint are described in the text. Diagram modified from Bolderson et al., 2009.

The sensor serine-threonine kinases ATR (ataxia talangiectasia and Rad3 related), ATM (ataxia talangiectasia mutated) and DNA-PK (DNA-ativated protein kinase), are crucial transducers of the DNA damage response. ATM and DNA-PK are activated in response to DSB and they are recruited via Nbs1 and Ku80 respectively to sites of damage (Falck et al., 2001; Uziel et al., 2003; You et al., 2005). ATR respond mainly to ssDNA RPA (replication protein A) coated ssDNA stimulates the recruitment of ATR to the lesion by its direct interaction with ATRIP (ATR interacting protein) (Zou & Elledge, 2003).

During S phase the DNA is particularly vulnerable to insults. When damage is induced during replication, the replicative DNA polymerase stalls while helicase continues to unwind DNA, generating long stretches of ssDNA (Petermann & Helleday, 2010). The coated RPA-ssDNA recruits ATR-ATRIP and Rad17-RFC, the later of which functions as a loader for the Rad9-Rad1-Hus1 (9-1-1) clamp complex that is necessary for the activation of ATR (Ellison & Stillman, 2003; Zou et al., 2003). In mammals the activation of ATR also requires TopBP1, that directly stimulates kinase activity of ATR (Delacroix et al., 2007; Kumagai et al., 2006). Once activated, ATR phosphorylates several adaptor proteins in order to drive the signal to the effector kinase Chk1 (Jazayeri et al., 2006). In yeast Rad9 is required to supply this role, however, in mammals several adaptor proteins have been identified, suggesting a grand array of mechanisms for the activation of Chk1 (Choi et al., 2007; Kumagai et al., 2004; Sweeney et al., 2005; Wilson & Stern, 2008). Chk1 acts as an effector kinase, and is mainly activated via ATR-dependent phosphorylation of the C-terminal residue S317-

S345, this blocks intramolecular interactions, exposing the N-terminal kinase domain (Jazayeri et al., 2006; Tapia-Alveal et al., 2009).

On the other hand, DSB are detected by MRN complex (Mre11-Rad50-Nbs1) that recruit ATM that in turn induces the phosphorylation of H2A variant, H2AX at the site of damage(Burma et al., 2001). The phosphorylation of H2AX acts as a signal to recruit the adaptor protein MDC1 (mediator of DNA damage checkpoint 1) that promotes the ATM-dependent phosphorylation of H2AX in long stretches of DNA surrounding the DSB (Rogakou et al., 1998; Stucki et al., 2005). MDC1 also promotes the binding of the several ubiquitin E3-ligase factors that ubiquitylate of histone H2A and H2AX. This serves as a signal for the recruitment of adaptors 53BP1 (p53-binding protein1) and BRCA1 that further promote the activation of p53 and the effector kinase Chk2 (Pinato et al., 2009; Wilson & Stern, 2008) (Mailand et al., 2007). ATM predominantly phosphorylates Chk2 at Thr68, promoting activation via intramolecular trans-autophosphorylation at Thr383-387 (Lee & Chung, 2001; Matsuoka et al., 2000; Melchionna et al., 2000). Furthermore, the Mre11 subunit of MRN supports endonuclease activity that may be responsible for mediating the resection of DSB to generate ssDNA. The ssDNA is recognized and activate the ATR signaling pathway to reinforce repair of the lesion (Williams et al., 2008).

Activated effectors kinases Chk1 and Chk2 are able to promote the phosphorylation and inactivation of Cdc25, this prevent further activation of CDKs to promote cell cycle progression (Figure 1.2). Phosphorylated Cdc25a is targeted for ubiquitination and proteosomal degradation (Mailand et al., 2000; Molinari et al., 2000).

The inhibition of Cdc25a prevents the activation of cyclin E and cyclin A-CDK complex, promoting the arrest in $G_1$/S transition and S phase, respectively(Bolderson et al., 2009a). In contrast, phosphorylated Cdc25c is excluded from the nuclear compartment and sequestered in the cytoplasm through the binding to 14-3-3 proteins (Peng et al., 1997; Sanchez et al., 1997; Zeng & Piwnica-Worms, 1999). The absence of Cdc25c prevents the activation of cyclin B-CDK, promoting the $G_2$/M checkpoint (Bolderson et al., 2005). In addition, Chk1 activation via ATR also plays a dominant role in response to replication stress (intra-S checkpoint). Chk1 directly phosphorylates S phase kinases DDK (Abf4 Cdc7 dependent kinase) and Tlk1 (tousled-like kinase). The phosphorylation of DDK prevents efficient initiation of DNA replication (Liu et al., 2006). Tlk1 phosphorylation induces inhibition of its activity, which is required for chromatin assembly and elongation of DNA replication (Beckerman et al., 2009). Also, Chk1 phosphorylates histone H3, responsible for DNA damage induced transcriptional repression of cell cycle regulatory genes (like cyclin B1 and Cdk1) through loss of histone acetylation (Shimada et al., 2008).

Furthermore, ATM and effector kinases directly phosphorylate p53 and its ligase Mdm2, which promote p53 stabilization. The accumulation of p53 induces the transcription of p21. P21 acts as a CDK inhibitor (Chehab et al., 1999; Hirao et al., 2000; Shieh et al., 2000). The inactivation of Cdc25 and p21 prevents the entry to S phase (Figure 1.2).

The activation of checkpoints induce delays in the progress of cell cycle by preventing the activation of CDKs, these delays give the necessary time to promote

DNA repair pathways. The two major strategies to repair damaged DNA are the non-homologous end joining (NHEJ) and the homology bases recombination repair (HR) pathways (Harper & Elledge, 2007). In human cells, NHEJ is active during all the phases of the cell cycle, but is the preferred mechanism for repair during $G_1$. DSB, induced during $G_1$ are recognized by the heterodimer Ku70-Ku80, Ku80 by direct interaction recruit DNA-PK to the break (Falck et al., 2005). The further recruitment of ligase IV-XRCC4 complex is responsible for the direct ligation of the two ends of DNA (Barlow et al., 2008). Since the repair mediated by NHEJ does not require a template for the ligation of two ends some loss or translocation may occur.

During S and $G_2$ phase the presence of sister chromatids promote repair mediated by HR. The major difference between HR and NHEJ is the fidelity of the repair. HR uses undamaged DNA template to restore the integrity of the damaged region without any loss of genetic information (Moynahan & Jasin, 2010). DSB are recognized by MNR that recruits ATM and starts the resection of the lesion to form ssDNA. The recruitment of Sgs1 helicase and Exo1 extends the stretch of ssDNA (Mimitou & Symington, 2008; Zhu et al., 2008). RPA coated-ssDNA stabilizes ssDNA, however Rad52 promotes the exchange of RPA for Rad51 (Moynahan & Jasin, 2010). BRCA2 is recruited by Rad51 and acts as an accessory factor to overcome the inhibitory effect of RPA and promote the formation of Rad51 filaments (Carreira et al., 2009; Yang et al., 2005). Once the filaments are formed, several orthologs of Rad51 are recruited to promote the strand invasion. DNA synthesis is primed from the invading strand, branch

migration occur to form Holliday junctions. Holliday junctions are resolved and the distal ends are ligated together (Liberi & Foiani, 2010).

Once checkpoints are activated, the phosphorylation cascade also promotes repair pathways. As an example, Chk1-dependent phosphorylation of Rad51 is required for the replacement of RPA on ssDNA, and facilitates the further formation of Rad51 filaments (Sleeth et al., 2007; Sorensen et al., 2005).

Since complete and precise DNA duplication is essential to maintain fidelity of genetic information, S phase is the most susceptible stage to experience catastrophic insults. When DNA damage is induced during replication, the intra-S phase checkpoint is activated and several responses are triggered in order to prevent further synthesis. The direct modulators of this response are components of the replication machinery. Below I present a detailed view of how the initiation for DNA replication (replication origins) are organized in different eukaryotes.

**Replication initiation in eukaryotic systems**

Jacob and Brenner (1963) postulated the classic *replicon hypothesis*, this is the principal concept behind the study of the control of DNA replication. This hypothesis, propose that specific DNA sequences serve as *origins of replication* which are activated by factors called *initiators* (Jacob & Brenner, 1963). Based on this, a *replicon* is a distinct stretch of DNA that replicates from a single origin. This hypothesis was rapidly corroborated in prokaryotes. However, eukaryotic chromosomes contain multiple origins and only in few model systems are these origins defined by specific DNA sequences.

Furthermore, trans-acting factors or *initiators* of DNA replication are very well conserved in most eukaryotes, suggesting that they can play a stronger role in the regulation of DNA replication than sequences alone. Also, replication initiation is affected by structural chromatin contexts and other processes intrinsic to the cell cycle, suggesting that the control of DNA replication is more intricate than was originally envisioned.

**Basic determinants of DNA replication in budding yeast**

Replicons were formerly identified by an assay first described by Struhl and colleagues (1979) where specific sequences confer the ability to promote autonomous replication of transformed plasmids (autonomous replication sequences -ARS- assay) (Struhl et al., 1979). In the budding yeast, *S. cerevisiae*, replicons are comprised of AT-rich sequences (Newlon & Theis, 1993). The most studied origin, ARS1, consist of only 150 base pairs of DNA and linker scanning mutations identified cis-acting elements that co-localize with the site of replication initiation (Marahrens & Stillman, 1992). These elements include the essential ARS consensus sequence (ACS), that is an 11 bases pair long AT-rich sequence that is necessary but not sufficient for ARS1 activity. Additional elements B1, B2, and B3 were also identified, individually these elements are not essential, but they are required for functional origins (Figure 1.3A) (reviewed in Aladjem et al., 2006). However, genome-wide analysis revealed that from all the ACS sequences predicted in budding yeast, only a fraction represents active origins. This

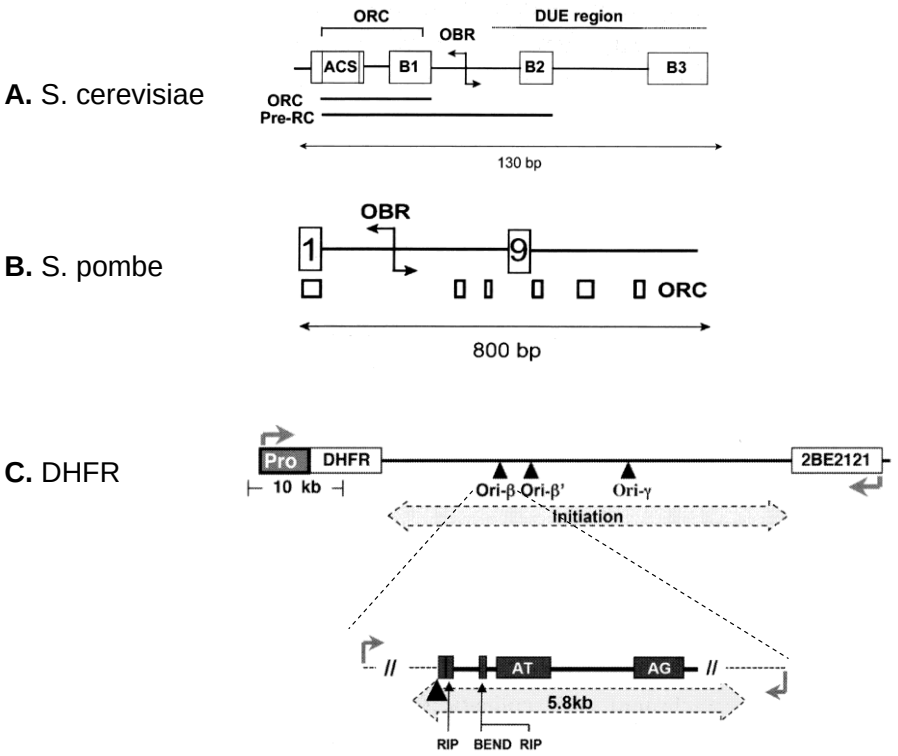


Figure 1.3 Functional elements in eukaryotic replicons. A. ARS1 replicon in budding yeast. Showing different cis-acting elements important for replication that are described in the text (ACS, B1, B2 and B3); (DUE) DNA unwinding element ; (ORC) origin recognition complex and showing its binding region; (OBR) represent the exact point where bidirectional replication start. The region protected by ORC and pre-RC is indicated. **B.** ARS1 replicon in fission yeast. Strongly required regions are marked by a numbered box. ORC binding seqiences are indicated by small box. Scale for each replicator is indicated. **C.** DHFR replicator regions. Bulk arrow indicates the initiation region. (Pro) gene promoter. Arrows indicate the direction of transcription. The structural detail of DHFR ori-β is indicated. (AT) indicates AT-rich stretches; (AG) indicates asymmetric purine:pyrimidine tracks. (BEND) indicate regions where the DNA is bent. (filled triangle) mark the initiation site. Diagram modified from Aladjem et al., 2006.

suggests that the ACS alone cannot be used to predict origin location (MacAlpine & Bell, 2005).

The eukaryotic chromosomal *initiator*, ORC is the six subunit origin of recognition complex first identified as nuclear binding activity that specifically associates with double stranded ARS1 A element, and corroborated by protection assay in presence of ATP (Bell & Stillman, 1992)ORC is a trans-acting factor essential for origin site selection and the nucleation of the replication machinery(Liang et al., 1995). The ATP-dependent binding of ScORC complex to ARS is directed to sequences present at ACS and B1. ACS is directly bound by Orc1, Orc2 and Orc4 subunits, while B1 is recognized by Orc5(Lee & Bell, 1997). The B2 element is proposed to function as a DNA unwinding element (DUE) since it has a low DNA helical stability and mutation of its sequences induce reduction in the origin activity (Huang & Kowalski, 2003; Lin & Kowalski, 1997). The B3 element is directly bound for an ARS binding factor 1, Abf1 (Diffley & Stillman, 1988). Abf1 is a multifunctional factor; whose role in replication is to act as boundary element for chromatin structure, preventing the spread of nucleosomes toward ACS and in this way facilitating ScORC binding (Li et al., 1998; Marahrens & Stillman, 1992; Venditti et al., 1994).

**Fission yeast: first challenge for the replicator hypothesis**

Like in *S. cerevisiae*, replicons were also identified by ARS assays in *Schizosaccharomyces pombe* (Sp). However, the sequences involved are considerably larger (500 to 1000 bases) than those identified in budding yeast (Figure 1.3B)(Okuno et

al., 1999). While they are composed of AT-rich DNA, they do not contain highly specific consensus sequences(Kim & Huberman, 1998). Genetic dissection of origins showed the presence of multiple redundant elements, which have an additive functional contribution to plasmid stability; moreover these determinants can be replaced with random AT-rich sequences without substantially affecting origin activity(Okuno et al., 1997). The only conserved characteristic of *S. pombe* origins is the presence of clusters of A residues with the complementary T-rich sequences; these regions are essential to form a functional origin (Okuno et al., 1999). Furthermore, genome-wide analysis revealed that the 90% of these AT-rich clusters (also called AT-islands) co-localize with active origins(Segurado et al., 2003).

The binding of SpORC complex is direct to origin sequences but it is not ATP-dependent(Lee et al., 2001). Since there is no ACS, SpORC utilizes a particular feature of one of its subunits in order to bind origins specifically. The SpOrc4 subunit contains an AT-hook domain that is known to mediate DNA binding to the minor groove of AT-rich sequences (Chuang & Kelly, 1999; Kong & DePamphilis, 2001). Replicons in *S. pombe* contain multiple AT-islands and it has been shown that ORC complexes are associated with all of them (Ogawa et al., 1999).

As described below, the actual activation of the origin occurs when a helicase is loaded onto the origin sequences. In *S. pombe*, this activation depends in the number of ORC complexes bound to AT-islands, and suggests that the lack of consensus sequences is compensated by the presence of multiple binding sites for ORC at each replicon

(Figure 1.3B) (reviewed in Aladjem et al., 2006). To date no non-ORC DNA binding protein, analogous to ABF1, has been show to play a role in *S. pombe* origin activation.

**An example of origins of replication in metazoan**

Replicons in higher eukaryotes share some similarities with those of *S. pombe*. Cis-acting regulatory sequences are spread in long chromosomal regions (up to 5.8 Kb for DHFR replicon). Replicators lack an apparent consensus sequence for ORC recognition and have higher AT-rich sequences content. However, the action of trans-acting factors, chromatin structure and transcriptional activity may have a key role in the determination of an origin than the DNA sequence alone (reviewed in Aladjem et al., 2006). Most of the origins in metazoans have been identified by ectopic replicator assays, where putative origin sequences are removed from their native environment and inserted into an ectopic chromosomal region that is then tested for the ability to support initiation of DNA replication.

The origin of replication of the dihydrofolate reductase (DHFR) in chinese hamster ovary methotrexate-resistant cells, is one of the most studied metazoan replicons and was the first mammalian origin identified (Heintz & Hamlin, 1982). In contrast to the budding yeast, *S. cerevisiae*, replication of the DHFR locus occurs within a very broad initiation zone of about 55 kb (Figure 1.3C). DNA replication starts from three major origins, called ori-β, ori-β' and ori-γ (Heintz & Hamlin, 1982; Ma et al., 1990). Ori-β is approximately 17 kb downstream from the DHFR gene, closely followed by ori-β', while ori-γ is more distally placed at 23 kb downstream of the gene (Figure 1.3C).

Ori-β region is necessary and sufficient for the initiation of DNA replication in ectopic chromosomal locations (Altman & Fanning, 2001). However, analysis by two dimensional gel electrophoresis from the endogenous chromosome, showed that most initiation events occur within a 12.5 kb region that contains both ori-β, ori-β' (Kobayashi et al., 1998). Also, in the endogenous locus, a 3.2 kb fragment present at the 3' end of DHFR gene is required for all initiation activity in the 55 kb DNA region (Altman and Fanning, 2004). Similar to other eukaryotic replicons, DHFR ori-β present asymmetrical AT-rich stretches and contains a stably bent DNA sequence necessary for origin activity (Altman & Fanning, 2004; Caddle et al., 1990).

The binding of metazoan ORC complexes to DNA is ATP-dependent, but it exhibits no specificity for DNA binding(Chesnokov et al., 1999). However, non-ORC DNA binding factors can play an important role in the recruitment of ORC to origins in metazoans. In *Drosophila*, the binding of a multiprotein complex (DmMyb) that contains the Myb protein is required for the recruitment of ORC to chorion gene origins and subsequent amplification of this region in differentiated follicle cells (Beall et al., 2002). Also, AIF-C a transcriptional repressor in rat, recognizes a specific sequence at the aldolase B origin, and is able to recruit ORC to this origin by direct physical interaction. Since rat ORC binds DNA non-specifically, the loss of AIF-C or elimination of the AIF-C DNA binding site prevents ORC recruitment and origin activation, the binding of AIF-C is necessary for replication from this origin (Minami et al., 2006).

Moreover, it has been described that the presence of unusual DNA structures, as a negatively supercoiled fragments, favors ORC binding to partially unwound AT-rich

sequences (Remus et al., 2004). Furthermore, factors that contribute to the formation of an "open" chromatin also contribute to origins activation and ORC binding. In *Drosophila melanogaster* (Dm), the ORC complex localizes to sequences enriched in histone variant H3.3 that is a characteristic replacement in nucleosomes of regions that are transcriptionally active (MacAlpine et al., 2010). Also in *Drosophila*, the tethering of Chameau acetyltransferase to origins at the chorion gene promotes the recruitment of ORC complex, suggesting that histone acetylation modulates the binding or activation of ORC in follicle cells (Aggarwal & Calvi, 2004). In humans, a genome-wide analysis showed that almost half of the origins are localized within or near CpG islands (Cadoret et al., 2008). All these data support the idea that the epigenetic chromatin environment strongly influences the binding of ORC, and primary DNA sequence, plays a minor, if any, role in defining active sites for replication initiation in higher eukaryotes.

**Formation and regulation of pre-replication complex (pre-RC)**

The pre-RC is a multiprotein complex that is assembled at all potential origins of replication. Pre-RC were first described by DNase protection assays in *S. cerevisiae*, as a complex that protect origins in a cell cycle regulated manner (Diffley et al., 1994).

The assembly of pre-RC is limited to late M and $G_1$ phases, when S-CDK levels are low (Figure 1.4). This mechanism ensures that the genome replicates only once in every cell cycle. Once ORC is bound to origins, Cdt1 is recruited to chromatin which in turn binds directly to Cdc6 (Figure 1.4) (Cook et al., 2004; Maiorano et al., 2000). In metazoan the recruitment of Cdt1 is negatively modulated by geminin, as an additional

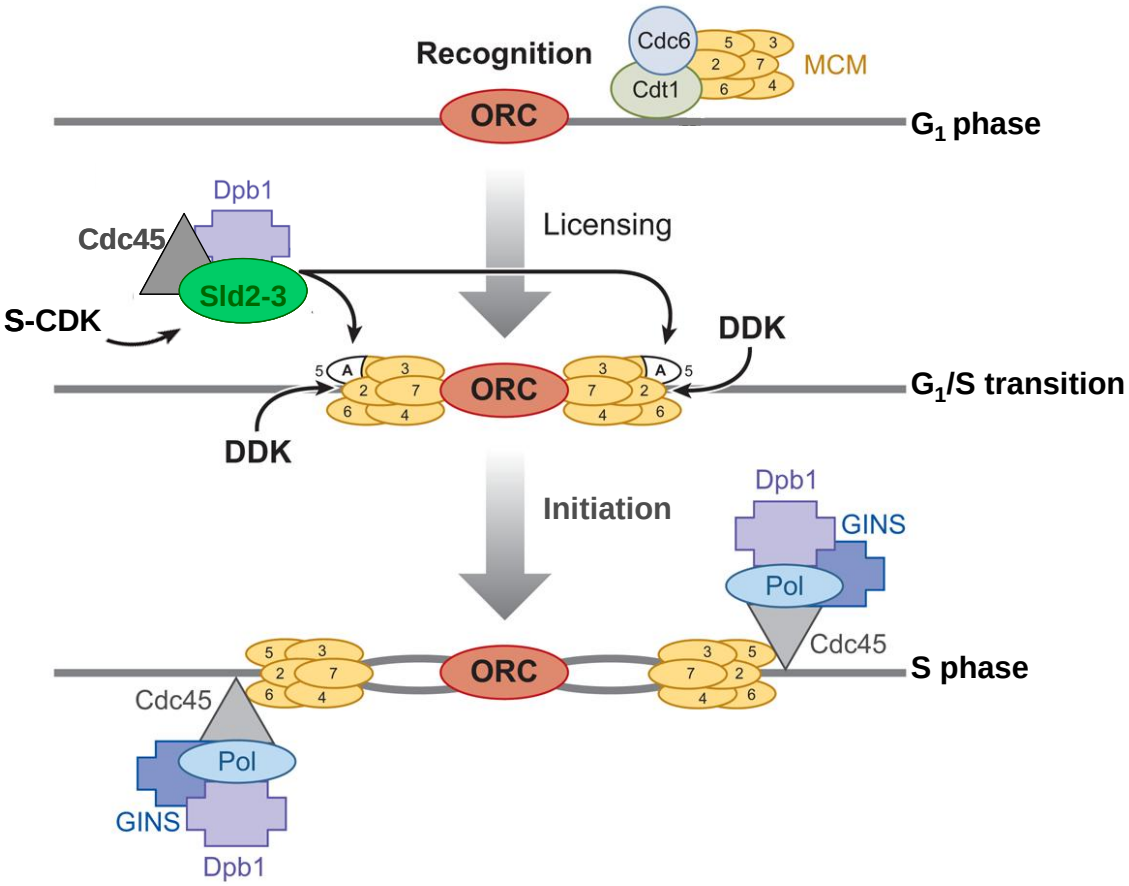


Figure 1.4 Model for the regulation of DNA replication. Origins of replication are recognized by ORC follow by the loading of Cdt1, Cdc6 and MCM helicase. In protozoans geminin inhibit Cdt1 and pre-RC formation. CDK and DDK are activated in the transition G1/S phase to promote the loading of DNA polymerases. Additionally CDK prevent any further activation of pre-RC. CDK also induce phosphorylation of Sld2, Sld3 and Mcm5 that promotes the initiation of DNA synthesis. Diagram modified from Sclafani and Holzen (2007).

mechanism to restrict pre-RC formation to only once per cell cycle (Lutzmann et al., 2006). Cdc6 in budding yeast stimulates the Abf1 binding activity (Feng et al., 1998). These events promote the recruitment of MCM2-7 complex, the replicative helicase, to all the origins and complete the pre-RC assembly conferring replication competency or licensing to the origin (Figure 1.4).

In the transition to S phase, S-CDK and DDK, two key kinases are universally required for the regulation of replication (Figure 1.4). DDK (Dbf4 dependent kinase) is composed of the Cdc7-Dbf4 heterodimer, where Dbf4 acts as regulatory subunit of Cdc7 kinase (Sclafani, 2000). S-CDK promotes the phosphorylation of Sld2 and Sld3 inducing their binding to Dpb11. The interaction between Dpb11 and phosphorylated Sld2 induces the formation of a pre-loading complex (pre-LC), which also includes Cdc45 (Figure 1.4) (Kanemaki & Labib, 2006; Tanaka et al., 2007; Zegerman & Diffley, 2007). The formation of the pre-LC complex is S-CDK dependent, but independent of the pre-RC formation and DDK activity (Muramatsu et al., 2010). It has been proposed that pre-LC is responsible to deliver GINS to pre-RC in order to promote helicase activity of MCM2-7 (Muramatsu et al., 2010).

On the other hand, DDK induces the phosphorylation of the amino terminus of Mcm4 (Figure 1.4), stimulating a change in the structural conformation of MCM complex (most likely dependent on Mcm5). This promotes the interaction of MCM complex with Cdc45, which is essential for the subsequent recruitment of polymerase α/primase (Sheu & Stillman, 2010).

Furthermore, in the transition to S phase different strategies are applied in order to avert pre-RC re-assembling. Between the initial events, S-CDK phosphorylate Orc2 and Orc6 subunits to prevent them from interacting with other pre-RC components. Also, S-CDK alters phosphorylation of Cdc6 which is targeted for proteolysis, as well S-CDK phosphorylate Mcm2-7 and Cdt1 which prevents their nuclear accumulation (McGarry & Kirschner, 1998; Wohlschlegel et al., 2000). Simultaneously, DDK reinforce the action of S-CDK by phosphorylating Mcm2, Mcm4 and Mcm6 preventing the interaction with other pre-RC components (reviewed in Sclafani and Holzen, 2007).

**Initiation of DNA replication**

During S phase the activation of origins (firing) is asynchronous during S phase, the timing at which origins are activated will define them as early, middle or late origins (Tanaka & Araki, 2010). The timing of replication initiation reflects the activation of the replicative helicase (Figure 1.4). The recruitment of pre-LC to licensed origins promotes the actual activation of the Mcm2-7 that consists in the direct interaction of Mcm2-7 with Cdc45 and GINS to promote helicase activity (Gambus et al., 2006; Ilves et al., 2010).

Pre-LC is associated during $G_1$ to early firing origins and loaded to late origins during S phase (Tanaka & Araki, 2010). As was already mentioned, pre-LC includes Sld2 and Sld3, multiple phosphorylation sites in this two factors suggested that they could act as sensors for S-CDK activity and trigger replication initiation (Tanaka et al., 2007; Zegerman & Diffley, 2007). Particularly Sld3, which is required for initiation but

not for elongation of replication and has been proposed that its release from the origin, may promote recruitment of factors necessary for elongation of replication forks (Tanaka & Araki, 2010).

Furthermore, it has been suggested that chromatin structure might be one of the determinant factors (Wu & Nurse, 2009). However, heterochromatin at the silent mating-type locus and pericentromeric regions is replicated during early S phase in *S. pombe* (Kim et al., 2003; Kim & Huberman, 1998). Recently it has been showed that heterochromatic factor Swi6 is responsible for the recruitment of Sld3 to heterochromatic origins via interaction with a DDK subunit and promoting its activation (Hayashi et al., 2009).

From all the origins licensed during $G_1$, only a fraction fire during S phase. Origins that fire every cell cycle are called constitutive, but most of the origins are flexible or are maintained in dormant state and passively replicated (Blow & Ge, 2008). In budding yeast, early firing origins are efficiently utilized in consecutives cell cycles, suggesting a strong correlation between timing and origin efficiency (Heichinger et al., 2006). Flexible origins are those that can be used stochastically, in case the cell is under unfavorable growth conditions or under genotoxic stress. Beside S-CDK and DDK modulation of origin firing, in presence of DNA damage or replication fork stalling, checkpoint kinases are also able to regulate origin activation (Santocanale & Diffley, 1998). Origin firing is inhibited by checkpoint kinases, allowing more time for pre-RC assembly increasing the efficiency of flexible origins, and activating dormant origins.

These allow completion of DNA replication during S phase when the re-licensing of origins is inhibited (Santocanale et al., 1999).

Finally, the recruitment of pre-LC also promotes the loading of Pol ε by direct interaction with Dpb11 (Masumoto et al., 2000). The loading of Mcm10 is necessary for the stable association of polymerase to chromatin (Ricke & Bielinsky, 2004; Wohlschlegel et al., 2002). Once helicases are activated double stranded DNA is unwound, polymerases α and δ and accessory proteins are loaded to form the replisome. This include replicator factor C (RFC) clamp loader, clamp proliferating cell nuclear antigen (PCNA) and replication protein A (RPA) for stabilization of local ssDNA and the establishment of bidirectional replication.

**Replicative checkpoint response**

The intra-S phase checkpoint is responsible for regulating DNA replication in cells that are under replication stress, blocking the advance of ongoing replication forks and inhibiting the firing of late replication origins (Machida & Dutta, 2005). During S phase damage may be accumulated endogenously when replication forks are stalled by the block of polymerase progression. As was previously described, DSB or exposed ssDNA may initiate a signal cascade that culminates with the activation of effectors kinases Chk1 and Chk2, which directly prevent the progression of the cell cycle by regulation of CDK activity.

Also several mediators are necessary for the activation of effector kinases. Besides their roles as mediators, some of them play an active role in the DNA damage response.

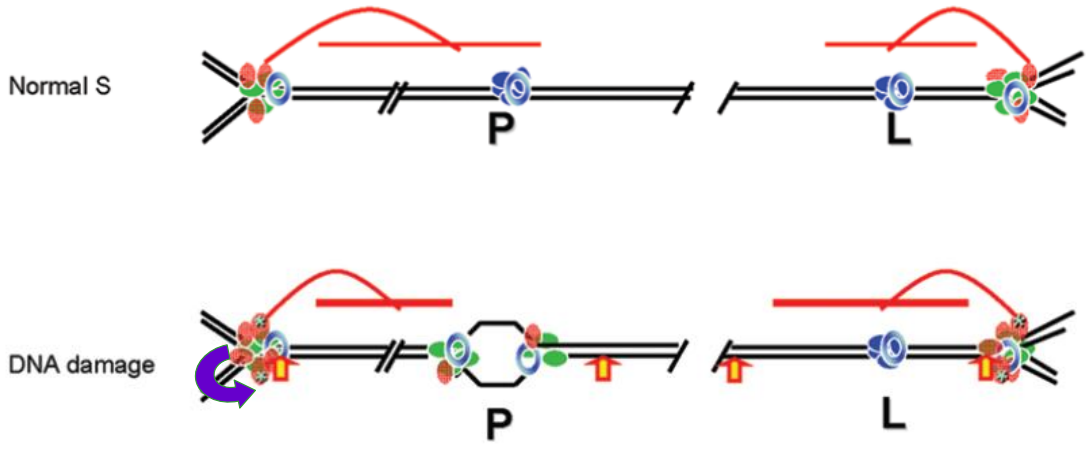


Figure 1.5 Regulation of origin firing during replicative checkpoint response. (Normal S) Shows the regulation of origin firing in unperturbed S phase with two replications forks progressing from each extreme. A (P) dormant origin that is passively replicated and a (L) Late firing origin. Pre-RC components (blue ovals) and components of replisome (green circles). Also showing (red circles) representing factors involved in the activation of checkpoint that are constitutively associated to chromatin during unperturbed S phases (like claspin, ATR and Chk1). Also illustrating the mechanism of origin interference, where the active origins inhibit the firing of redundant origins (red inhibitory arrows). (DNA damage) showing S phase in presence of genotoxic stress. The (P) dormant origin is fired before the threshold that activates the checkpoint is reached. Once intra-S phase checkpoint is activated, other components of the checkpoint (red circles) are recruited to the site of damage (red and yellow arrow). Activation of the checkpoint promotes strong inhibition of redundant origins. Diagram modified from Grallert and Boye (2008).

One of these mediators, claspin, is localized at replication forks in unperturbed cells and is necessary for normal rates of fork progression during active DNA synthesis by direct binding to two of the subunits of polymerase Pol ε (Osborn & Elledge, 2003; Petermann et al., 2008; Tourriere et al., 2005). During activation of the intra-S checkpoint, claspin is phosphorylated by Chk1, this promotes the dissociation of one of the subunits of Pol ε (Chini & Chen, 2006). Since claspin also binds Mcm2-7 it has been proposed that claspin may be able to sense the separation between helicase and polymerase activity and this way inhibit further replication (Figure 1.5) (Katou et al., 2003; Lou et al., 2008; Osborn & Elledge, 2003; Petermann et al., 2008; Tourriere et al., 2005)

Furthermore, ATR is also an integral component of replisomes. In *Xenopus* ATR associates with chromatin after initiation of replication and dissociates upon completion of replication (Hekmat-Nejad et al., 2000). This explains why the disruption of ATR causes chromosomal fragmentation and promotes lethality in embryos and somatic cells (Brown & Baltimore, 2000; Cortez et al., 2001). During genotoxic stress ATR is accumulated at the damaged site as discuses above.

Chk1 is also an essential gene in embryos and necessary for normal proliferation of somatic cells (Lam et al., 2004; Takai et al., 2000). In addition, Chk1 is required for the activation of origins and for the normal progression of forks in unperturbed cells (Maya-Mendoza et al., 2007; Petermann et al., 2006). During genotoxic stress the activation of Chk1 responds to a threshold sufficient for checkpoint activation, Chk1 activation induces inhibition of S-CDK that reduces to minimal the firing of origins and only dormant origins may fire when replication proceed in suboptimal conditions and before

checkpoint activation (Figure 1.5) (Ge et al., 2007; Grallert & Boye, 2008) (Shechter et al., 2004; Shimada et al., 2002).

The phosphorylation of S-CDK, also induces the activation and the phosphorylation of the Cdc25a phosphatase. As a result, Cdc25a is targeted for degradation and unable to promote the loading of Cdc45 for the initiation of DNA synthesis (Sorensen et al., 2004; Suryadinata et al., 2010). However, late firing origins and dormant origins are bound by pre-RC, dormant origins that are not activated during normal S phase are trigger in presence of DNA damage (Doksani et al., 2009; Santocanale et al., 1999). Recently, Petermann and colleagues (2010) suggested that Chk1 directly regulate the speed of replication forks in normal cell cycles by acting as an inhibitor of excessive origin firing. The observation that depletion of Chk1 increased origin firing but at the same time reduces the speed of replication forks, suggest that Chk1 dependent phosphorylation of Cdc25a promotes fork progression in order to revert the effect of low frequency of firing origins (Petermann et al., 2010) .

Furthermore, the activation of the intra-S phase checkpoint induces Chk2 activity. Chk2 induces the direct phosphorylation of Dbf4 (the regulatory subunit of DDK) and also the phosphorylation of replication initiation protein Sld3, preventing this way the formation of pre-RC at origins that already were fired (Lopez-Mosqueda et al., 2010; Zegerman & Diffley, 2010).

**DNA synthesis with different set of rules**

Re-replication and endoreplication are examples of deviations from strict regulation of replication that exist during mitotic cell cycles.

Endoreplication is a variation of the normal cell cycle that result in the generation of polyploid cells, which are required to support growth and development at early embryonic stages in metazoans. Endocycles consist of a synthesis (S) phase followed by a gap phase without cell division; this generates a cell with a single polyploid nucleus (Lee et al., 2009). Endocycling require pre-RC assembly at origins and is governed by the activation and inactivation of cyclin E, which is necessary for licensing of origins (Muramatsu et al., 2010). In addition, endoreplicating cells do not express cyclin B, cyclin A or Cdc25c, essential regulators of $G_2$ and mitosis (Figures 1.1 and 1.2), suggesting that polyploidization is under a tight control of S-CDK, but subjected to a different set of rules than mitotic cell cycles. An ongoing controversy is the role of Orc1p in endocycles. Recent studies in *Drosophila* salivary glands deficient in Orc1p showed that Orc1p is dispensable for endoreplication since this mutants complete endocycles as efficiently as wild type cells (Park & Asano, 2008). This opens the possibility of an alternative mechanism for the regulation of DNA replication during endocycles.

Polyploidization by endoreplication is also a characteristic feature of cancer cells, where polyploids cells are considered intermediates between normal cells and cancer-associated aneuploids (). Early lesions are often characterized by transient activation of DNA damage that fails to respond to genotoxic stress, polyploidy and genetic instability

(Ganem et al., 2007). In fact recently it has been established that the simultaneous elimination of p53 and telomerase mimics the tetraploidization by endoreplication observed in epithelial cancer cells, suggesting a possible mechanism for the transformation of humans cells(Davoli et al., 2010).

Another alternative replication process includes the re-amplification of specifics sites in chromosomes. This occurs in terminally differentiated cells such as *Drosophila* follicle cells that amplify genes necessaries for the egg shell formation (Tower, 2004). Re-replication was originally defined by an aberrant process characterized by uncontrolled continuous re-initiation of DNA synthesis at individual origins within a single S phase (Blow & Dutta, 2005). This lead to DNA damage, checkpoint activation, aneuploidy, genomic instability and tumor formation(Hook et al., 2007). In metazoans the recruitment of Cdt1 is negatively modulated by geminin as a primary mechanism to restrict the pre-RC formation to only once per cell cycle and to prevent re-replication (Lutzmann et al., 2006; Saxena & Dutta, 2005). In humans and *Drosophila* the depletion of geminin promote re-replication during early S phase (Ding & MacAlpine, 2010; Dorn et al., 2009). However, a recent genome-wide analysis showed that pericentromeric heterochromatin was preferentially re-replicated in the absence of geminin (Ding & MacAlpine, 2010), suggesting that re-replication is not a totally uncontrolled process. Furthermore, Gomez and Antequera (2008) showed that short regions that overlap origin are re-replicated several times when the origin fired during S phase. The re-replicated fragments are double stranded 200 base pairs long, have an RNA primer attached and are derived from nucleosome free regions (Gomez & Antequera, 2008). The authors suggest

that the level of these short controlled re-replicated fragments is not high enough to activate intra-S checkpoint. It is not known whether this over-replication plays any role in the control of DNA synthesis, but clearly has changed our notion of re-replication in mitotic cell cycles.

**Biology of *Tetrahymena thermophila***

*Tetrahymena thermophila* is one the most well characterized species in ciliate protozoans. As most ciliates, *Tetrahymena* contains two nuclei within the same cytoplasm, which are genetically related but differ in structure and function. The micronucleus (MIC) contains five metacentric chromosomes and divides by conventional mitosis during vegetative cell cycles and meiosis during development (Gorovsky & Woodard, 1969; Mayo & Orias, 1981; Yao & Gorovsky, 1974). The micronucleus plays an important function acting as the reservoir of genetic material that is exchanged during conjugation. It is actively transcribed during a brief period during development and considered transcriptionally inactive during the vegetative life cycles (Jahn & Klobutcher, 2002; Karrer, 2000; Prescott, 1994).

The macronucleus (MAC) serves as the somatic nucleus; it is transcriptionally active during vegetative growth, responsible for expressing all genes necessary for vegetative growth and initiation of the conjugation program (Bruns & Brussard, 1974; Mayo & Orias, 1981). The macronucleus contains ~280 autonomously replicating chromosomes ranging from 20 kb to over 2 Mb long. These chromosomes are derived

from site-specific fragmentation and rearrangement of the five micronuclear chromosomes during sexual development (Coyne et al., 1996; Woodard et al., 1972).

The macronucleus divides amitotically during vegetative cell division and is not transmitted to progeny following conjugation. The amitotic transmission of MAC chromosomes does not use any visible mitotic spindle. Indeed the macronucleus elongates and constricts to generate two daughter nuclei with approximately half of the parental macronuclear DNA, when the cell divides by binary fission during vegetative growth (Orias et al., 1991). Microtubules invade the dividing MAC, but appear principally to establish the plane for MAC division (Katz, 2001). The unequal division of the MAC generates two heterozygous daughter cells, the vegetative propagation of these cells generate subclones with macronucleus functionally haploid. This phenomenon, denominated macronuclear phenotypic assortment, is a random and stochastic process that promotes the elimination of one of the two alleles from the MAC (Merriam & Bruns, 1988; Prescott, 1994; Sonneborn, 1974).

*Tetrahymena* sexual phase is called conjugation (Martindale et al., 1982). In order to initiate conjugation cells must first be starved for at least one nutrient, be of different mating types and have reached sexual maturity, which occur ~70 cell divisions after the previous conjugation (Allewell et al., 1976). Cells conjugate by generating temporary junctions and forming mating pairs, allowing for the reciprocal exchange of gametic pro-nuclei (Wolfe, 1982). Exchange is followed by fertilization and nuclear differentiation during which the old parental macronucleus is destroyed and replaced by

a new macronucleus that is derived from the new micronucleus of progeny (Karrer & VanNuland, 1999).

In detail, once two *Tetrahymena* cells have formed mating pairs (Figure 1.6a) the micronucleus moves away from the macronucleus and elongates increasing its length by over 50-fold, forming a structure called crescent. This micronuclear crescent, stretches the entire length of the cell and curves around the macronucleus (Figure 1.6b) (Wolfe et al., 1976). Following crescent formation chromosomes condense (Figure 1.6c) and undergo two rounds of meiosis (Figure 1.6d). After meiosis one of the nuclei is selected and moves to the anterior portion of the cell while the other nuclei are degraded (Figure 1.6e) (Gaertig & Gorovsky, 1992). The selected micronucleus then undergoes mitosis forming two genetically identical pronuclei (Figure 1.6f). One of these pronuclei will migrate to the fusion point of the mating pair and be transferred to the mating partner while the other pronucleus remains in the cell of origin (Kaczanowski et al., 1991). After pronuclear exchange the two pronuclei will fuse to form the fertilized micronucleus (Figure 1.6g). This micronucleus undergoes two postzygotic rounds of mitosis (Figure 1.6h) (Kaczanowski et al., 1991). Two of the nuclei are selected which chromatin decondenses and initiate the macronuclear developmental process, at this point the new macronuclei is called anlagen (Figure 1.6i) (Martindale et al., 1982). During the second stage of macronuclear development, the two micronuclei and anlagen macronuclei move to the center of the cell while the old macronucleus moves to the posterior of the cell where it undergoes condensation and apoptotic DNA fragmentation (Figure 1.6j) (Mpoke & Wolfe, 1996). The mating pair then separates and one of the micronuclei will

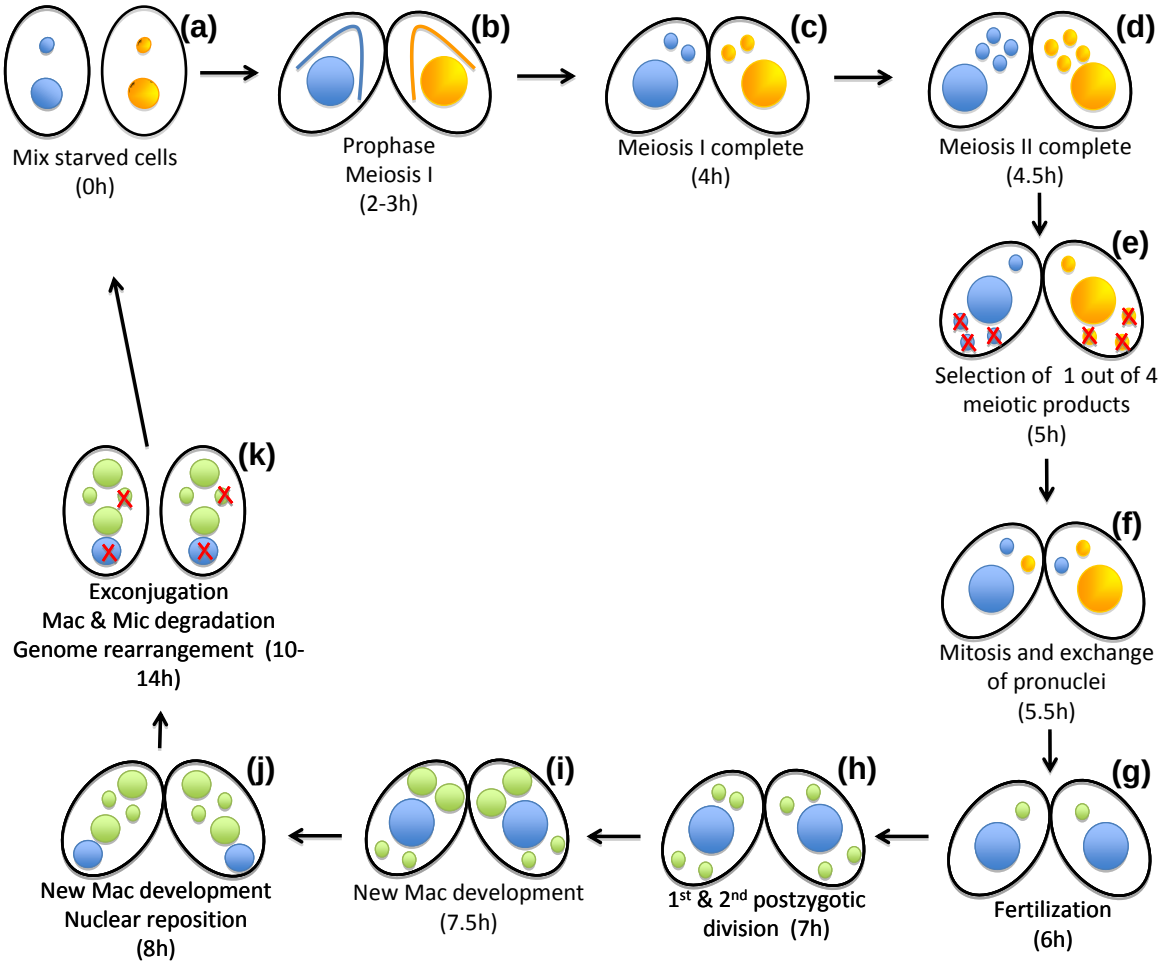


Figure 1.6 Nuclear events during conjugation of *Tetrahymena*.

also be degraded (Figure 1.6k). Finally the remaining micronucleus undergoes mitosis and the cell divide by binary fission to produce two cells which are the progeny of the mating pair.

During macronuclear differentiation (Figure 1.6i) developmentally programmed DNA rearrangements occur. One of these DNA rearrangements involves the elimination of internal DNA fragments following ligation of the flanking sequences (Karrer, 2006). The internal eliminated sequences (IES) are most likely removed by a scan mechanism that involves synthesis of small RNAs, denominated scnRNA (Yao & Chao, 2005). This scnRNA (28-29 bases) are synthesized in the MIC during meiosis and are processed by a dicer-like protein Dcl1p followed by association with an Argonaut protein Twi1p (Malone et al., 2005; Mochizuki & Gorovsky, 2004; Mochizuki & Gorovsky, 2005). Dcl1p and Twi1p are conserved essential components of the RNA interference machinery and involved in transcriptional and post-transcriptional gene silencing in several eukaryotes (Chu and Rana, 2007). IES are repetitive elements that close resemble transposons and their deletion eliminates about 15% of the MIC sequence (Cherry & Blackburn, 1985; Patil et al., 1997).

A second rearrangement is the site specific fragmentation of the five MIC chromosomes at the chromosome breakage sequences (Cbs, Figure 1.7) that generate ~280 minichromosomes. Telomeres are added de novo to the new chromosomes end and these minichromosomes are amplified to ~45 copies (Figure 1.7) (Coyne et al., 1996; Fan & Yao, 1996; Yao, 1982; Yao et al., 1987).

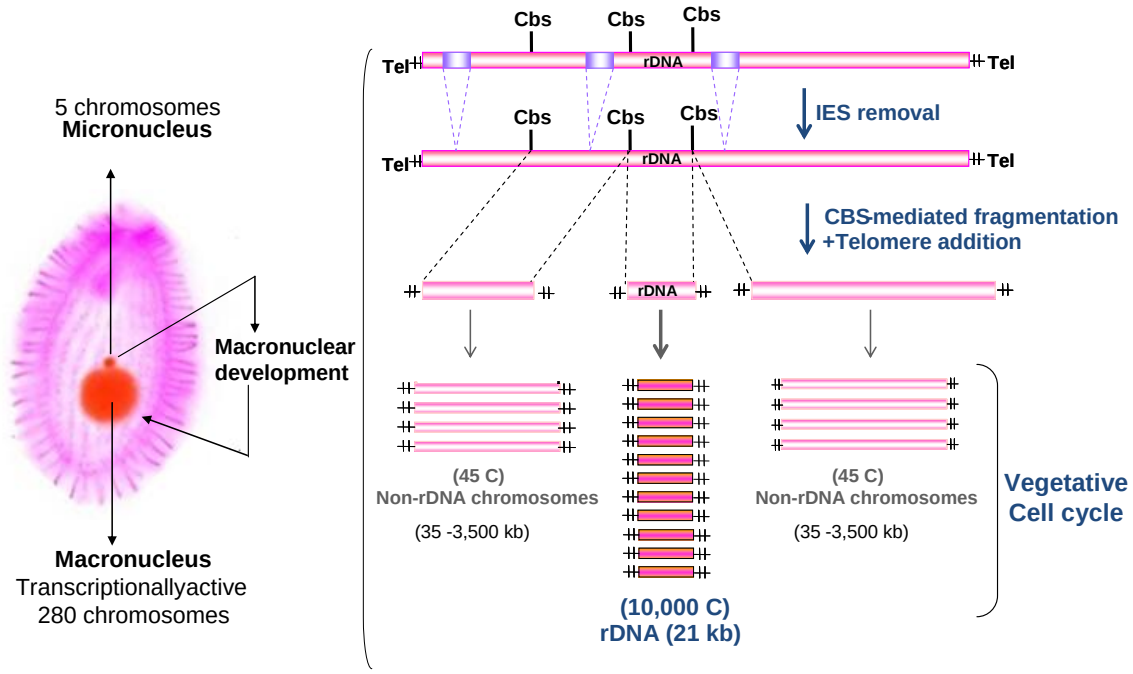


Figure 1.7 Differential DNA replication and developmentally programmed DNA rearrangement during macronuclear development. Left panel is a composite representation of bi-nucleate *Tetrahymena* cell. Macronuclear development key steps are shown in the right panel, during macronuclear development, (Cbs), chromosome breakage, (IES) internally eliminated sequences. Endoreplication of the non-rDNA minichromosomes occurs to generate 45 copies. Locus specific amplification of the rDNA increase the copy number in the developing macronucleus up to 10,000 copies. The number of copies is maintained in every vegetative cell cycle.

Another programmed DNA rearrangement that occurs during macronuclear development is the rearrangement and amplification of the rDNA minichromosome. During this process the single copy of the *Tetrahymena* gene for the 35S ribosomal RNA precursor is excised from the MIC genome (Figure 1.7). This 10.5 kilobase fragment then undergoes head-to-head palindrome formation resulting in a 21 kilobase inverted repeat to which telomeres are added de novo (Gall, 1974; Yasuda & Yao, 1991) The rDNA is amplified to 10,000 copies in the developing macronucleus (Yao & Gorovsky, 1974). Developmental amplification of *Tetrahymena* differs from gene amplification in other model organism in that it does occur in the normally differentiated cells. Endoreplic cycles precede to rDNA gene amplification during development. Furthermore, all the replic origins are subsequently utilized during vegetative cell division. Hence, non-rDNA replicons that are silenced during vegetative cell cycle need to be reactivated during conjugation. As for the previously described chromosomes rDNA amplification occurs during a single S phase and the resulting minichromosomes are maintained at this level during subsequent vegetative division (Karrer and Blackburn, 1989).

**The rDNA replicon in *Tetrahymena***

The ribosomal minichromosome (rDNA) is a 21 kilobase palindromic sequence that is maintained vegetatively in 10,000 copies in the macronuclear nucleus and replicated only once every cell cycle. It contains two distinct sites for DNA replication initiation localized in two 430 base pair tandem imperfectly duplicated direct repeats at

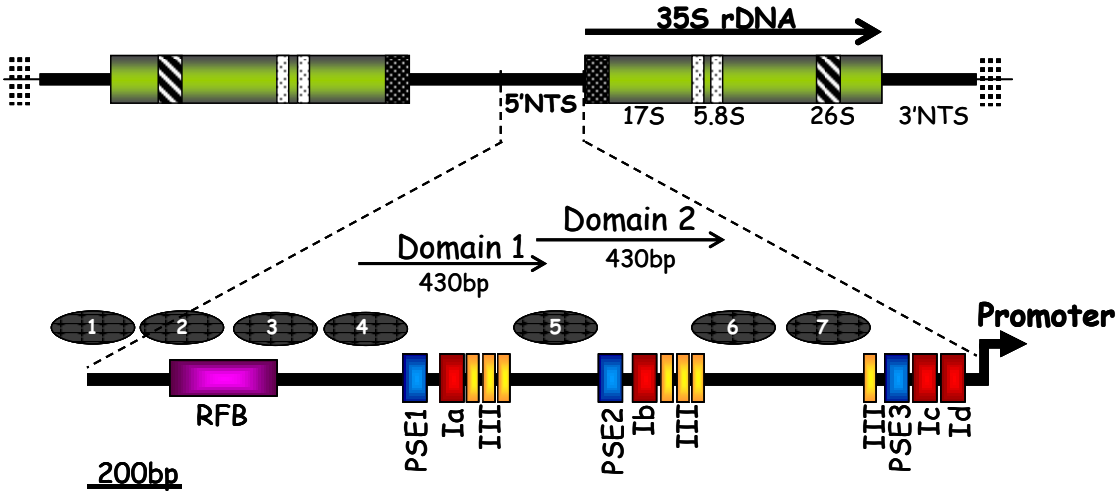


Figure 1.8 Schematic of the *Tetrahymena* rDNA minichromosome. The 2.1 Kb macronuclear rDNA minichromosome consisted a palindromic arrangement of two copies of the rDNA gene (in green) that encode for 17S, 5.8S and 26S ribosomal rDNA. The region encompassing the 5'NTS is expanded and includes cis-acting determinants for DNA replication. Type I, II, III and pause site elements are phylogenetically conserved sequences. Type I elements are showing in red, Type III in yellow, replication fork barrier (RFB) in purple and pause site elements (PSE) in blue. The locations of the seven positioned nucleosomes are depicted by black ovals.

the 1.9 kilobase of the 5' non-transcribed spacer (5' NTS, Figure 1.8) (Zhang et al., 1997). These replication origins are designated Domains 1 and 2 and reside in two of three nucleosome-free regions in the 5' NTS (Palen & Cech, 1984). D1 and D2 are part of a single replicon that contains several reiterated cis-acting regulatory elements essential for DNA replication (Figure 1.8) (Reischmann et al., 1999).

The type I element is a 33 base pair sequence that is phylogenetically conserved in the rDNA of tetrahymenid species (Challoner et al., 1985). There are four type I elements in the 5' NTS of *Tetrahymena*, one in each replication origin (type IA and IB) and two situated at the promoter region (type IC and ID; (Figure 1.8). It has been shown that mutations within or downstream of a type element cause rDNA minichromosome maturation or maintenance defects (rmm mutant). Strains containing rmm mutant alleles present single base mutations and are defective in one of these two mechanisms but not both(Kapler & Blackburn, 1994; Yaeger et al., 1989) As example, rmm3 mutant is able to complete development, but exhibit defects in vegetative propagation of the rDNA chromosome (Gallagher & Blackburn, 1998). This phenotype is only evident when rmm mutants are placed in competition with wild-type rDNA alleles. Some of these mutations (rrm1, rmm4, and rmm7) map to the type IB element found in the D2 region (Larson et al., 1986; Yaeger et al., 1989) while others (rmm3 and rmm8) are found in the type IC and ID elements in the promoter region (Gallagher & Blackburn, 1998).

Analysis of mutants with alteration at the promoter proximal type I elements reveal that type IC and ID elements are part of the rDNA promoter, and consequently regulate rRNA transcription as well as rDNA replication (Gallagher & Blackburn, 1998;

Pan & Woodson, 1998). However, mutations in this region affect either replication or transcription suggesting that these processes may be controlled by different DNA binding factors.

Type I elements have also been shown to regulate DNA replication fork movement by causing forks to arrest transiently at specific, conserved nearby PSEs (MacAlpine et al., 1997). This arrest in replication fork movement occurs in an orientation-dependent manner. Together these results indicate that type I elements regulate replication initiation, elongation of replication forks, and rRNA transcription.

Other phylogenetically conserved sequences are the pause site elements (PSE). Three PSE are found in the rDNA replicon and coincide with sites of transient replication fork arrest (MacAlpine et al., 1997). PSE is a 52 base pair sequence and contain three blocks of conserved sequence separated by two spacers. PSE1 and PSE2 reside in D1 and D2 respectively and map to the 5'-border of the nucleosome-free regions of the two DNA replication origins (Figure 1.8), while PSE3 is promoter-proximal, but is not part of the minimal rRNA promoter (Miyahara et al., 1993). However, PSE3 has been shown to be essential for DNA replication since the replacement of its sequences disrupts the ability to maintain rDNA molecules that are transformed into the developing *Tetrahymena* (Saha et al., 2001).

Recently, the first two non-rDNA replicon were described in *Tetrahymena* and named ARS1-A and ARS1-B of 700 and 1,200 base pair respectively (Donti et al., 2009). Non-rDNA ARS lacks the phylogenetically conserved sequences present at the rDNA. Furthermore, no significant sequence similarity exists between ARS1-A and –B,

resembling somehow the case in higher eukaryotes, where no sequences are conserved between origins.

**Trans-acting factors for *Tetrahymena* rDNA replication**

*Tetrahymena thermophila* (Tt) ORC is a high molecular multisubunit complex which binds to type I elements in an ATP dependent and sequence specific manner (Mohammad et al., 2003; Mohammad et al., 2007). One of the unique features of TtORC is that it contains an integral RNA subunit that uses Watson-Crick base pairing to bind to the T-rich strand of the type I element (Mohammad et al., 2003; Mohammad et al., 2007). The ORC RNA subunit, 26T RNA, corresponds to the terminal 282 nucleotides (nt) of 26S rRNA, and mutations that perturb RNA-DNA base pairing disrupt rDNA origin recognition and activation (Mohammad et al., 2003; Mohammad et al., 2007). Furthermore, TtORC also regulates activation of non-rDNA origins (Donti et al., 2009). Since non-rDNA origins do not contain sequences similar to type I element, this suggest that TtORC utilizes a different mechanism for targeting to non-rDNA origins in *Tetrahymena*.

Type I elements are also recognized by other single-stranded binding factors, called TIFs, three distinct type I element binding factors (TIF1-3) have been identified in *Tetrahymena* extracts using electrophoretic mobility shift assays (Mohammad et al., 2000; Mohammad et al., 2003). Each of these binding activities appears to be independent, since those binding activities are differentially regulated during development and the cell cycle. Furthermore, the differentially regulated expression of

these factors suggests that they compete for type I binding in vivo (Mohammad et al., 2000).

Tif2p is an 85 kDa protein that binds to both the A-rich and T-rich strands of the type I element. The binding activity of Tif2p increases in cells undergoing vegetative replication or rDNA gene amplification (Mohammad et al., 2000). Tif3p is a 32 kDa protein that also binds to both the A-rich and T-rich strands of the type I element. Binding activities of Tif3p increase notably in extract prepared from starved cells. However, binding activity of Tif3p is lost when cells are growing vegetatively, suggesting that it may play a role as a negative regulatior of rDNA replication in adverse environmental conditions (Mohammad et al., 2000; Saha et al., 2001).

Tif1p is a 21 kDa protein that forms a homotetramer in vivo. Tif1p binds independently A-rich or T-rich single-strand DNA of the type I element, suggesting that it may stabilize unwound DNA in these regions (Saha & Kapler, 2000). Tif1p also binds the essential PSE, suggesting an important role in the regulation of DNA replication. Furthermore, in vivo footprinting analysis revealed that Tif1p regulates the occupancy of origin and promoter proximal type I element in vivo, consistent with a role in the regulation of replication initiation and possible rRNA transcription (Saha et al., 2001). Additionally, strains that are depleted from TIF1 replicate the rDNA precociously in S phase. These findings suggest that Tif1p play an inhibitory role in the replication of rDNA minichromosome (Morrison et al., 2005). Morrison and colleagues also showed that Tif1p serves a more global role in both MIC and MAC and is required to maintain the integrity of the mitotic MIC chromosomes and for proper division of the amitotic

MAC (Morrison et al., 2005). The remaining chapters will form my dissertation studies of Tif1p and unexpected features of *Tetrahymena* DNA damage response.

# CHAPTER II

# TIF1 ACTIVATES THE INTRA-S PHASE CHECKPOINT RESPONSE IN THE DIPLOID MICRONUCLEUS AND AMITOTIC POLYPLOID MACRONUCLEUS OF TETRAHYMENA*

## Overview

The ribosomal DNA origin binding protein Tif1p regulates the timing of rDNA replication and is required globally for proper S phase progression and division of the *Tetrahymena thermophila* macronucleus. Here, we show that Tif1p safeguards chromosomes from DNA damage in the mitotic micronucleus and amitotic macronucleus. Tif1p localization is dynamically regulated as it moves into the micro- and macronucleus during the respective S phases. TIF1 disruption mutants are hypersensitive to hydroxyurea and methylmethanesulfonate, inducers of DNA damage and intra-S phase checkpoint arrest in all examined eukaryotes. TIF1 mutants incur double-strand breaks in the absence of exogenous genotoxic stress, destabilizing all five micronuclear chromosomes. Wild-type *Tetrahymena* elicits an intra-S phase

---

*Reprinted with permission from "Tif1 Activates the Intra-S Phase Checkpoint response in the Diploid Micronucleus and Amitotic Polyploid Macronucleus of Tetrahymena" by J. Sebastian Yakisich, Pamela Y. Sandoval, Tara L. Morrison and Geoffrey M. Kapler, 2006. *Molecular Biology of the Cell*, 17, 5185-5197, Copyright [2006] by Molecular Biology of the Cell.

checkpoint response that is induced by hydroxyurea and suppressed by caffeine, an inhibitor of the apical checkpoint kinase ATR/MEC1. In contrast, hydroxyurea-challenged TIF1 mutants fail to arrest in S phase or exhibit caffeine-sensitive Rad51 overexpression, indicating the involvement of TIF1 in checkpoint activation. Although aberrant micro- and macronuclear division occurs in TIF1mutants and caffeine-treated wild-type cells, TIF1p bears no similarity to ATR or its substrates. We propose that TIF1 and ATR function in the same epistatic pathway to regulate checkpoint responses in the diploid mitotic micronucleus and polyploid amitotic macronucleus.

## Introduction

The coordinate regulation of nuclear and cytoplasmic cell cycles ensures that daughter cells receive a complete complement of chromosomes. Consequently, perturbations in DNA replication, chromosome segregation, or nuclear division arrest the cell cycle before cytokinesis. Recent studies have identified an intra-S phase DNA damage checkpoint that protects chromosomes from lesions associated with the elongating replication fork (for review, see Lambert and Carr, 2005). Sources of genotoxic stress, such as the chemical mutagen methylmethanesulfonate (MMS) or depletion of DNA precursors with hydroxyurea (HU), trigger the activation of the damage sensor/transducer protein Ataxia Telangectasia and RAD3-related (ATR) (MEC1 in *Saccharomyces cerevisiae*). This phosphatidylinositol 3 (PI3)-kinase–related protein kinase initiates a signaling cascade by phosphorylating downstream effector kinases Chk1p (in mammals), Rad53p (Chk2p) in budding yeast, and additional

regulatory proteins (Foss, 2001; Gilbert et al., 2001; Tanaka and Russell, 2001). Uninitiated replication origins are repressed, and elongating replication forks are stabilized until the impediment to DNA replication is resolved by recombination or repair. Inactivation of the damage checkpoint is lethal in all examined eukaryotes.

The coordinate regulation of nuclear and cytoplasmic cell cycles is subjected to unusual challenges in ciliated protozoa, such as *Tetrahymena thermophila*, because members of this ancient lineage contain two nuclei within a single cytoplasm. These nuclei serve nonoverlapping roles and harbor chromosomes that are organized and segregated in fundamentally different ways (for review, see Karrer, 2000). The transcriptionally silent, diploid micronucleus functions as the germline nucleus and contains five chromosome pairs that are transmitted by conventional mitosis and meiosis. In contrast, the transcriptionally active, polyploid (~45 C) macronucleus has >250 distinct chromosomes that lack centromeres and segregate by a poorly understood amitotic mechanism.The macronuclear genome is not inherited after conjugation. Instead, a new macronuclear "anlage" is generated by differentiation of a toti-potent postzygotic micronucleus in progeny cells. Macronuclear chromosomes are produced by site-specific fragmentation and rearrangement of their micronuclear precursors. With the exception of the 21-kilobase rDNA minichromosome, which is amplified to ~9000 copies, macronuclear chromosomes attain a copy number of ~45 C.

Once macronuclear development is complete, *T. thermophila* divides by binary fission. Because the timing of micro- and macronuclear DNA replication and division are offset in the cell cycle, these nuclei must respond to different cell cycle cues.

Although macronuclear chromosomes segregate randomly, chromosome copy number is maintained in a manner somewhat analogous to bacterial plasmids (for review, see Dobbs et al., 1994). The imprecision of amitotic macronuclear division raises the possibility that an ATR-like intra-S phase checkpoint is dispensable for macronuclear chromosome homeostasis. Furthermore, unconventional mechanisms have evolved to compensate for the associated genic imbalances. Partial endoreplication cycles and the elimination of "excess DNA" in the form of macronuclear extrusion bodies maintain macronuclear DNA content and gene copy number within a narrow range (Cleffmann, 1968; Doerder and Debault, 1975; Bodenbender et al., 1992).

Because these compensating pathways do not operate in the diploid, mitotic micronucleus, one would predict that the micronucleus uses conventional DNA damage checkpoint pathways to maintain genome stability. One argument against this idea is the fact that micronuclear aneuploidy does not arrest vegetative cell cycle progression. "Functionally amicronucleate," hypo-diploid "star" strains divide normally and have an unlimited life span (Allen, 1967), and some related tetrahymenid species lack a micronucleus. The integrity of the micronucleus only comes into play during conjugation, because it contains the sole source of transmitted nuclear genes.

We obtained preliminary evidence for a macronuclear S phase checkpoint during our analysis of tif1-1::neo mutants, which among other things are partially defective in macronuclear S phase progression (Morrison et al., 2005). TIF1-deficient cells exhibit a prolonged macronuclear S phase, that once complete, is followed by a further delay in macronuclear division and cytokinesis (Morrison et al., 2005). Whereas macronuclear

divisions are frequently aberrant in TIF1 mutants, the observed defect in S phase progression and subsequent delay in macronuclear division and cytokinesis argue that macronuclear and cytoplasmic cell cycles are coordinately regulated. Tif1p binds essential cis-acting replication determinants in the rDNA origin, in vitro and in vivo (Saha and Kapler, 2000; Saha et al., 2001) and was recently shown to regulate rDNA origin activation, functioning in a repressive capacity to prevent precocious initiation during macronuclear S phase (Morrison et al., 2005). Because macronuclear S phase is prolonged in Tif1p-deficient strains, Tif1p might regulate initiation and/or the elongation of replication forks in other (non-rDNA) macronuclear chromosomes.

Here, we show that Tif1p is required to maintain genome integrity in the mitotic germline micronucleus. We demonstrate that wild-type *T. thermophila* elicits an intra-S phase DNA damage checkpoint response that has the hallmarks of the highly conserved ATR-dependent pathway. Furthermore, we show that the intra-S phase checkpoint pathway promotes chromosome homeostasis in both the diploid mitotic micronucleus and the polyploid amitotic macronucleus. Most significantly, we demonstrate that Tif1p is required to activate the intra-S phase checkpoint response in both nuclear compartments. These observations, in conjunction with the previously described role for Tif1p at the rDNA origin (Morrison et al., 2005), suggest that this protein contributes to chromosome homeostasis through its action at origins and at elongating replication forks.

**Material and methods**

Manipulation of *T. thermophila* strain

The relevant features of the micro- and macronucleus in wild-type and TIF1-deficient strains are listed in Table 2.1. Standard methods were used for strain propagation, mating, and selection or screening for drug-resistant markers [100 μg/ml paromomycin (pm), 12.5% (wt/vol) 2-deoxygalactose (2-dgal), or 15 μg/ml cycloheximide (cycl); Sigma-Aldrich, St. Louis, MO] (Orias and Bruns, 1976). The homozygous tif1-1::neo null strain (TXk202), macronuclear TIF1/tif1-1::neo knockdown mutant (TXh48), and heterozygous TIF1/tif1-1::neo germline disruption strains (TXh102 and TXh106) were generated previously by biolistic transformation with the tif1-1::btu1-neo (neomycin phosphotransferase) disruption cassette (Morrison et al., 2005). The latter three strains were serially propagated in increasing concentrations of pm to obtain phenotypic assortants with elevated levels of the tif1-1::neo disruption and diminished amounts of the wild-type gene in the transcribed polyploid macronucleus (wild-type macronuclear TIF1 DNA copy number relative to untransformed control: TXh48, ~ 25%;TXh102, ~20%; and TXh106, ~20%). The homozygous null strain TXk202 eventually senesced and repeated attempts to generate another homozygous null strain were unsuccessful. The macronuclear anlage cotransformant TAM101 is heterozygous for the tif1–2allele that contains 6xhis/5xmyc epitope tag on its carboxy terminus (Brown et al., 1999). Cotransformation of the developing macronucleus and screening for partial replacement of wild-type macronuclear TIF1 were performed as described previously (Morrison et al., 2005).

Table 2.1 *T. thermophila* strains used. chx1-1, cycloheximide-resistance; gal1-1, 2-deoxygalactose-resistance; tif1-1::neo, paromomycin resistance conferred by cadmium-inducible neomycin phosphotransferase transgene targeted to the TIF1 locus; and ts29, recessive temperature-sensitive allele at locus of unknown function.[a] TIF1gene disruption: the MTT1neoBTU1transgene was introduced into the macronuclear anlagen or premeiotic germline micronucleus (note the micronuclear genotype indicates whether the strain is a [germline] micronuclear and macronuclear anlagen transformant). Partial replacements contain wild-type TIF1 macronuclear gene dosages that are ~20–25% relative to wild type (macronucleus = 45 C). [b] Macronuclear anlagen cotransformants carrying his-myc epitope-tagged TIF1 and MTT1neoMTT1 at the respective TIF1 and MTT1 loci. [c] Heterokaryon strains.

| Strain | Micronuclear genotype | Macronuclear genotype/ phenotype |
|---|---|---|
| TXh102[a] | *TIF1/tif1-1::neo* | *TIF1* disruption (partial replacement) pm resistant |
| TXh106[a] | *TIF1/tif1-1::neo* | *TIF1* disruption (partial replacement) pm resistant |
| TXk202[a] | *tif1-1::neo/tif1-1::neo* | *TIF1* disruption (complete null) pm resistant |
| TXh48[a] | *TIF1/TIF1* | TIF1 disruption (partial replacement) pm resistant |
| TAM101[b] | *tif1-2/tif1-2* | C terminal his-myc *TIF1* Epitope tag (partial replacement) pm resistant |
| CU427[c] | *TIF1/TIF1* *CHX1/chx1-1* | pm sensitive Cycloheximide-sensitive |
| CU428[c] | *TIF1/TIF1* | pm sensitive |
| SB210[c] | *TIF1/TIF1* *gal1-1/gal1-1* | pm sensitive 2-deoxygalactose-sensitive |
| SB1969[c] | *TIF1/TIF1* *ts29/ts29* | pm sensitive Temperature resistant |

Micronuclear cytology in mating cells

For mating experiments, wild-type strains (CU427 and CU428) were distinguished from TIF1 knockout (TXk202), knockdown (TXh48), or A* strains by incorporation of MitoTracker dyes (Invitrogen, Carlsbad, CA). Starved vegetative cell cultures were incubated overnight with 0.1 μg of MitoTracker Green FM (wild type) or MitoTracker Red-CMXRos (mutants). Cells were subsequently mated at a concentration of 2 x $10^5$ cells/ml. One-milliliter aliquots were harvested at defined intervals, stained with 0.1 μg/ml 4',6'-diamidino-2-phenylindole (DAPI; Sigma-Aldrich), and examined by fluorescence microscopy (Morrison et al., 2005). The functionally amicronucleate A* strain served as a reference strain for aberrant development. This strain contains a DAPI-staining micronucleus that fails to transmit genetic information to progeny. Vegetative nuclei were also visualized in living cells withApoFluor (0.001% acridine orange and 5 μg/ml Hoechst 33342; Sigma-Aldrich).

Immunocytological studies were performed using antibodies directed against human Rad51p, 5'-bromo-2'-deoxyuridine (BrdU), or the myc-epitope tag in the Tif1-2p fusion protein. Fixed cells were incubated with antibodies before mounting onto slides (Morrisonet al., 2005) or mounted before antibody incubation (Loidl and Scherthan, 2004). For cell cycle studies, vegetative cultures were starved, refed, and harvested at 30-min intervals as described previously (Mohammad et al., 2003).

Molecular biology techniques

Standard molecular biology techniques, including genomic DNA isolation, polymerase chain reaction (PCR), and Northern blottingwere performed as described previously (Mohammad et al., 2000; Saha et al., 2001). Micronuclear genome instability was examined with PCR primers that span chromosome breakage sequence elements that demarcate the sites of chromosome fragmentation in the developing macronucleus (Hamilton et al., 2005; Yakisich and Kapler, 2006). Total cellular RNA was prepared using an RNAeasy mini-kit (QIAGEN, Valencia, CA) according to the manufacturer's recommendations, resolved on formaldehyde agarose gels, and hybridized to random primer radiolabeled RAD51 or TIF1 coding region probes (Morrison et al., 2005).

For Western blot analysis, protein samples were prepared by direct lysis in 1x Laemmli buffer ($5 \times 10^4$ cells), resolved on a 12% SDS-PAGE gel, and transferred to a polyvinylidene difluoride membrane (Millipore, Billerica, MA) according to the manufacturer'srecommendations. Blocked membranes were incubated overnight at 4°C with mouse anti-human Rad51p polyclonal antiserum (1:2500 dilution; NeoMarkers, Fremont, CA) or rabbit polyclonal antiserum directed against the myc epitope tag (1:2500 dilution;Delta Biolabs, Gilroy, CA) to monitor Tif1p. Membranes were washed and then incubated with secondary anti-mouse (1:3000) or anti-rabbit (1:5000) antibody coupled to horseradish peroxidase (Jackson ImmunoResearch Laboratories, West Grove, PA) for 3 h at 4°C. After washing twice with $H_2O$ and once with phosphate-buffered saline/0.05%Tween 20 (15 min each) and five times with $H_2O$ (5 min each), the membranes were developed using enhanced chemiluminiscence (Millipore). Human

Rad51p antibody detects a single DNA damage-inducible polypeptide of the size predicted for *T. thermophila* Rad51p (34 kDa; EMBL accession no.AF064516) (Campbell and Romero, 1998; Loidl and Scherthan, 2004).

DNA damage and S phase checkpoint analysis

For studies involving the DNA-damaging agent MMS, wild type (CU428) or TIF1 knockdown (TXh48) cultures were grown to a concentration of 1 x $10^5$ cells/ml. Cultures (30 ml) were treated with varying concentrations of MMS (Sigma-Aldrich). Cells were grown at 30°C for 1 h before a 30-min pulse labeling with 100 μg/ml BrdU. Samples (15 ml) were harvested and prepared for BrdU immunofluorescence analysis with mouse monoclonal anti-BrdU antibody (GE Healthcare, Little Chalfont, Buckinghamshire, United Kingdom), and rhodamine-conjugated goat anti-mouse antibody (Jackson ImmunoResearch Laboratories) (Morrison et al., 2005). Secondary antibody treatment and DAPI staining were performed as noted above. MMS time courses were also used to examine Tif1p and Rad51p localization and abundance.

The intra-S phase checkpoint was examined by treating cells with HU and/or caffeine (Sigma-Aldrich). HU inhibits ribonucleotidereductase and depletes dNTP stores in S phase, whereas caffeine inhibits the $G_1$ checkpoint kinase Ataxia Telangectasia Mutated(ATM) and intra-S phase checkpoint kinase ATR in all examined eukaryotes (for review, see Lambert and Carr, 2005). The effectof wortmannin (WM), which preferentially inhibits conventional (non-ATM/ATR) PI3-kinases, was also tested (Yakisich and Kapler, 2004). Stock solutions of HU and caffeine were prepared in water.

Wortmannin stocks were prepared in dimethyl sulfoxide. Mock treatments involved the addition of drug vehicle alone to culture media. HU dose–response curves were generated by measuring tritiated thymidine incorporation into trichloroacetic acid-insoluble material and by assessing cell cycle progression with flow cytometry to determine the $ID_{50}$ (Morrison et al., 2005).

Log phase cultures were subsequently grown for 12 h in HU-containing media to induce cell cycle S phase arrest (or HU + caffeine), washed twice with 10 mM Tris, pH 7.5, and then resuspended in drug-free media to measure culture outgrowth, viability of treated cells, and cell division during the first cell cycle after drug removal. Cell viability was determined by serially diluting cells into 100 μl of growth media in 96-well microtiter dishes immediately after drug treatment. The number of confluent wells (clonally derived lines) was recorded 4 d later in plates that contained <33% positive wells and related to the number of input cells in the relevant dilution. For cell division analysis, DAPI-stained cells were examined microscopically at defined intervals after drug treatment and removal. The input cells for the latter analysis were synchronized by starvation and refeeding before the addition of HU and/or caffeine (Mohammad et al., 2003). The cell division index corresponds to the percentage of cells exhibiting a cytokinetic furrow, as determined by light microscopy.

**Results**

Tif1p is required for the maintenance of a functional micronucleus

The previously described array of macronuclear aberrations associated with Tif1p-deficient *Tetrahymena* (Morrison et al., 2005) indicates that this protein plays a global role in macronuclear chromosome biology. Preliminary studies suggested that Tif1p functions in the diploid micronucleus as well, because the intensity of micronuclear DAPI staining was reduced in Tif1-1::neo mutant strains (Morrison et al., 2005). To investigate the contribution of Tif1p to micronuclear chromosome stability, we monitored the transmission of genetic markers from TIF1-deficient parents to progeny. First, we mated two heterozygous tif1-1::neo/TIF1 mutants to one another. Before mating, strains TXh102 and TXh106 were propagated in pm for >100 fissions to allow cells to reach sexual maturity and to select for phenotypic assortants with high levels of the tif1-1::neo disruption allele in the amitotic polyploid macronucleus. Mature cells were mated, and 48 clonal lines were established by plating cells at limiting dilutions 24 h after initiating the mating.

If the micronucleus of tif1-1::neo/TIF1 mutants is intact and low levels of Tif1p expression do not effect meiotic chromosome transmission, then one of four progeny should be homozygous wild type (12/48clones). However, because the pairing efficiency of this mating was ~80%, the predicted frequency of pm-sensitive progeny is 20% (9.6 clones). The 48 lines were expanded and tested for pm resistance and sexual immaturity. None of the clonal lines were pm sensitive (Table 2.2, cross 1), suggesting that

Table 2.2 Chromosome transmission in TIF1 heterozygote and heterokaryon strains. Resistance to 2-deoxygalactose, cycloheximide, or paromomycin is encoded in the micronucleus of SB210 (gal1-1), SB1969 (chk1-1), and TIF1:tif1-1::neo heterozygotes, respectively. For cross 1, n is the number of clonal progeny tested for pm resistance. For cross 2, n is the number of small-scale matings in which the nonclonal progeny pool was tested for pm resistance. [a] The predicted frequency for $pm^s$ progeny is 25%. However, because the pairing efficiency in this cross was ~80%, the expected frequency of $pm^s$ clones is ~20% (9.6 clones of 48 rather than 12 of 48).

| Cross | Strain | Phenotype | Expected % | Observed % |
|---|---|---|---|---|
| 1 | TXh102 × TXh106 | $pm^s$ clonal progeny | 20[a] | 0, n = 48 |
| | | Sexual immaturity | 100 | 0, n = 48 |
| 2a | TXh102 × SB210 | $2dgal^r/pm^r$ progeny | 50 | 0, n = 40 |
| 2b | TXh106 × SB210 | $2dgal^r/pm^r$ progeny | 50 | 0, n = 40 |

they failed to transmit the wild-type allele or had aborted development altogether and consequently retained their parental macronucleus. The second prediction was confirmed in a subsequent cross, in which a tester strain was immediately mated to the presumed F1 progeny (at ~20–30 fissions) to determine whether they were juveniles or sexually mature. True progeny require at least 70 fissions before they can form mating pairs (for review, see Karrer, 2000). All 48 clones formed mating pairs in this cross, indicating that they did not contain a new macronucleus. These results are consistent with the presence of a severely compromised micronucleus in heterozygous TIF1/tif1-1::neo mutants. An alternative possibility is that the observed macronuclear retention reflects a maternal requirement for Tif1p during new macronuclear anlage development. To distinguish between these possibilities, we directly mated TIF1/tif1-1::neo mutants to a wild-type tester strain. Because genetic exchange is reciprocal, half of the progeny that inherit the tif1-1::neo allele will undergo macronuclear development in a wild-type cytoplasm. Eighty clonal lines were established from two different heterozygous tif1-1::neo/TIF1 transformants (TXh102 and TXh106), and subsequently mated to the wild-type heterokaryon strain SB210, which contains a 2-deoxygalactose (2-dgal)–sensitive macronucleus and is homozygous for 2-dgal resistance in the transcriptionally silent micronucleus (1000 cells/mating). True progeny were selected en mass for 2-dgal resistance and then screened for pm resistance, conferred by the introduced tif1-1::neo disruption allele. Because many progeny were generated in each cross, all of the cultures should include pm-resistant progeny if micronuclear chromosomes from the tif1-1:neo/TIF1 parent were successfully transmitted. This was not the case, because all of

the 2-dgal–resistant progeny died in pm (Table 2.2, crosses 2a and 2b). This result, in conjunction with the aborted development observed in cross 1, argues that the TIF1/tif1-1-1::neo micronucleus underwent extensive genome instability during vegetative propagation.

**Aberrant meiosis in Tif1p-deficient cells**

As cells enter meiosis, the spherical micronucleus migrates away from the macronucleus and elongates into a crescent that encircles a significant portion of the macronucleus. TIF1 mutants generate a very small crescent micronucleus that stains weakly with DAPI relative to wild-type controls (Morrison et al., 2005). Although these observations and genetic studies (Table 2.2) suggest that micronuclear DNA is lost, examination of the meiotic program provides more definitive information on the fate of germline chromosomes. Consequently, we mated homozygous tif1-1::neo and heterozygous TIF1/ tif1-1::neo mutants with a wild-type strain and compared meiotic progression, mating pair synchrony and chromosome composition to a control mating involving two wild-type strains. Cells were examined by DAPI staining, before prophase I through anaphase II.

In contrast to a mating involving two wild-type strains (our unpublished data), the progression of tif1-1::neo/TIF1 mutants through meiosis frequently lagged behind the wild-type partner (Figure 2.1A, micrographs i–iii). In mating pairs in which the wild-type micronucleus revealed multiple, extended metaphase or anaphase chromosomes, the tif1-1::neo/TIF1 partner displayed one or two condensed micronuclear DNA masses (Figure

2.1A, micrographs i and ii, arrows). The scarcity of anaphase structures in Tif1p-deficient mating partners suggested that the residual chromosomes failed to segregate.

Asynchronous meiosis and the apparent loss or fusion of micronuclear chromosomes is a hallmark of micronuclei derived from the functionally amicronucleate star strains, which contain a cytologically visible, but genetically compromised micronucleus that fails to transmit genetic information to progeny (Allen, 1967). Both tif1-1::neo/TIF1 and A* strains exhibited this phenotype in crosses with wild-type tester strains (our unpublished data). In rare instances where a tif1-1::neo/TIF1 mutant micronucleus seemed to complete meiosis II, qualitative differences in the DAPI staining intensity of the four postmeiotic pronuclei were evident, suggesting that meiotic chromosome segregation was impaired (Figure 2.1A, micrograph iv, arrows). Whereas DAPI is not ideally suited for quantification, the often diminutive and highly variable size of micronuclei (crescents and pronuclei) and meiotic chromosomal masses supports the notion that micronuclear DNA content is diminished in the TIF1 mutant background. This prediction was subsequently borne out at the molecular level (see below).

Progressive micronuclear genome instability was evident in cytological studies of siblings derived from freshly established clone lines of the homozygous knockout strain TXk202. For example, when clonal line KO-C2 was mated with a wild-type partner (CU428), one mutant cell exhibited two large globular DNA masses during meiosis, whereas a sibling produced a single, more compact DNA mass (Figure 2.1B, micrographs i and ii).

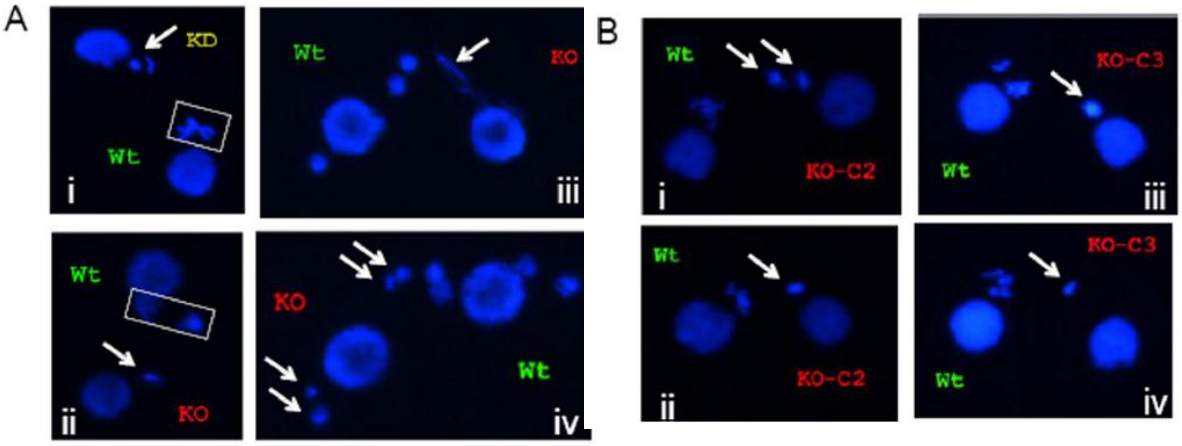


Figure 2.1 Cytogenetic evidence for micronuclear genome instability, developmental delay, and/or meiotic arrest in TIF1-deficient strains. The wild-type strain (CU428) was mated with TIF1mutants (TXh48 [KD, knockdown]; TXk202 [KO, knockout/null]), and mating pairs were examined at various times during development by DAPI fluorescent staining. Wild-type and mutant strains were prelabeled with MitoTracker Red and Green dyes, respectively, to identify each partner. (A) Meiotic aberrations in TIF1-deficient strains. Meiotic stages: i, wild type: metaphase, mutant: prophase (?); ii, wild type: anaphase, mutant: prophase (?); iii, wild type: postmeiotic pronuclei, mutant: meiotic crescent or aberrant anaphase (?); and iv, wild type and mutant: postmeiotic pronuclei. Arrows point to mutant nuclei. (B) Comparative cytogenetic analysis of siblings cells in subcloned parental lines KO-C2 and KO-C3 derived from the tif1-1::neo knockout strain TXh202. The newly generated clonal lines were briefly expanded and then mated with the wild-type strain CU428 to examine meiosis. Arrows point to condensed, micronuclear-derived DAPI-staining chromosomes in siblings within the same mating culture. Micrographs i and ii, representative tif1-1::neo/TIF1 knockout clone C2 siblings; micrographs iii and iv, representative tif1-1::neo knockout clone C3 siblings.

All siblings from the KO-C3 clone contained a single DAPI-staining micronuclear mass; however, the DAPI-staining intensity varied considerably (Figure 2.1B, micrographs iii and iv). Thus, the sterility of TIF1 mutants is reflected by an apparent diminution in DNA mass, chromosome number, and aberrant meiotic cell cycle progression. It should be noted that the homozygous null strain TXh202 eventually senesced, suggesting that the long-term absence of Tif1p affects macronuclear genic balance as well. Repeated attempts to generate new homozygous null strains failed with freshly generated heterozygous germline transformants, even when selective pressure for the disruption allele was removed immediately after identifying transformants (our unpublished data). We conclude that partial Tif1p depletion has a greater effect on the function of the diploid micronucleus relative to the polyploid macronucleus.

**Molecular analysis of micronuclear chromosomes reveals ongoing genome instability**

The genetic and cytological studies described above indicate that Tif1p is required for micronuclear chromosome transmission. To gain insight into the fate of chromosomes at the molecular level, we subjected 10 freshly generated subclones of strain Txh48 to PCR analysis with primer combinations that span sites for programmed DNA fragmentation of the five germline chromosomes in the developing macronucleus (Hamilton et al., 2005). These primer sets will only amplify products derived from intact micronuclear chromosomes.

All 10 examined subclones failed to amplify markers derived from the left (L) and right (R) arms of chromosomes 4 and 5 (Figure 2.2, early). The chromosome 2L marker was absent from all 10 clones as well; however, the 2R marker was retained, consistent with the formation of a double-strand break (DSB). These results suggest that chromosome arms and possibly entire chromosomes are missing. Heterogeneity was detected among the subclones for other markers (1L, 2R, and 3R), indicating that the stochastic loss of these markers occurred after the parental TXh48 strain was generated. When these lines were reexamined ~250 fissions later, additional markers were missing (Figure 2.2, late). These results indicate that the micronucleus of sterile Tif1p-deficient strains is hypodiploid and undergoes progressive and massive DNA loss during vegetative cell divisions.

**Elevated levels of DNA damage in MMS-treated TIF1 mutants**

The micronuclear and macronuclear chromosome transmission defects associated with a Tif1p deficiency suggest that both nuclei accumulate DNA damage at an elevated rate, even in the absence of exogenous genotoxic stress (Morrison et al., 2005; this work).To test this prediction, we first asked whether tif1-1 mutants were hypersensitive to the alkylating agent MMS, which mutagenizesDNA and promotes activation of the intra-S phase checkpoint response (Chang et al., 2002; Lupardus et al., 2002). BrdU incorporation was used to monitor the DNA damage response (Liu et al., 2003). Log

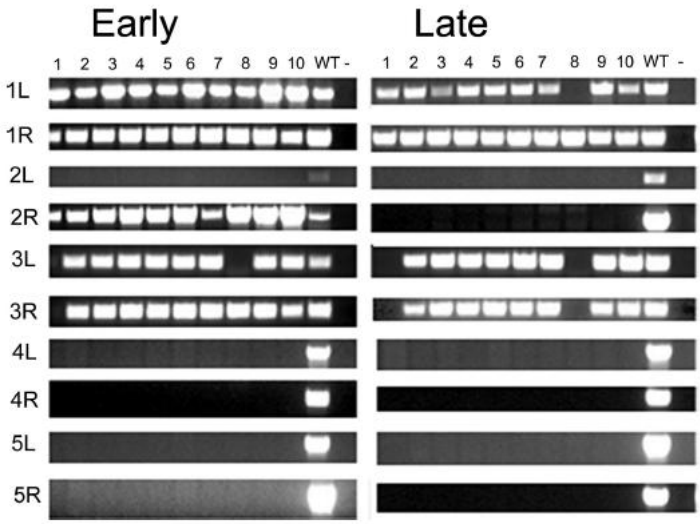


**F**igure 2.2 Micronuclear genome instability in TIF1-deficient *T. thermophila*. Ten clonal lines derived from the tif1-1::neo/TIF1 knockdown strain TXh48 were established and subjected to PCR analysis with primers sets that span sites for chromosome breakage sequence (CBS)-mediated chromosome fragmentation in the developing macronucleus. PCR primers derived from the right (R) and left (L) arms of all five micronuclear chromosomes were tested. 1–10, clonal TXh48 knockdown lines; WT, CU428. Early, ~150 fissions after conferring resistance to high concentrations of pm (encoded by thetif1-1::neo disruption); late, ~250 fissions later than "early".

phase wild-type and mutant cultures were exposed to various concentrations of MMS for 1 h, pulse labeled for 30 min with BrdU, and examined by indirect immunofluorescence. Due to the close physical association of micro- and macronuclei throughout most of the vegetative cell cycle, definitive information was not obtained for the micronucleus. Therefore, we focused our attention on the macronucleus.

Untreated wild-type and mutant strains exhibited a comparable percentage of BrdU-positive macronuclei in log phase cultures,indicating a similar cell cycle distribution in asynchronous populations (Table 2.3). MMS treatment inhibited BrdU incorporation in a dose-dependent manner in both genetic backgrounds; however, partial and complete inhibition occurred at lower MMS concentrations in the tif1-1::neo/TIF1 mutant background (Table 2.3). For example, Tif1p-deficient cells showed a marked decrease in BrdU-positive macronuclei in 0.06% MMS, whereas comparable inhibition occurred at a threefold higher concentration in the wild-type strain (0.18% MMS). This concentration abolished BrdU labeling in the mutant. These results raise several nonmutually exclusive possibilities. First, the elevated basal level of DNA damage in the TIF1 mutant lowers the threshold for exogenous damaging agents. Second, the TIF1 mutant fails to activate a checkpoint response, leading to the collapse of replication forks at DNA adducts. Third, the TIF1 mutant is defective in a repair or recombination pathway that removes or bypasses the lesion.

Table 2.3 MMS DNA damage response.

| | % BrdU-positive macronuclei | |
|---|---|---|
| % MMS (vol/vol) | Wild type | TIF1 mutant |
| 0 | 40 | 39 |
| 0.03 | 38 | 36 |
| 0.06 | 36 | 26 |
| 0.12 | 32 | 23 |
| 0.18 | 23 | 0 |
| 0.24 | 0 | 0 |

More than 300 cells were examined at each MMS concentration.

**Differential regulation of TIF1 and RAD51 in MMS-treated cells**

Intrinsic and MMS-induced DNA damage can lead to the formation of DSBs during S phase. ATR activates the double-strand break repair response by phosphorylating Rad52p, which acts in concert with replication protein A (RP-A) and the RecA homologue Rad51p to promote homology-mediated repair at DSBs or stalled replication fork (for review, see Lambert and Carr, 2005). Romero and colleagues previously showed that RAD51 gene expression is induced by MMS and UV light (Campbell and Romero, 1998; Smith et al., 2004a), and heterologous antibodies have been used to monitor *T. thermophila* Rad51p abundance and localization (Loidl and Scherthan, 2004).

To assess DNA damage in tif1-1 mutants and examine the integrity of the repair response, we first assayed the accumulation ofRAD51 mRNA and protein in MMS-treated cells. The basal levels of RAD51 mRNA were barely detectable by Northern blot analysis in untreated wild-type and mutant strains (Figure 2.3A). The steady-state RNA level increased in response to MMS in both backgrounds and was approximately twofold higher in the tif1-1 mutant (range 0.03–0.18% MMS). RAD51 mRNA levels dropped precipitously at high MMS concentrations (0.24% MMS and above) (Figure 2.3A); however, microscopic examination revealed that most cells had lost motility and were dying. Similar responses were observed at the protein level: Rad51p was induced by MMS and consistently higher in the mutant (Figure 2.3B, 1-h induction).

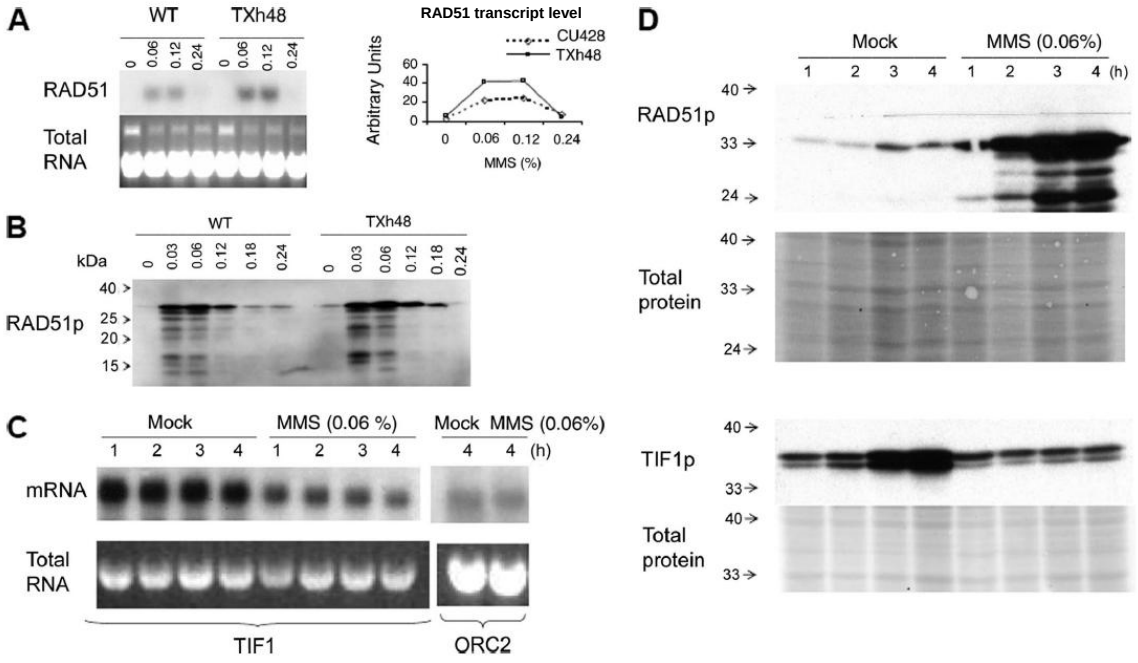


Figure 2.3 Regulation of RAD51 and TIF1 by MMS. (A) RAD51 Northern blot analysis after a 1-h exposure to MMS [0–0.24% (vol/vol)]. Top left, hybridization with a RAD51coding region probe. Bottom left, ethidium bromide staining of total RNA before transfer to GeneScreen Plus membranes (New England Biolabs, Beverly, MA). Right, graphic representation of RNA hybridization signals quantified on a PhosphorImager (Bio-Rad, Hercules, CA). Dotted line, wild type (CU428); solid line, TIF1 knockdown mutant (TXh48). (B) Western blot analysis of Rad51p in wild-type and mutant whole cell lysates (1-h MMS treatment). (C) Northern blot analysis of TIF1 mRNA in MMS-treated wild-type cells. Strain CU427, same MMS treatment regimen as in C. Probes, TIF1 and origin recognition complex, subunit 2 (ORC2) protein-coding regions. Bottom, ethidium bromide staining of RNA preparations for normalization. (D) Rad51p and Tif1p levels in mock and MMS-treated cells (0.06% MMS; 1–4 h). The Tif1p Western blot probe was directed against the myc epitope in the tif1-2–tagged strain TAM101. Membranes were stained with Ponceau S to compare the amount of total protein loaded in each lane.

Because 0.06% MMS induced the most robust RAD51 response, we examined TIF1 mRNA and protein levels across a 4-h interval at this MMS concentration. Northern blot analysis showed a rapid and substantial decline in TIF1 mRNA following the addition of MMS, whereas ORC2 mRNA levels were unaffected (Figure 2.3C). This decline may reflect the arrest of cell cycle progression,because TIF1 mRNA levels peak before the onset of macronuclear S phase, well before the peak for maximal TIF1 in vitro DNAbinding activity (Morrison et al., 2005).

To monitor Tif1p, we transformed *Tetrahymena* with a TIF1 derivative encoding a reiterated his-myc epitope tag on the carboxy terminus (tif1-2). The tagged allele was targeted to the endogenous TIF1 locus during macronuclear development (Cassidy-Hanleyet al., 1997), generating a partial gene replacement in which the transgene was under the control of its native promoter. Transformants expressing an unlinked marker were screened for epitope-tagged tif1-2 by PCR and by Western blotting (our unpublished data). Cotransformant strain TAM101 was analyzed further.

To best compare the TIF1 and RAD51 S phase responses, we synchronized wild-type and TIF1-tagged strains by growing cultures to stationary phase and briefly starving cells for 8 h before refeeding in the absence or presence of MMS (0.06%, 0- to 4-h time course). Western blot analysis showed modest and comparable increases in Rad51p and Tif1-2p protein levels over time in mock-treated cells, consistent with a single round of cell division and hence a doubling in cell number (Figure 2.3D, compare signal to mock controls). Whereas Rad51 protein levels increased significantly over this time interval in MMS-treated cells, Tif1-2 protein levels remained constant. A doublet was detected at

the expected molecular weight for tagged Tif1-2p, suggesting that this protein is subjected to posttranslational modification.

Indirect immunofluorescence was then used to examine the subcellular localization of Tif1p. Concurrent staining of the macronucleus and cytoplasm was observed in a subpopulation of wild-type cells; however, Tif1p was markedly diminished in the macronucleus in most cells (Figure 2.4B and C). To our surprise, the Tif1p immunofluorescence signal was significantly reduced in MMS-treated cells (Figure 2.4B, 0.06% MMS for 4 h). In contrast, Rad51p, which was not detected in untreated cells, produced a robust micro- and macronuclear immunofluorscence signal in MMS-treated cells (Figure 2.4A). Because Tif1p levels do not decline (Figure 2.3D), this result raises the possibility that the myc epitope tag might be partially masked after DNA damage.

Localization of Rad51p to the micronucleus was previously reported during meiosis (Loidl and Scherthan, 2004), whereas a separate study of vegetative cells reported Rad51p staining of just the macronucleus in MMS-treated cultures (Campbell and Romero, 1998). The discrepancy in vegetative micronuclear staining between our work and the previous study may reflect the more robust reactivity of heterologous antibodies that were used in our analysis. The cumulative RAD51 data suggest that MMS promotes the formation of DSBs in both nuclear compartments and indicate that the micro- and macronucleus elicit comparable responses.

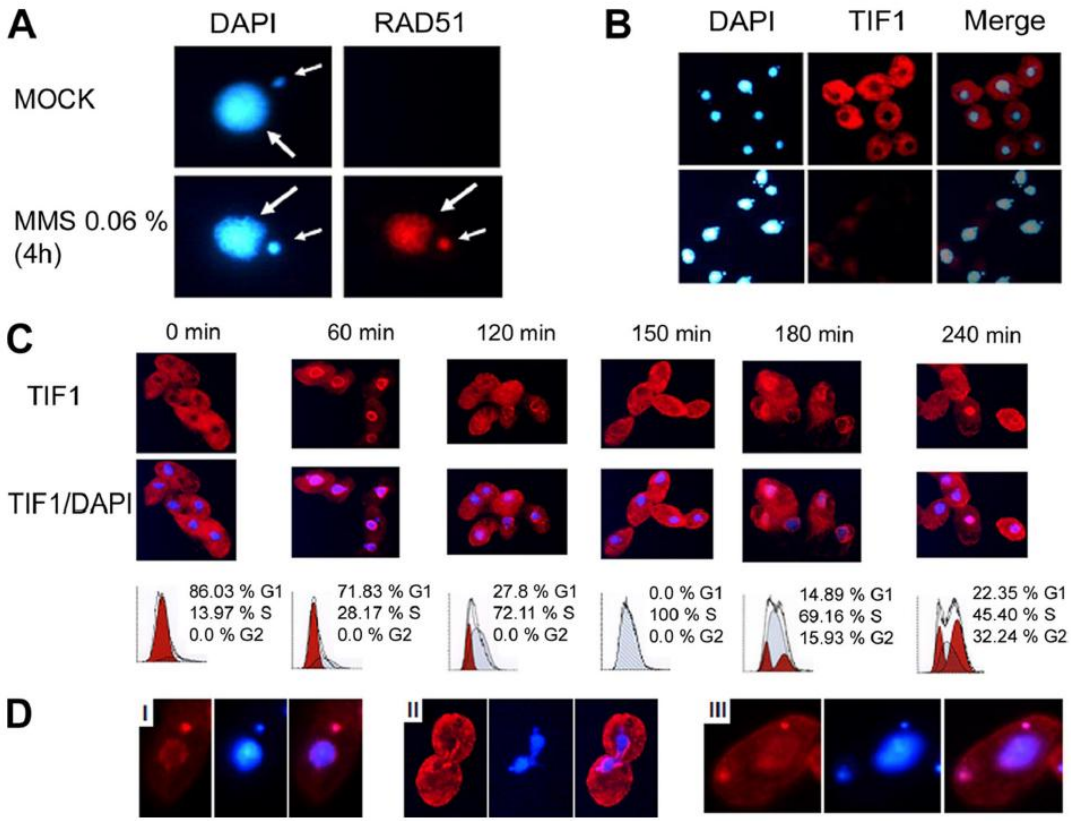


Figure 2.4 Immunolocalization of Rad51p and Tif1p in control and MMS-treated cells. (A) Rad51p immunolocalization in wild-type cells (0.06% MMS; 4 h). Red, Rad51p immunofluorescence; blue, DAPI. Small arrow, micronucleus, large arrow, macronucleus. (B) Immunolocalization of Tif1p in asynchronous control and MMS-treated cultures (strain TAM101; 0.06% MMS, 4 h). Red, Tif1p immunofluorescence; blue, DAPI. (C) Cell cycle localization of Tif1p. Strain TAM101 was synchronized by starvation and refeeding and assayed at 30-min intervals for TIF1p localization (red, TIF1p immunofluorescence; blue, DAPI) and DNA content (flow cytometry). Alternating time points are shown. (D) Immunolocalization of Tif1p late in the cell cycle (240 min). Note the micronuclear localization of Tif1p in micrographs i and iii and exclusion from dividing macronuclei in micrograph ii.

Cell cycle regulated localization of Tif1p

The heterogeneous pattern of Tif1p staining in asynchronous cultures raised the possibility that nuclear localization of this protein might be cell cycle regulated. To address this possibility, TAM101 cells were synchronized by starvation and refeeding, and then they were harvested at 30-min intervals for flow cytometry and immunofluorescence analysis (Figure 2.4C). Dynamic changes in micro- and macronuclear localization were observed across the cell cycle. Tif1p localized exclusively to the cytoplasm in starved cells. Before the onset of macronuclear S phase (Figure 2.4C, 60 min), a fraction of Tif1p associated with the macronucleus, forming intensely staining perinuclear foci. Diffuse, homogeneous macronuclear staining was observed during the peak interval for macronuclear DNA replication (Figure 2.4C, 120–180 min), and a return to punctate perinuclear staining was seen in a subpopulation at late S phase cells (Figure 2.4C, 180 min), suggesting that Tif1p relocalizes to the periphery in $G_2$. The mixed localization and heterogeneous flow cytometry profiles at 240 min are indicative of increased asynchrony.

Previous studies showed that micronuclear and macronuclear S phases are offset, with micronuclear DNA replication occurring later in the cell cycle (for review, see Karrer, 2000). Tif1p localized to the micronucleus at late time points in the cell cycle (i.e., 240 min), consistent with a role during micronuclear S phase. Cells that displayed intense micronuclear staining exhibited punctate perinuclear staining of the replicated but an undivided macronucleus (Figure 2.4D, micrograph i). Tif1p was present in both postmitotic micronuclei, indicating that this association persists through mitosis. In

contrast, macronuclear staining was generally lost before or during macronuclear division (Figure 2.4D, micrograph ii). The localization of Tif1p to S phase micro- and macronuclei suggests that its primary role occurs when chromosomes are actively replicating.

**Identification of a macronuclear intra-S phase checkpoint**

The elongated macronuclear S phase of TIF1 mutants could result from damage-induced activation of an intra-S phase checkpoint. However, the elevated rate of aberrant macronuclear division suggests that this checkpoint can be overridden in Tif1p-deficient *Tetrahymena* (Morrison et al., 2005). A bioinformatics search of the *T. thermophila* genome database (http://tgd.org) identified putative orthologues of the three intra-S phase checkpoint kinases: ATR, CHK1, and CHK2, but it failed to yield a candidate orthologue for the $G_1$ checkpoint kinase ATM. The e values for the predicted *Tetrahymena* proteins relative to humans were very high: ATR, $2.0^{-40}$; CHK1, $2.0^{-29}$; and CHK2, $2.0^{-61}$. Consequently, we asked whether wild-type and Tif1p-deficient *Tetrahymena* elicit a classical intra-S phase checkpoint response. To do so, we used the ribonucleotide reductase inhibitor HU, which induces S phase arrest and activates the intra-S phase checkpoint in all reported eukaryotes. We then tested the effect of caffeine, a potent inhibitor of the phosphatidylinositol kinase-related protein kinases ATM and ATR, on HU-arrested *Tetrahymena* (for review, see Abraham, 2001).

HU dose–response curves were generated by using tritiated thymidine and flow cytometry to monitor DNA synthesis and cell cycle progression. Pulse labeling with

thymidine revealed no substantive difference in the rate of DNA synthesis in wild-type and Tif1p-deficient strains. HU inhibited thymidine incorporation in a concentration-dependent manner, with the majority of cells arresting with a $G_1$ DNA content (tested HU concentrations 0.1–20 mM, $ID_{50}$ = 10 mM; flow cytometry). The recovery from HU arrest was subsequently assessed in cultures treated with increasing concentrations of HU and then reseeded at a fixed cell density in drug-free media. No lag in the outgrowth of wild-type cells was observed at all tested HU concentrations, indicating that HU-induced cell cycle arrest is reversible (Figure 2.5A).

Caffeine was added to the HU regimen to determine whether S phase arrest can be reversed by inhibition of an ATR-like protein kinase. Caffeine alone (0.3 or 1 mM) was not toxic and did not induce cell cycle arrest or aberrant macronuclear division (Figure 2.5A and B, wild type, 0.3 mM caffeine; 1 mM caffeine). The addition of caffeine to wild-type cells partially reversed HU inhibition (Figure 2.5B) and caused a modest lag in outgrowth of the culture upon removal of both drugs (Figure 2.5B). To assess whether this lag corresponds to a recovery period for the resumption of replication or reflects a decrease in cell viability, HU + caffeine-treated cells were plated into 96-well dishes at limiting dilutions, and the outgrowth of clonal lines was quantified relative to mock and single drug regimens. The exposure to caffeine + HU did not decrease cell viability (Figure 2.5C, wild type). However, this regimen greatly perturbed DNA partitioning during macronuclear division (Figure 2.5D).

Grossly abnormal macronuclear divisions were observed in dividing wild-type cells examined 7 h after removal of HU and caffeine (Figure 2.5D, penetrance ~40%).

Figure 2.5 Response of wild-type and tif1-1::neo mutants to HU and caffeine. (A) Wild-type (CU428) and tif1-1::neo/TIF1 mutant (TXh48) strains were grown to a density of 3x $10^4$/ml and incubated for 12 h in growth media containing a range of HU concentrations (0–20 mM, +HU; stock solution in water) to induce S phase–specific cell cycle arrest. Outgrowth of cultures after removal of the drug (–HU), refed cells were adjusted to a density of 1 x $10^5$/ml and counted at 3-h intervals. The mean and SEs for three experiments are shown. (B) Outgrowth of cultures treated for 12 h with 20 mM HU and/or 0.3 mM caffeine (stock solution in water) and released into drug-free media. Cell densities were adjusted to 1 x $10^5$/ml after washing out the drug(s), and the cultures were counted at 3-h intervals. The mean and SE for two experiments are shown. (C) Cell viability analysis in cultures treated with HU and/or caffeine. Wild-type and TIF1-deficient strains were incubated for 12 h in media containing no drug, 0.3 mM caffeine, 20 mM HU, or both. Cells were washed repeatedly to remove the drugs and plated out at decreasing concentrations into two 96-well dishes/dilution. For comparative analysis, the percentage of wells that was positive for growth in mock-treated cultures (plating density 0.3 cells/well) was normalized to 20 for each of the three experiments. The representative data for drug-treated strains were similarly normalized and correspond to the mean and SE of the three experiments. (D) Examples of macronuclear division defects in wild-type cells treated for 12 h with 20 mM HU and 0.3 mM caffeine and then propagated for 7 h in drug-free media.

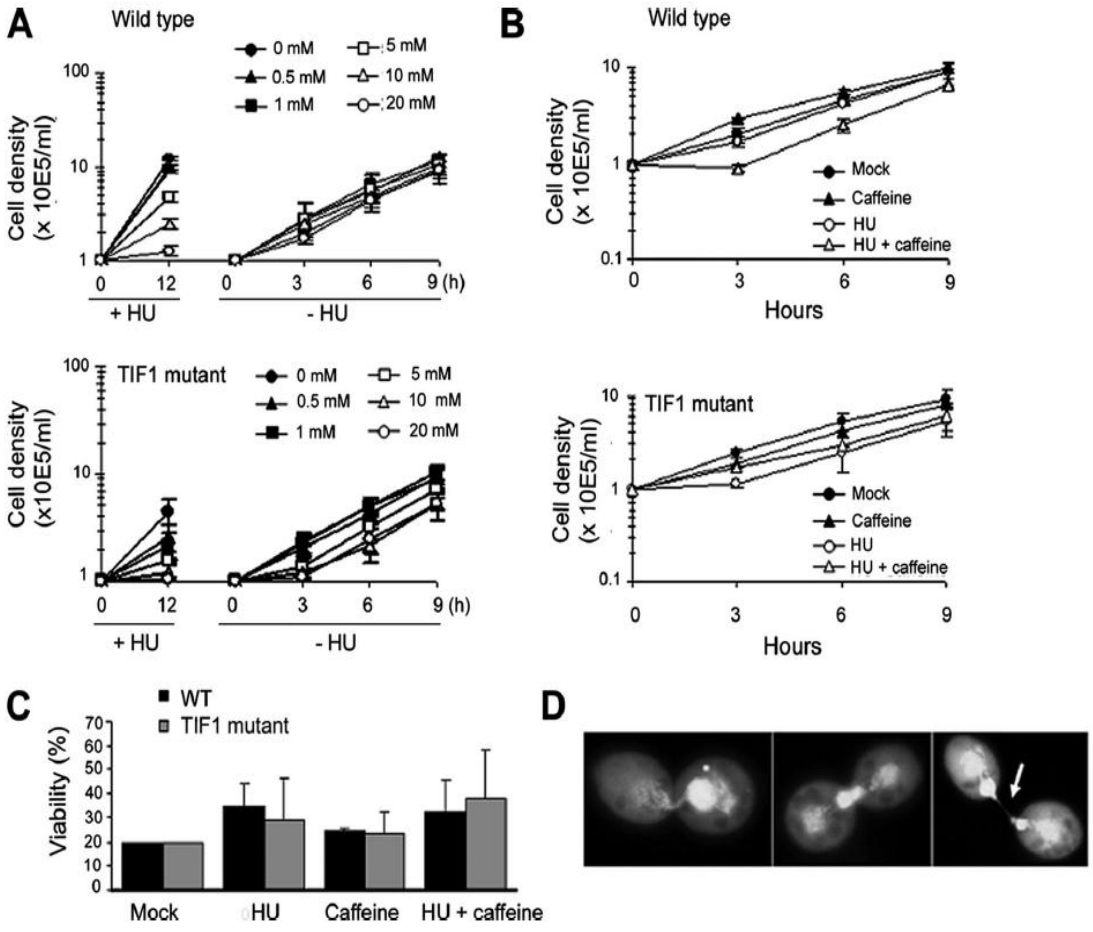
A
Wild type
0 mM
0.5 mM
1 mM
5 mM
10 mM
20 mM
Cell density (x 10E5/ml)
100
10
1
0
12
0
3
6
9 (h)
+ HU
- HU
TIF1 mutant
Cell density (x10E5/ml)
B
Wild type
Cell density (x 10E5/ml)
10
1
0.1
Mock
Caffeine
HU
HU + caffeine
0
3
6
9
Hours
TIF1 mutant
C
WT
TIF1 mutant
Viability (%)
70
60
50
40
30
20
10
0
Mock
HU
Caffeine
HU + caffeine
D

The most frequently observed phenotype consisted of dividing cells that had two properly partitioned daughter macronuclei and contained an additional large bolus of DNA at the cleavage furrow (Figure 2.5D, middle and right micrographs; note the wisp of DNA connecting the two daughter cells in the micrograph in the right micrograph [arrow]). The small fraction of wild-type cells that failed to arrest in HU exhibited similarly severe macronuclear division defects (our unpublished data). Amacronucleate cells were occasionally observed, along with dividing cells with large differences in macronuclear DAPI staining (Figure 2.5D, left micrograph). The severity of these phenotypes lessened at later times during the recovery, and normal macronuclear division was restored by 36 h (our unpublished data).

To further investigate the effect of caffeine on the intra-S phase checkpoint response, we synchronized wild-type cells by starvation and refeeding and examined cytokinesis and nuclear division during the first cell cycle in the presence of HU or HU + caffeine. As expected, the majority of the synchronized wild-type cells arrested cell division in HU-supplemented media (Figure 2.6A, WT, open triangles). Rare escapees divided >1.5 h later than untreated controls. Furthermore, the addition of caffeine after the onset of S phase (150 min postrefeeding) suppressed cell cycle arrest in a significant fraction of HU-treated cells (Figure 2.6A, wild type, closed squares) and accelerated the timing of cytokinesis relative to HU treatment alone. Whereas the appearance of dividing cells during the 150- to 300-min interval after refeeding was reduced to 14% in cultures treated with HU alone, the addition of caffeine largely reversed the HU inhibition (HU + caffeine: 60%).

Caffeine-induced suppression of HU cell cycle arrest was similarly observed when both drugs were added at the time of refeeding, with HU + caffeine-treated cells divided later than mocked-treated and earlier that cells treated with HU alone. The cumulative data indicate that macronuclear S phase progression is mediated by a caffeine-sensitive factor, a hallmark of ATR. Abrogation of the intra-S phase checkpoint allows macronuclear division and cytokinesis to occur in the absence of completereplication of macronuclear chromosomes.

**The caffeine sensitive intra-S phase checkpoint is active in the mitotic micronucleus**

Previous studies revealed that the mitotic micronucleus is dispensable to vegetative *Tetrahymena* (for review, see Karrer, 2000). However, the micronucleus contains all of the nuclear genes that are transmitted during conjugation. Because amicronucleate strains fail to undergo cell cycle arrest, it was unclear whether the intra-S phase checkpoint pathway described above regulates micronuclear genome stability. To best address this question, we examined micro- and macronuclear division during the first cell cycle of synchronized cultures in the presence of HU + caffeine. Microscopic examination of dividing cells (Figure 2.6B) revealed defects in micronuclear division. The micronucleus normally divides and is partitioned to daughters before the onset of macronuclear division (Figure 2.6B, left panels and accompanying schematic). In contrast, micronuclear division was delayed in cells treated with HU + caffeine and frequently occurred concurrently with macronuclear division and cytokinesis (Figure 2.6B, right panel,bottom three micrographs). In these instances, segregating daughter

micro- and macronuclei were typically connected by an extended segment of DAPI-staining material (Figure 2.6B, bottom micrograph). These results indicate that an ATR-like factor regulates the micronuclear cell cycle. Inhibition of this pathway eliminates the temporal regulation of micronuclear division and cytokinesis.

**Tif1-1:neo mutants fail to activate the intra-S phase checkpoint response**

The previously documented defect in macronuclear S phase progression, "cut" macronuclear division phenotype (Morrison et al., 2005), and hypersensitivity of tif1-1::neo/TIF1 mutants to MMS (Table 2.2) are consistent with a role for Tif1p in the S phase DNA damage checkpoint response, similar to the caffeine-sensitive ATR-like target. To explore this possibility, we examined the response of tif1-1::neo mutants to HU and caffeine. tif1-1::neo mutants were slightly more sensitive to HU than wild type, and they displayed a modest, but reproducible dose-dependent lag in outgrowth after removal of the drug (Figure 2.5A). Although HU treatment alone slowed the outgrowth of tif1-1::neo mutants, this lag period was not extended when the presumed ATR response was blocked with caffeine (Figure 2.5B). By comparison, HU + caffeine generated a lag in outgrowth and slower doubling time in wild-type cells.Furthermore, macronuclear division defects were not exaggerated in HU + caffeine-treated tif1-1::neo mutants. Although the incidence of aberrant macronuclear division was ~40% in HU + caffeine-treated wild-type cells, the severity of the cell division defect did not increase in frequency (~20%) or magnitude in HU + caffeine-treated tif1-1::neo/TIF1 mutants relative to mock controls (our unpublished data).

Similar to HU + caffeine-treated wild-type cells, examination of synchronized tif1-1::neo/TIF1 cultures revealed simultaneous defects in micro- and macronuclear division, even in the absence of HU (Figure 2.6F). Because the ATR-dependent RAD51 responseis muted in TIF1 mutants (Figure 2.6D) and Rad51p is targeted to both the micro- and macronucleus after genotoxic stress (Figure 2.4B), this result suggests that Tif1p is a component of the micronuclear S phase checkpoint. Finally, similar to wild-type cells, tif1-1::neo mutant cell viability was not decreased after HU and/or caffeine exposure (Figure 2.5C), supporting the contention that the polyploid macronucleus is largely buffered from the effects of genotoxic stress.

The most compelling evidence for the involvement of Tif1p in the S phase checkpoint response came from the analysis of cultures that were synchronized by starvation and then released into media containing HU, caffeine or HU + caffeine. As reported previously (Morrison et al., 2005), cytokinesis is delayed in tif1-1::neo mutants relative to wild-type controls (Figure 2.6A, filled diamonds). In contrast to wild-type cells, a significant fraction of TIF1p-deficient cells continued to divide in the presence of 20 mM HU (Figure 2.6A, open triangles). These cells divided earlier than the rare wild-type cells that escape the HU block. Caffeine treatment alone had no effect on the incidence or timing of cell division in wild-type or mutant strains. Furthermore, the addition of caffeine at the beginning of S phase (Figure 2.6A; T = 150 min, filled squares) or immediately upon refeeding of the mutant did not generate an increase in the percentage of dividing HU-treated cells. The failure to arrest in HU or exhibit and more

pronounced defect in HU + caffeine argues that Tif1p is required to activate the intra-S phase checkpoint response.

The final marker that we examined for S phase checkpoint activation was Rad51p, which participates in recombination-mediated repair at stalled forks or replication-induced DSBs (for review, see Lambert and Carr, 2005). As noted, the basal levels of RAD51mRNA and protein are elevated in tif1-1::neo mutants (Figure 2.3 A and B). To examine the contribution of Tif1p and the ATR-like checkpoint to the Rad51p response, synchronized cells were released into media containing HU and/or caffeine. HU-treated wild-type cells exhibited a dramatic increase in Rad51 protein levels (Figure 2.6C). The majority of this response was eliminated by the addition of caffeine, consistent with inactivation of the checkpoint target. In contrast, HU generated a very modest increase in the Rad51p level in the tif1-1::neo mutant. Caffeine had minimal effect on the Rad51p level, indicating a central role for Tif1p in the DNA damage checkpoint response. The absence of homology between TIF1p and ATR orthologues argues that TIF1p is not the caffeine-sensitive target. In support of this contention, caffeine did not alter Tif1 protein levels or the relative abundance of the two Tif1 protein isoforms (Figure 2.6D).

To verify that caffeine was not targeting a previously documented wortmannin-sensitive non-ATM/ATR PI3-kinases (Smith et al.,2004b; Yakisich and Kapler, 2004),

Figure 2.6 Identification of an intra-S phase checkpoint defect in Tif1p-deficient *T. thermophila*. (A) Wild-type (CU428) and tif1-1::neo/ TIF1 mutant (TXh48) strains were grown to saturation, starved, and then released into drug-free media (filled diamonds) or media containing 20 mM HU (open triangles and filled squares). Caffeine (1 mM) was added before the onset of macronuclear S phase (T = 150 min) (filled squares), and cell division was monitored by light microscopy. The cell division index corresponds to the percentage of cells with a cytokinetic furrow. (B) DAPI analysis of micro- and macronuclear division in mock and HU + caffeine-treated wild-type cells (same treatment as in A). (C) Rad51p Western blot analysis in synchronous wild-type and TIF1 mutant cultures, 5 h after refeeding with media containing HU, caffeine, or both. (D) Tif1p Western blot analysis of untreated and caffeine-treated wild-type strain (CU428; 1 mM caffeine for 4 h). (E) Rad51p Western blot analysis in synchronous wild-type cultures, 5 h after refeeding with media containing WM, HU, or both. (F) DAPI analysis documenting aberrant micro- and macronuclear division in tif1-1::neo mutant cells (TXh48) grown in normal culture media (no HU added). Arrow: cytokinetic furrow.

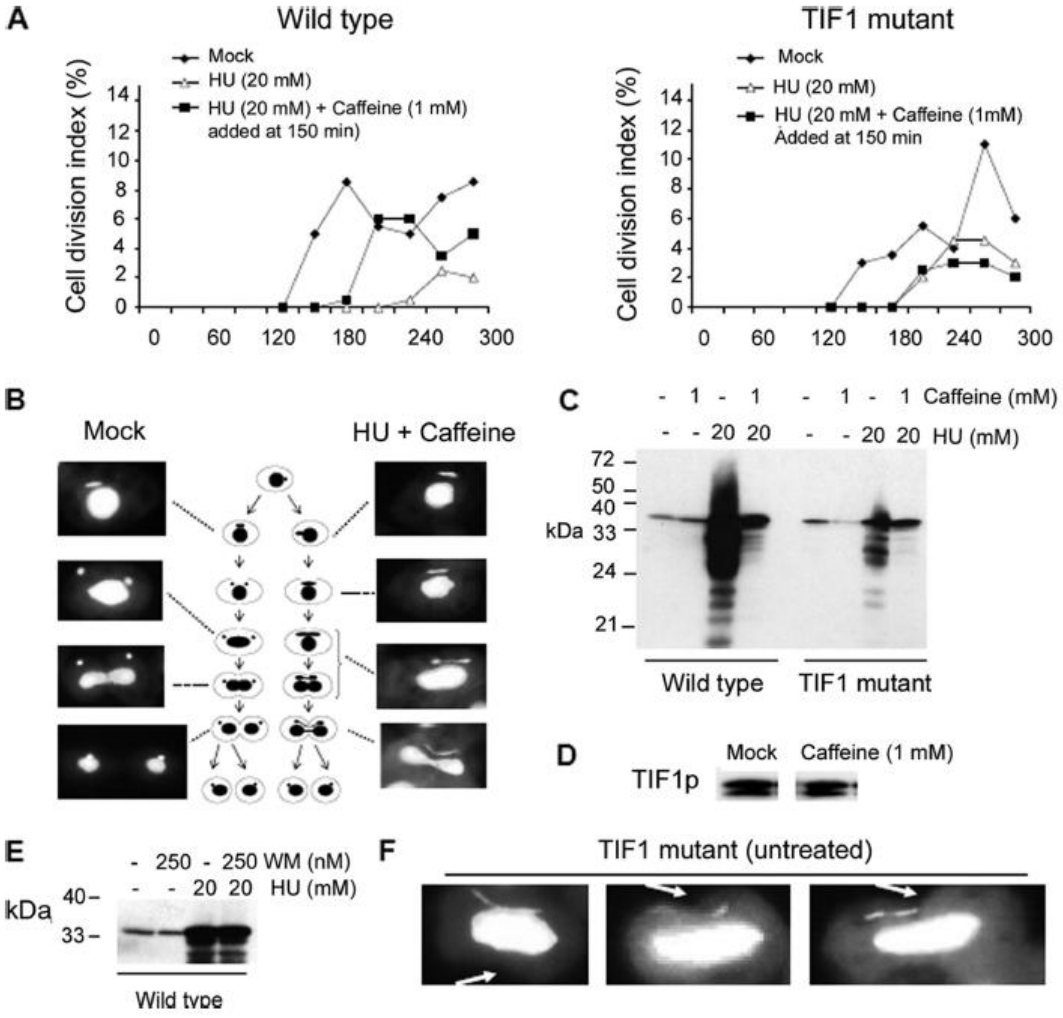
A
Wild type
TIF1 mutant
Mock
HU (20 mM)
HU (20 mM) + Caffeine (1 mM) added at 150 min)
HU (20 mM + Caffeine (1mM) Added at 150 min
Cell division index (%)
B
Mock
HU + Caffeine
C
Caffeine (mM)
HU (mM)
kDa
Wild type
TIF1 mutant
D
TIF1p
Mock
Caffeine (1 mM)
E
WM (nM)
HU (mM)
F
TIF1 mutant (untreated)

we tested whether WM could suppress HU-induced activation of the intra-S phase checkpoint response by monitoring the production of Rad51p in wild-type cells treated with HU, WM, or both, under the same conditions used for Figure 2.6C. WM at 250 nM failed to repress the induction of Rad51p (Figure 2.6E). This concentration exacerbates nuclear division defects in cells expressing paclitaxel-hypersensitive β-tubulin allele btu1-1 (Smith et al., 2004b), and it inhibits programmed nuclear death during *Tetrahymena* development (Yakisich and Kapler, 2004). Conversely, 1 mM caffeine did not block acidification of the old parental macronucleus in mating progeny, as is observed in WM-treated cells (our unpublished data). We conclude that the caffeine-sensitive intra-S phase checkpoint is activated by an ATR-like protein kinase. Consistent with this model, we have identified a strong candidate ATR orthologue in the *T. thermophila* genome database as well as other conserved components of this checkpoint pathway.

**Discussion**

DNA damage checkpoints facilitate the repair of potentially catastrophic lesions before DNA replication. ATR is an S phase–specific sensor/transducer kinase that activates downstream targets that stabilize stalled replication forks and inhibit initiation from late firing origins (for review, see Abraham, 2001). Although this pathway is conserved from yeast to human, it is unclear whether the demands on this pathway are diminished in polyploid organisms or tissues. Members of the ancient eukaryotic branch, the Ciliophora, are unusual in that they contain two nuclei within a single cytoplasm, the diploid micronucleus and polyploid macronucleus. In this study we provide evidence that a common S phase checkpoint pathway functions in both types of nuclei. One component of the *T. thermophila* checkpoint seems to be functionally analogous to mammalian ATR, because its ability to induce S phase arrest is inhibited by caffeine. The second component, Tif1p,has no obvious homologue in yeast and higher eukaryotes; however, we have identified a candidate orthologue in a distantly related ciliate, Paramecium tetraurelia (e value $6^{-13}$, 27% sequence identity, 56% sequence similarity; Kapler and Sperling, unpublisheddata). Sequence conservation outside of ciliates is limited principally to the carboxy terminus of Tif1p, which resembles the oligomerization domain of whirly transcription factors in plants, that like Tif1p, assemble into homotetramers and bind single-strand DNA in a sequence-specific manner (Desveaux et al., 2000, 2002). It is plausible that Tif1p functions in the intra-S phase checkpoint pathway are broadly conserved.

Tif1p and the cell cycle

TIf1p undergoes dynamic relocalization during normal cell cycles (Figure 2.4C and D). It is exclusively in the cytoplasm of $G_1$ phase cells. Intense localization to the macronuclear periphery occurs before and during early macronuclear S phase. This distribution suggests that Tif1p may initially be targeted to rDNA-containing nucleoli. Tif1p is found throughout the macronucleus later in S phase, and it relocalizes to the periphery or is excluded from the macronucleus before cytokinesis. Tif1p is similarly targeted to the micronucleus during S phase, and it is transiently retained in postmitotic micronuclei. It is unclear how Tif1p is differentially localized to distinct nuclei that inhabit the same cytoplasm. By analogy, the subcellular localization of the TIF4 Orc2p cross-reactive subunit Tt-p69 is similarly regulated (Mohammad et al., 2003). We speculate that these proteins are imported into micro- and macronuclei by nucleus-specific "licensing factors." Whatever the mechanism, we show that Tif1p is most prominently associated with replicating nuclei, suggesting that its primary role occurs during S phase.

One well-defined role for Tif1p is to regulate the timing of rDNA replication initiation (Morrison et al., 2005). Several lines of investigation illustrate a more global role for Tif1p in the macronucleus, because it is required for normal macronuclear S phase progression, the coordinate regulation of macronuclear division and cytokinesis (Morrison et al., 2005), and functions in the checkpoint response to intrinsic or extrinsic inhibitors of DNA replication (this work). tif1-1::neo mutants contain elevated basal levels of Rad51p (Figure 2.3) and are hypersensitive to external sources of genotoxic

stress (Table 2.3 and Figures 2.5 and 2.6), arguing that tif1-1::neo mutants accumulate DNA damage in unperturbed cell cycles. Moreover, because MMS and HU destabilize elongating replication forks and Tif1p localizes to the micro- and macronucleus during S phase, we speculate that the role of Tif1p in checkpoint activation occurs at the replication fork. By analogy, yeast and metazoan checkpoint sensor and effector proteins, such as Xenopus laevis ATM and ATR (Shechter et al., 2004), and *S. cerevisiae* Mrc1 (Szyjka et al., 2005), are targeted to elongating replication forks during unperturbed cycling cells.

Macronuclear genome stability is influenced by many factors, some of which efficiently compensate for the aberrant amitotic divisions associated with the loss of TIF1 or natural fluctuations in chromosome transmission. However, the conventional mitotic micronucleus lacks these compensatory mechanisms and is more dependent on Tif1p. Nine of 10 chromosomal markers were absent from the micronucleus in unselected TIF1/tif1-1::neo mutant cell populations (Figure 2.2). Although the micronuclear chromosome loss leads to germline sterility, TIF1/tif1-1::neo mutants fail to undergo cell cycle arrest. One possible reason is that Tif1p is required to activate the intra-S phase checkpoint (Figure 2.6).

Induction of the intra-S phase checkpoint by genotoxic stress

Our studies indicate that wild-type *Tetrahymena* elicits a classic intra-S phase checkpoint response. Cell cycle arrest is induced by HU and suppressed by further addition of caffeine, a known inhibitor of ATM and ATR kinases (Figure 2.6A; see

model in Figure 2.7). Cells that escape HU arrest undergo aberrant micro- and macronuclear division (Figures 2.5D and 2.6B), indicating that both nuclei are regulated by the caffeine-sensitive factor. Tif1p functions in S phase checkpoint activation as well. tif1-1::neo mutants are hypersensitive to MMS and HU (Table 2.3 and Figure 2.5A) and fail to arrest in the presence of HU (Figure 2.6A). Aberrant macronuclear division occurs frequently, producing a cut phenotype, in which the macronucleus is bisected by the cleavage furrow (Morrison et al., 2005). Aberrant micronuclear division is also observed in the absence of exogenous genotoxic stress (Figure 2.6F). Micronuclear genome instability is rampant as no chromosome is spared (Figure 2.2).

Several lines of evidence argue that Tif1p and the presumed ATR kinase function in the same epistatic pathway (Figure 2.7). First, HU blocks cell cycle progression in wild-type cells, but it fails to induce cell cycle arrest in a significant fraction of tif1-1::neo mutant cells. Caffeine suppresses HU-induced cell cycle arrest in wild cells, but it fails to do so in the mutant, suggesting a role for TIF1 in the ATR response (Figures 2.6A and 2.7, bottom schematic). Second, HU-treated tif1-1::neo cells and HU + caffeine-treated wild-type cells divide with similar kinetics (Figure 2.6A). Cell division is associated with aberrant micro- and macronuclear division in both situations (Figure 2.6B and F). Third, the induced expression of RAD51, a marker for checkpoint activation, is largely suppressed intif1-1::neo mutants (Figure 2.6C). HU-treatment leads to a substantive increase in RAD51 mRNA and protein in wild-type cells, the majority of which is suppressed by caffeine (Figure 2.7). In contrast, TIF1 mutants exhibit a very modest increase in Rad51 protein, and this induction is refractory to the addition

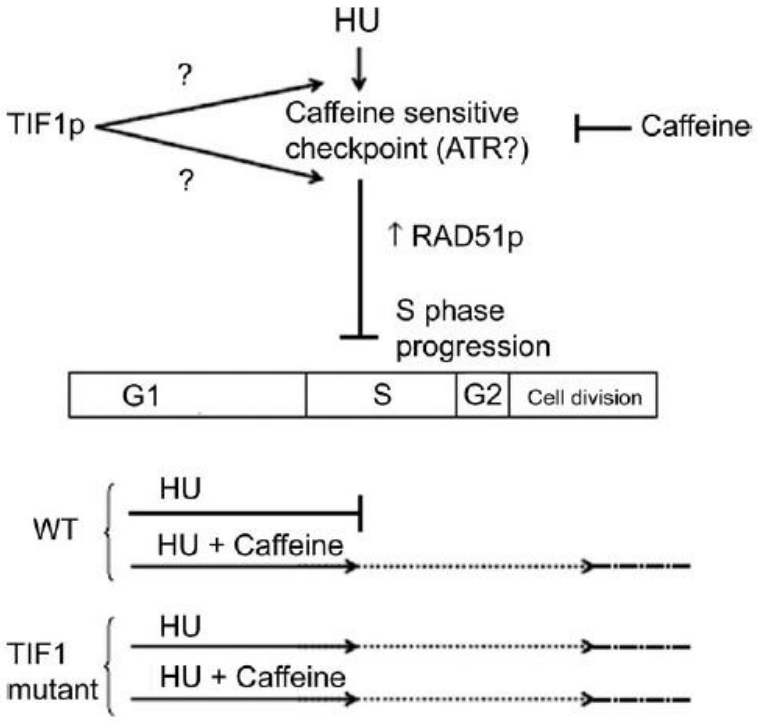


Figure 2.7 Proposed models for the epistatic relationship between TIF1p and caffeine-sensitive intra-S phase checkpoint protein.

of caffeine.

Rad51p interacts with the ATR substrate Rad52p in a recombination pathway that repairs DSBs and lesions ahead of stalled replication forks (for review, see Lambert and Carr, 2005). Although Rad51p has not been commonly used to assess checkpoint activation, we show that the up-regulation of RAD51 mRNA and protein is induced by HU and suppressed by further addition of caffeine. Consequently, robust expression of RAD51 is part of the *Tetrahymena* intra-S phase checkpoint response. RAD51 induction served as a reliable marker that illustrated the contribution of TIF1 to checkpoint activation.

It remains to be determined whether Tif1p acts upstream or downstream of ATR in the intra-S phase checkpoint pathway (Figure 2.7). Bioinformatic analyses suggest the presence of ATR, CHK1, and CHK2 orthologues in the *T. thermophila* genome. We predict that Tif1p is not a direct substrate of ATR, because it lacks the clustered SQ/TQ motifs present in most ATM/ATR substrates (Traven and Heierhorst, 2005). Consistent with this prediction, caffeine does not alter the abundance or stoichiometry of Tif1p isoforms (Figure 2.6E). Because Tif1p does not display homology to other downstream mediator or adapter proteins, we propose that it serves a novel role in the intra-S phase checkpoint response. The propensity of Tif1p for single-stranded DNA raises the possibility that it might act in concert with persistent chromatin-bound replication protein A to recruit ATR to sites of DNA damage (Figure 2.7) (Zou and Elledge, 2003). Furthermore, because Tif1p represses early initiationfrom the rDNA origin during

normal cell cycles (Morrison et al., 2005), this repressive function might be extended to other origins during normal cell cycles and/or in response to genotoxic stress.

## Chapter II Addendum

The work described in Chapter II, was published in *Molecular Biology of the Cell* (Vol. 17, 5185–5197, December 2006) and I was a co-first author. Here I summarize my specific contribution to the published work and their significance.

In the work described in Chapter II, I generated the strain TAM101 that expresses an epitope-tagged TIF1 allele containing a 6xHis-5xMyc at the carboxy terminus (Tif1p-HM-C) to study the cell cycle-regulated localization of Tif1p. The intracellular localization of Tif1p was dynamic throughout the cell cycle with a strong perinuclear staining immediately prior to S phase. This perinuclear staining was present in macro nuclei in cultures synchronized at the $G_1$/S border (71% in G1 and 28% in S phase). Since rDNA is mostly encapsulated in nucleoli, which are evenly distributes around the macronucleus throughout the cell cycle, we speculated that this staining correlates with the binding of TIF1p to type I elements at the rDNA origin. The timing of this binding is consistent with the idea that Tif1p acts as an inhibitor of rDNA replication during early S phase. In general, Tif1p localizes to the cytoplasm during $G_1$, followed by a peripherical staining of the macronucleus and later relocalization throughout the macronucleus during S phase. Tif1p localization to the macronucleus is lost before cytokinesis, arguing that the main role for this protein occurs before and during S phase. Micronuclear localization of Tif1p was also observed prior and

throughout micronuclear S phase, suggesting that Tif1p is involved in DNA replication in the micronucleus as well.

I also characterized the macronuclear response of wild-type and TIF1-knockdown strains to hydroxyurea (HU) and caffeine. HU is an inhibitor of ribonucleotide reductase, which induces depletion of deoxynucleotides precursors from the cell (Slater 1973). The absence of these precursors during S phase induces replication fork stalling and activates an ATR-dependent response that inhibits further DNA synthesis (Santocanale and Diffley 1998). Treatment with 20mM HU inhibits the growth of wild type unsynchronized cultures and this arrest is reversible upon removal of the drug. This ability to recover from the depletion of deoxynucleotide suggests that stalled forks are stabilized during treatment, a key feature of the intra-S phase checkpoint response. Caffeine acts as inhibitor of ATR/ATM kinases (Sarkaria et al., 1999). The addition of caffeine to wild type cultures is not toxic and reversed the effect of hydroxyurea, suggesting that *Tetrahymena* uses an ATR-like pathway to regulate the response to genotoxic stress. TIF1 mutants are hypersensitive to HU during vegetative growth and also show a delay in the recovery from HU-induced genotoxic stress during the recovery time (5- 20mM HU). This delay suggests that the intra-S phase checkpoint response is defective in these mutants, and that Tif1p could play an important role in the ATR-like pathway of *Tetrahymena*.

# CHAPTER III

# THE IN VIVO ASSOCIATION OF TIF1P WITH rDNA MINICHROMOSOMES DOES NOT REQUIRE SPECIFIC TARGET SEQUENCES

## Overview

Previous studies using TIF1 knockdown strains showed that Tif1p has a global role in the maintenance of genome stability in *Tetrahymena*. Tif1p preserves the integrity of chromosomes in the micronucleus and macronucleus, and prevent aberrant nuclear division by activation of the intra-S phase checkpoint response to genotoxic stress. Tif1p also regulates the timing of ribosomal DNA (rDNA) replication, suggesting that it acts directly on the rDNA origin. The mechanisms for activation of rDNA replication and the checkpoint response have not been elucidated. In my initial efforts to study Tif1p function, different epitope tags were placed at either the amino or carboxyl terminus of the preotein. In all cases, Tif1p function was compromised, highlighting the essential role of structure at both the amino and carboxy terminus. Whereas the amino terminus is predicted to be involved in DNA binding, epitope tags added to the carboxy-terminal oligomerization domain affected Tif1p binding to rDNA minichromosomes. These data argue that the overall architecture of TIF1 homotetramer is important for DNA binding. The altered phenotypes include defects in macronuclear development,

aberrant amitotic macronuclear division and macronuclear genomic stability. This data further illustrate the global role for Tif1p in genome maintenance.

Since epitope tags perturbed Tif1p functions, heterologous antiserum was generated against an exposed peptide loop in Tif1p. In chromatin immunoprecipitation experiments I determined that Tif1p association with the rDNA minichromosome extends beyond the replication origin. Tif1p binding was observed throughout the rDNA coding region. Furthermore, Tif1p was largely excluded from non-rDNA chromosomes. These findings suggest that mechanism for targeting Tif1p to rDNA and non-rDNA minichromosomes is fundamentally different.

**Introduction**

Accurate replication and segregation of chromosomes is essential for the successful completion of the cell cycle and cell viability. In order for a replication origin to be competent to initiate DNA replication, it minimally needs to be populated by the essential origin recognition complex (ORC) (Bell & Stillman, 1992). The six subunits of ORC are highly conserved among eukaryotes (Gavin et al., 1995). ORC is responsible for nucleation of pre-replication complexes (pre-RCs) at specific sites in chromosomes. This occurs during late mitosis and early $G_1$ when the levels of kinases that promote replication initiation are low (Diffley et al., 1994; Okuno et al., 2001; Zou & Stillman, 2000). ORC recruits the pre-RC that contains Cdc6, Cdt1 and MCM2-7, the hetero-hexameric replicative helicase. After MCM2-7 is loaded, the pre-RC is competent (licensed) for initiation. Conversion of the pre-RC into a pre-initiation complex (Pre-IC)

occurs at the $G_1$/S phase transition, and is promoted by the kinases Cdk2/cycE and Cdc7/Dbf4 (Walter, 2000; Zou & Stillman, 2000). At this time Mcm10 is loaded and recruits Cdc45, which is essential for DNA unwinding (Gregan et al., 2003). Cdc45 acts as a physical link between initiation and elongation factors (DePamphilis, 2005). The loading of replication protein A (RPA) stabilizes single-stranded DNA and promotes DNA unwinding (Walter & Newport, 2000). In order to initiate replication polymerases are loaded and replication proceeds in a semi-continuous manner from bidirectional origins.

Replication origins are also bound by non-ORC proteins; however their contribution to replication initiation is less well understood and can differ from one protein to the next. The most extensively studied non-ORC origin binding protein is *S. cerevisiae* ARS binding factor 1 (Abf1,(Diffley, 1998; Diffley & Stillman, 1988). Abf1 serves many roles in the nucleus. It promotes replication initiation and is involved in transcriptional regulation, DNA repair and gene silencing (McBroom & Sadowski, 1995; Reed et al., 1999; Trawick et al., 1992). Abf1 is a site-specific DNA binding protein, and facilitates replication initiation by functioning as barrier for nucleosome occupancy, creating a nucleosome-free structure at the ARS1 origin that favors ORC binding to adjacent sequences (Lipford & Bell, 2001; Rhode et al., 1992; Venditti et al., 1994).

Studies in higher eukaryotes revealed that non-ORC DNA binding proteins can facilitate ORC recruitment by physically interacting with ORC and tethering ORC to origins. In *Drosophila melanogaster*, binding of a multiprotein complex (DmMyb) to the chorion gene replication origin is required for recruitment of ORC to ACE3 and

subsequent amplification of this region in differentiated follicles cells (Beall et al., 2002). Another recently described protein, AIF-C, recognizes a specific sequence at the rat aldolase B origin, and is able to recruit ORC to this origin through protein:protein interactions (Minami et al., 2006). The binding of AIF-C to this origin is required to initiate replication from this site. Since rat ORC binds DNA non-specifically, the loss of AIF-C or elimination of the AIF-C DNA binding site prevents ORC recruitment and origin activation. Whereas metazoan ORC complexes exhibit no specificity for DNA binding in vitro, tethering provides a mechanism for bringing ORC to specific chromosomal sites in vivo. The current data do not provide a compelling argument that this is the sole mechanism for recruiting ORC to metazoan origins.

Mutations in ORC or non-ORC proteins not only promote the failure to support replication initiation but also compromise other cellular mechanisms. For example, the depletion of *S. cerevisiae* Orc6 does not affect the binding of ORC to origins, but strongly impairs the maintenance of pre-RC and S phase progression, leading to the activation of the intra-S phase DNA damage checkpoint response (Chen et al., 2007). In human cells, depletion of Orc2 induces a decrease in the level of other ORC subunits, thereby preventing the initiation of DNA replication. However, low levels of ORC do not activate the intra-S phase DNA damage checkpoint signal (Machida et al., 2005). These differences not only reflect the intricate regulation of replication initiation, but also reveal the diversity between different model systems. There are several examples in which mutations of replication factors compromise other cellular processes. Mutations in Orc2p and Orc5p subunits, have revealed their role in transcriptional gene silencing,

cohesion of sister chromatids and assembly of mitotic chromosomes in yeast and Drosophila (Dillin & Rine, 1998; Kato et al., 2008; Pflumm & Botchan, 2001; Suter et al., 2004).

In *Tetrahymena* the 5' non-transcriptional sequences (NTS) of the rDNA minichromosomes contains three evolutionarily conserved, repeated sequences, referred to as Type I, II, and III elements (Figure 3.1) (Challoner et al., 1985). Type I elements reside in two nucleosome-free regions where origins of replication have been mapped, as well as the nucleosome-free rDNA promoter (Zhang et al., 1997). Promoter-proximal type I element regulate both replication initiation and transcription of the 35S ribosomal RNA precursor (Tower, 2004). Type I elements are recognized *in vitro* by factors designated Type I Factors 1 through 4 (Tif1p through 4). Tif1p was shown to bind to single-stranded DNA in a sequence-specific manner (Hou et al., 1995). Electrophoretic mobility shift assays (EMSAs) showed that S100 extracts from wild type *Tetrahymena* contains a DNA binding activity (Tif1p/ssA-TIBF) that strongly binds to the central A-rich portion of the Type I element (Umthum et al., 1994). Tif1p also binds specifically to the type I element T-rich strand, as well as pause site elements (PSE), which were previously shown to regulate rDNA origin activation (Saha et al., 2001). Using in vivo footprinting of wild type and TIF1-depleted *Tetrahymena*, our laboratory demonstrated that Tif1p regulates the occupancy of type I and PSE elements *in vivo*. Specifically, partial depletion of Tif1p affects the occupancy of the type I element A-rich strand and PSE element at the rDNA origin, and the complementary T-rich strand at the promoter (Saha & Kapler, 2000). The most parsimonious model is that Tif1p specifically and

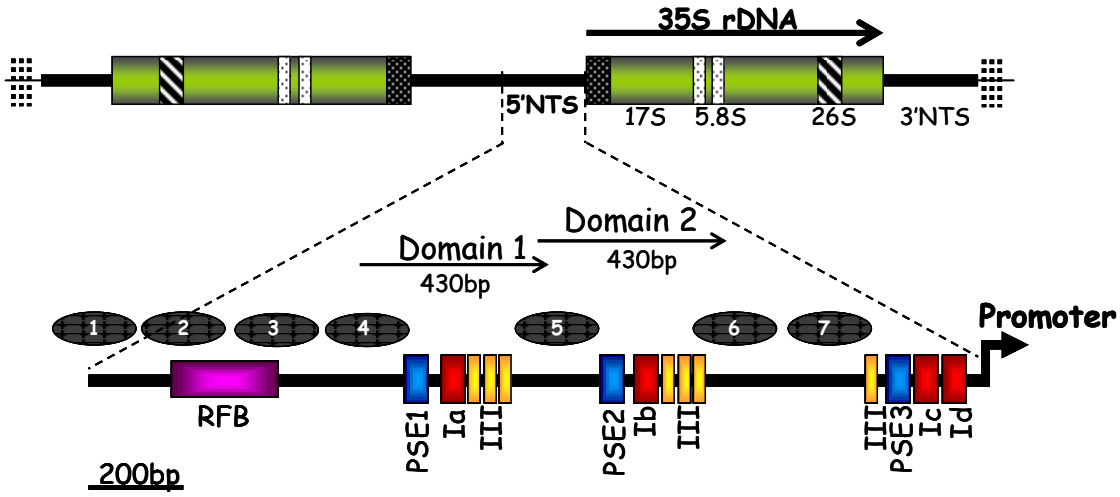


Figure 3.1 Schematic of the *Tetrahymena* rDNA minichromosome. The 2.1 Kb macronuclear rDNA minichromosome consisted a palindromic arrangement of two copies of the rDNA gene (in green) that encode for 17S, 5.8S and 26S ribosomal rDNA. The region encompassing the 5'NTS is expanded and includes cis-acting determinants for DNA replication. Type I, II, III and pause site elements are phylogenetically conserved sequences. Type I elements are showing in red, Type III in yellow, replication fork barrier (RFB) in purple and pause site elements (PSE) in blue. The locations of the seven positioned nucleosomes are depicted by black ovals.

directly associates with these sequences in vivo. The work described in this chapter challenges this model.

Orthologs of Tif1p belong the whirly protein family in plants. Tif1p homology to members of this family is restricted to the whirly domain (Saha et al., 2001). Like Tif1p, plant transcription factor, Stwhy1 is a sequence-specific single-strand DNA binding protein (Desveaux et al., 2002). The crystallographic structure of Stwhy1 has been determined, providing significant information for the study of Tif1p (Desveaux et al., 2002; Saha et al., 2001).

Saha and Kapler determined that the oligomeric status of purified native Tif1p is a homotetramer, yet Tif1p binds just one molecule of DNA per homotetramer in vitro (Saha & Kapler, 2000). Studies in a mutant strain expressing low levels of TIF1 revealed that Tif1p acts as an inhibitor of rDNA origin firing in early S phase (Morrison et al., 2005). Furthermore, this protein is essential for accurate macronuclear S phase progression; TIF1 mutants exhibit an elongated macronuclear S phase that is associated with a reduced rate of DNA synthesis (Morrison et al., 2005). This finding suggests that Tif1p has a global role in macronuclear DNA replication that extends beyond its function at the rDNA origin.

Recently studies revealed that the multi-subunit TIF4 complex is *Tetrahymena* ORC (Mohammad et al., 2007). Like other type I binding factors, *Tetrahymena* ORC (TtORC) recognizes and binds in a sequence-specific manner to single-strand DNA (Mohammad et al., 2000). In contrast to TIF1, TtORC binding activity is ATP-dependent and specific for the T-rich strand only. The most unusual characteristic of

TtORC is that it is a ribonucleoprotein (RNP) complex. *Tetrahymena* ORC uses an integral RNA subunit to facilitate rDNA origin recognition by RNA:DNA base pairing (Mohammad et al., 2007). Since footprint analysis revealed that Tif1p interacts at the rDNA origin A-rich strand and TtORC is targeted to the complementary T-rich strand, it has been proposed that Tif1p regulates the timing of rDNA replication by directly affecting TtORC binding or regulation.

Several mechanisms can be envisioned for how Tif1p might repress rDNA origin firing (Figure 3.2). One possibility is that Tif1p *inhibits the assembly of pre-RCs* by physical obstruction of the rDNA origin (Figure 3.2, Model 1). If this were the case, we predict that Tif1p and ORC would not coexist at the rDNA origin at any point during the cell cycle. Alternatively, Tif1p and ORC might coexist at rDNA origins either transiently or stably. In one scenario (Figure 3.2, Model 2) Tif1p would prevent *pre-RC activation* by blocking recruitment of the MCM complex to the origin. Subsequent modification of the ORC-origin-Tif1p complex, such as phosphorylation of Tif1p, would release Tif1p from the DNA and render the origin competent for loading of the MCM complex and further pre-RC activation. Alternatively, Tif1p would not leave the origin, and the phosphorylation of Tif1p would allow for the recruitment of MCM to origins. In this case, *Tif1p would be included in the activated pre-RC complex* (Figure 3.2, Model 3).

To better understand how Tif1p regulates rDNA replication; I generated strains expressing epitope-tagged versions of TIF1. The present work shows that the addition of small peptide tags to Tif1p largely recapitulates the phenotypes associated with TIF1

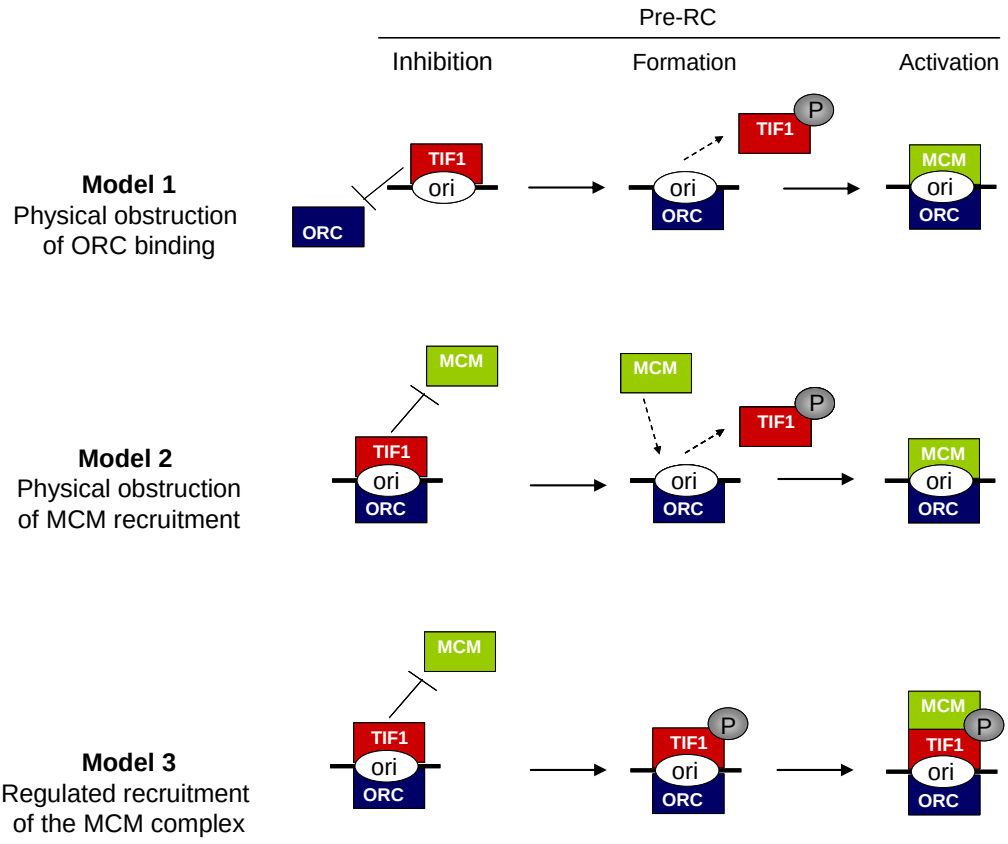


Figure 3.2 Proposed models for the negative regulation of rDNA replication by Tif1p.

knockdown mutants. Cultures with tagged Tif1p showed defects during macronuclear development. Defects during vegetative growth were also observed, including abnormal macronuclear division and genomic instability. Recruitment of Tif1p to the rDNA origin was also altered in tagged TIF1 strains. To overcome these problems, I designed a peptide antibody against Tif1p, and used this antibody to study the *in vivo* binding of Tif1p to chromosomes by chromatin-immunoprecipitation (ChIP) analysis. My results suggest that the binding of Tif1p to rDNA minihromosome goes beyond the type I element sequences during the cell cycle. However, this binding is limited to the 21 kb rDNA minichromosome, since no significant binding was observed in a 60 kb interval of a non-rDNA chromosome that includes a bonafide non-rDNA replication origin, TtARS1A.

**Material and methods**

*Tetrahymena thermophila* culture methods and transformation

Cultures were grown at 30°C in 2% PPYS (2% proteose peptone, 0.2% yeast extract, 0.003% sequestrine) supplemented with 250 μg/ml penicillin, 100 μg/ml streptomycin and 250 ng/ml amphotericin B.

To prepare cells for mating cultures were starved in 10 mM Tris-HCl (pH 7.4) for 20 h. Mating was induced between wild type strains CU428 and CU427 by mixing equal number of each strain at a density of 2x10e5 cells/ml. Acridine orange (0.001%) was used to stain mating pairs and monitor developmental stages with a fluorescence microscope to determine the timing for transformation.

Germline transformation was achieved by bioballistic bombardment 4 h after initiation of mating. Macronuclear anlagen transformation was performed at 8 h. For transformation, mating cultures were harvested by centrifugation at 4000 rpm for 5 min and resuspended in 1 ml of 10 mM Tris-HCl (pH 7.4). A 100 mm diameter petridish was used to support a sterile Whatman filter paper saturated with 1 ml of 10 mM Tris-HCl (pH 7.4) onto which the concentrated suspension of cells was transferred. The macrocarrier used for transformation (0.6 μm gold particles, Biorad) was coated with a DNA mixture containing 35 μg of the MTT1-neo-MTT1 plasmid and 35 μg of the experimental plasmid carrying a tagged version of TIF1. Restriction digested DNA fragments were then introduced into *Tetrahymena* by bioballistic transformation according to the manufacturer's instructions (Biorad). Homologous recombination between the end of the inserts and endogenous target sequences was used to integrate both the MTT1-neo-MTT1 and tagged-Tif1p fragments into their respective chromosomes. The expression of the neo-cassette (neomycin phosphotransferase provides drug resistance to the transformed cells) was driven by the MTT1 promoter which was induced by the addition of cadmium in form of cadmium chloride ($CdCl_2$) to the media.

After transformation, the cells were transferred into 500 ml flasks containing 50 mls of 10 mM Tris-HCl (pH 7.4) and incubated under stationary conditions at 30°C for 18 h to complete the developmental cycle. The cells were then refed with 5% PPYS to a final concentration of 2% supplemented with 1.2 μg/ml final concentration of $CdCl_2$ and incubated in a 30°C shaker for 6 h. Next, paromomycin (100 μg/ml final concentration)

was added to the transformed culture. To identify MTT1-neo transformants, cells were plated out in 96 well dishes, undiluted or diluted 1:10 or 1:100, and incubated in a dark, moist chamber at 30 °C for 4 days in the presence of paromomycin. Paromomycin-resistant wells were identified by light microscopy. Further screening for co-transformants that contained the epitope-tagged TIF1 transgene was achieved by PCR amplification or by western blotting with antibodies directed against the TIF1 epitope tag.

Synchronization of *Tetrahymena* culture

Synchronization of *Tetrahymena* cultures was achieved by starvation or centrifugal elutriation. To synchronize log phase cultures by starvation, cells were harvested by centrifugation and washed twice with 10 mM Tris-HCl (pH 7.4), and incubated in 10 mM Tris-HCl (pH 7.4) for 8 h at 30°C shaking at 100 rpm. This culture was synchronized in $G_1$ phase. Synchronized cells were refeed with 5% PPYS to a final concentration 2% at a density of 2.5x10e5 cells/ml and incubated at 30°C with gently agitation (100 rpm). The refed cells reached early S phase 2.5 h after refeeding. The subsequent G1 phase was evident by the end of 4 h, as confirmed by flow cytometry analysis.

To synchronize cultures by elutriation, three flasks of 2 L each with 500 mL of 2% PPYS were inoculated with 10 ml of a log phase culture (1x10e5 cells/ml) and incubated for 14 h at 30°C with 100 rpm, and grow to a density of 1x10e5 cells/ml. The culture was pumped into an elutriation chamber mounted onto a Beckman J6M/E

centrifuge at a rotor speed of 850 rpm and flow rate of 50 ml/min. Two hundred milliliters of a synchronized G1 cell population was recovered by increasing the pump flow rate to 65 ml/min. This fraction contains a cell population synchronized in G1 phase of the cell cycle. The elutriated culture reached early S phase after 1 h and the next G1 phase was evident at 3 h post-elutriation upon incubation at 30°C with shaking (100 rpm).

Flow cytometry

To determine the DNA content within a cell population at least 2.0x10e5 cells/ml were collected by centrifugation at 4000 rpm for 4 min. Cells were washed with 5 ml of cold phosphate buffer saline (PBS) re-centrifuged and the supernatant was aspirated. Cells were resuspended in a minimal volume (~10 µl) and fixed with 5 ml of ice cold 70% ethanol by incubating for 2 h on ice. Samples were stored at 4°C or stained immediately with propidium iodide (PI). Fixed samples were washed twice with PBS and resuspended in 0.4 ml of propidium iodide staining solution (PBS containing 0.1% Triton X10E0, 0.002% propidium iodide and 0.2 mg/ml RNase A). The samples were protected from the light and incubated at RT for at least 1 h. Stained samples were collected on BD FACSCaibur$^{TM}$ flow cytometer and cell cycle progression was determined by monitoring DNA content. Thirty thousand cells were analyzed for each sample and plotted as a function of the PI intensity, which reflects the DNA content of each cell.

Cryogenic preservation of *Tetrahymena*

Cells from 0.1 L of log phase culture (2.5x10e5 cells/ml) were harvested, washed twice, resuspended in the original volume with 10 mM Tris-HCl (pH 7.4) and starved for three days by incubation at 30°C (100 rpm) in a 500 ml flask. For cryogenic preservation, cells were concentrated by centrifugation and recovered in 10 ml of 8% DMSO in 10 mM Tris-HCl. Aliquots of 0.5 ml were dispensed in cryovials and slow frozen for 20 h at -80°C (Burns et al., 2000). The vials were transferred to a liquid nitrogen tank for permanent storage.

Immunoprecipitation and chromatin-immunoprecipitation

Ten ml of cell cultures (2x10e5 cells/ml) were crosslinked for 10 min at room temperature with 1% formaldehyde (270 µl from 37% stock). The crosslinking was stopped by adding 0.125 mM glycine (513.5 µl of 2.5 M stock) and mixed for 5 min. Next the samples were washed twice with PBS (pH 7.4) supplemented with a 1x protease inhibitor (complete EDTA free cocktail, #1873580, Roche); each wash was done by mixing for 5 min and centrifuging at 2,000 rpm for 1 min. The final pellet was resuspended in 0.6 ml of SDS lysis buffer (1% SDS, 10 mM EDTA, 50 mM Tris-HCl (pH 8.1) plus protease inhibitor) and incubated for 10 min in ice. The lysate was sonicated to shear DNA to a length of 200 and 1000 base pairs. Five pulses of 10 seconds were applied each with 10% duty in a Misonix Sonicator 3000. Samples were centrifuged at 17000xg for 10 min. An aliquot of 200 µl was stored at -20°C to test the input material. The remaining sample (400 µl) was diluted ten-fold with ChIP dilution

buffer (0.01% SDS, 0.01% Triton X-100, 1.2 mM EDTA, 16.7 mM Tris-HCl pH 8.1, 167 mM NaCl and protease inhibitor). To reduce non-specific background the sample was pre-cleared with 120 µl of a 50% slurry Protein A agarose coated with salmon sperm DNA (catalog #16-157, Millipore), and incubated for 30 min at 4°C with constant agitation in a small rotisserie rotator at 8 rpm. To pellet the agarose beads, the sample was centrifuged 2,000 rpm for 2 min. The supernatant was recovered and divided in to two aliquots. One aliquot was incubated overnight with 1:200 dilution of specific antibody at 4°C and constant gentle agitation. The other aliquot was used as control with no antibody added, but incubated under the same conditions. To collect the antibody-proteinchromatin complex, 60 µl of Protein A agarose was added to each aliquot; incubated for 1 h at 4°C and constant agitation. After centrifugation (1,000 rpm for 1 min) the supernatant was discarded and the beads were washed consecutively with 1 ml of low salt immunocomplex wash buffer (0.1% SDS, 1% Triton X-100, 2 mM EDTA, 20 mM Tris-HCl pH 8.1, 150 mM NaCl and protease inhibitor); high salt immunocomplex wash buffer (0.1% SDS, 1% Triton X-100, 2 mM EDTA, 20 mM Tris-HCl pH 8.1, 1.5 M NaCl and protease inhibitor); LiCl immunocomplex wash buffer (0.25 mM LiCl, 1% NP40, 1% deoxycholate, 1 mM EDTA, 10 mM Tris-HCl pH 8.1 and protease inhibitor) followed by two washes with TE buffer (pH 8.0). All the washes were done for 5 min at constant agitation and samples were subsequently centrifuged at 1,000 rpm for 1 min.

To check for immunoprecipitation of proteins the beads were recovered in 25 µl of Laemmli buffer (2% SDS, 10% glycerol, 5% 2-mercaptoethanol, 0.002%

bromophenol blue, 60 mM Tris-HCl (pH 6.8), boiled, loaded on a 12% or 6% SDS-polyacrylamide gel for Tif1p or Mcm6p examination, respectively, and analyzed by western blotting.

Alternatively, to elute the chromatin-crosslinked complexes from the antibody the samples were incubated twice with elution buffer (1% SDS, 0.1 M $NaHCO_3$) for 15 min at room temperature and constant agitation. Next, samples that contained protein-DNA complexes were treated in parallel to the input sample previously collected. To reverse protein-DNA crosslinking, 0.2 M NaCl was added, and the samples were incubated for 4 h at 65°C. Samples were deproteinized and phenol/chloroform extracted. The DNA was precipitated, washed and finally resuspended in 50 µl of Tris-HCl pH 8.0 for analysis by PCR or hybridization with radioactive probes.

Antibodies

To immunoprecipitate acetylated histone H3 a rabbit polyclonal antibody was used (06-599 Millipore, Billerica, MA). For immunoblotting detection of the Myc epitope tag a rabbit polyclonal antibody was used in at 1:2500 dilution (DB061CMyc-C10, Delta Biolabs, Gilroy, CA). For detection of Tif1p-FLAG-C tag a mouse monoclonal ANTI-FLAG® M2 affinity purified antibody was used at a 1:5000 dilution (F1804, Sigma, Saint Louis, MI). Anti-pan-MCM polyclonal antiserum against a synthetic peptide from hMcmc3p (residues 405 to 421) (a gift from Dr. MacAlpine) was used at a 1:1000 dilution.

Horseradish peroxidase-conjugated secondary antibodies for western blotting were used at a 1:5000 dilution and purchased from Jackson ImmunoResearch Laboratories (West Grove, PA).

**Results**

Amino terminal tagging of TIF1 affects vegetative growth and induces mutant phenotype

To create tools to explore the role Tif1p in rDNA origin regulation and checkpoint activation several strategies were use to generate a tagged Tif1 protein (Tif1p). In general, tagged transgenes ware targeted by homologous recombination to the endogenous TIF1 locus during macronuclear development (Cassidy-Hanley et al., 1997). Strains with a partial gene replacement were generated, and in all cases the TIF1 transgene was under the control of the endogenous promoter. These strains were generated by co-transformation with an unlinked selectable MTT1-neo transgene to first select cells that incorporated and expressed exogenous DNA during the initial screening of bioballistic transformants. TIF1 co-transformants were subsequently identified by PCR and western blotting analysis. The various tagged TIF1 alleles that were used in this study are described in Table 3.1.

To initiate these studies, a tag consisting of 6 histidine residues combined with 5 copies of C-myc tag was attached to the amino terminus of Tif1p (Tif1p-HM-N-tag). Anlagen co-transformants were screened by PCR using primers that flank the insertion site at the endogenous locus. Several Tif1p-6x<u>H</u>is-5x<u>M</u>yc amino tagged clonal

Table 3.1 Genetic and biochemical analysis of epitope-tagged TIF1 alleles.

| Strain name | Other name/ reference | Tag | Insertion site | Transformants Type | Tetramer formation EMSA assay | Defect |
|---|---|---|---|---|---|---|
| TM001 | **Tif1p-HM-N** | His-Myc | Amino | Anlagen | yes | Abnormal mac division and macronuclear extrusion bodies |
| TM002 | **Tif1p-HM-C** TAM101/Yakisich et al. 2006 | His-Myc | Carboxy | Anlagen | yes | Loss of specific binding to origins |
| TF005 | **Tif1p-FLAG-C** | FLAG | Carboxy | Germline | yes | Developmental defects |

(EMSA) electrophoretic mobility shift assay.

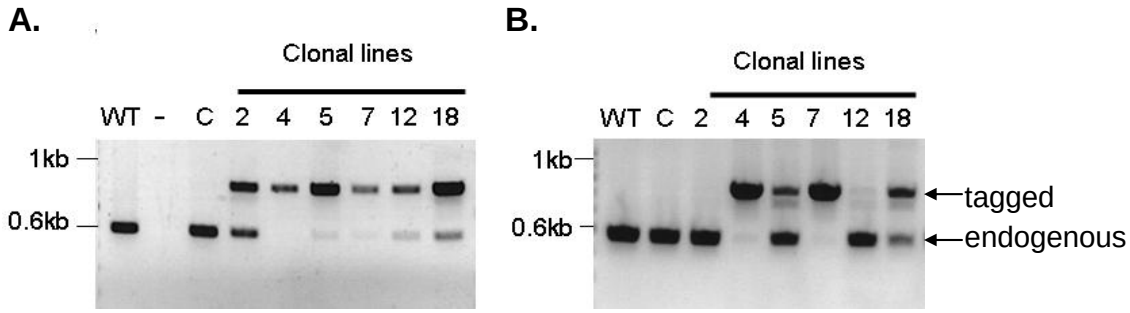


Figure 3.3 The replacement of the endogenous TIF1 gene by an TIF1-HM-N tagged transgene is not stably maintained in clonal lines. Negative image of an agarose gel stained with ethidium bromide showing PCR products. These fragments were amplified by primers that anneal with endogenous TIF1 sequences and that flank the side of the tag insertion. The tagged allele can be discriminated from the endogenous gene by the size of the amplified fragment. *Tetrahymena* genomic DNA was used as template. (WT) Wild type strain, (-) is a PCR reaction without template DNA, (C) control strain transformed with the MTT-neo-MTT transgene only, clonal lines 2-4-5-7-12-18 contain different amounts of the tagged TIF1 transgene. **A.** The genomic DNA used in these amplifications was prepared immediately after the clonal lines were isolated. **B.** Genomic DNA prepared after the clonal lines were grow for 168 generations.

cotransformants were generated, each one with different degree of gene replacement (Figure 3.3A). These clonal line cultures were propagated for 168 generations and a subsequent analysis by PCR revealed that the amino tagged-Tif1p was difficult to maintain in the amitotic macronucleus (Figure 3.3). Since macronuclear chromosomes segregate randomly, the rapid loss of the transgene from the entire population suggested that the tag was interfering with Tif1p function. Nevertheless, TIF1-HM-N-A4, one of the strains with highest gene replacement in the macronucleus, was selected for further experiments.

To asses whether the tag affect oligomerization and DNA recognition, in vitro DNA binding activity was analyzed. Since Tif1p was originally identified in crude cytosol S100 extracts as an activity that binds specifically to the single A-rich strand DNA sequence from rDNA type I binding element and pause site elements (PSE) (Mohammad et al., 2000; Saha & Kapler, 2000; Umthun et al., 1994), I decided to test this activity in cultures from Tif1p-HM-N-tag strain (Figure 3.4). No defect in DNA binding activity was noticeable in the tagged strain compared to wild type. Since the replacement of the endogenous TIF1 for the tag version was high, I suspected that the tagged version was responsible for most of the Tif1p binding activity. The mobility of the DNA:protein complex was identical to wild type suggesting that the protein exists as a homotetramer.

The expression of tagged-Tif1p was analyzed throughout the cell cycle by western blotting in synchronized cell cultures. Synchronization in $G_1$ phase was achieved by starvation-refeeding protocol and the cell cycle progression monitored by

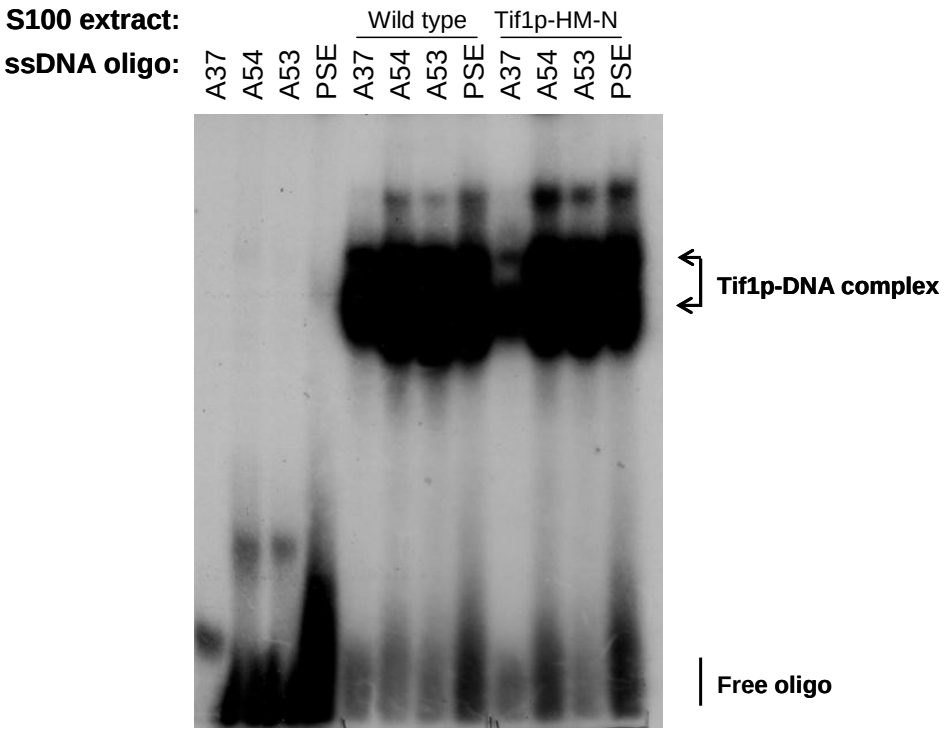


**ssA37** 5'-GGCAAAAAAAAAAACAAAAATAGTAAACCTTCCGAAC-3'

**ssA53** 5'-GGCAAAAAAAAAAACAAAAATAGTAAACCTTCCGAACTTTTGCAACTTTTGAG-3'

**ssA54** 5'-TGGCAAAAAAAAAAACAAAAATAGTAAACCTTCCGAACTTTTGCAACTTTTGAG-3'

**PSE** 5'-AAAAAATGAATGAAAACTGAAAAATTTACAAGGGATTGAAAATTTTGGC-3'

Figure 3.4 Tif1p-HM-N tag is able to bind to type I and PSE sequences of rDNA. The binding activity of Tif1p in S100 extracts from wild type and amino terminal tagged-Tif1p strains were compared by EMSA asay. Single stranded DNA (ssDNA) oligos representing different length of the A-rich strand of type I element were assayed (A37, A53, A54). The binding to an oligo corresponding to pause site element (PSE) was also analyzed. The migration of the TIf1p-DNA complex is indicated, as well as the free oligonucleotide substrate. The sequence of each oligonucleotide is showed in the bottom.

flow cytometry (Figure 3.5A). Similar to wild type, S phase was detectable by 3 h after refeeding and a peak for G2 was observed at 4 h. Tagged Tif1p was detected using an antibody against the myc-epitope tag (Figure 3.5C). Considering that the tag itself is about 10 KDa, the predicted size for the tagged Tif1p is around 34 KDa. Unexpectedly, two bands were detected with this antibody (45 and 55 KDa), strongly suggesting the presence of posttranslational modification. When the signals were normalized by total protein loaded in a parallel SDS-PAGE gels, (Figure 3.5B), no significant change in the level of Tif1p was observed across the cell cycle. By contrast, the abundance of the wild type TIF1 transcript was previously shown to be cell cycle regulated, with a increase during S phase (Mohammed et al., 2000; Saha & Kapler, 2000). These differences raised the possibility that addition of this tag to the N-terminus prevents cell cycle regulated turnover of TIF1 protein.

The primary indication that the amino terminal tag compromised Tif1p function was the high frequency of macronuclear extrusion bodies observed by direct microscopy of non-dividing cells (as shown in the figure on p.137, panel A). Extrusion bodies are extranuclear bodies of chromatin that are positively stained with acridine orange. Extrusion bodies were previously described as a mechanism to reduce macronuclear DNA content in normal cycling cells (Cleffmann, 1980). However, an excessive number of extrusion bodies that contain fragmented DNA has been reported in knockdown strains for genes involved in the maintenance of nuclear integrity (Wiley et al., 2005). As expected extrusion bodies were occasionally detected by direct microscopic observation in logarithmic growing cultures of a wild type strain. An excessive number extrusion

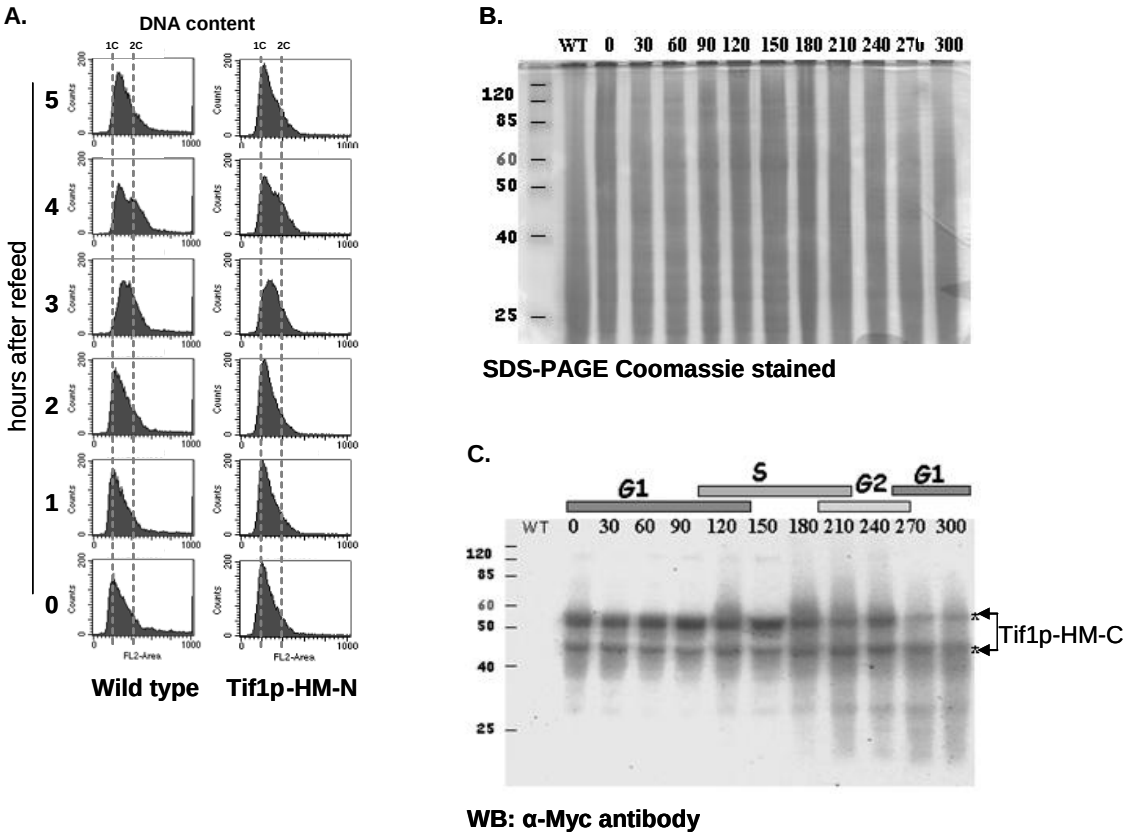


Figure 3.5 Cell cycle analysis of Tif1p-HM-N tag. A. Cell cycle progression was measured by flow cytometry. Synchronization was achieved by the starvation–refeeding protocol. Histograms showing number of cells (counts, ordinate) as a function of the DNA content (1C and 2C, abscissa). Wild type and tagged Tif1p strains were compared at indicated time after refeeding. **B.** 12% SDS-PAGE stained with Coomassie blue showing total protein loaded for each sample. **C.** SDS-PAGE and western blot analysis of whole cell lysates with α-myc antibody; this antibody recognize two distinct bands of Tif1p-HM-N tag (*). No detectable signal in wild type sample (WT).

bodies were present in Tif1p-HM-N strain, occurring in 80% of the TIF1-tagged cells (Figure 3.6A). Furthermore, abnormal macronuclear division was elevated in the tagged strain (Figure 3.6B). Cells undergoing cytokinesis without completion of division of the macronucleus were commonly observed in the tagged strain. In general these phenotypes are analogous to the ones observed in TIF1 knockdown strains (Morrison et al., 2005), suggesting that the addition of the tag to Tif1p severely affects the properties of Tif1p, and hence the overall integrity of the cell.

**Initial characterization of the His-myc carboxy terminal-tagging of Tif1p**

Since placement of the his-myc tag at the amino terminal of TIF1 was deleterious, a second construct was generated with the tag at the carboxy end of Tif1p. Since the carboxy terminus contains the oligomerization domain of Tif1p, we were not sure whether this tagged variant would form homotetramers. The observation that placements of a His tag at the carboxy terminus of whirly proteins did not affect crystallization of tetramers, suggested that insertion of the tag should not be an issue (Desveaux et al., 2002). An epitope-tagged TIF1 gene with 6xHis-5xMyc added at the carboxyl terminus (TIF1-HM-C-tag) was introduced to *Tetrahymena*. The ability of this tagged variant to form homotetramers and bind DNA was corroborated by EMSA (data not shown). Careful examination revealed no significant increase in the frequency of extrusion bodies or aberrant macronuclear division in this strain, suggesting that this tag-Tif1p was stable and maintained in the cell. Western blots analysis was used to

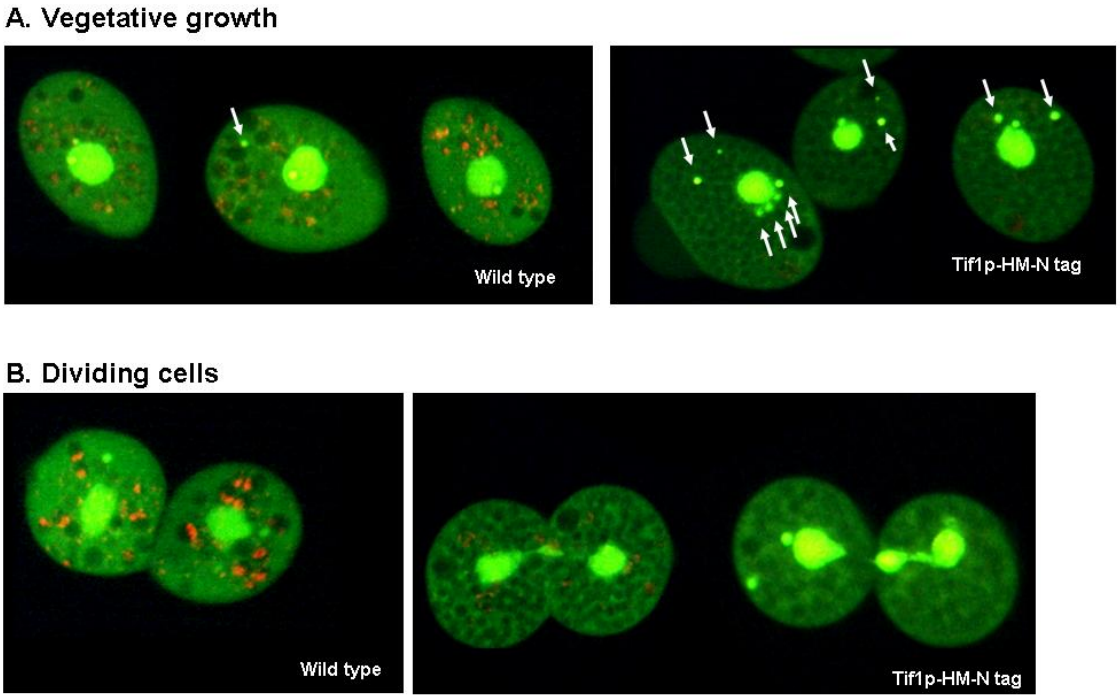


Figure 3.6 Insertion of tag at the amino terminus of TIF1 induce abnormal phenotype in *Tetrahymena* cells. Acridine orange stained cells. A. Log phase cultures from wild type and Tif1p-HM-C tagged TIF1 strain are compared. Arrows indicate extrusion bodies in the cells. B. Dividing cells from wild type and tagged Tif1p are compared. Progression of cytokinesis without complete macronuclear division is observed in tagged Tif1p strains. Acridine orange staining turns red in acid pH; I assume that the red spot presents in the wild type strain correspond to lysosomes.

determine the levels of TIF1-HM-C-tag proteins using an α-myc antibody. As for amino-terminal tagged Tif1p, the levels of the carboxy terminal tagged Tif1p did not oscillate across the cell cycle (Figure 3.7A). The temporal localization of Tif1p in both the micronucleus and macronucleus during vegetative cell division was determined and presented in Chapter II. The intracellular localization of Tif1p was dynamic throughout the cell cycle with a strong perinuclear staining immediately prior to S phase. This perinuclear staining was present in macro nuclei in cultures synchronized at the $G_1$/S border. Since rDNA is mostly encapsulated in nucleoli, which are evenly distributes around the macronucleus throughout the cell cycle, we speculated that this staining correlates with the binding of TIF1p to type I elements at the rDNA origin. Furthermore, the timing of this binding was consistent with the idea that Tif1p acts as an inhibitor of rDNA replication during early S phase (Yakisich et al., 2006).

As a first attempt to distinguish between the proposed models for how Tif1p regulates rDNA origin activation (Figure 3.2), I tested for the loading of Tif1p into chromatin, and for physical interactions between Tif1p and ORC or the MCM complex. Crosslinked chromatin was used for this analysis. Consequently, direct interaction between Tif1p and ORC or MCM2-7 would be detected, as well as co-occupancy of a DNA fragment. Since ORC and MCM2-7 are high molecular weight complexes (~500 KDa Mohammad et al., 2003) and *Tetrahymena* ORC contains an integral RNA subunit (Mohammad et al., 2007), it was essential to include formaldehyde in the chromatin precipitation to preserve DNA-protein, RNA-protein and protein-protein interactions.

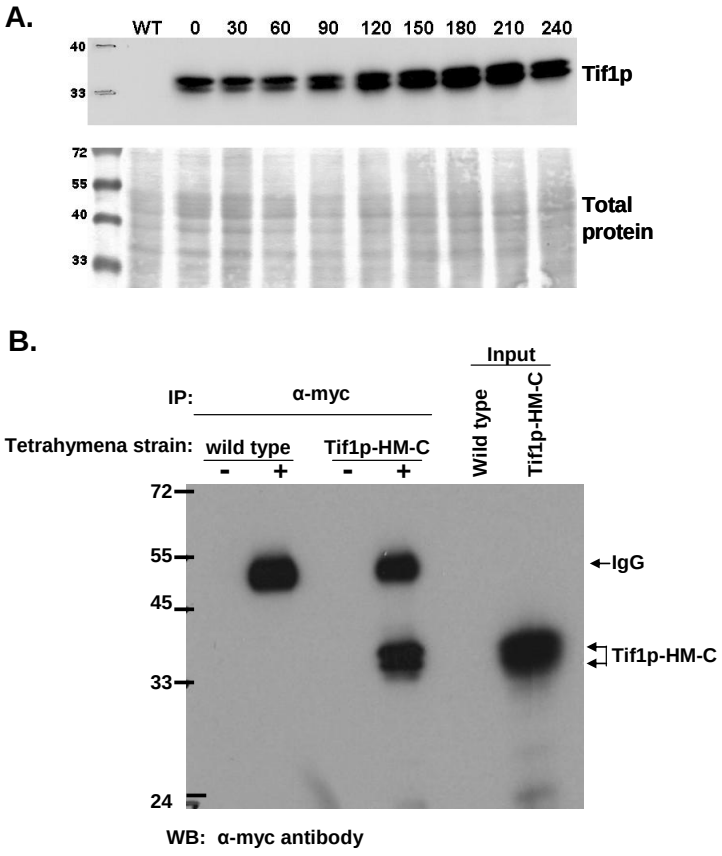


Figure 3.7 Detection of C-terminal tagged Tif1p. A. Myc antibody was used to monitor tagged TIf1p during cell cycle. Culture was synchronized by starvation-refeed protocol. Samples were collected every 30 min after refeeding. Logarithmically growhing wild type strain was used as a negative control. Ponceau S stained membrane is showing the comparable loading of total protein **B.** Tif1p-HM-C-tag is effectively immunoprecipitated by myc antibodies. Whole cell extract from a wild type and TIf1p-HM-C strains were subjected to IP. Immunoprecipitates from samples treated with (+) or without (-) myc antibody were compared. The IP antibody against myc epitope was used for western blotting. HRP-goat anti rabbit was used for detection.

To determine whether the C-terminal epitope tag in Tif1p was accessible to the antibody, Tif1p-HM-C-tag was immunoprecipitated using antibodies against Myc and the imunoprecipitated fraction was assayed by western blot using the same antibody (Figure 3.7B). The antibody specifically recognize tagged-Tif1p in the fraction immunoprecipitated which contained soluble and chromatin bound Tif1p. Having established the parameters for immunoprecipitation and western blotting, I proceed to test the models for the role of Tif1p in the regulation of replication.

The models proposed in Figure 3.2 predict that Tif1p is loaded onto the rDNA origin during the stage of the cell cycle where Tif1p is known to inhibit rDNA replication. If Tif1p is interfering with the formation of pre-RC by preventing the loading of ORC (Figure 3.2, model 1), then origin sequences should be immunoprecipitated by Tif1p mainly during $G_1$ and early S phase when the rDNA origin is repressed by Tif1p. Additionally, Tif1p is not expected to be present at the origin once ORC is loaded or when pre-RCs are activated at the $G_1$/S border (MCM loading, Figure 3.2, model 1). As a first step in this analysis, a ChIP assay was performed on synchronized starvation-refed cultures to examine the temporal association of Tif1p with rDNA origins across the cell cycle. Following formaldehyde crosslinking and fragmentation of the chromatin, Tif1p-HMC-tag was immunoprecipitated with α-myc polyclonal antibody. Segments spanning known in vitro and presumed in vivo binding sites for Tif1p (type I element at the origin and at the rRNA promoter) were amplified. Additional segments of the 5' NTS were also amplified to serve as negative controls. No enrichment for known target sequences for Tif1p or negative controls was

Figure 3.8 Binding of Tif1p to rDNA origin sequences. Top panel showing a schematic representation of the 5'NTS of the rDNA. Cis-acting elements (Type I in red, Type II in purple, Type III in yellow, pulse site elements in blue and replication fork barrier in waved pattern) and nucleosome position (black ovals) are indicated. Amplified fragment are also indicated. **A.** ChIP with α-myc antibody on wild type and Tif1p-HM-C-tag strain was compared. Starvation-refeed protocol was used to synchronize the cells in $G_1$ phase. Formaldehyde (HCHO) alone or plus a homobifunctional amine (HCHO+EGS) was used as a crosslinker. PCR products for indicated regions are shown. Input (I), plus antibody (+) and no antibody (-) as indicated. **B**. Control ChIP assay using synchronized cultures of wild type strain. Antibodies against acetylated histone H3 were used. (**N4 and N7**) fragments where nucleosome 4 and 7 are respectively positioned in the 5' NTS.

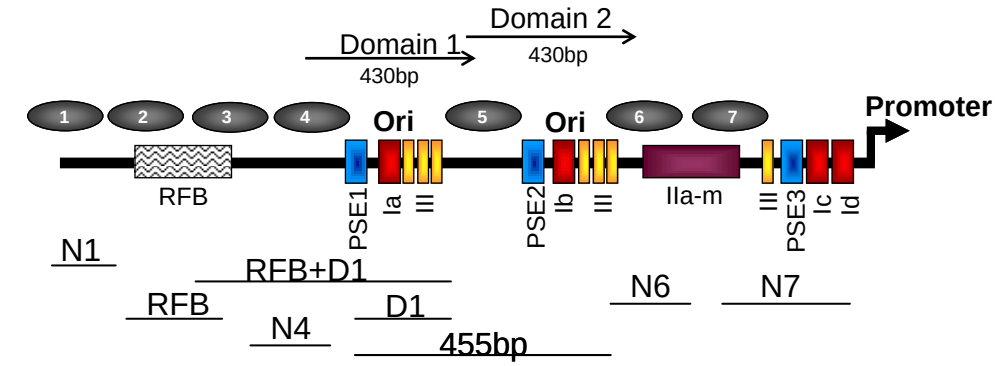
Domain 1
430bp
Domain 2
430bp
1
2
3
4
Ori
5
Ori
6
7
Promoter
RFB
PSE1
Ia
III
PSE2
Ib
III
IIa-m
III
PSE3
Ic
Id
N1
RFB+D1
RFB
D1
N6
N7
N4
455bp

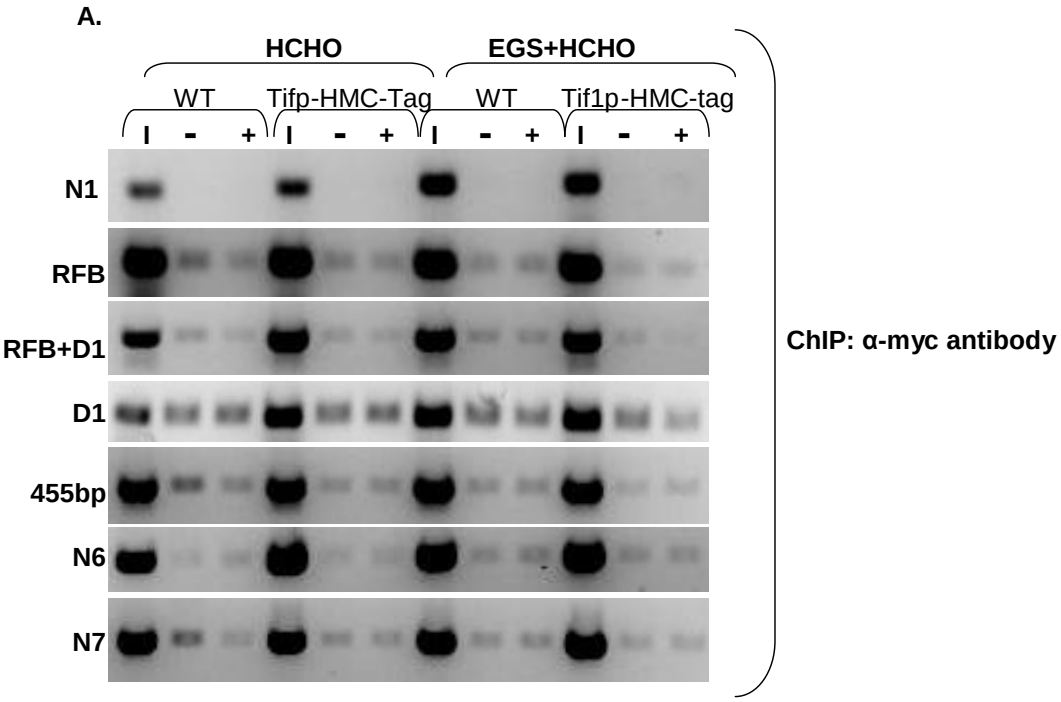
A.
HCHO
EGS+HCHO
WT
Tifp-HMC-Tag
WT
Tif1p-HMC-tag
I - + I - + I - + I - +
N1
RFB
RFB+D1
D1
455bp
N6
N7
ChIP: α-myc antibody

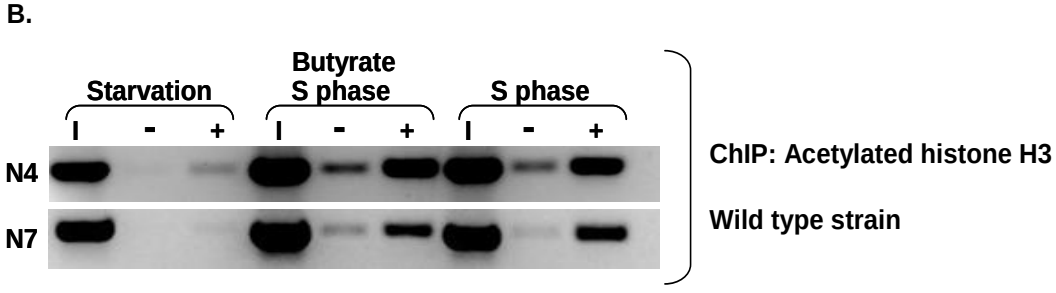
B.
Starvation
Butyrate
S phase
S phase
I - + I - + I - +
N4
N7
ChIP: Acetylated histone H3
Wild type strain

observed (Figure 3.8A). To improve protein-protein crosslinking before the pull down, the homobifunctional amine, EGS, was added (Pierce, Rockford, IL). Still no enrichment was evident for type I and PSE sequences. To check whether the ChIP protocol was suitable for *Tetrahymena*, the binding of acetylated histone H3 to specific sequences in the rDNA 5' NTS was assayed. ChIP was performed in a starved culture, where acetylation is expected to be minimal, and on S phase cells, plus an S phase control where hyperacetylation of histones was enriched by inhibiting histone deacetylases with sodium butyrate. Binding sequences were pulled down with antibodies against acetylated histone-H3 and enrichment was evident in both S phase cultures, arguing that the protocol was appropriate for our objective (Figure 3.8B). These data suggest that either Tif1p does not maintain a direct association with rDNA origin and promoter sequences, or that addition of the tag was interfering with the function of Tif1p.

The interaction of Tif1p with ORC or MCM complexes was also assayed. Myc antibody was used to pull down complexes that include Tif1p-HM-C-tag in starvation-refed synchronized cultures of TM002 strain (Table 3.1). The immunoprecipitated fraction was assayed by western blotting to detect the co-occupancy of Tif1p with ORC or MCM. However, no interaction between Tif1p and Mcm2-7 or ORC was observed (data not shown). This suggested either that no interaction between Tif1p and pre-RC complexes occur, or an obstruction of these interactions produced by the adition of the tag to Tif1p. The possibility that the carboxy terminal tag in Tif1p was modulating the interactions between Tif1p and pre-RC was a concern. Furthermore, based in the crystallographic data, Desveaux and colleagues predicted that mutating one specific

residue at the carboxy-terminus (Lys 188) would interfere with the ssDNA binding activity. Their experimental data suggests that the carboxy terminus modulates the affinity of whirly proteins for DNA (Desveaux et al., 2002).

The first approach to address whether this tag interferes with Tif1p function was to replace his-myc tag with a smaller peptide. Three copies of FLAG tag were added at the carboxyl terminus of Tif1p. The size of this tag was considerably smaller compared with the previous one (3 vs 10 KDa). However, preliminary screening of transformants expressing FLAG-tagged Tif1p demonstrated that the addition of FLAG tag induced genome instability in the micronucleus. Specifically, in a test cross between wild type and TF005 strains (Table 3.1), the progeny failed to complete macronuclear development. This reinforced the idea that the addition of tags to the carboxyl terminus interferes with functions of Tif1p. Induction of genomic instability in the transcriptionally silent micronucleus is another characteristic of TIF1-depleted strains (Morrison et al., 2005).

**Design of a peptide antibody to study endogenous Tif1p**

In silico analysis showed that the predicted isoelectric point for Tif1p of 9.17 (using ProtParam at http://ca.expasy.org), which is consistent with that of a DNA-binding protein. This parameter changed to 7.61 and 5.51 in Tif1p-FLAG-tag and Tif1p-HM-C-tagged, respectively. Furthermore, the instability index based on statistical predictions (ProtParam) suggests that the tags may induce some instability in Tif1p particularly when the His-Myc tag was added (Table 3.2).

Table 3.2 Instability index based on statistical predictions (ProtParam). This software predicting in vivo stability of a protein from its primary sequence by the overall charges of the protein and its dipeptide composition (Guruprasad et al., 1990). Stable proteins are designated as those that show instability index lower than 40. Protein sequences from Tif1p wild type and carboxy terminal tagged Tif1p either with FLAG or his-myc tag were compared.

| | Tif1p | Tif1-3xflag | Tif1-His-Myc |
|---|---|---|---|
| **Total number of negatively charged residues (Asp + Glu):** | 22 | 34 | 49 |
| **Total number of positively charged residues (Arg + Lys):** | 29 | 35 | 40 |
| **Instability index:** | **28.50** | **32.92** | **42.34** |
| **This classifies the protein as stable.** | yes | yes | no |

To overcome these shortcomings, a peptide antibody was designed to study the endogenous TIF1 protein. As was previously reported, the alignment of Tif1p and StWhy1 (former P24, Desveaux et al., 2000) revealed a high degree of sequence similarity (Saha et al., 2001). Crystallographic evidence showed that four StWhy1 molecules are most likely organized into a homotetramer, and the tetramerization is mediated by α-helixes 2 and 3 in the C-terminal portion of the protein (Figure 3.9B, Desveaux et al., 2002). To model Tif1p tertiary structure, the Swiss Model Software (htt://swissmodel.expasy.org) was used to compare the solved structure of StWhy1 with Tif1p (Figure 3.9A). The three-dimensional model of Tif1p predicts structural conservation with StWhy1. For StWhy1, it is known that the C-terminal helix mediates tetramer formation. Taking in to account peptide recommendations from in silico analysis, 16 residues (Ac-CSKDNTGKVNIDYSKR-Amide) were selected as an immunogen for rabbit antibody production using services offered by COVANCE laboratories. This peptide is present in the exposed unstructured loop between β3 and β4 that forms part of the whirly domain (Figure 3.9A and B indicated by an arrow).

The affinity-purified antibody recognized a single protein band of the expected size (24 KDa) in western blot analysis of wild type strain (Figure 3.10A). As expected, the intensity of this band was diminished in the TIF1 knockdown strain (Figure 3.10A), suggesting that endogenous Tif1p was specifically detected by the peptide antibody. Immunoprecipitation of tagged Tif1p from Tif1p-HM-C-tag strain with α-myc antibody was recognized by Tif1p peptide antibody (Figure 3.10B). As a control, a strain that contain Mcm6-myc tag was also immunoprecipitated with α- myc antibody.

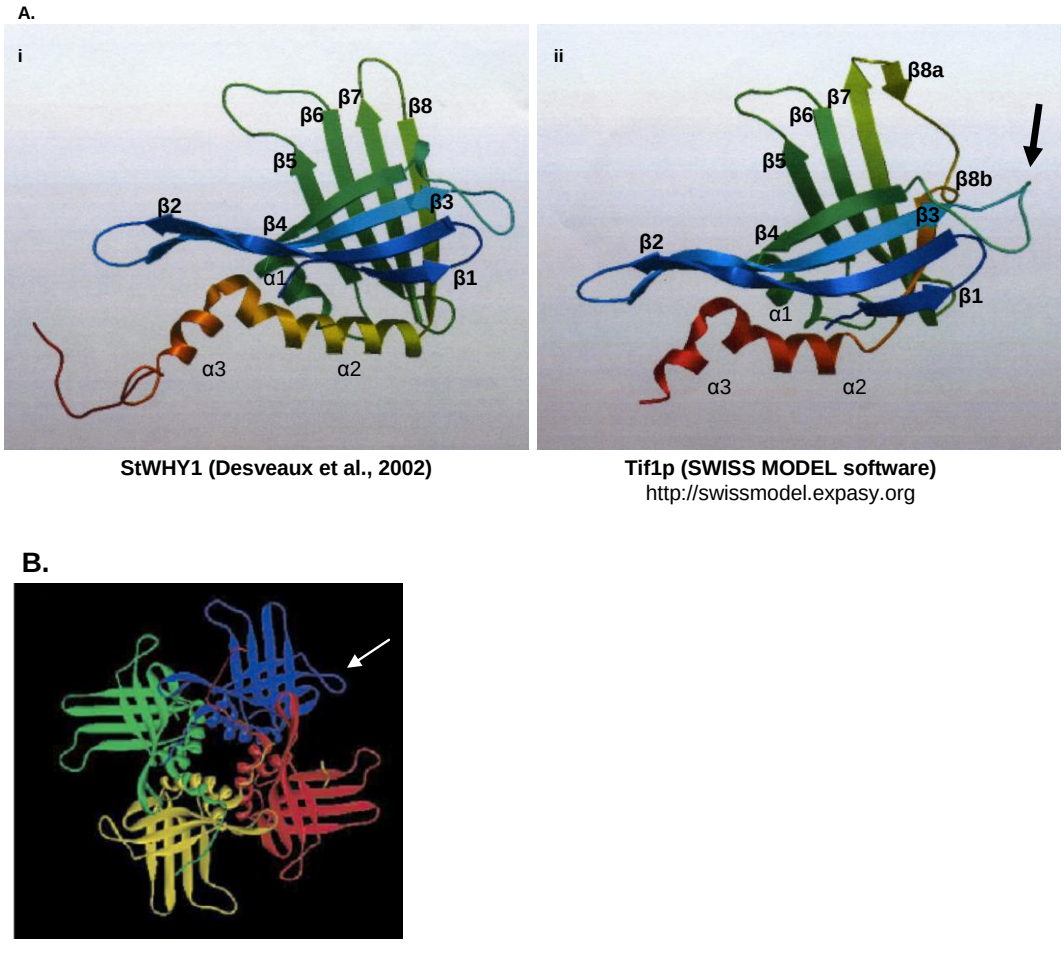


**StWHY1 (Desveaux et al., 2002)**

**Tif1p (SWISS MODEL software)**
http://swissmodel.expasy.org

Figure 3.9 Three-dimensional model of Tif1p is related to the solved structure of StWHY1. A. Ribbon representation of StWHY1 (panel i) from Desvaux e al., 2002 and Tif1p (panel ii) modeled by Swiss Model Software (htt://swissmodel.expasy.org). The arrow demarcates the location of the sixteen residues between β3 and β4 to which Tif1p-peptide polyclonal antiserum was raised against. B. Illustration of tetrameric structure formed by StWHY1 from Desvaux et al. 2002. Each StWHY1 is represented in a different color. The arrow indicates the exposed loop to show the region recognized by Tif1-peptide antibody.

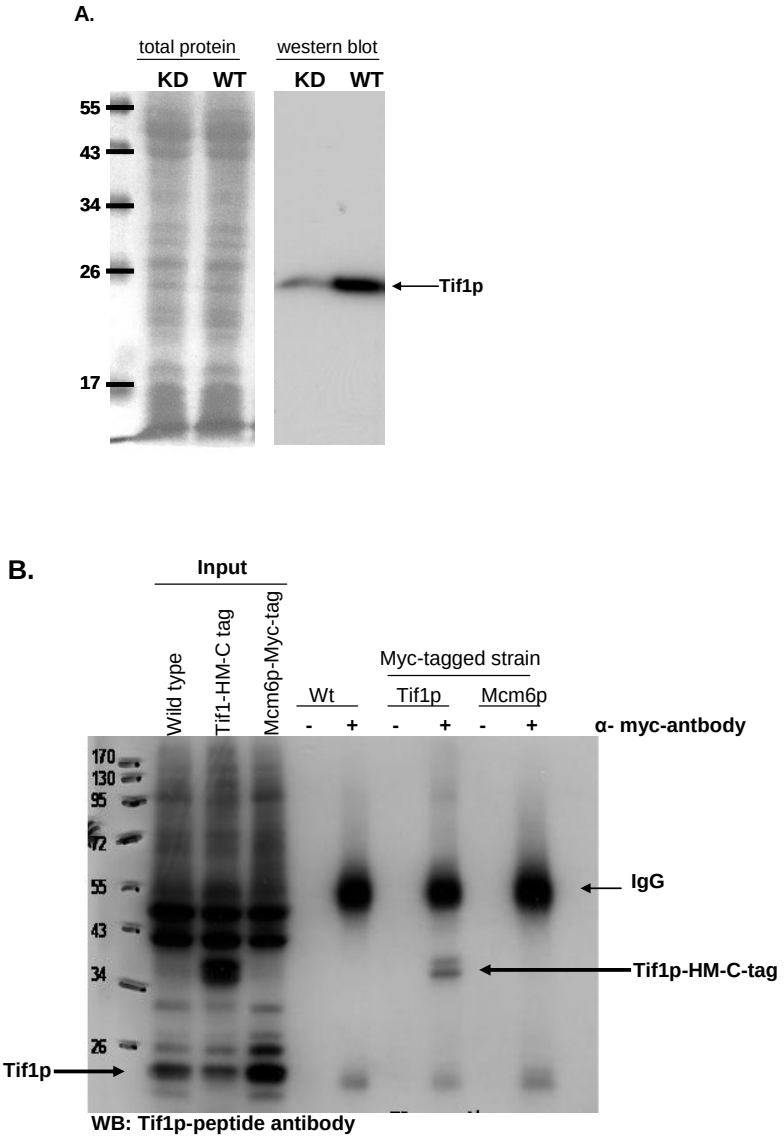


Figure 3.10 Detection of Tif1p with peptide antibody. A. Western blot analysis of whole cell lysate from log phase cultures of wild type (WT) and TIF1-knockdown (KD) strains. Ponceau S was used to stain PVDF membranes and shows the uniform loading of total proteins (left panel). Tif1p-peptide-antibody identified a single band of 24 KDa that correspond to the predicted size for endogenous Tif1p (right panel). B. Immunoprecipitation of myc-tag proteins in S phase synchronized cultures. Samples were crossinked with formaldehyde. Wild type, Tif1p-HM-C-tag and Mcm6p-myc-tag were IP with α-myc antibody. Tif1p was detected pull down in samples by western blot using the Tif1p-peptide-antibody.

No major background was detected with the Tif1p peptide antibody in this strain (Figure 3.10B). Unexpectedly, antibodies against the endogenous

Tif1p only recognize a single band in wild type protein extracts compared with two bands revealed in the tagged Tif1p. This raised two possibilities: (1) that a modified TIF1 protein was not detected by the peptide antibody in the wild type strain, or (2) that a truncated version of Tif1p was expressed in the tagged strain.

To better resolve Tif1p, wild type cytosolic proteins extracts were analyzed on two-dimensional gel electrophoresis (isoelectric focusing pH 6-11 SDS-PAGE). Tif1p peptide antibody recognizes at least three possible isoforms of the native Tif1p which suggested some post-transcriptional modifications (Figure 3.11A). Two of this isoform contain the same molecular weight but slightly different isoelectric points. Using NetPhos 2.0 (http://www.cbs.dtu.dk/services/NetPhos) twelve possible sites for phosphorylation in Tif1p were predicted (seven serines, three tyrosines and two threonines). One of the threonine is included in the sequence of the peptide that is recognized by the antibody against Tif1p opening the possibility that this antibody only recognizes the unphosphorylated isoform of this protein. In order to determine whether Tif1p is phosphorylated at this site, mock and phosphatase treated samples were compared. Alkaline phosphatase was used specifically to release phosphate groups from phosphorylated tyrosine, serine and threonine residues in Tif1p. Also, sodium orthovanadate was used in higher concentrations as a phosphatase inhibitor. Since orthovanadate (0.1-0.5 mM) causes a defect ciliary movement and interferes with elongation of the dividing macronucleus in *Tetrahymena* (Nilsson 1999), the assays to

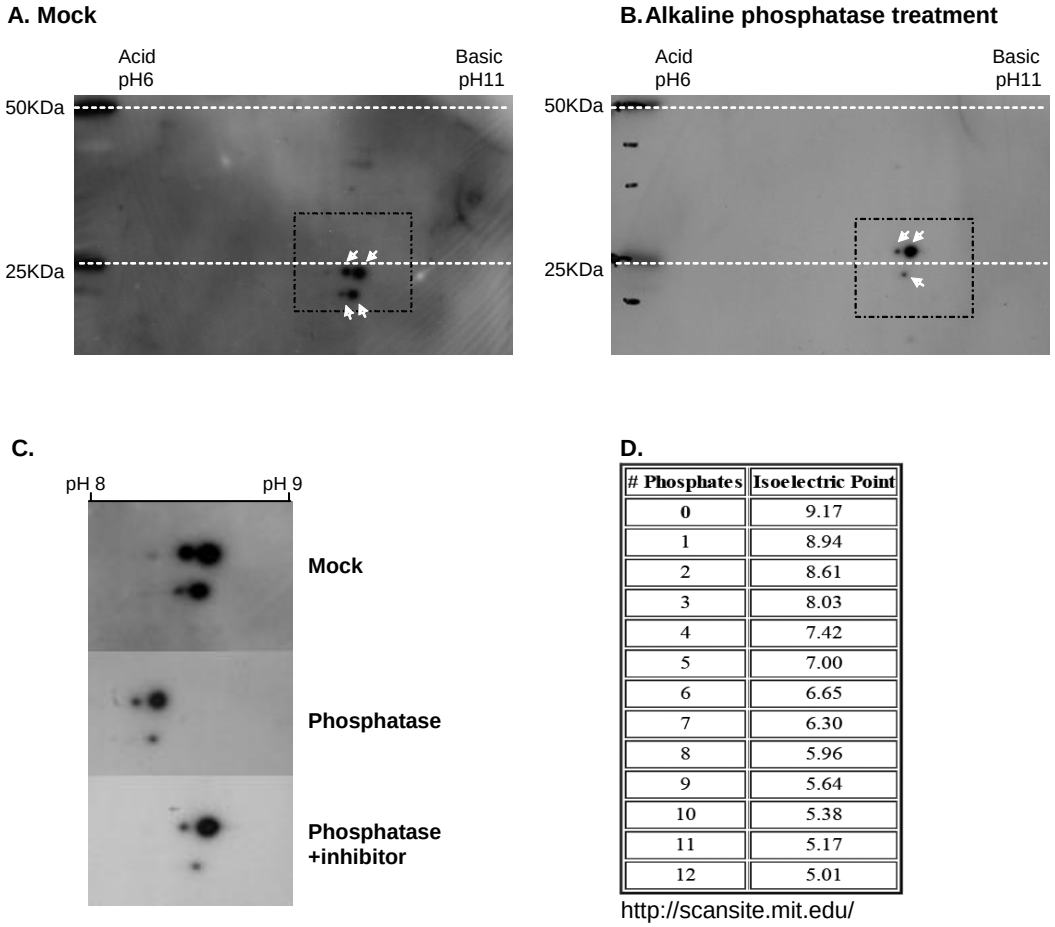


| # Phosphates | Isoelectric Point |
|---|---|
| 0 | 9.17 |
| 1 | 8.94 |
| 2 | 8.61 |
| 3 | 8.03 |
| 4 | 7.42 |
| 5 | 7.00 |
| 6 | 6.65 |
| 7 | 6.30 |
| 8 | 5.96 |
| 9 | 5.64 |
| 10 | 5.38 |
| 11 | 5.17 |
| 12 | 5.01 |

Figure 3.11 Tif1p isoforms. Cytoplasmic extract from wild type strain was analyzed by two-dimensional isoelectric focusing gel (15 % SDS-PAGE pH 6-11). A. Mock treated sample. B. Sample treated with alkaline phosphatase to remove phosphate groups. White dashed lines were addd to help the visualization of the molecular marker. Dashed square are showing the area that was amplified for better visualization. C. Cropped areas showing in detail the changes in pH for Tif1p in the different treatments. Sodium orthovanadate was used as phosphatase inhibitor. D. Analysis of the impact of Tif1p phosphorylation in changes of isoelectric point. This prediction was obtained by submitting the primary sequence of Tif1p in ScanSite pI/Mw (expasy.org/tools). Multiple phosphorylation states are listed and the predicted effect in the molecular weight and isolelectric point of Tif1p.

determine phosphorylation were limited to in vitro approaches.

If phosphorylation of Tif1p blocks its detection by the peptide antibody, the elimination of a phosphate group in Tif1p should increase the signal for the desphosphorylated form. Mock, phosphatase and phosphatase plus inhibitor treated samples were subjected to two dimensional gel electrophoresis and endogenous Tif1p was detected by western blotting. Phosphatase treatment did not increase the western blot signal for Tif1p, arguing against the idea that a phosphorylation prevent the detection of Tif1p. Furthermore, an adjustment of the pH occurred under alkaline phosphatase treatment due to the dephosphorylation of Tif1p (Figure 3.11C). The dephosphorylation was prevented by the addition of orthovanadate to alkaline treatments. The shift in the pH occurs within pHs 8 and 9 (Figure 3.11C) and ScanSite pI/Mw prediction site was used to estimate the number of phosphate groups presents in Tif1p. The addition of three phosphate groups is predicted to change the isoelectric point of Tif1p from pH 9.17 to pH 8.03 (Figure 3.11D). This suggests that Tif1p is potentially phosporylated in three different sites and that phosphorylation does not prevent the detection of Tif1p by the peptide antibody.

**Tif1p abundance during vegetative cell growth and macronuclear development**

As previously described TIF1 mRNA levels are cell cycle regulated, showing a maximal signal during macronuclear S phase, that is approximately seven-fold greater than the abundance of this transcript during development where TIF1 mRNA transcripts levels are constant (Morrison et al., 2005).

Taking advantage of the antibody against the endogenous Tif1p, I followed Tif1p during the vegetative and developmental cycle. Up to this point, I used starvation-refeeding protocol to synchronize cultures for cell cycle studies. However, by using Tif1p-peptide antibody I noticed that starvation treatments leads to a decrease in Tif1p (Figure 3.12A). To avoid this situation, centrifugal elutriation protocols were used to obtain synchronized $G_1$ cultures for further experiments during vegetative cell cycles.

Wild type cultures were synchronized by elutriation and the abundance of Tif1p was followed by western blotting throughout the cell cycle (Figure 3.12B). Early in the cell cycle low levels of Tif1p were detected (Figure 3.12B, 0 and 30 min after elutriation). At the $G_1$/S transition Tif1p levels increased, suggesting that the protein was directly reflecting the abundance already described for TIF1 transcript. However, the down regulation observed at the beginning of the cell cycle was not reproducible in the second cell cycle (Figure 3.12B, 150, 180 or 210 min after elutriation). This data suggest that Tif1p was stabilized after elutriation, but does not necessarily cycling during synchronized vegetative growth. I speculate that Tif1p may be sensing mechanical damage imposed during elutriation, but indeed the origin of this down regulation is unknown. The abundance of Mcm6p was used to show its cell cycle regulated levels during this experiment (Figure 3.12B). Mcm6 is highly abundant during G1 phase and G1/S, followed by a decrease during S phase and its low level is maintained until next G1. For better comparison between Tif1p and Mcm6p during the cell cycle, the abundance of each protein was quantified directly from the western blot signal by using ImageJ (Figure 3.12B). The collective data show no evidence of cyclic pattern for Tif1p

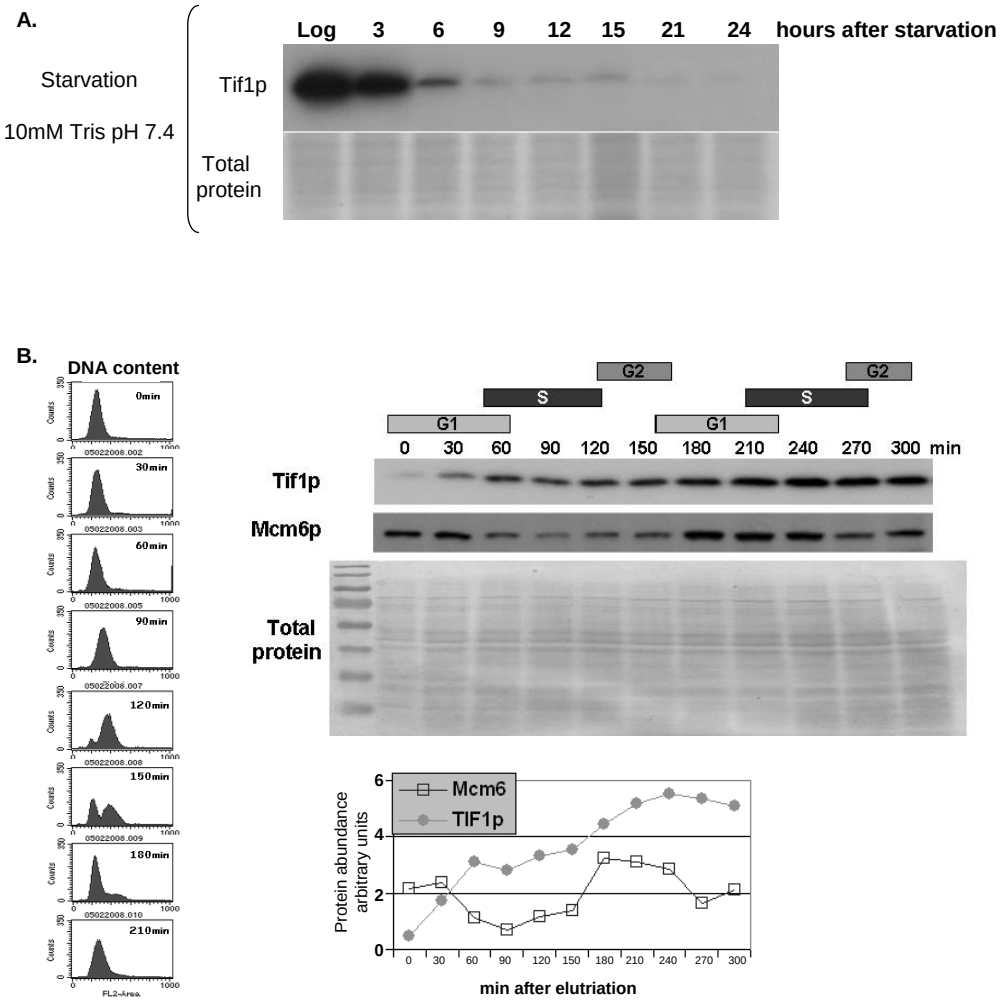


Figure 3.12 Tif1 protein levels during starvation and the vegetative cell cycle of elutriated log phase cells. A. Tif1p peptide antibody was used to monitor endogenous Tif1p in a starved wild type culture (top panel). Samples from log phase culture and different times point samples during starvation were compared. Ponceau S stained membranes (total protein) showing the even loading of protein for different time points. B. Cell cycle analysis of wild type *Tetrahymena* synchronized by elutriation. Histograms showing cell cycle progression in samples taken every 30 min until 210 min. Cell cycle detection of Tif1p and Mcm6p by western blot using the corresponding peptide antibody. Synchronized samples were compared. PVDF membranes were stained with ponceau S to show equal loading of total proteins (left panel).

during the vegetative cell cycle.

The transcription profile for TIF1 extracted from a genome-wide analysis of *Tetrahymena* during starvation and macronuclear development (Miao et al., 2009) was compared with the protein abundance (TGED, TTHERM_00048810; Figure 3.13A). During starvation TIF1 transcript decreased, supporting the results obtained with Tif1p-peptide-antibody that show a gradual decrease in the Tif1p levels during starvation. However, a contradictory piece of data was observed during conjugation. Here the TIF1 transcript shows a prominent increase in expression at two hours, probably associated with meiosis and a shoulder of expression between 10 and 14 h post mating when macronuclear anlagen are developing. These observations correlate with the increased TIF1 binding activity observed in extract from cells undergoing macronuclear development (Mohammad et al., 2000), but disagree with previous mRNA data obtained in our lab where the TIF1 mRNA was present at constant low levels throughout development (Morrison et al. 2005). To address this discrepancy western blotting was performed with Tif1p peptide antibody to directly monitor the levels of Tif1p during development. Tif1p was not detected during the pre-meiotic and post-zygote S phases (2-6 h) or during macronuclear development (9-24 h) (Figure 3.13B). In case that Tif1p is actually expressed during development Tif1p levels are very low compared to vegetative growth and the detection by western blotting was not sensitive enough. These data indicate that Tif1p is down regulated in mating cells and exconjugant progeny.

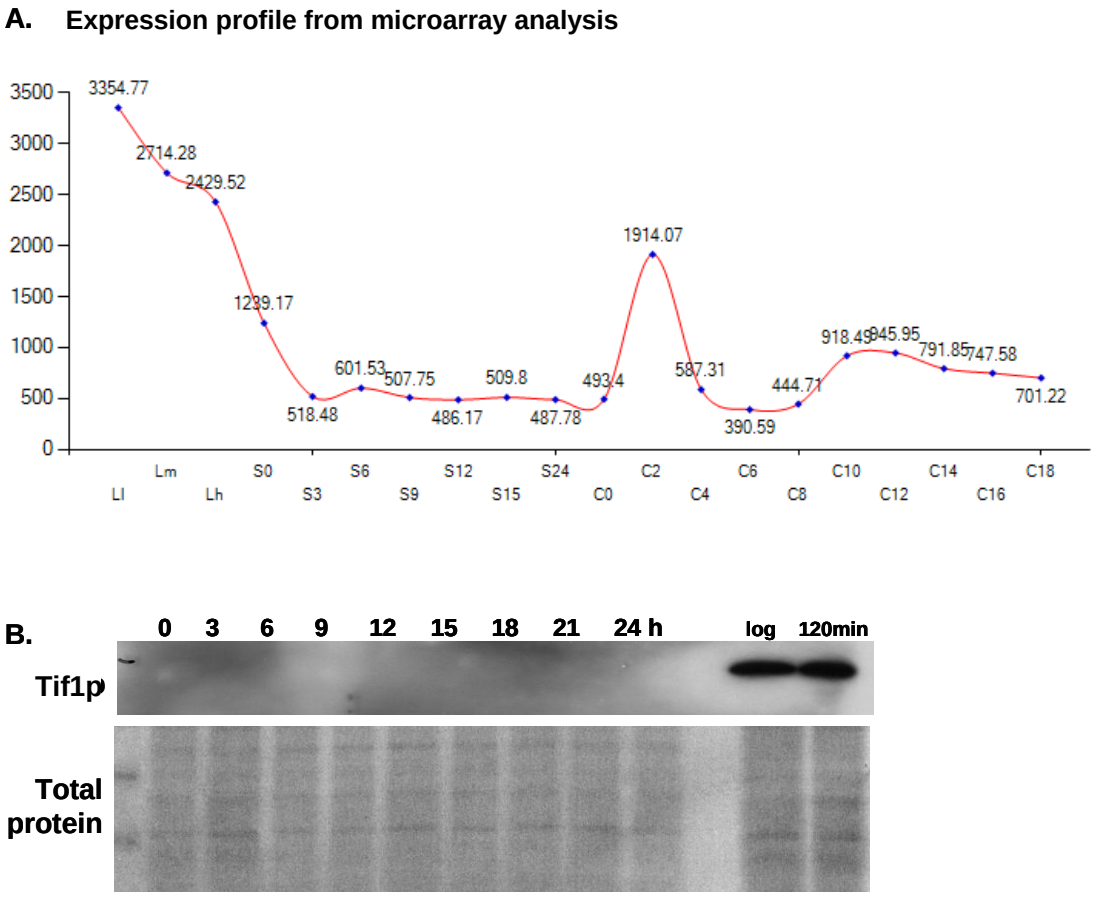


Figure 3.13 Expression profile for TIF1. A. Microarray data for TIF1 (gene ID TTHERM_00048810 from http://tged.ihb.ac.cn). Growing cells, **L-l**, **L-m** and **L-h** correspond respectively to ~$1\times10^5$ cells/ml, ~$3.5\times10^5$ cells/ml and ~$1\times10^6$ cells/ml. For starvation, ~$2\times10^5$ cells/ml were collected at 0, 3, 6, 9, 12, 15 and 24 hours (referred to as **S-0, S-3, S-6, S-9, S-12, S-15** and **S-24**). For macronuclear development, equal volumes of B2086 and CU428 cells were mixed, and samples were collected at 0, 2, 4, 6, 8, 10, 12, 14, 16 and 18 hours after mixing (referred to as C-**0, C-2, C-4, C-6, C-8, C-10, C-12, C-14, C-16** and **C-18**). B. TIF1 protein is not detected during macronuclear development. Western blotting showing the abundance of Tif1p every 3 h for 24 h during macronuclear development. A logarithmically growing culture and a starved-refed synchronized culture sample taken at 120 min after refeeding are shown as positive controls.

**Analysis of chromatin binding sites for Tif1p using peptide antibody**

ChIP assays were used to examine the specific binding of Tif1p to type I element in a log phase culture (Figure 3.14A). After crosslinked chromatin was sheared the native Tif1p bound to DNA was immunoprecipitated with αTif1p peptide antibody. Standard PCR with specific set of primers were used to determine the enrichment of specific DNA fragments in the immunoprecipitated fraction. A marginal but reproducible enrichment of type I elements present at the origin was observed (Figure 3.1, domain 1), arguing that specific binding occurred. However, no enrichment of the type I element at the promoter was detected (Figure 3.14A). As a negative control, the binding of Tif1p to the coding region of β-tubulin was analyzed and no enrichment was detected suggesting that the binding of Tif1p was specific for type I elements. Since the macronucleus contains only 45 copies of non-rDNA chromosome versus 10,000 copies of the rDNA, these data opened the possibility that the absence of enrichment of the β-tubulin locus could be a detection issue due to the difference in the copy number. To resolve this, a sequence analogous to type I element present in the RAD51 promoter was analyzed and added as a second ChIP control. Type I-like sequence at RAD51 promoter showed enrichment similar to the rDNA origin. These results suggest that Tif1p binding is specific to type I element.

Given that Rad51 mRNA is induced by DNA damage and the fact that Tif1p is able to bind to RAD51 promoter, suggested that Tif1p could be modulating RAD51 expression during genotoxic stress. The binding of Tif1p to RAD51 promoter sequence

was further analyzed by in vitro assay and the collective data will be shown in the Chapter IV of this dissertation.

The modest enrichment observed at the rDNA origin in log phase cultures (Figure 3.14A) suggested that the binding of Tf1p might be transient during the cell cycle. Since Tif1p acts as repressor of replication, it was expected that its binding would be high to origins in G1, and low in late S phase. To address this possibility, ChIP assays were used to analyze the binding of Tif1p in synchronized cultures. A $G_1$ population of wild type cells obtained by centrifugal elutriation was cultivated and samples of the synchronized early and late S phase were compared to a $G_1$ culture. Since the levels of Tif1p were low in recently elutriated cells (Figure 3.12B), samples representing $G_1$ phase were obtained at the beginning of the second cell cycle (Figure 3.14A, 180 min). As a negative control the binding of Tif1p to non-rDNA sequences was analyzed, here TIF1 coding region did not present any evidence of Tif1p binding. Segments spanning type I elements at the origin and rDNA promoter were amplified (Figure 3.14A). A very modest enrichment of the rDNA origin and promoter regions was detected (Figure 3.14A). No evidence for cell cycle regulation was observed.

Since Tif1p is permanently bound to rDNA origins throughout the cell cycle, models 1 and 2 (Figure 3.2) cannot explain the inhibitory effect of Tif1p in the regulation of DNA replication. However, model 3 suggests that Tif1p is always bound at the origin and the activation of origins is controlled by a modification in Tif1p which promote the recruitment of the MCM complex (Figure 3.2, model 3). In this case Tif1p should be included in the activated pre-RC complex.

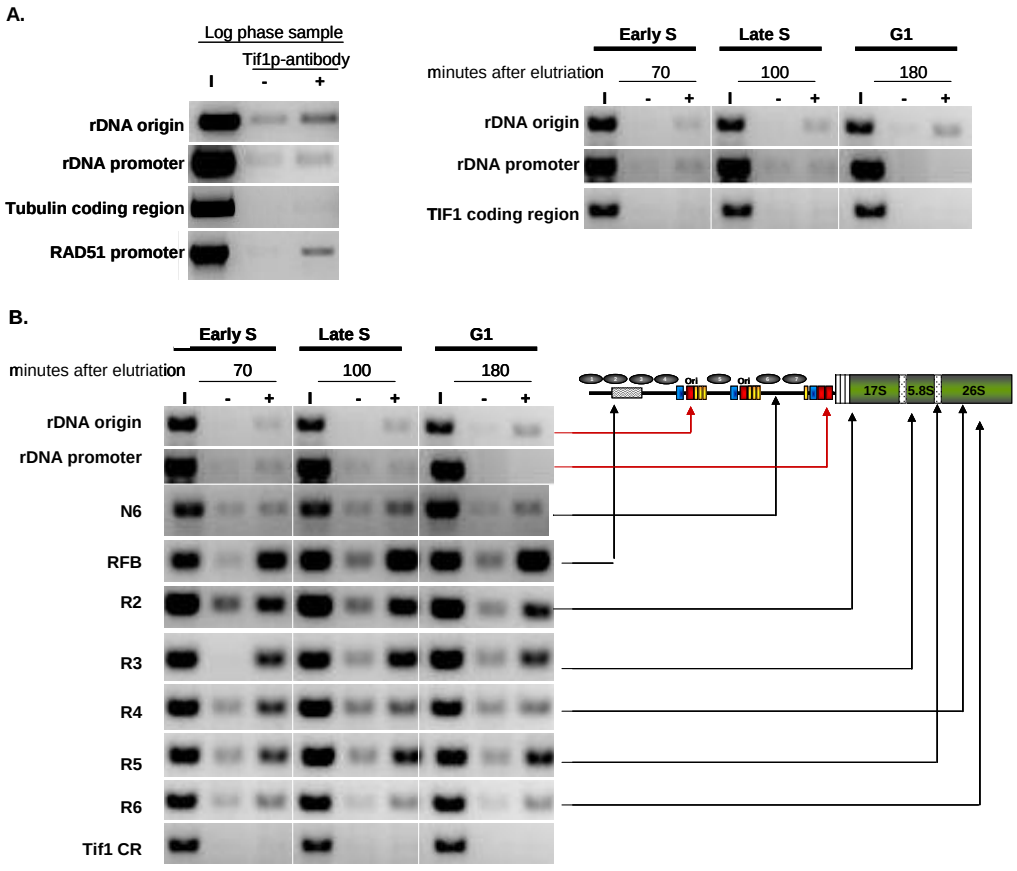


Figure 3.14 In vivo association of Tif1p with the rDNA minichromosome. A. ChIP analysis of wild type strain in log phase culture (right panel) and synchronized cultures (left panel) using Tif1p-peptide antibody. Crosslinked, sheared chromatin was immunoprecipitated with Tif1p-peptide antibody. After reverse the crosslinking, immunoprecipitated DNA was amplified using primer sets specific to the regions indicated. (1:100) dilution of total input DNA (I), immunoprecipitated samples with (+) or without (-) antibody. B. (right panel) Binding of Tif1p to rDNA sequences in synchronized vegetative cells. Wild type culture was synchronized by elutriation and samples from G1, early S and late S phase of the cell cycle were compared. (Left panel) diagram of one copy of rDNA minichromosome showing regulatory elements in the 5' NTS and coding regions fragments that were amplified.

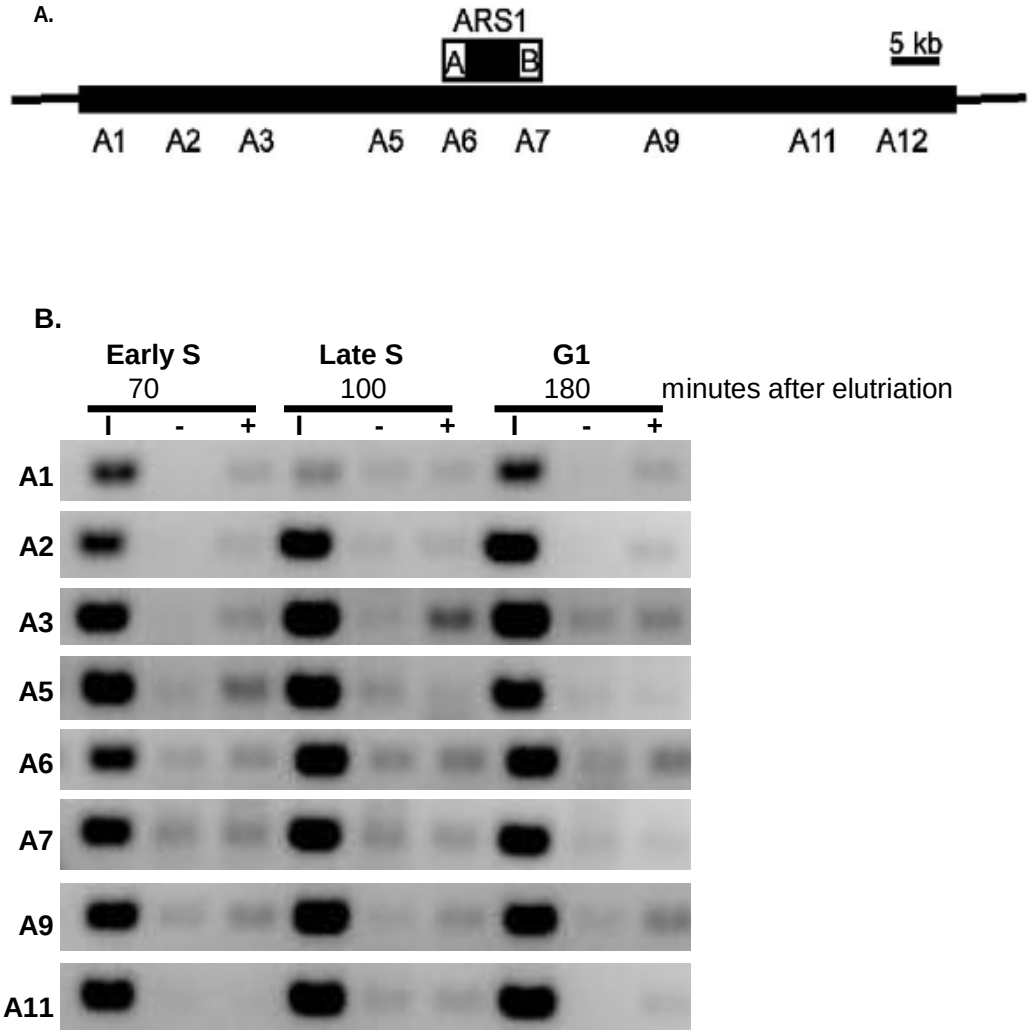


Figure 3.15 Cell cycle associate binding of Tif1p to non-rDNA sequences. A. Diagram showing 60Kb spanning the non-rDNA origin of replication, ARS1, in the endogenous macronuclear chromosome. Sequences detected by PCR are indicated (A1 to A12) B. ChIP analysis of the ARS1 surrounding sequences (showed in A) with tif1p peptide antibody. (1:1000) dilution of total input DNA (I), immunoprecipitated samples with (+) or without (-) antibody.

Along with the origin regions rDNA intervals where the binding of Tif1p was not predicted to occur were tested by PCR from the immunoprecipitated fractions as controls (Figure 3.14B): these segments included developmentally regulated replication fork barrier (RFB, Zhang et al., 1997), sequences close to the promoter (previously showed to be occupied by nucleosome 6 (N6)), and randomly chosen sequences in the rDNA coding region (R2-6) (Figure 3.14B). An unexpected extremely robust enrichment of sequences from coding region of rDNA was observed (Figure 3.14B, R2, R3, R4, R5, R6). These fragments did not contain a type I-like sequences suggesting that the binding of Tif1p to rDNA coding region is not sequence specific.

To test whether the enrichment seen at rDNA coding region was common to other macronuclear chromosomes a 60 Kb segment encompassing the 0.9 Kb non-rDNA origin of replication, ARS1, was analyzed by ChIP (Figure 3.15A, A1-12). ARS1A and B are the only non-rDNA origins of replication described for *Tetrahymena* (Donti et al., 2009). In contrast to rDNA coding sequences no strong enrichment was observed in this interval. Modest enrichment was detected for regions A3 and A5, similar to the signal for rDNA origin and promoter (Figure 3.15B). However, neither of these segments functions as a replication initiation site in endogenous non-rDNA chromosome.

To better compare these results, amplified PCR products were quantified using ImageJ program. The same area for each amplified fragment was quantified. No antibody treated samples count as a background signal and the values were subtracted from the immunoprecipitated sample. Enrichment was normalized to the input and plotted as a function of the phase in the cell cycle (Figure 3.16). In general, rDNA

coding regions (CR2-6) were highly enriched in the immunoprecipitated fraction, suggesting they are preferred binding sites for Tif1p. Surprisingly the expected binding sites for Tif1p, the origin and rDNA promoter, were not enriched greater than 15% of the input. Randomly chosen non-rDNA sequences from the ARS1 replicon were enriched up to a 25%, which is higher than rDNA regulatory sequences.

These results revealed that the binding of Tif1p extends beyond the A- and T-rich sequences present at the rDNA origin and promoter, suggesting that rDNA coding regions may be targeted for the binding of Tif1p. These unexpected findings rise the possibility that Tif1p is preferentially sequestered in the rDNA minichromosome.

**Discussion**

Tif1p is a non-ORC protein originally characterized as a single-strand binding protein that interact specifically with type I elements at the 5' NTS of the rDNA minichromosome in *Tetrahymena* (Umthun et al., 1994; Saha & Kapler, 2000). *In vivo* footprinting assays revealed that Tif1p was responsible for the occupation of the A-rich strain at the origin and T-rich strand at the promoter region of rDNA, suggesting that Tif1p might play a role in the recruitment of machineries for replication and transcription initiation, respectively (Saha et al., 2001). Furthermore, *in vivo* binding assays also revealed that Tif1p was able to protect sequences corresponding to PSE, emphasizing the idea that Tif1p plays a role in the regulation of replication.

Studies with TIF1 hypomorphic strain revealed that the deficiency of Tif1p resulted in early firing of the rDNA origin, suggesting that Tif1p acts as an inhibitor of

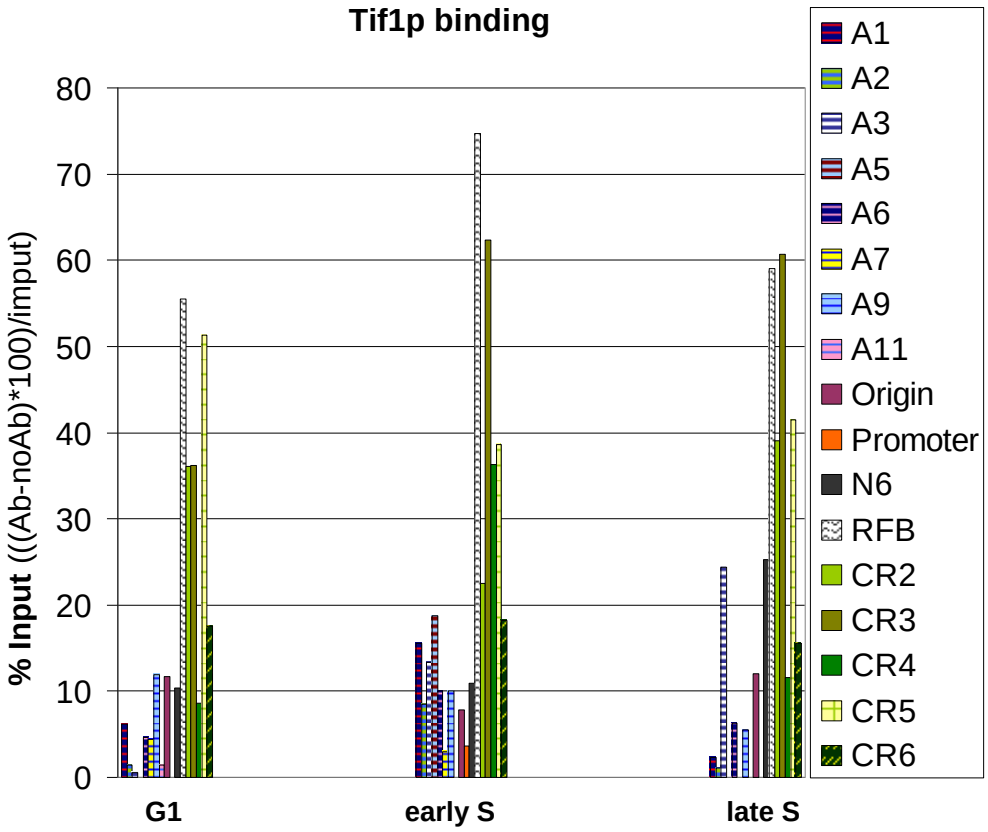


Figure 3.16 Quantification of the binding of Tif1p to rDNA and non-rDNA regions.

replication initiation (Morrison et al., 2005). In addition, mutant strains displayed defects in the progression through macronuclear S phase and cell division, loss of micronuclear chromosomes and defects during macronuclear development (Morrison et al., 2005, Yakisich et al., 2006). Furthermore, TIF1 mutants accumulate double strand break the in absence of genotoxic stress and present hypersensitivity upon DNA damage induction, suggesting that Tif1 is necessary for the activation of the DNA damage response (Yakisich et al., 2006). These collective experimetns revealed that Tif1p is responsible for the maintenance of genome integrity in the micro- and macronucleus

To monitor Tif1p during cell cycle progression, I used several strategies to generate a tagged Tif1p. The addition of small epitopes to Tif1p has a profound impact on cells. Similar to the depletion of wild type Tif1p in TIF1 knockdown strains, the addition of a FLAG tag to the carboxy terminus of Tif1p prevents successful completion of macronuclear development. Cellular phenotypes associated with TIF1 knockdown strains were also seen during vegetative growth of cells expressing N-terminal tagged TIF1. These phenotypes include the presence of numerous macronuclear extrusion bodies and abnormal macronuclear division in vegetative growing cells. These findings confirm that Tif1p is crucial for micro- and macronuclear genomic stability. The addition of a his-myc tag to the C-terminus of Tif1p did not arouse afore mentioned abnormal phenotypes or defects in the oligomerization of Tif1p. However, the Tif1p-HM-C tagged protein failed to interact with rDNA origins as determined by ChIP. Since untagged Tif1p binds to origin and promoter *in vivo*, we conclude that the C-terminus of Tif1p plays a role in DNA recognition.

Tif1p is a non-ORC protein that regulates the timing for rDNA replication and is involved in the checkpoint response. Non-ORC proteins play a key role in the establishment of initiation of replication in eukaryotic chromosomes. Two common features of non-ORC initiation proteins are their multifunctional roles and the fact that are essential for cell viability (Mucenski et al., 1991). The *S. cerevisiae* transcription factor, Abf1, is one of the best studied non-ORC origin binding factors. Abf1 originally described as a sequence specific DNA binding protein, is responsible for promoting the correct nucleosome positioning at sequences adjacent to the origin to favor ORC binding. A recent genome-wide analysis that combined computational predictions of Abf1 binding sequences with DNA binding assays, revealed that Abf1 associates with numerous DNA sequences that were previously uncharacterized (Schlecht et al., 2008). Furthermore, surprising results showed that Abf1 had two-fold higher affinity for sequences that deviate significantly from the consensus binding site (Beinoraviciute-Kellner et al., 2005). These data suggest that Abf1 has considerable flexibility in the recognition of target sequences (Diffley & Stillman, 1988; Marahrens & Stillman, 1992; Schlecht et al., 2008).

Tif1p shares sequence similarities with a nuclear transcription factor in the plant, *S. tuberosum*, StWhy1. Like Tif1p, StWhy binds to single-stranded DNA and form homotetramers by the association of a 24 KDa subunit. StWhy1 belongs to such called whirly family due to the whirling appearance of its quaternary structure (Desveaux et al., 2002). Whirly proteins have been characterized as transcriptions factor in different plants systems (Desveaux et al., 2004; Xiong et al., 2009). *A. thaliana* codes for three

homologues of StWhy1 (AtWhy1-3), which have been implicated in modulation of telomere length, and promote genomic stability of circular plastids and mitochondrial genomes (Cappadocia et al., 2010; Marechal et al., 2009; Yoo et al., 2007). A recent detailed report of the crystal structure of DNA-Why2 complex in *Arabidopsis* showed that single-stranded DNA is preferentially bound in a sequence-independent manner (Cappadocia et al., 2010). Cappadocia and colleagues showed that the mechanism for this binding is dominated by hydrophobic interactions between adjacent nucleotides and aromatic/hydrophobic interaction between protein residues. They also propose that the binding of whirly proteins to single stranded DNA in the nucleus is limited by the low concentration of this protein in this organelle relative to plastids and mitochondria (Krause et al., 2005).

Since Tif1p and ORC bind to complementary DNA sequences at the origin it has been suggest that Tif1p directly affects the binding or activation of TtORC at the rDNA origin. In this Chapter I set out to analyze how Tif1p regulates initiation of rDNA replication. The works presented here show that the binding of Tif1p extends beyond rDNA origin and promoter. Chromatin-immunprecipitation with a Tif1p specific antibody was used to examine Tif1p occupancy of binding sites at the rDNA origin and promoter during $G_1$, early S and late S phase. To our surprise only modest enrichment of type I element-containing fragments at the rDNA origin and promoter was observed. Furthermore, the binding of Tif1p to rDNA origin is not cell cycle regulated, suggesting that Tif1p is a component of pre-RC and the activation of these origins occur while Tif1p is bound (Figure 3.2, model 3).

Interestingly, a much stronger enrichment of chromatin was detected in randomly chosen sequences in the rDNA coding region and 5' NTS (RFB). Considering the high content of AT-rich sequences in *Tetrahymena*, it would be easy to imagine that Tif1p could be distributed throughout the whole genome. However, the in vivo chromatin binding of Tif1p appears to predominantly involve the rDNA minichromosome. Binding of Tif1p to non-rDNA minichromosomes was assayed by chromatin-immunoprecipitation across a 60 kb segment spanning the endogenous ARS1 chromosomal locus. Minor enrichment was observed in sequences that flank ARS1A replicon (Figure 3.15), fragments A3 during late S phase and A5 in early S phase and a very marginal $G_1$ phase binding was detected in A6, which include the non-rDNA origin, ARS1A. These ChIP signal were comparable to those observed for the rDNA origin and promoter and markedly lower than enrichments of rDNA coding region sequences. Donti and colleagues (2009) showed that ORC1p binds to A6 segment in synchronized $G_0/G_1$ cultures and dissociates during S phase when TtORC is degraded. This implies that ORC and Tif1p populate non-rDNA origins simultaneously. These suggest that the model proposed to explain how Tif1p inhibit rDNA replication (Figure 3.2, model 3) can be generalized for non-rDNA origins.

With respect to the cellular distribution of Tif1p, no mitochondrial targeting peptide signal can be predicted from Tif1p sequence (data not shown). However, the alignment of the original peptide sequence of Tif1p obtained by Edman degradation with the predicted protein sequence shows differences at the amino terminus (23 residues) suggesting that some transit peptide sequences might be lost during the purification of

Tif1p (Saha et al., 2001). Considering that Tif1p was purified from a S100 extract, this opens the possibility that Tif1p may be targeted to a specific subcellular region before it accumulates in the cytoplasm. If this was the case, the binding of Tif1p in the macronucleus could be also limited by the accessibility of Tif1p, as was proposed for whirly proteins in plants. However, once in the nuclear compartment Tif1p would need to find several unwound segments in the rDNA in order to bind to. Could this mean that the rDNA in the macronucleus is intrinsically unwound, and that Tif1p has a protective role to ensure genomic stability, especially to the rDNA?

Recent studies have shown that structural components of the nucleolar remodeling complex (NoRC) and the number of rDNA arrays in higher eukaryotes, mediate the establishment of rDNA silencing and the formation of heterochromatin in the nucleus (Guetg et al., 2010; Paredes & Maggert, 2009), reinforcing the idea that genomic stability is highly dependent of the formation and maintenance of heterochromatic regions (Peng & Karpen, 2008). In *Tetrahymena*, the macronucleus is responsible for gene expression during vegetative cell cycles; it is amitotically maintained during vegetative growth and its chromosomes lack any apparent chromosome condensation (Tucker et al., 1980; Karrer, 2000). The rDNA minichromosomes are contained in approximately 100 nucleoli distributed around the macronuclear periphery, and are physically isolated from other chromosomes (Nilsson & Leick, 1970). Nucleoli segregation during macronuclear amitotic division is independent of the bulk chromosomes (Cervantes et al., 2006). Little is known about classical heterochromatin formation in fully developed macronuclei compared to the detailed

studies of micronuclei developing macronucleus (Chalker, 2008). In fact, the best recognized factor involved in chromatin organization in macronuclear chromosomes is the linker histone H1. Histone H1 is dephosphorylated during development when the old macronucleus turns into a highly condensed structure and averts transcription, priori to its complete degradation (Lin et al., 1991). Macronuclear histone H1 is phosphorylated in macronuclear chromatin of vegetative growing cultures, suggesting a link to chromatin decondensation and gene transcription (Allis et al., 1980). Macronuclear histone H1 is not essential for viability, but the chromatin of this nucleus in H1 knockout strains is less condensed than in wild type cells (Mizzen et al., 1999; Shen et al., 1995). The evidence that a TIF1-deficient strain conveys global defects in *Tetrahymena* cells (Morrison et al., 2005) and the observation of a homogeneous binding of Tif1p to rDNA minichromosome support the idea of Tif1p being responsible for protection of rDNA minichromosomes.

# CHAPTER IV

# CHARACTERIZATION OF THE DNA DAMAGE RESPONSE DURING S PHASE IN TETRAHYMENA TERMOPHILA

## Overview

*Tetrahymena thermophila* has been the source of many paradigm shifting discoveries that have changed our understanding of fundamental molecular biological processes, such as the maintenance of chromosome ends, epigenetic remodeling of chromatin and the catalytic capacity of RNA. However, the mechanisms that regulate *Tetrahymena* cell cycle are poorly understood. *Tetrahymena* contains two functionally distinct nuclei that replicate and divide at different stages of the cell cycle, and partition daughter chromosomes by remarkably different mechanisms. Despite these differences, our previous studies revealed that *Tetrahymena* elicits a DNA damage cell cycle checkpoint response in both the diploid mitotic micronucleus and polyploid amitotic macronucleus, and that this pathway shares common characteristics with checkpoint signaling in other eukaryotes.

Induction of DNA damage with the alkylating agent, MMS, or depletion of DNA precursors with hydroxyurea, HU, triggers S phase checkpoint-induced cell cycle arrest in *Tetrahymena* that is most likely mediated by an ortholog of the human ATR/budding yeast Mec1 kinase. Furthermore, mutations in factors that directly regulate replication initiation or elongation (ORC1, MCM6, TIF1) activate this checkpoint response.

Abrogation of the checkpoint with the inhibitor caffeine leads to elevated levels of DNA damage, aberrant macronuclear division and micronuclear genome instability.

Several features of the *Tetrahymena* macronucleus suggest that the requirements for accurate and complete duplication of the genome may be more relaxed compared to other eukaryotes. They include the polyploid composition of the somatic macronuclear chromosomes, and the absence of a mitotic mechanism for segregation of daughter chromosomes. In this chapter I studied the DNA damage response to replication stress. To distinguish between $G_1$ and S phase checkpoint responses, DNA damaging agent MMS and HU were added before and during periods for macronuclear DNA synthesis. Here I provide evidence that HU and MMS elicit different checkpoint responses that differentially impact on the fate of Mcm6p, a subunit of the DNA helicase, present at all replication forks. Mcm6p was stabilized in cells treated with MMS at $G_1$ or S phase, presumably allowing for the rapid resumption of DNA replication once DNA damage is repaired. In sharp contrast, treatment with the second agent, HU, resulted in the degradation of Mcm6p when the drug was added at $G_1$ or S synchronized cells. The removal of HU from S phase arrested cells resulted in the resumption of DNA replication, macronuclear division and cytokinesis after a brief lag. Aberrant macronuclear division was not elevated in recovered cells compared to wild type controls, suggesting that the integrity of macronuclear chromosomes was not compromised.

To obtain a better understanding of the $G_1$ and S phase checkpoint response, flow cytometry and fluorescence microscopy were used to assess cell cycle progression in

genotoxic stressed cells, monitoring DNA content of the polyploid macronucleus, cellular and macronuclear division, and the potential formation of macronuclear extrusion bodies. These studies uncovered a novel response to DNA damage induced during S phase, in which the S phase DNA content returns to a $G_1$/1N DNA level without the completion of DNA replication (formation of $G_2$/2N peak) and/or cell division. The formation of the new $G_1$/1N peak was not associated with the biogenesis of macronuclear extrusion bodies, previously shown to remove "excess DNA" that arises from asymmetric macronuclear division. While the mechanism for re-establishing a $G_1$/1N DNA content remains to be determined, we predict that ATR is not directly involved, since this apparent cell cycle regression in not inhibited by caffeine. Pulse chase experiments with tritiated thymidine suggest that the newly synthesized DNA is actively degraded in MMS-treated S phase cells.

The role of ATR in checkpoint activation was further investigated in wild type and ATR-mutant strains and similar to higher eukaryotes, ATR is required during unperturbed vegetative cell cycles in *Tetrahymena*. Compared to wild type, ATR-deficient cells contained elevated levels of the DNA repair protein, Rad51p, when cultured in the absence of exogenous genotoxic stress. Studies with synchronized cultures suggest that DNA damage occurs predominantly during macronuclear S phase.

Finally, in vitro analysis of kinase activity in extracts from mock and HU-treated *Tetrahymena* revealed that DNA damage stimulates a response distinct from that described in other eukaryotes. Budding yeast and mammalian cells induce a characteristic and prominent autophosphorylation of the ATR/Mec1 substrate, Chk1

following activation of the intra-S phase checkpoint. While *Tetrahymena* contains a bona fide ATR ortholog and several candidate Chk1 genes, in vitro kinase assays of HU-treated *Tetrahymena* leads to a decrease in the phosphorylation state of unidentified protein compared to mock-treated controls. Our findings on the differential regulation of Mcm6p, unprecedented cell cycle response to S phase-induced DNA damage, and protein phosphorylation in stressed cells, collectively illustrate that *Tetrahymena* has developed novel strategies to cope with DNA stress and the failure to completely duplicate chromosomes in the polyploid amitotic macronucleus.

## Introduction

In response to exogenous and endogenous genotoxic stress, cells have evolved mechanisms to coordinate cell cycle progression, DNA replication, DNA repair and chromosome segregation to maintain genome integrity. When the level of DNA damage exceeds a threshold, cell cycle progression is arrested to allow more time for repair. The DNA damage response includes an intricate association of proteins that can be regulated at multiple levels.

The intra-S phase DNA damage checkpoint maintains genome integrity by sensing replication stress. Activation of effectors proteins arrests cell cycle progression by blocking the firing of late replication origins, stabilizing stalled replication forks, and recruiting DNA repair proteins to arrested forks (Abraham, 2001; Cortez, 2005). In the presence of DNA damaging agents, such as methyl-methanesulphonate (MMS) (Tercero & Diffley, 2001) or inhibitors of DNA replication, such as aphidicolin or hydroxyurea

(HU) (Santocanale & Diffley, 1998), the activity of the MCM2-7 replicative helicase and DNA polymerase are uncoupled at replication forks, generating long stretches of single-stranded DNA (Byun et al., 2005). Replication protein A (RPA) coats the exposed single-stranded DNA and recruits the apical checkpoint protein kinase, ATR (ataxia telangiectasia and Rad3 related protein), to activate the checkpoint signaling pathway. ATR is loaded onto stalled replication forks in a complex with ATRIP (ATR interacting protein) (Cortez et al., 2001; You et al., 2002; Zou & Elledge, 2003). A parallel event that is essential for optimal ATR activation is the formation of a complex between Rad9, Rad1 and Hus1 (9-1-1) that is recruited to DNA damage foci by Rad17 (Zou et al., 2002). The 9-1-1 complex facilitates the phosphorylation and recruitment of several other factors that are required to promote phosphorylation of downstream ATR targets, such Chk1 kinase (Byun et al., 2005; Delacroix et al., 2007; Liu et al., 2000; Roos-Mattjus et al., 2003; Zou et al., 2002) Chk1 represses initiation of replication from late origins by phosphorylating Cdc25 inducing its degradation and preventing activation of Cdk2, thereby blocking progression though S phase (Mailand et al., 2002; Shirahige et al., 1998). Activation of ATR and ATM can be inhibited by the addition of caffeine to the growth media, and this effect is conserved in all examined eukaryotes (Sarkaria et al., 1999). Following repair, stalled replication forks must be re-activated, and late firing origins must be rendered competent to assure that each chromosome is fully replicated once during cell cycle.

In addition to their roles in the DNA damage checkpoint response ATR, ATM (apical checkpoint kinases) and Chk1 (effector kinase) regulate the activation of

replication origins in unperturbed S phases. In higher eukaryotes cells ATR and Chk1 are essential for normal cell growth and maintenance of genomic stability (Brown & Baltimore, 2000; Liu et al., 2000; Wakabayashi et al., 2010).

In several model systems, mutations that compromise the function of MCM complex are associated with genome instability and an increased level of DNA damage, suggesting that MCM complex is essential for an adequate response. In mammalian cells Mcm 2 and 3 are phosphorylated in response to treatments with DNA damaging agents (Cortez et al., 2004). Also, in mammalians cells, another member of the putative helicase, Mcm 7, has been shown to be directly associated with ATRIP. Furthermore, in yeast the C-terminal domain of Mcm 4 is essential to prevent excess of single strand DNA formation during HU treatment (Nitani et al., 2008). All these observations suggest a key role for the MCM complex during the DNA damage response.

*Tetrahymena thermophila* has been used as a model system to study the DNA damage response during the vegetative cell cycle. Like most ciliated protozoa, *Tetrahymena* contains two genetically related, but functionally distinct nuclei within a common cytoplasm: the diploid micronucleus and the polyploid macronucleus (Figure 4.1B). The micronucleus plays important functions acting as the reservoir of genetic material that is exchanged during conjugation. It is actively transcribed during a brief period during development and exists as transcriptionally inactive heterochromatin during the vegetative cell cycle. Accordingly, micronuclear chromatin is enriched with histone modifications largely associated with heterochromatic DNA, like methylation of histone H3-K9 and H3-K27 (Chalker, 2008).

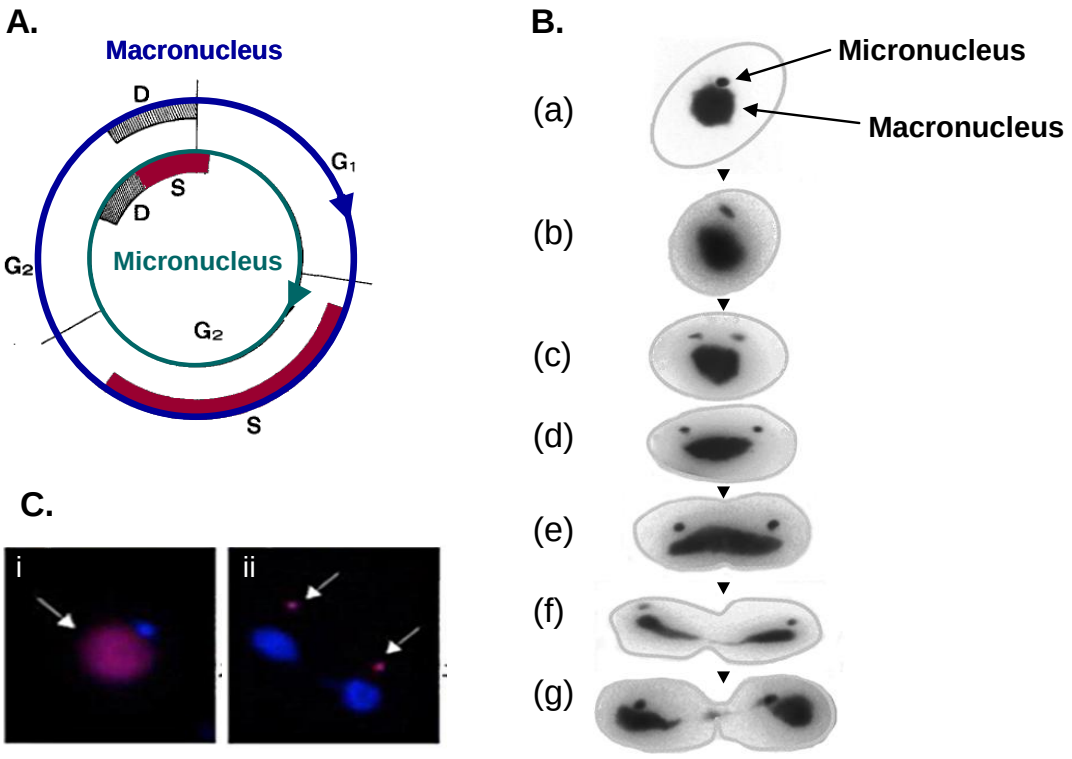


Figure 4.1 Vegetative cell cycle in *Tetrahymena*. A. Illustration for the cell cycle in *Tetrahymena*. Representation of events during vegetative cell cycle for micronucleus (inner circle) and macronucleus (outer circle), modified from Flickinger, 1965. (G) gap phase, (S) synthesis phase, (D) cell division B. Composite of *Tetrahymena* cell division. C. Micrograph extracted from Morrison et al., 2005. Showing DNA stained with Dapi (blue staining) and BrdU incorporation (red staining, white arrow) during (i) macro and (ii) micronucleus replication period.

The macronucleus serves as the somatic nucleus, it is transcriptionally active during vegetative growth and contains all the features of euchromatin, such as acetylation and phosphorylation of specifics residues in histone H3 and H4, methylation of histone H3 (K4), and the presence of histone variants H3.3 and H2A.Z (Lin et al., 1991; Stargell et al., 1993; Strahl et al., 1999; Vavra et al., 1982a; Vavra et al., 1982b).

These profound differences in chromatin structure and function suggest that the packaging, replication and repair of DNA in the micronucleus and macronucleus may be differentially regulated. In support of this, micro- and macronuclear S phases are offset in the cell cycle, as was demonstrated by the incorporation of base analogs in vegetative growing cells (Figure 4.1A and C). The micronucleus starts DNA replication as soon as cell division is complete, while macronuclear division is coupled to cytokinesis (Figure 4.1A and C-ii). Relative to micronuclear events, $G_1$ is absent and $G_2$ takes place during the most part of the cell cycle. On the other hand, macronuclear $G_1$, S and $G_2$ phases are equally distributed across the vegetative cell cycle (Figure 4.1A).

More profoundly, micro- and macronuclei use unrelated strategies to transmit their chromosomes. The micronucleus is diploid and contains five metacentric chromosomes that condense and divide by conventional mitosis during vegetative cell cycle. In contrast, the 280 distinct chromosomes in the polyploid (45C) macronucleus lack centromeres. They show no evidence for condensation during macronuclear division and are randomly segregated without spindle formation to daughter cells via a poorly understood amitotic mechanism (Orias et al., 1991). Microtubules and components of the condensin complex can be found within the macronuclear

compartment, and are essential for the distribution of chomosomes during cell division; however, no mechanism has been described for their exact roles in this process (Cervantes et al., 2006; Numata et al., 1999).

The micronucleus lies in a depression in the macronucleus during most of the cell cycle and its detachment is the first visible sign of commitment to cell division (Figure 4.1B, a). Micronuclei increase in size and elongate while mitosis occurs (Figure 4.1B, b-c). Once mitosis is complete the two daughter micronuclei migrate to opposite poles in the cell (Figure 4.1B, d-e). Macronuclei elongate and divide amitotically, the elongation is progressive towards each pole of the cell until two new discrete macronuclei are formed (Figure 4.1B, d-e-f). As soon cytokinesis is complete the macronucleus recovers its spherical shape and the micronucleus returns to the depression at the macronucleus (Figure 4.1B, g).

Remarkably, the copy number of macronuclear chromosomes is relatively stable. The high copy number of each chromosome suggests that DNA damage checkpoints might play little if any role in maintenance of chromosomes in the polyploid amitotic macronucleus. However, we discovered that DNA damaging agents activate a caffeine-sensitive checkpoint response that regulates S phase progression and nuclear division of both the micro- and macronucleus (Yakisich et al., 2006). We further identified a candidate ATR ortholog in the *Tetrahymena* genome database that was subsequently shown to be required for meiotic transmission of micronuclear chromosomes (Loidl & Mochizuki, 2009). Furthermore, we determined that the novel *Tetrahymena* gene, TIF1, plays a global role in the ATR-like checkpoint response in both the micro- and

macronucleus (Yakisich et al., 2006). TIF1p was originally identified biochemically as a macronuclear rDNA origin binding factor and shown to regulate the timing of rDNA origin activation (Mohammad et al., 2000; Morrison et al., 2005; Saha & Kapler, 2000). TIF1-depleted cells are hypersensitive to MMS and HU, exhibit an elongated macronuclear S phase, undergo aberrant macronuclear division and exhibit extensive micronuclear genome instability (Morrison et al., 2005; Yakisich et al., 2006).

Since MMS can induce cell cycle arrest in G1 or S phase through different checkpoint activators (ATM/G1 and ATR/S) in other systems, we developed an approach to specifically study the macronuclear S phase checkpoint response. In the work presented here we used flow cytometry to monitor cell cycle progression in wild type *Tetrahymena* that were exposed to DNA replication stress priory and during S phase. These studies not only reveal differences in the response to genotoxic stress, they suggest the existence of a novel pathway for the removal of incompletely replicated chromosomes from the macronucleus.

**Material and methods**

*Tetrahymena* strains, culturing and cell cycle synchronization

To synchronize log phase cultures by starvation cells were harvest by centrifugation and washed twice with 10 mM Tris-HCl (pH 7.4). The cells were diluted with10 mM Tris-HCl (pH 7.4) and incubated for 8 hours at 30°C shaking at 100 rpm. This culture was synchronized in G0/G1 border. The synchronized culture was refed with 5% PPYS to a final concentration 2% at a density of 2.5x105 cells/ml and

incubated at 30°C with 100 rpm. This synchronized culture reach early S phase after 2.5 hours. The subsequent G1 phase was evident by the end of 4 hours as was confirmed by flow cytometry analysis.

To synchronize cultures by elutriation three flasks of 2 L each with 500 mL of 2% PPYS were inoculated with 10 ml of a log phase culture (1x10e5 cells/ml) and incubated for 14 hours at 30°C with 100 rpm to a density of 1x10e5 cells/ml. The culture was pumped into an elutriation chamber mounted onto a Beckman J6M/E centrifuge at a rotor speed of 850 rpm and flow rate of 50 ml/min. Two hundred milliliters of a synchronized G1 cell population was recovered by increasing the flow rate of the pump to 65 ml/min. This fraction corresponds to a population synchronized in the G1 phase of the cell cycle. The elutriated culture reach early S phase after 1 hour and the next G1 phase was evident at 3 hours post-elutriation upon incubation at 30°C with 100 rpm.

Flow cytometry

To determine the DNA content within a cell population at least 2.0x105 cells/ml were collected by centrifugation at 4000 rpm for 4 min. Cells were washed with 5 ml of cold PBS and centrifuged again and the supernatant was aspirated. Cells were resuspended in a minimal volume (~10 μl) and fixed with 5 ml of ice cold 70% ethanol by incubating for 2 hours on ice. Samples were stored at 4°C or stained immediately with propidium iodide. Fixed samples were washed twice with PBS and resuspended in 0.4 ml of propidium iodide staining solution (PBS containing 0.1% Triton X100, 0.002% propidium iodide and 0.2 mg/ml RNase A). The samples were protected from the light

and incubated at room temperature for at least 1 hour. Stained samples were collected on BD FACSCalaibur$^{TM}$ flow cytometer and cell cycle progression was determined by monitoring DNA content. Thirty thousand cells were collected from each sample and plotted as a function of the PI intensity which reflects the DNA content in each cell.

Drugs and chemicals

Caffeine, hydroxyurea (HU) and methylmethanesulophonate (MMS) were purchased from Sigma-Aldrich (Saint Louis, MI) and used at a final concentration of 1 mM, 20 mM and 0.06% respectively.

Western blot analysis

One ml of culture was collected and washed with 0.5 ml of 10 mM Tris-HCl (pH 7.4). The samples were finally resuspend in 40 ul of 10 mM Tris-HCl and kept at -70°C. Once all the samples were collect 10 ul of SDS-loading buffer (Laemmli 1970) were add to each sample and boiled for 5 min. After a short spin the samples were load in a SDS-PAGE. SDS-polyacrylamide gels of 12% and 7% were use for the analysis of Rad51p and Mcm6p respectively. Samples were then transfer to a nylon membrane. The membranes were stained with Ponceau S (Sigma-Aldrich) for visual analysis of the loading and transference control. Later membranes were blocked with 10% low fat milk in PBS solution containing 0.1% Tween 20. Antibodies for Rad51p were obtained from NeoMarkers (51RAD01, Fremont, CA) Mcm6p antiserum was generated as was previously described in Donti et al., 2009.

**Results**

DNA replication factor reveal two alternatives pathways in response to DNA damaging agents

To better understand how activation of the intra-S checkpoint affects replication factors in *Tetrahymena*, the level of MCM6p was monitored following treatment with two different DNA damaging agents. In order to activate checkpoint response, we initially treated asynchronous logarithmically growing cultures with HU and MMS, which induce $G_1$ arrest via ATM and S phase arrest via ATR/Mec1 in yeast and other eukaryotes. Caffeine, HU + caffeine and MMS + caffeine treatments were added in order to determine if apical checkpoint activators, ATM and ATR, were involved. It is known that Rad51p plays an active role during recombination mediated repair at stalled forks or replication induced DSB, and is directly regulated by Chk1 in mammalian cells(Sorensen et al., 2005). Consequently, the activation of this intra-S phase checkpoint was followed by western blotting using specific antibody against Rad51p. As expected, both inducers of genotoxic stress, HU and MMS, caused Rad51p levels to increase (Figure 4.2A). When caffeine was added in combination with HU or MMS, the levels of Rad51p were similar to mock treatment, revealing the inactivation of the ATR-like pathway in both HU and MMS-treated cells. Caffeine alone did not have a major effect in Rad51p levels (Figure 4.2A).

At the same time we monitored the levels of Mcm6p. HU treatment decreased the levels of MCM6p and the addition of caffeine to HU-treated samples did not maintain Mcm6p mock-treated levels. These data indicate that a component of the

Mcm2-7 helicase is degraded rather than reversible phosphorylated in response to DNA damage, unlike other models systems. Next, Mcm6p was monitored in the presence of MMS. Unexpectedly we observed an increase in Mcm6p; the abundance was about 6-fold greater in the MMS-treated samples compared with mock (Figure 4.2A). Despite this MMS was able to arrest cell division (see below). The addition of caffeine did not suppress the MMS induction of Mcm6p, suggesting that this MMS response is regulated by an ATR-independent pathway (Figure 4.2A).

**Induction of the DNA damage response in synchronized cultures**

In order to better study the DNA damage response, HU and MMS were added at specific times to synchronized cell cultures. Since Mcm6p plays a key role in the activation of pre-RCs and acts at the replication fork, we decided to induce damage during S phase when DNA molecules were being actively replicated.

Previous studies in yeast showed that the activation of the intra-S phase checkpoint can be achieved by adding HU to $G_1$ synchronized cultures (Santocanale & Diffley, 1998). To address this, mock-treated *Tetrahymena* cultures were synchronized by centrifugal elutriation. Flow cytometry of elutriated cultures reveal a very sharp peak that represents a well synchronized $G_1$ population of cells (Figure 4.2B, 0 h post elutriation, mock treatment). The synchronization was well maintained for at least two cell cycles, where 1N and 2N peaks of DNA content are clearly measured by flow cytometry (Figure 4.2B, mock treatment).

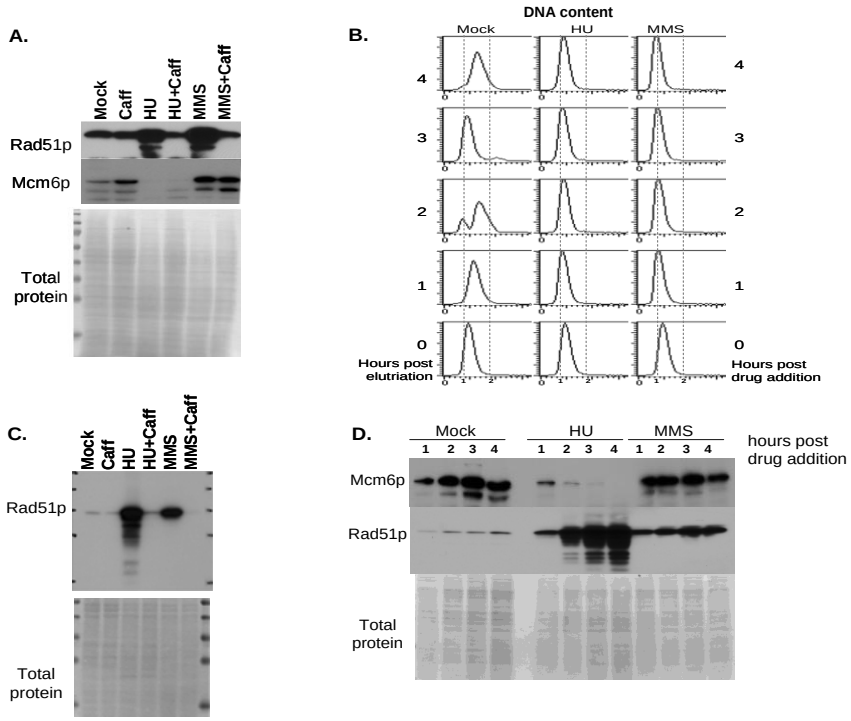


Figure 4.2 Responses to HU and MMS. A. Log phase cultures treated for 4 h with caffeine (caff, 1mM), HU (20mM), MMS (0.06%) or in combination. Western blots showing the abundance of Rad51p as a marker for the activation of the intra-S checkpoint and the differential regulation of MCM6p under DNA damage agents. B. Flow cytometric analysis of synchronized cultures treated with mock, HU (20 mM) or MMS (0.06%). All the treatments were added as soon the cells were collected from elutriator. Each histogram represents the number of counted cells versus DNA content (1 and 2). Samples were taken every hour after addition of the treatments. C. Western blotting showing checkpoint activation by abundance of Rad51p. Genotoxic agents (HU and MMS) were added to $G_1$ synchronized cells, which were analyzed after 4 h of incubation with the respective treatments. Also inhibition of the ATR-like pathway was assayed by adding caffeine to the treatments. Samples correspond to the 4 h post drug addition showed in panel B. D. Comparison of the abundance of Mcm6p and Rad51p by western blotting. Samples from mock, HU and MMS-treated cultures taken every hour after addition to $G_1$ cells (as panel B). Total protein loading is showed by Ponceau S stained membrane.

To study the activation of the intra-S checkpoint response, elutriated cells were treated with HU and MMS as soon as they were recovered from the elutriator. According to other systems we expect to see a G1 arrest for MMS and intra-S phase arrest for HU treated cultures. The DNA content was monitored by flow cytometry every one hour. Surprisingly, the initial peak was maintained showing an arrest in $G_1$ phase after treatment with both HU and MMS (Figure 4.2B). In order to confirm that the treatments were effectively inducing DNA damage, Rad51p was monitored at hourly intervals by western blotting (Figure 4.2C). After 4h of treatment, the level of Rad51p was elevated by at least ten-fold for HU and two-fold for MMS compared to mock treated cultures. HU treatment induced a stronger response and since HU mainly affect the elongating forks, we presumed that this may reflect a greater fraction of cells that enter S phase.

Caffeine treatment did not induced changes in the levels of Rad51p compared to mock treatment (Figure 4.2C). As was expected, when caffeine was used in combination with HU or MMS, inactivate the ATR-like pathway, reversing the induction of Rad51p in presence of either toxic agent. Since caffeine was efficiently blocking the activation of the checkpoint, we expect to see a progression in the cell cycle reflected by an incremental increase in DNA content, primary in MMS-treated cells where Mcm6p was present. However, caffeine did not have any effect in the flow cytometry histogram (data not shown), suggesting that the genotoxic agents was activating more than one response pathway. One of these pathways is modulated by caffeine and responsible for activation of repair mechanisms, most likely through the previously described ATR-like pathway.

The second pathway is unresponsive to caffeine, and closely monitors the DNA

content of damaged cells. When Rad51p was monitored every hour after HU addition, clearly showed that the level of Rad51p is elevated by the first hour of treatment and this induction was proportionally increased with the length of the treatment. In contrast, the induction of Rad51p by MMS was maximal by the end of the first hour of treatment. By the end of the 4 h of treatment with MMS, Rad51p did not present major variation compared with the levels induced during the first hour of treatment (Figure 4.2D).

To determine how Mcm6p abundance was affected by the genotoxic treatment in synchronized cells, samples were taken every hour after the addition of HU or MMS and analyzed by western blotting (Figure 4.2D). Similar to the asynchronous cultures (Figure 4.2A), HU treatment induced the gradual degradation of Mcm6p. By the end of 3 h post HU addition undetectable signal for Mcm6p was observed (Figure 4.2D). In contrast, MMS treated cells showed a modest increase in the level of Mcm6p 1 h post treatment, and the level was maintained (Figure 4.2D). Furthermore, both treatments were insensitive to caffeine (data not shown). These result support the idea that two different pathways are activated during the DNA damage response in *Tetrahymena*, one affecting Rad51p and another affecting Mcm6p.

**Activation of the intra-S phase checkpoint in *Tetrahymena***

From the above experiments I speculate that adding DNA damaging agents in $G_1$ phase induces a caffeine-sensitive pathways (induction of Rad51p) as well as a caffeine-insensitive pathway (affecting Mcm6p). Alternatively, the different effects of HU and MMS on Mcm6p reflect arrest at different stages of the cell cycle. To better focus

attention on the intra-S phase DNA damage response, drugs were directly added after synchronized cultures had clearly progressed into S phase.

Elutriated cultures were collected and cultured for 1h to reach S phase (Figure 4.3A, 1h post elutriation). Once in S phase, cultures were treated with HU or MMS (0 h post drug addition). Mock-treated samples show a mix population of $G_2$/dividing and a new $G_1$ by 2 h post elutriation. As was expected, 1h after HU treatment the culture was efficiently arrest in S phase (Figure 4.3A, HU 1h post drug addition). However, the flow cytometry profile contained cells with a small 1N DNA ($G_1$) content peak 2 h after HU addition (Figure 4.3A, HU, arrow). This $G_1$ peak became prominent when cells were further incubated in HU. By 4 hours cultures treated with HU partitioned in two clear peaks; one corresponding to the initial S phase population and a second population with a 1N DNA content. In MMS-treated samples the original S phase peak was not maintained 1 h post treatment and did not progress towards $G_2$ content. Instead the S phase peak gradually shifted towards a 1N/ $G_1$ DNA content without progressing towards $G_2$/2N. Similar responses were obtained when cells were synchronized by starvation-refeeding. While the synchrony obtained by starvation-refeeding was not as good as for elutriation. The absence of an obvious $G_2$ (2N) DNA content peak was evident in HU and MMS treated cells. Furthermore the cells treated with HU revealed two DNA content populations ($G_1$ and S). These results suggest that the HU and MMS treatments were having a similar effect on DNA content.

The increased abundance of Rad51p confirmed that the DNA damage response was activated when HU or MMS were added to S phase cultures (Figure 4.3B).

Furthermore, Mcm6p levels were regulated in the same fashion observed when HU and MMS were added in $G_1$ (Figure 4.3B). Furthermore, the addition of caffeine, as in G1 checkpoint activation, repressed the ATR-dependent increased in Rad51p but was unable to reverse the effect of HU or MMS on Mcm6p levels (Figure 4.3C). Since MMS affects both $G_1$ and S phase checkpoints responses these data suggest that $G_1$ and S phase regulation of Mcm6p may be governed by a common mechanism.

Treatment of budding yeast with HU results in the very slow progression of replication forks and activation of Mec1 (ATR) checkpoint (Alvino et al., 2007). The shift in DNA content from S phase values to G1 without progression to G2 DNA content in HU and MMS treated cells has not been previously described in *Tetrahymena* or any other eukaryote. I decide to follow the nature of such phenomena, focusing in HU-treated cells which generated a more distinct $G_1$-like peak in response to genotoxic stress. Several mechanisms can be envisioned for how the G1 population was generated. The simplest explanation is that cultures treated with HU were induced to divide without completion of macronuclear S phase. This model makes two predictions: (1) there should be a significant increase in cell number and (2) a significant formation of a sub $G_1$ peak should also occur. To better interpret the flow cytometry data, histograms representing an S phase culture and a culture with a mix population of $G_1$ and $G_2$ phase cells were simultaneously overlaid to provide references for the analysis of HU-treated samples. A synchronized S phase culture was treated with HU, samples were collected

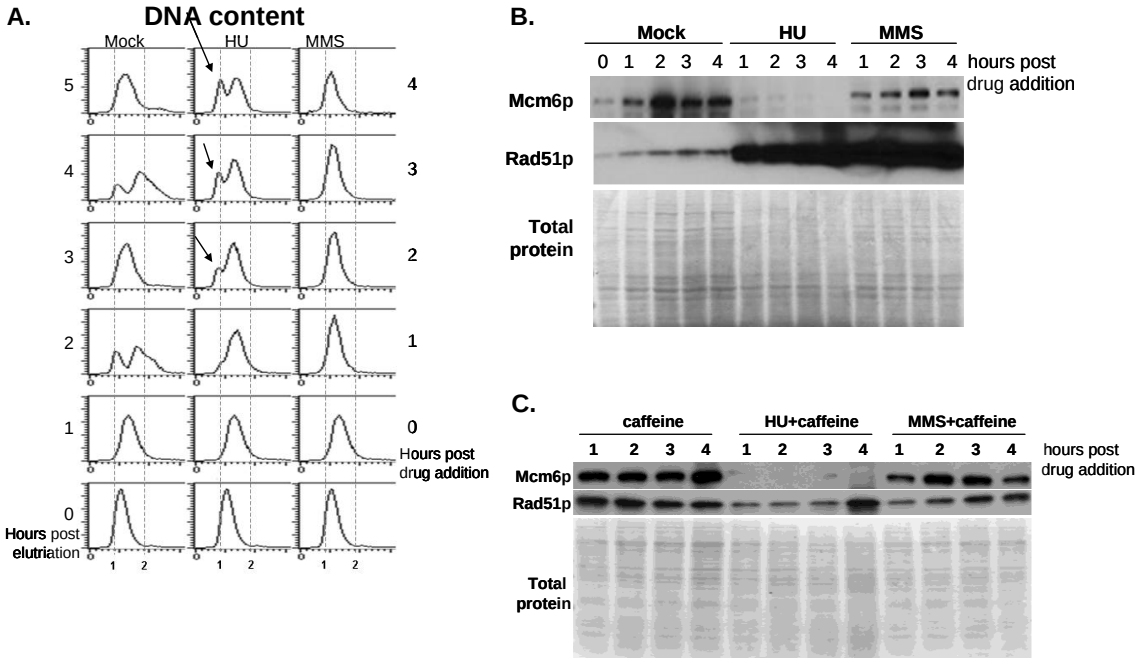


Figure 4.3 DNA damage responses during S phase. A. Flow cytometry outputs of cultures synchronized by elutriation, DNA damaging agents were added during S phase and samples analyzed ever hour. Arrow showing a new 1N peak in HU treated samples. B. Comparison of the abundance of Mcm6p and Rad51p by western blotting. Samples from mock, HU and MMS-treated cultures were taken every hour after addition to cells in S phase (as panel A). Total protein loading is showed by Ponceau S stained membrane. C. Comparison of the abundance of Mcm6p and Rad51p in cells treated with caffeine alone or in combination with HU or MMS, samples collected as in B.

every hour after drug addition for 6h. Flow cytometry histograms were overlapped with the controls already mentioned (Figure 4.4A). After 1 h of HU treatment a small shoulder was noticeable on left side of the curve. However, the right side of the curve did not shift to a higher DNA content. The 1N peak becomes more prominent during prolonged incorporation of HU. Moreover the leading shoulder of the S phase peak did not shift further to the right. Thus no increase in DNA content was observed during 6 h of treatment (Figure 4.4A, pink curve). Furthermore, when a G1 synchronized culture was added to the overlapped histograms obtained after 4 h HU treatment, it was apparent that the new 1N peak falls within the DNA range of the control G1 peak, suggesting that this profile was not generated by cell death or macronuclear division (Figure 4.4A, bottom). Additional experiments support this conclusion (see below).

In order to better resolve the accumulation of the 1N peak, samples from mock and HU treatments were collected every 10 min (Figure 4.4B). The presence of the shoulder for 1N peak was consistent in all the experiments. Furthermore, no evidence for the transient accumulation of a 2N/ $G_2$ DNA content was detected.

**The new 1N peak is not the product of cell division**

Previous work with starved/refeed cultures revealed that 10% of HU-treated cells escape cell cycle arrest (Yakisich et al., 2006). If the prominent 1N peak in HU treated S phase cultures was the product of dividing cells, an increase in the culture density or at

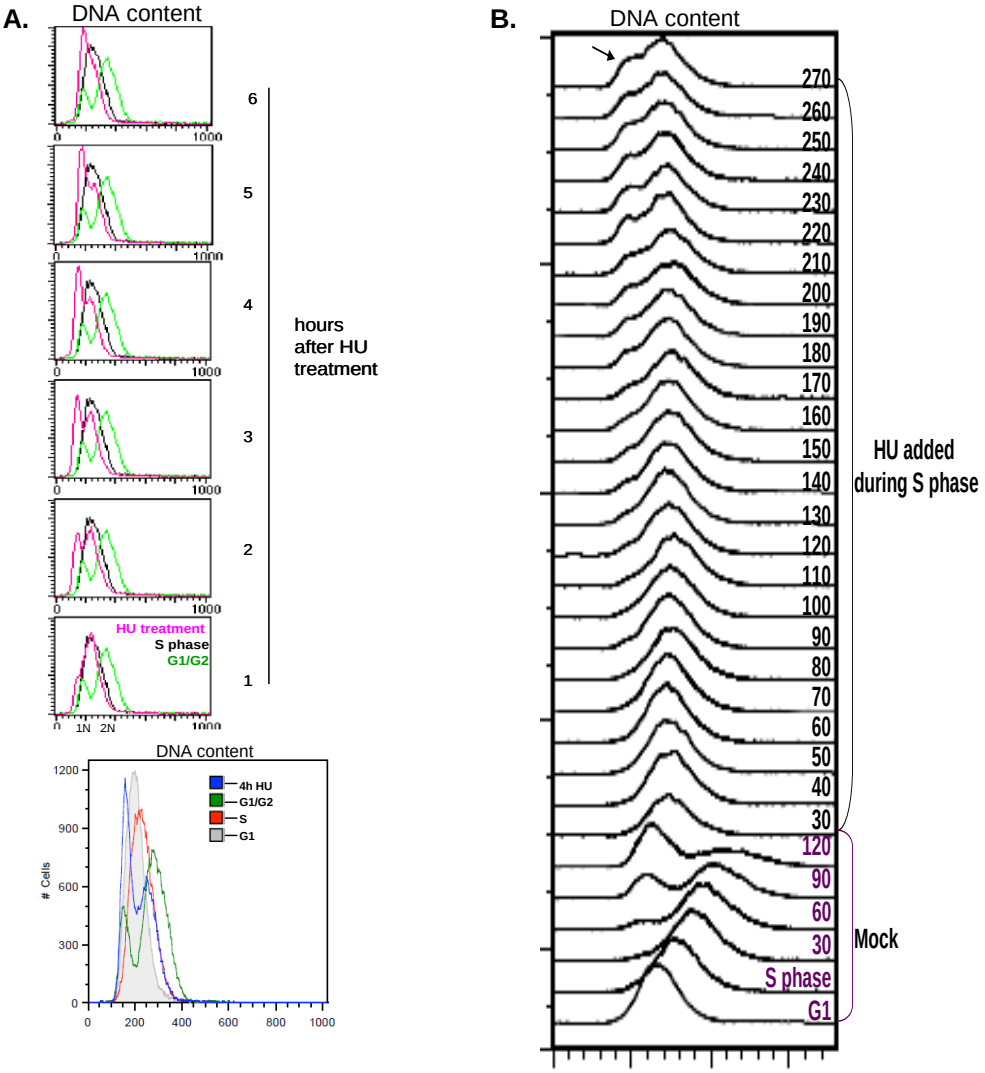


Figure 4.4 Detection of 1N population by flow cytometry. A Cultures synchronized by elutriation. S phase synchronized cultures were treated with HU, samples were taken every one hour after HU treatment for six consecutives hours. Overlays of a mock treated culture synchronized in S phase is showed in black, a mix population of G1/G2 in green and the corresponding HU treated cultures in pink. The bottom panel shows a summary with the overlapping curves corresponding to a G1 elutriated culture (grey background), S phase cultures showed in a red curve, G1/G2 mix population showed in green and culture treated for 4 h with HU is showed in blue. **B.** Flow cytometry analysis for mock-treated cultures every 30 min up to 120 min is show. DNA content was measured every 10 min for 260 min in S phase cultures treated with HU.

least an increase in the percentage of dividing cells should be detected when genotoxic agents were added to the cultures.

To address this, S phase synchronized cultures were treated with HU or MMS and the density of the cultures were measured every two hours and compared with the density of a mock-treated sample (Figure 4.5A). The result indicate that while the density of mock treated cells increased exponentially over time, S phase cultures treated with HU or MMS were maintained at a constant cell density for the 8 hours duration of experiment. To assess the percentage of dividing cells in mock, HU and MMS treated S phase cultures, cells were stained with acridine orange and quantified by direct microscopic observation (Figure 4.5B). Vegetative division (Figure 4.1B, b-g) was quantified in three independent experiments for each treatment. One hour after S phase, ~40% of the cells in mock-treatment were undergoing cell division (Figure 4.5B), correlating with the appearance of the G2 phase peak detected by flow cytometry (Figure 4.3A, 2 h post elutriation). Out of 300 cells scored at every time point in each independent experiment (n=3), less that 5% of the population of HU or MMS treated cells showed evidence of cell division. This frequency is too low to account for the predominant 1N peak.

A second possible explanation for the shift in DNA content is that cells under genotoxic stress induced the elimination of macronuclear DNA, through the formation of macronuclear extrusion bodies. Extrusion bodies are extranuclear vesicles that contain chromatin and are positively stained with acridine orange. Extrusion bodies were previously described as a mechanism to reduce DNA content in normal cycling cells

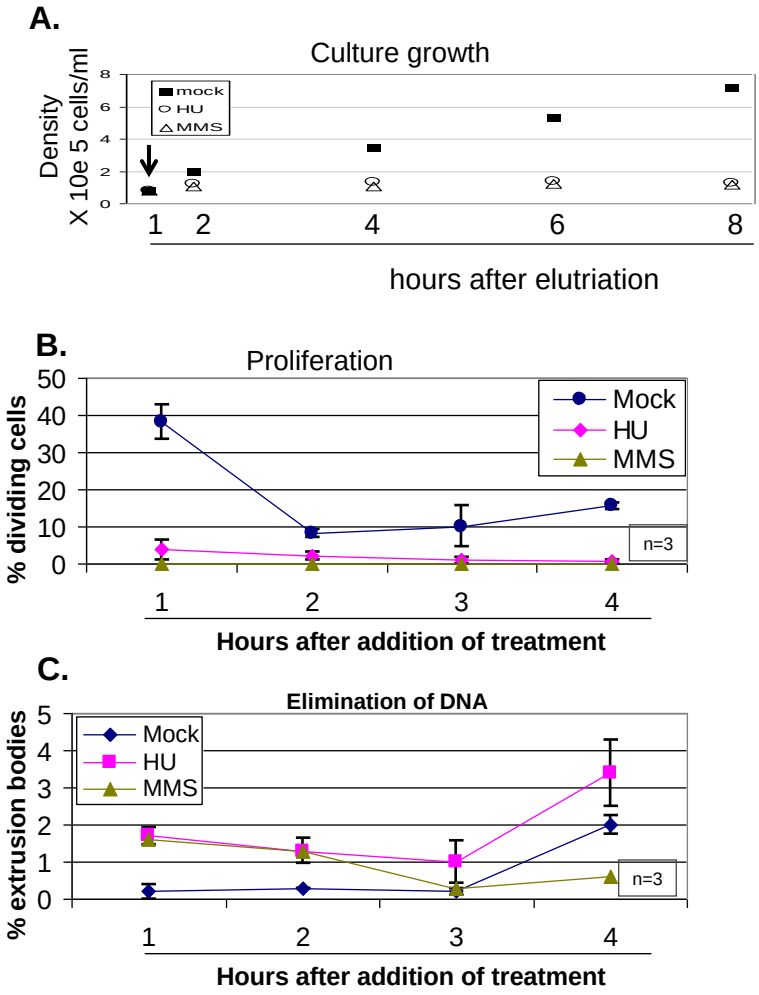


Figure 4.5 Determination of cell density, number of dividing cells and presence of extrusion bodies in synchronized cultures. A. Showing the density of synchronized cultures treated with HU or MMS. Cultures were synchronized by elutriation and allowed to reach S phase (arrow) at that point all the treatments were added and the density of the cultures were follow over time. B. Evaluation of the number of cell in division present in each treated culture. S phase cultures were treated and the number of dividing cells was quantified every hour up to the end of 4 h of treatment. C. Extrusion bodies were quantified in the same cultures used in B.

following asymmetric amitotic macronuclear division (Cleffmann, 1980). Recently, extrusion bodies were described as a mechanism for eliminating fragmented DNA in mutant strains that undergo macronuclear instability (Wiley et al., 2005). The percentage of extrusion bodies was measured by microscopic observation of cells stained with acridine orange in mock, HU and MMS treated cultures. As expected extrusion bodies were detected in a very small percentage of mock-treated cells, 2% by the end of 4 h post S phase. HU and MMS treated samples contained a similarly small percentage of cells with extrusion bodies (ranging from 1% to 3.5%).

The collective quantitative measurements of density and dividing cells do not support the idea that HU and MMS-treated S phase cells are dividing with less DNA or eliminating DNA via previously described and poorly understood mechanism. The data suggest that in the presence of HU or MMS, S phase synchronized cultures employed a different mechanism to establish a 1N DNA to S phase arrested cells.

**Dissection of the 1N peak by flow cytometry**

Since this $G_1$/1N, S and $G_2$/2N flow cytometry peak was could be resolved, it was possible to compare flow cytometry parameters of different cell cycle populations in mock- and HU-treated cells. Cells synchronized, by elutriation were cultured until they reached S phase and left untreated (mock) or treated with HU, and samples were collected every thirty minutes. First, DNA content was monitored by the propidium iodide (PI) staining (Figure 4.6A). As was expected mock treated samples showed the highest DNA content 30 min after S phase (maroon triangle), where the DNA in the

macronucleus had completed replication and cells were preparing to divide (Figure 4.6A). At 60 min after S phase, the lowest DNA content was observed suggesting that cells had divided. From this point DNA content gradually increased and a second cell division was evident at 240 min. The amount of DNA seems to be higher in dividing cells for the second cell cycle, however, this could also reflect a decrease in the synchrony of the culture. HU-treated synchronized S phase cells exhibited a gradual decrease in PI signal starting 30 min after drug addition (Figure 4.6, red X)

Forward scatter (FSC) was used to compare the relative size of mock and HU-treated cells. This parameter assesses the amount of laser beam signal that passes around each cell and is ideally suited for spherical cells. Since *Tetrahymena* are usually oblong (50 μm long and 30 μm wide), it remained to be determined whether this parameter could detect differences between mock and HU-treated cells. However, when these cultures were compared by FSC, a clear difference in the average FSC was evident. FSC in mock treated samples decrease at 60 min post S phase correlating with cell division, suggesting that the average FSC could be used to monitor the size of *Tetrahymena* (Figure 4.6A, dark blue diamonds). HU-treated samples exhibit a constant increase FSC values compared to mock (Figure 4.6A, light blue boxes), suggesting that cells with decreased DNA content had increased in size rather than divided.

Another parameter obtained by flow cytometry is the amount of the laser beam signal that refracts off of particles inside the cell. This signal is collected and scored as SSC (side scatter), and represents cell complexity. In mock treated samples SSC is fairly consistent across the cell cycle, and the lowest value was detected in recently divided

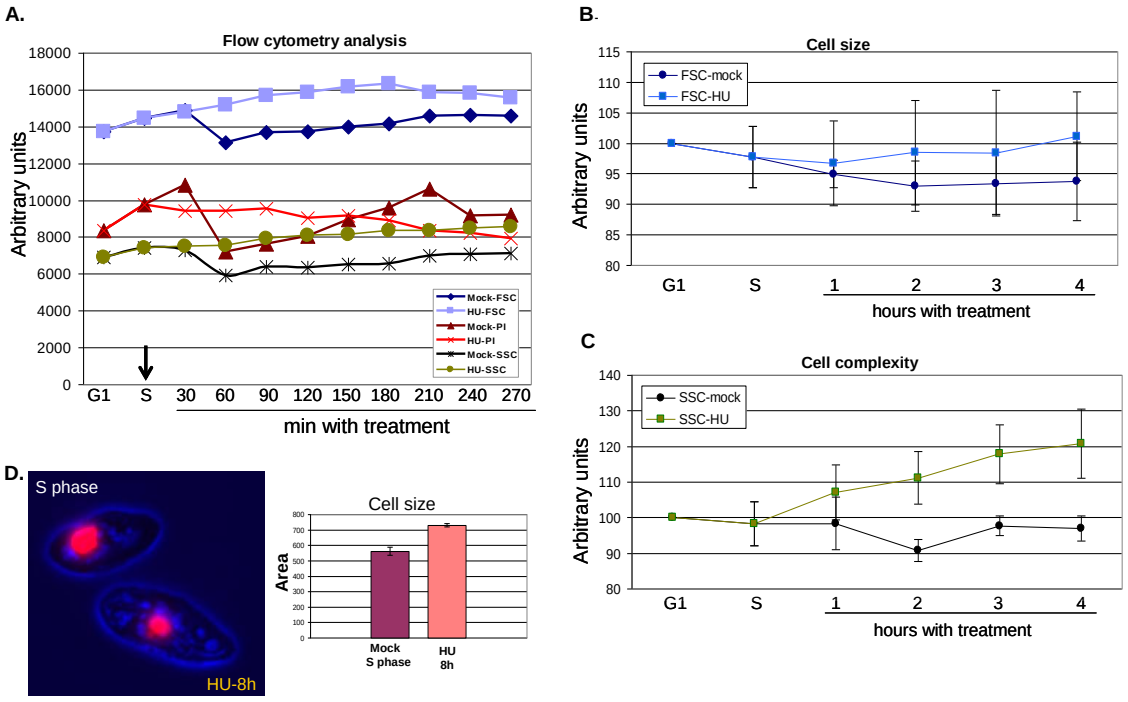


Figure 4.6 Flow cytometry analysis of HU-treated cells A. Detailed analyses of the DNA content (PI), forward scatter (FSC) and side scatter (SSC) in mock and HU-treated cells. S phase synchronized cells were treated with HU (arrow). Samples were collected every 30 min and 30.000 counts were scored at each time point. B. and C. Statistical comparison of forward scatter (FSC) and side scatter (SSC) respectively, between mock and HU-treated cells. HU treatment was added during S phase and samples collected every hour. Plot was generated by the results of three independent experiments (n=3). D. (left panel) Representative micrograph illustrating the difference in size between an untreated cell in S phase and HU-treated cell for 8 h. (right panel) The area of n=100 cells mock or HU-treated was measured and plotted to stress the statistical differences between the size upon treatment.

cells (60 min after S phase, dark black starts). In HU treated samples, SSC showed a constantly increasing signal during the time of treatment (Figure 4.6A, green circles).

To determine if the average differences in SSC and FSC were statistically significant, three independent experiments were used to compare mock and HU treated samples (Figure 4.6B and C). The collective data revealed that FSC in HU-treated samples is not significantly different from the values found in mock-treated samples (Figure 4.6B). In contrast, in HU-treated cells exhibit clear increase in SSC values compared to mock, arguing that treated cells were 'more complex' than mock (Figure 4.6C). To determine whether increased SSC in HU-treated samples could be related not only to activation of intracellular machineries, but also to size, direct microscopic measurements of the size of cell in different treatments was registered. Since mock-treated cells did not suffer major variation in SSC across the cell cycle, representative S phase cells were compared with HU treated cells. Since SSC increases proportionally to the time in HU treatment, cells treated with HU for 8 h were used to stress the difference when compared with S phase culture (Figure 4.6D). This analysis shoe that HU treated cells are bigger than those present in S phase cultures. The area of 100 cells in S phase was measured and compared to the area of the same number of HU treated cells (Figure 4.6D). This suggested that SSC could be use as parameter for size in *Tetrahymena*.

In general HU induced an increase in the cellular size as the 1N peak appeared in the culture. This 1N peak is gradually generated concomitant with a decrease in the amount of DNA in the macronucleus.

**Identification of higher SSC population in HU-treated G1 and S phase cells**

Since the increase in SSC correlates with an enlarge in cell size, I decide to monitored the population with higher SSC in HU-treated cells and determine whether the increased complexity was a common factor between $G_1$ and S phase treated cells in response to DNA damage.

Cells were synchronized by elutriation and cultivated for 7 h, mock-treated cultures, DNA content as well as the change of SSC in function of the FSC was monitored. Mock-treated cells showed a well synchronized initial $G_1$ population (Figure 4.7, A, left panel), a prominent 2N peak was evident by 2 h after elutriation, corresponding to cells in $G_2$. As noted above, SSC in mock-treated cells did not present any major variation in the 7 h analysis (Figure 4.7, A, right panel).

Hydroxyurea was added either to $G_1$ or S phase synchronized cells (Figure 4.7B and C respectively). HU addition to $G_1$ synchronized cells induced the activation of the checkpoint and inhibits synthesis of DNA, as confirmed by the maintenance of the 1N DNA content for the 7 h of treatment (Figure 4.7, B, left panel). However, a noticeable change in SSC occurred over time, the whole $G_1$ population gradually acquires a more homogeneous FSC and a higher SSC (Figure 4.7, B, right panel).

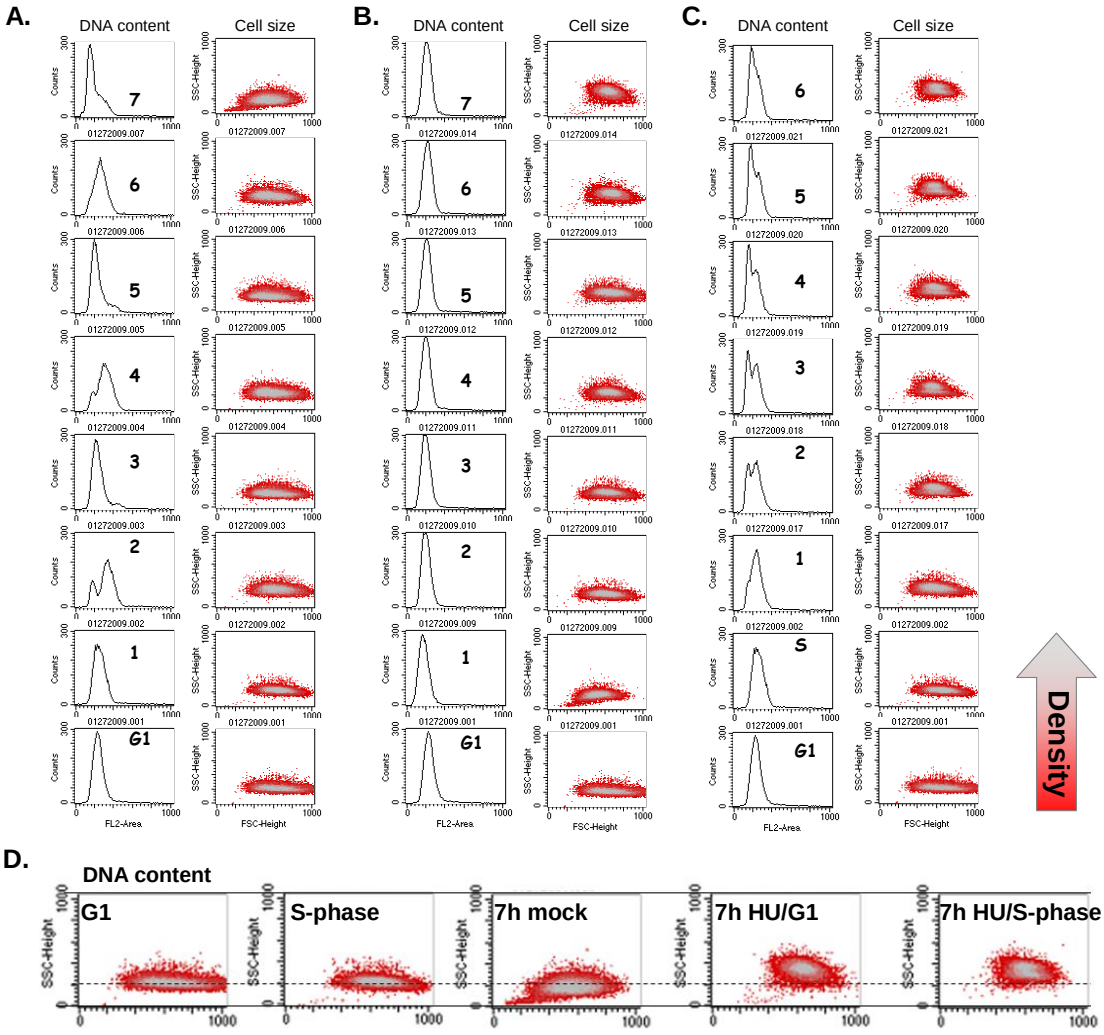


Figure 4.7 HU treatments induce an increase in the SSC of the cells. Flow cytometry analyses. (Left panel) showing number of events scored (counts) versus the DNA content (PI intensity). (Right panel) SSC versus FSC for cells synchronized by elutriation and cultivated in mock (A), HU added in $G_1$ phase (B) or HU added in S phase (C). Numbers indicate the hours of incubation with the corresponding treatment. D. Showing a detail for better comparison of cells in G1, S phase and after 7 h of treatment with mock, HU added in $G_1$ and HU added in S phase.

After HU addition to synchronized cells in S phase the expected 1N peak appeared as a shoulder beginning 1 h after HU addition (Figure 4.7, C, left panel). This 1N peak, as was showed before, became more prominent while the HU treatment was maintained, by the end of 6 h of treatment a clear 1N peak was generated. Similar to G1 HU-treated cells, the addition of HU to S phase synchronized cells induced a gradual shift to a higher SSC in the population (Figure 4.7, C, right panel).

These data showed that HU-treated cells are clearly different from normally dividing cells. They also illustrate the increase in SSC is shared between HU-treated cells either during $G_1$ or S phase. Since $G_1$ HU-treated cells are clearly not increasing their DNA content while increasing in size.

**Recovery from HU-induced genotoxic stress**

Treatment with HU promotes the stalling of replication forks due to depletion of dNTPs and activation of the DNA damage response. Once the damage is eliminated or damaging agent removed, arrested cells should resume cell cycle progression. The resetting of the cell progression during recovery from HU is associated with the inactivation of Chk1 kinase (Pellicioni et al., 1999) and the maintenance of the activated and hyperphosphylated state of Chk1 depends on ATR (Lopez eta al, 2001).

To address the recovery from inhibition of DNA replication, synchronized S phase cultures were treated with HU for 8 h, following by the removal of HU and further culturing of the cells in fresh media. To assess the effect of premature inactivation of the ATR-like pathway, a fraction of the HU-treated culture was recovered in the presence of

caffeine. Samples from these cultures were analyzed by flow cytometry to determine the DNA content and progression through the cell cycle. The levels of Rad51p were determined by western blotting to monitor the status of the DNA damage response. Since we speculated that the activation of the DNA damage response is dependent on the ATR-like pathway, the addition of caffeine should decrease the levels of Rad51p early during recovery time. Furthermore, since Mcm6p was degraded in HU-treated cells the fate for this protein was also monitored during recovery period.

As we already noticed, HU-treatment added to S phase synchronized cells induces the formation of a well synchronized 1N peak (Figure 4.8A, 0 h). Cells that recovered in the absence of caffeine progressed through the cell cycle with less synchrony, however a clear S/G2 peak is detected by the end of 2 h after recovery. Evidence for a new cell cycle was observed 3 h post HU release. These data suggest that replication forks were competent to initiate a normal cell cycle as soon as the HU was removed from the culture. Furthermore, this timing is coincident with the completion of a normal cell cycle, suggesting that after 8 hours of HU treatment cells were synchronized in G1 phase. Cultures released in the presence of caffeine clearly attempt to progress through the cell cycle, however no clear 2N content peak is observed and a population with a sub-G1 DNA content indicate a provable effect in the viability of the culture (Figure 4.8A, +caffeine).

The saturating Rad51p signal after 1h of recovery suggest that cells undergo a great deal of repair in order to maintain viability after 8 h of HU treatment (Figure 4.8B). The levels of Rad51p are only decreased after 5 h in recovery media. However, the

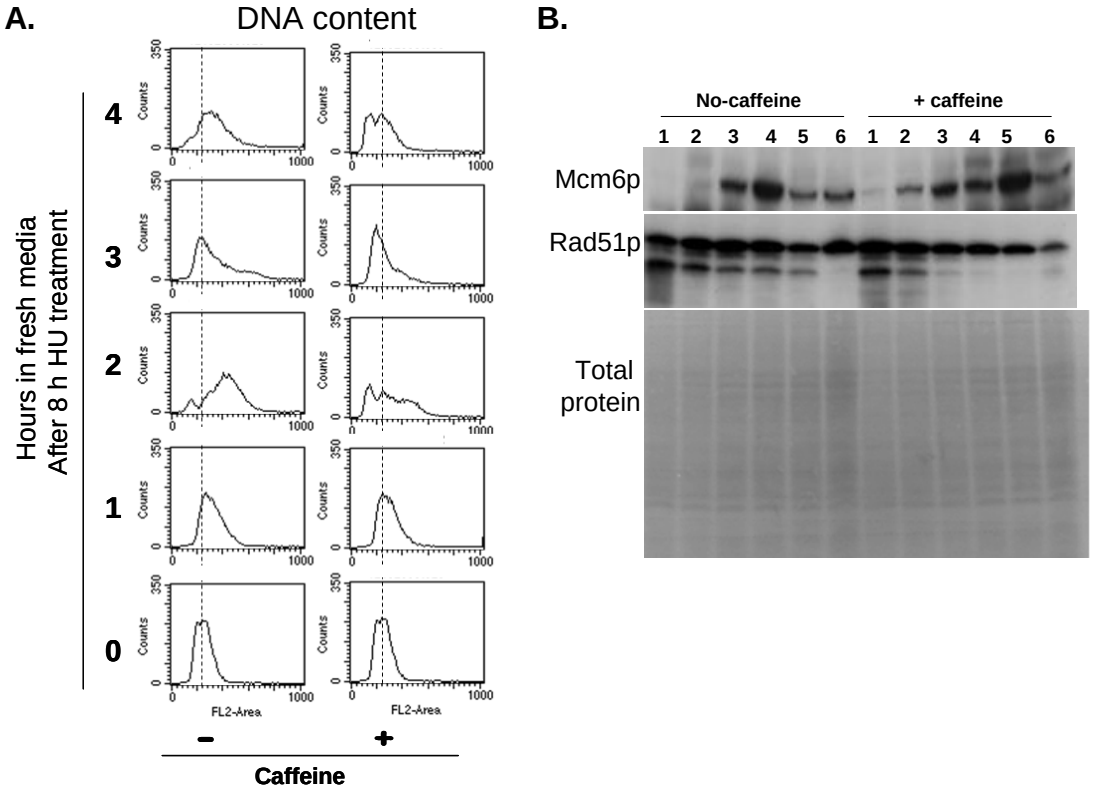


Figure 4.8 Recovery from HU-treatment added in S phase synchronized cells and maintained for 8 h. A. Flow cytometry analysis showing number of event scored (counts) versus DNA content in recovery media supplemented (+) or not (-) with caffeine. Dotted line indicating the synchronized peak obtained after 8 h of treatment with HU added in S phase synchronized cells. B. Comparison of Mcm6p and Rad51p level in recovery media by western blotting. The samples were collected every hour upon incubation in recovery media supplemented (+) or without caffeine.

addition of caffeine induces a early reduction in the Rad51p levels suggesting that ATR-like pathway was responsible for the activation of the DNA damage response.

The levels of Mcm6p after HU treatment are completely depleted from the cell and are initially recovered 2 h after HU removal (Figure 4.8B). In unperturbed cell cycles the levels of Mcm6p are low during S phase, and this correlate well with the 1 and 2 h in recovery media, when the recovered cell undergo S phase (Figure 4.8A). What is not clear is how these cells are able to complete S phase during recovery period without Mcm6p, this open few possibilities. (1) Mcm6p is not necessary for the first cycle after genotoxic stress. (2) The levels of Mcm6p are very low and escape from our detection method. Interestingly, the presence of caffeine in the recovery media promote an early increase in the levels of Mcm6p corroborating the idea that activation of the DNA damage response is directly modulating the levels of Mcm6p in absence of genotoxic agent in *Tetrahymena*.

**Formation of the new 1N peak in relation to incorporation of base analogs**

The fact that the total DNA content in HU treated samples was decreasing, suggested the presence of a DNA elimination mechanism was active. This mechanism of DNA elimination was not related to the formation of extrusion bodies but probably more relate to degradation of the DNA. To study this possibility, the incorporation of 3H-methylated-thymidine was measured in treated cultures. In case that the newly synthesized DNA in synchronized cultures where degraded upon HU treatment, a decrease in the tritiated thymidine should be observed in HU-treated cells compared to

the initial incorporation (control). Since the DNA damage response is activated a minor background corresponding to DNA repair mechanisms was expected. However, the addition of caffeine to HU or MMS-treated samples prevents that activation of the ATR-like pathway, promoting further incorporation of thymidine.

To evaluate the DNA synthesis due to replication and/or repair G1 phase cells synchronized by elutriation were cultured, 50 min after elutriation tritiated-thymidine was added to the culture in order to label newly synthesized DNA. After 10 min of incorporation, an aliquot was saved as control and the culture at this point reached S phase was subjected to different treatments (Figure 4.9A). HU, MMS, caffeine or a combination of HU-caffeine, MMS-caffeine treatments were added and maintained for 4 h. Tritiated-thymidine was still present in the culture to monitor further incorporation. Finally samples were collected and TCA precipitable thymidine was quantified. Each treatment was evaluated by five independent aliquots (Figure 4.9A). The control sample corresponded to the amount of thymidine incorporated into newly synthesized DNA during the 10 min prior to the addition of different treatments (Figure 4.9A). As expected, mock-treated samples incorporated significant amounts of thymidine during the 4 h incubation. As previously shown, caffeine did not affect the cell cycle progression and the amount of thymidine incorporated was similar to mock-treated cells. Furthermore, HU and MMS-treated cells incorporated low levels of thymidine, probably due to repair mechanism. The addition of caffeine to MMS-treated cells did not impact in the level of thymidine incorporated. Interestingly, the addition of caffeine to HU-treated samples showed a minor increase in the incorporation of thymidine, supporting

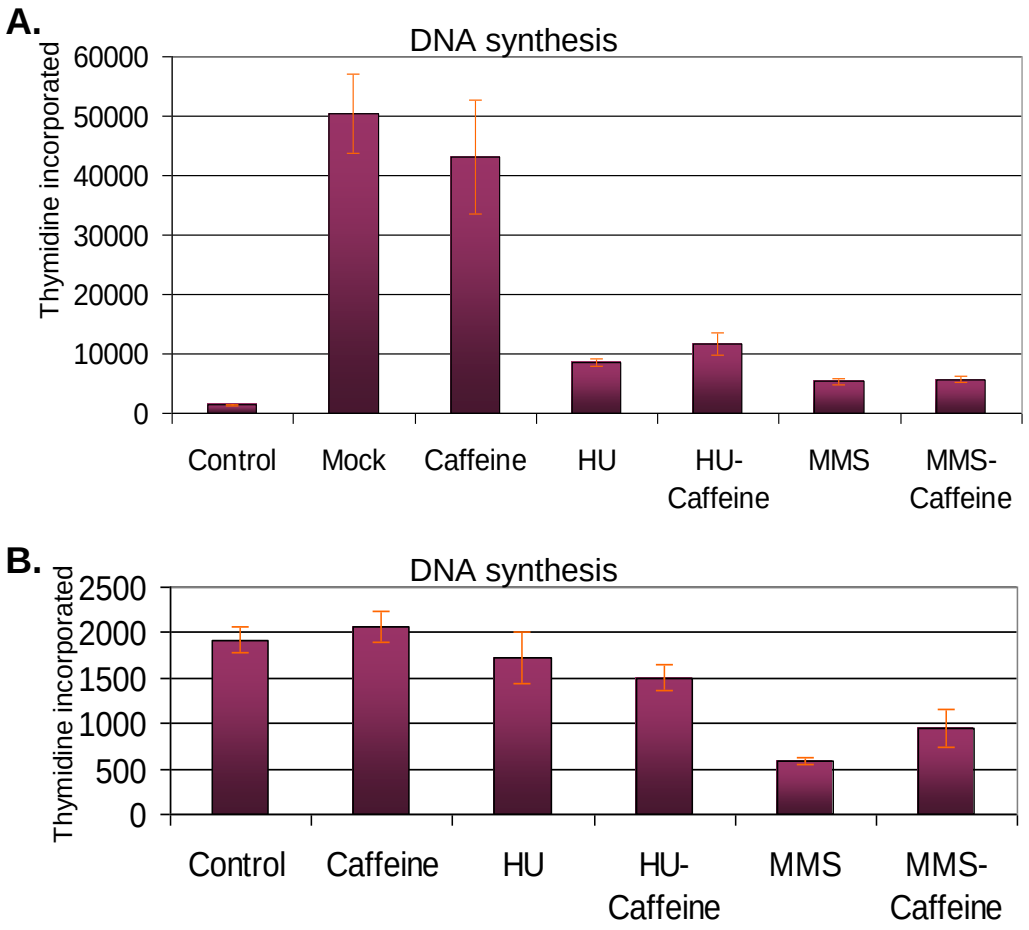


Figure 4.9 Incorporation of tritiated thymidine. A. Incorporation of activity for 10 min of pre-labeled period (control). Treatments were added to S phase cell and cultured for 4 h in presence of thymidine. Graphs are representing the radioactivity incorporated through the length of the treatments. B. Newly synthesized DNA was labeled with thymidine (control), which was removed before addition of the treatments to S phase synchronized cultures. Treatments were maintained for 4 h. Graphs representing the residual amount of tritiated thymidine upon treatment were added and maintained for 4 h.

the idea that the activation of DNA damage response is differential between these two genotoxic agents (Figure 4.9A).

To address the possibility of DNA degradation during genotoxic stress, G1 phase cells synchronized by elutriation were cultured for 30 min before tritiated-thymidine was added. After 30 min of incorporation, the thymidine was removed and labeled cells resuspended in fresh media. An aliquot of the labeled newly synthesized DNA was saved as a control and the culture that at this point reached S phase was subjected to different treatments which were maintained by 4 h (Figure 4.9B). The initial levels of thymidine incorporated were maintained in caffeine-treated cells. Minor decrease in the thymidine incorporation was observed in HU and HU-caffeine-treated cultures. Interestingly, MMS-treated cells presented an important decrease in the incorporated thymidine, suggesting that a significant fraction of the newly synthesized DNA was undergoing degradation (Figure 4.9B). The addition of caffeine to MMS-treated samples partially prevents decrease of thymidine initially incorporated. These results suggested that the activation ATR-like pathway induce degradation of the newly synthesized DNA in MMS-treated samples but not in HU-treated cells.

### *Tetrahymena* ATR mutants accumulate DNA damage during S phase and are hypersensitive to genotoxic stress

To better understand the DNA damage response in *Tetrahymena* and to clarify the difference in the response to different genotoxic agents I decide to study the response to HU and MMS in ATR-deficient strains.

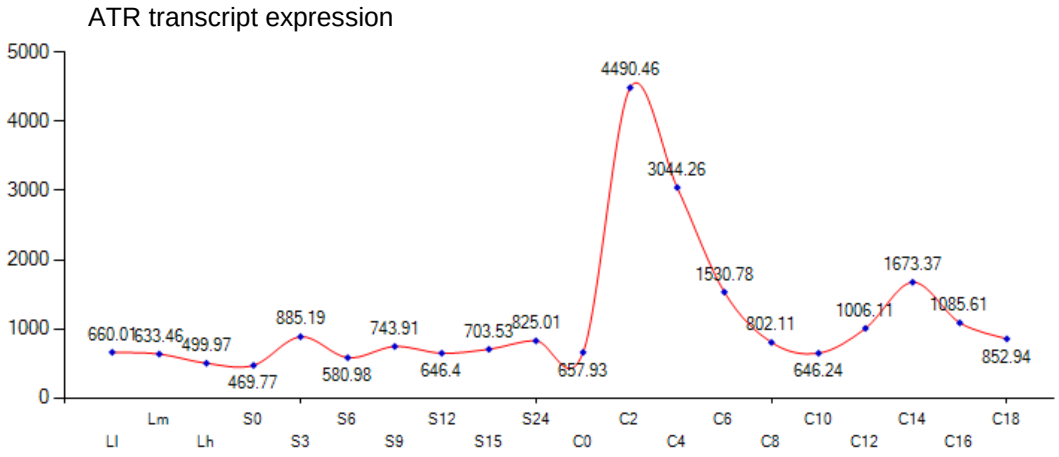


Figure 4.10 Expression profile for TtATR. Gene ID TTHERM_01008650. Growing cells**,** L-l**,** L-m and L-h correspond respectively to ~$1\times10^5$ cells/ml, ~$3.5\times10^5$ cells/ml and ~$1\times10^6$ cells/ml. For starvation, ~$2\times10^5$ cells/ml were collected at 0, 3, 6, 9, 12, 15 and 24 hours (referred to as S-0, S-3, S-6, S-9, S-12, S-15 and **S**-24). For macronuclear development, equal volumes of B2086 and CU428 cells were mixed, and samples wer e collected at 0, 2, 4, 6, 8, 10, 12, 14, 16 and 18 hours after mixing (referred to a**s** C-0, C-2, C-4, C-6, C-8, C-10, C-12, C-14, C-16 and C-18).

We previously identified a candidate ATR gene in the *T. thermophila* genome database (TTHERM_01008650). The transcription profile for ATR extracted from a genome-wide analysis of *Tetrahymena* during logarithmically growing phase, starvation and macronuclear development (Miao et al., 2009) showed that macronuclear ATR expression is marginal in logarithmically growing cultures compared to the expression during development (Figure 4.10). However, ATR expression might be transient during the cell cycle.

Recent deletion of the macronuclear copy of ATR suggests that it is not required for viability during vegetative cell cycles, but necessary for the elongation of micronucleus in early stages of *Tetrahymena* conjugation (Loidl and Mochizuki, 2009). We obtained the ATR mutant strains (ATR/KO-CU428(8)4 and ATR/KO-B2086(2)3) and assayed for defects in vegetative cell cycle progression and the DNA damage response. In the absence of exogenous DNA damage, ATR mutants exhibited a dramatic activation of the DNA damage response as monitored by the levels of Rad51p (Figure 4.11A, log phase samples). This suggests that ATR is actively utilized during normal vegetative growth and that the absence of ATR leads to the accumulation of DNA damage.

Examination of synchronize cultures of the ATR-mutant strain did not revealed major defects in progression through the cell cycle (Figure 4.11B). ATR-mutant showed a major peak corresponding to a new $G_1$ phase 3 h after elutriation. The time that ATR-mutants took to complete one cell cycle was comparable to wild type. However, a

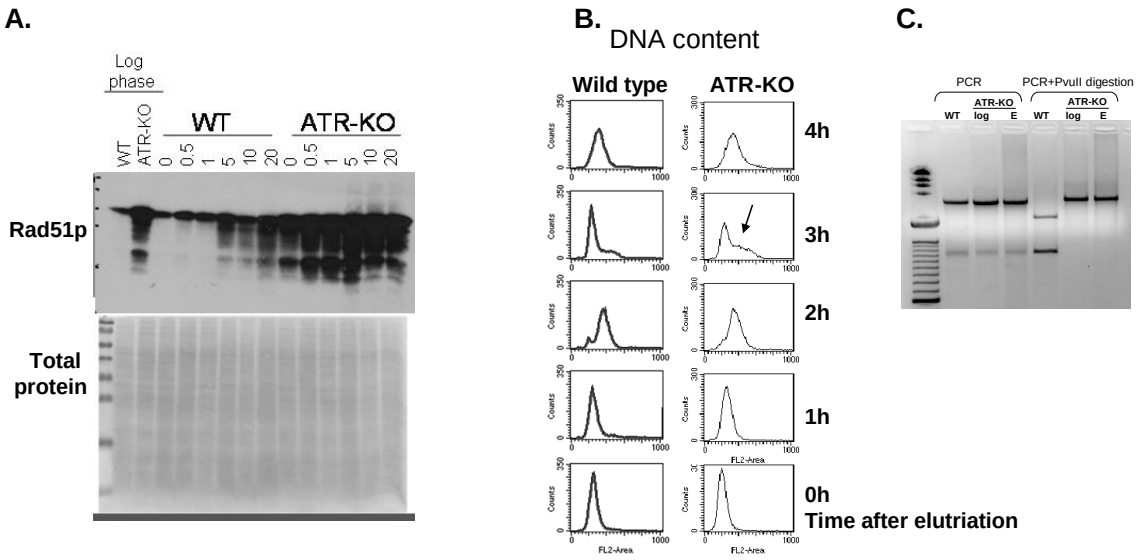


Figure 4.11 ATR-mutants accumulate DNA damage but do not show major delay during cell cycle. A. Log phase wild type and ATR-mutant strains were compared. DNA damage response was monitored by the levels of Rad51p in log phase cultures treated with increasing amounts of HU (mM). B. Wild type and ATR-mutant cultures were synchronized by elutriation and cell cycle progression was monitored by flow cytometry. C. Genotype for ATR-mutant culture. Wild type (WT), ATR-mutant strain a log phase (log) and elutriated (E) cultures were compared. Fragment from ATR locus were amplified by PCR and then digested with PvuII, which only cut wild type sequences.

small population of cells in ATR-KO strain were delayed in the cell cycle progression (Figure 4.11B arrow at 3 h after elutriation).

To test the level of replacement of the wild type ATR gene with the disruption allele, the genotype of the ATR-KO strain was checked by PCR combined with restriction digestion (Figure 4.11C). Primers that anneal to the ATR locus were used to amplify a 3.5 Kb fragment and the PCR product was digested with PvuII which only cleaves the wild type allele. This revealed that ATR strain hold a complete replacement with the disrupted allele. This suggests that the polyploid nature of macronuclear chromosomes and the random segregation of the minichromosomes allowed the cell to be propagated without defect in the viability of cells that hold a great level of DNA damage.

In order to determine the ability of ATR mutant strains to respond genotoxic stress, log phase culture was treated with different concentrations of HU (Figure 4.11A). The activation of the DNA damage response measured by the levels of RAD51p was difficult to assess due to saturation of the Rad51p signal in the mutant strain compared with wild type (Figure 4.11A). These data suggest that as in other eukaryotes, in *Tetrahymena* ATR is necessary for the normal progression of S phase in unperturbed cells cultures.

To better study the DNA damage response, cell cultures synchronized by elutriation were treated with HU and MMS (Figure 4.12A). The induction of Rad51p in mock-treated samples after 4 h of treatment was 6-fold higher in ATR-mutant strain compared to elutriated samples and 5-fold higher than the signal detected in wild

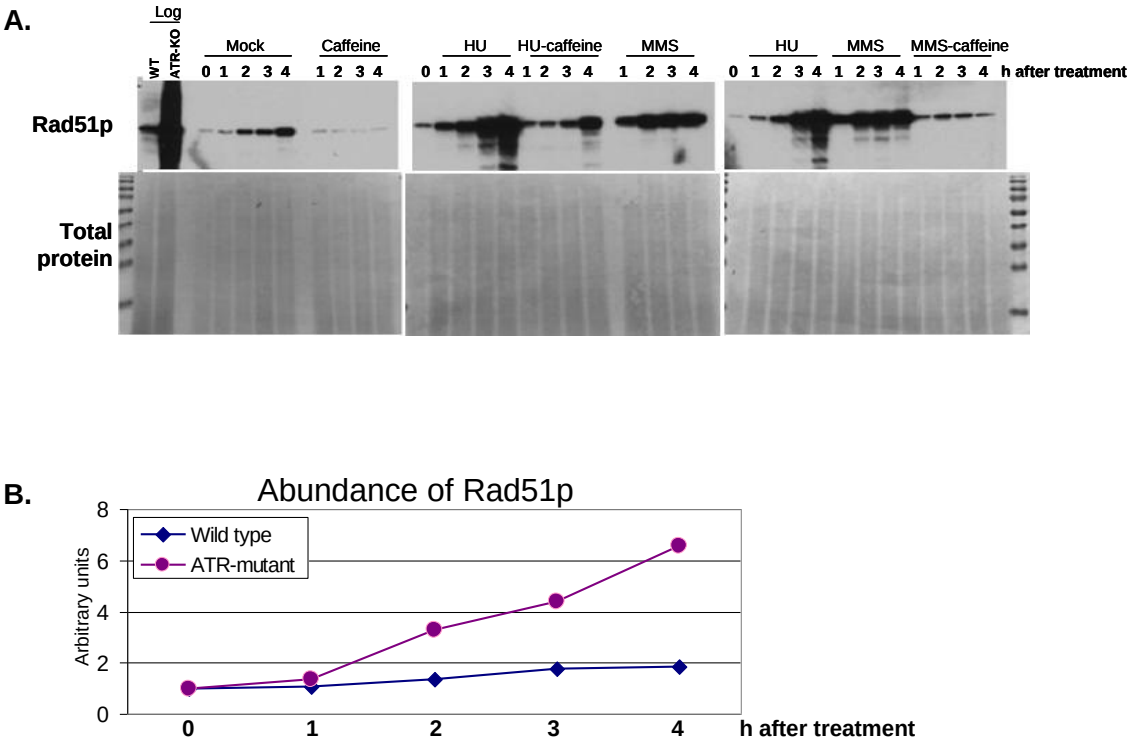


Figure 4.12 Induction of Rad51p in ATR-mutant strains. (A) Abundance of Rad51p in wild type and ATR-mutant strains in logarithmical phase compared with ATR-mutant strain synchronized by elutriation in $G_1$ (0h). Also showing mock, caffeine, HU, HU-caffeine, MMS, MMS-caffeine treatment for 1, 2, 3or 4 h. Bottom panel showing total protein as a loading control by membranes stained with Ponsoe S. (B) Quantification of the abundance of Rad51p in wild type and ATR-mutant cultures. Cultures were synchronized by elutriation (0 h) and cultured for 4 h, the level of Rad51p was detected by western blotting and quantified with ImageJ (http://rsbweb.nih.gov/ij/).

type strains (Figure 4.12B). Since elutriated samples reach S phase 1 h after elutriation (Figure 4.12B), these data suggest that the accumulation of damage in the ATR-mutant strain originates during S phase and could be the product of defects in the progression of DNA replication. Treatments with HU and MMS produced a robust increase in the level of Rad51p indicating the activation of DNA damage response mechanism (Figure 4.12A). The fact that cells are able to detect the genotoxic stress and respond by increasing the abundance of Rad51p in a total absence of a functional ATR kinase, suggest that an alternative mechanism is activated in order to response to DNA damage. This alternative response also detect the damage induced by HU and MMS treatments, as is revealed by the induction of Rad51p (Figure 4.12A).

Surprisingly, caffeine treatment decreased the levels of Rad51p in the ATR-mutant strain (Figure 4.12A). As was noticed above, caffeine-treated wild type cells progressed normally (as mock) through the cell cycle, the ability of caffeine to reduce the abundance of Rad51p in ATR-mutant strains suggest that the alternative pathway is governed by other kinase activity that is also sensitive to caffeine. This is also observed in HU-caffeine and MMS caffeine-treated cells, were the presence of caffeine revert the induction of Rad51p caused by HU and MMS (Figure 4.12A).

The caffeine-sensitivity of the macronuclear ATR-mutant strain raised three possibilities; (1) the disrupted gene in the mutant strain is not ATR, (2) in addition to ATR, caffeine regulates checkpoint at a downstream step (Chk1 and/or Chk2), as has been proposed in mammals (Cortez, 2003), (3) *Tetrahymena* contains another caffeine

sensitive pathway that is independent of ATR. Since orthologues sequences for ATM have not been detected in *Tetrahymena* genome (Yakisich et al., 2006) the other caffeine-sensitive pathway is provably independent of ATM as well.

**An alternative phosphorylation state in response to DNA damage in *Tetrahymena***

To determine whether the caffeine-sensitivity of the macronuclear ATR-mutant strain was modulated by a downstream effector kinase, I decide to follow the ability of Chk1 of autophosphorylation in the response to DNA damage.

One of the most studied targets of ATR in *S. cerevisiae* is the effector kinase Rad53p, which is directly phosphorylated and activated by ATR. The functional homolog of Rad53 in mammals is Chk1. Once activated, Chk1/Rad53 undergoes autophosphorylation necessary for complete activation (Feijoo et al., 2001; Walworth & Bernards, 1996) In yeast and higher eukaryotes, the basal levels of autophosphorylated Rad53 are undetectable, however the exposure to genotoxic agents (like HU and MMS) increases the levels of autophosphorylated Rad53 (Pellicioli et al., 1999).

In *Tetrahymena*, five Chk1 candidate genes with E values ranging from 10e-20 to 10e-29 can be found. Since gene duplication is not common in *Tetrahymena* genome the possibility that these genes are redundant is low, however, no clear candidate has been yet identified.

To examine the phosphorylation of Chk1 in *Tetrahymena*, I used a renaturation assay to measure autophosphorylation in situ. This assay was previously applied in yeast to identify autophosphorylated Rad53 (Pelliconi et al., 1999). Autophosphorylation is

measured by the incorporation of $^{32}P$ from radioactively label ATP. There are several proteins that could be autophosporylated in this assay, however when Rad53p is specifically activated its molecular weight increase. Furthermore, the identity of autophosphorylated Rad53 was corroborated by western blotting using specific antibodies against Rad53 (Pelliconi et al., 1999). Since Chk1 have not been characterized in *Tetrahymena*, I cannot directly relate the incorporation of $^{32}P$ to this kinase. However, the activation of the DNA damage response initiates a phosphorylation cascade in all characterized eukaryotes, and in the absence of ATR this signal can be used to evaluate mechanism of activation of DNA damage response independent of ATR.

As a control for the activation of Chk1, extracts from logarithmically growing wild type yeast strain 14WW (MATa ade2 trp1 leu2 ura3-52 cit1::LEU2) cultured for 3 h in the presence of mock or HU were used. As was expected, phosphorylated Chk1 was undetectable in mock-treated cells (Figure 4.13A). HU-treated yeast cells incorporate a significant amount of radioactivity in the 95 KDa band, that corresponds to the hyperphosphorylated form of Chk1 in yeast (Figure 4.13A, arrow head). Once the phosphorylated form of Chk1 in yeast was clearly identified, logarithmically growing wild type *Tetrahymena* strain mock and HU-treated for 3 h were subjected to the same assay. Surprisingly, mock-treated *Tetrahymena* cells present a large amount of phosphorylated proteins ranging from 43 to 56 KDa. Furthermore, HU-treatment induces a reduction of the phosphorylated signal (Figure 4.13A). These data are extraordinarily opposite to what was expected, first suggest that logarithmically growing *Tetrahymena*

cells contain a great number of proteins that are autophosphorylated in comparison to yeast. Second, *Tetrahymena* phosphorylation level is down regulated in response to DNA damage.

To determine whether the phosphorylation in mock-treated cells was dependent of ATR, logarithmically growing ATR-mutant strain were left untreated or treated with HU for 3 h. The ability of ATR-mutant mock-treated extract of incorporate radioactive label was mostly eliminated, suggesting the presence of a second kinase responsible for this residual phosphorylation. These data also suggest that the majority of the cells phosphorylated during vegetative growth are target of ATR, this is consistent with the role of ATR in other eukaryotes where is regulating the progression of DNA replication in unperturbed cell cycles. Furthermore, the residual phosphorylation present in mock-treated ATR-mutant extracts was completely eliminated upon HU treatment, this suggest that in contrast to yeast response to HU where the phosphorylation state increase in damaged cells, in *Tetrahymena* the tendency is to dephosphorylation in response to DNA damage.

Since logarithmically growing mock-treated *Tetrahymena* extract present a unique high level of kinase activity, I decide to analyze kinase activity of proteins in *Tetrahymena* during vegetative cell cycles. Wild type *Tetrahymena* culture synchronized be elutriation was cultured and samples were collect every hour post elutriation for 4h (Figure 4.13B). In synchronized *Tetrahymena* G1 cultures, a high incorporation of $^{32}P$ was detected ranging from 43 to 72 KDa. The lower portion of this range was permanently phosphorylated across the cell cycle, as was evidenced by the 32P

Figure 4.13 Autophosphorylation assay. Protein extracts of yeast (25 ug) and *Tetrahymena* (50 ug) were loaded in a 10% SDS-PAGE and blotted into PVDF membranes. After denaturation/renaturation treatments the membrane was incubated with 10μCi of [ϒ-32P]ATP and after 1h of incubation membranes were exposed. Arrow-head showing the hyperphosphorylated form of Rad53 in yeast. (A) Logarithmically growing yeast and *Tetrahymena* (wild type and ATR-mutant) strains, mock and HU-treated were compared by its ability of incorporation of 32P-radioctively labeled ATP. (B) Logarithmically growing yeast was compared to synchronized wild type *Tetrahymena* cultures. Samples taken every hour after elutriation (0 h). (C) Logarithmically growing yeast used as control was compared with synchronized wild type *Tetrahymena* treated with HU or MMS. Treatments were added during G1 or S phase, aliquots were saved every hour after treatment. Top panel showing the phosphorylation level and bottom panel total protein as a loading control. (D) Quantification of the $^{32}P$ incorporation in (C) by using ImageJ.

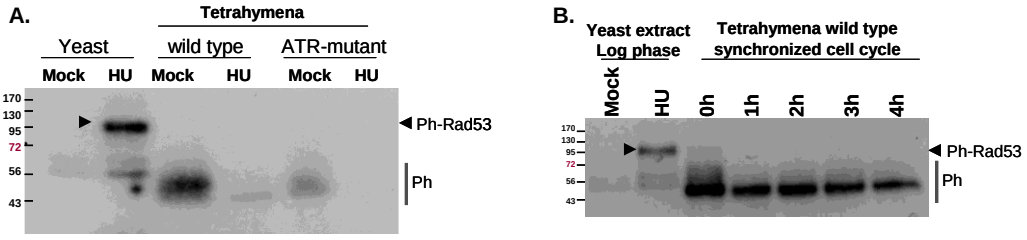
A.
Tetrahymena
Yeast
wild type
ATR-mutant
Mock
HU
Mock
HU
Mock
HU
170
130
95
72
56
43
Ph-Rad53
Ph
B.
Yeast extract
Log phase
Tetrahymena wild type
synchronized cell cycle
Mock
HU
0h
1h
2h
3h
4h
170
130
95
72
56
43
Ph-Rad53
Ph

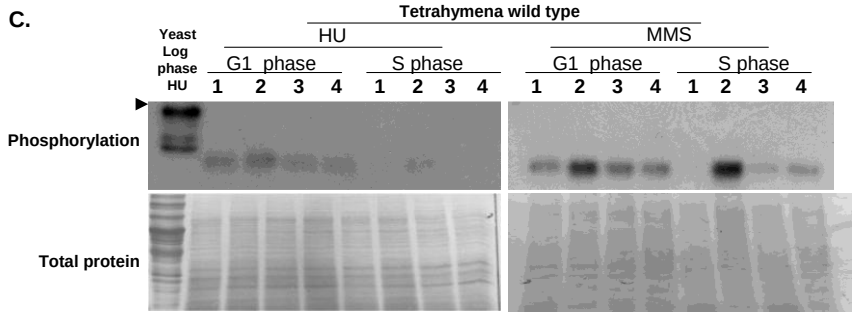
C.
Tetrahymena wild type
Yeast
Log
phase
HU
HU
MMS
G1 phase
S phase
G1 phase
S phase
1 2 3 4 1 2 3 4 1 2 3 4 1 2 3 4
Phosphorylation
Total protein

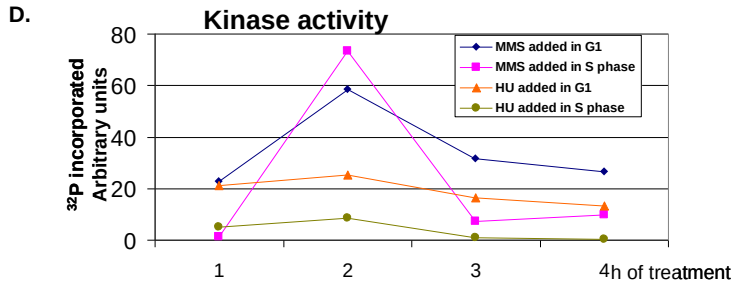
D.
Kinase activity
32P incorporated
Arbitrary units
80
60
40
20
0
1
2
3
4h of treatment
MMS added in G1
MMS added in S phase
HU added in G1
HU added in S phase

incorporation in samples from 1, 2, 3 and 4 h post elutriation. Elutriated cultures usually evidenced a $G_1$ peak from a second cell cycle by 3 h after elutriation, however the higher level of phosphorylation observed in 0 h was not reproduced by the end of 3 h.

This in vitro phosphorylation assay showed that *Tetrahymena* proteins decrease their level of phosphorylation in response to DNA damage. To determine how this kinase activity was modulated by genotoxic agents synchronized G1 and S phase wild type *Tetrahymena* cultures were treated with HU or MMS (Figure 4.13C). The level of phosphorylation in *Tetrahymena* extracts was compared to the autophosphorylated Rad53 band in yeast. HU-treated cells synchronized in $G_1$ present a low and persistent signal through the 4 h of treatment, however when the signal for the incorporation of $^{32}P$ was quantified, normalized against the yeast control and plotted, a minor increment was observed at 2h of treatments (Figure 4.13D). When HU was added to cell synchronized in S phase, almost no detectable signal was observed, the quantification of these samples indicate a signal above background was detected 2 h after the HU was added (Figure 4.13D). Treatments with MMS added to $G_1$ synchronized cells show and transient increased level of 32P incorporated by 2 h of treatments, during the 3 and 4 h post treatment the levels are decrease similar to levels detected at 1 h post treatment. These signals were also quantified by using ImageJ and plotted for further comparison (Figure 4.13D). Finally, when MMS was added to S phase synchronized cells no detectable incorporation of $^{32}P$ was observed by the end of the first hour of treatment. However, an important increase in the $^{32}P$ incorporation was detected 2 h post treatment, this level of incorporation did not persist in the following time points (Figure 4.13C and D). These

data suggest that the ability of phosphorylation revealed by this kinase assay is down regulated in response to DNA damage. Furthermore, mechanisms that regulate this decreased ability to uptake $^{32}P$ are coordinated and they are also able to rearrange this response as is suggested by the collective increased incorporation of $^{32}P$ at 2 h post treatment.

**Discussion**

*Tetrahymena* contains two functionally distinct nuclei, micro- and macronucleus. The S phases and division of these nuclei are offset in the cell cycle, indicating that mitosis is not coordinated with division as in other eukaryotes. Checkpoint proteins shape cell cycle progression by monitoring the presence of DNA damage and coordinating cell propagation. *Tetrahymena* can survive to aberrant division due to the polyploid character of the macronucleus. Despite this, *Tetrahymena* contain checkpoint factors that modulate cell cycle progression.

In this work, DNA damage was induced in G1/S boarder or S phase to study specifically the intra-S phase damage response. In addition, two different genotoxic agents were used, HU and MMS, and the origin of the damage differentially impact on the fate of Mcm6p. Furthermore, during the recovery from genotoxic stress Mcm6p were undetectable suggesting that resumption of replication involve novel mechanisms in *Tetrahymena*.

In general, the features for the control of cell cycle progression in ciliates had not been studied in detail. The progression through cell cycle events is strictly regulated by

machinery that is common between eukaryotes systems. Opportune initiation of DNA synthesis, accurate chromosome segregation, recognition of DNA damage and activation of appropriated DNA damage responses must all be coordinated to maintain genomic stability (Eserink and Kolodner, 2010).

Regulation of the cell cycle is mostly controlled by cyclin dependent kinases (CDK) and their association with specifics cyclins, which act as regulatory subunit. Little is known about cell cycle regulation in ciliated protozoa. *Tetrahymena* and Paramecium are the most studied members of this protozoa family. Regarding to the regulation of the cell cycle, Paramecium contains at least three different CDKs, two CDK1s with different molecular masses (34 and 36 KDa) and are activated at different points in the cell cycle (Tang et al., 1994). The smaller CDK1 is maximally active at the end of the cell cycle, suggesting its involvement in the control of cell division (Tang et al., 1994). The 36KDa-CDK1 probably regulates progression at earlier stages of the cell cycle; its peak of activity is broad and overlaps with DNA replication of the macronucleus (Tang et al., 1995). The other identified CDK, designated as CDK2, is also associated with the regulation of cytokinesis (Zhang & Berger, 1999). Furthermore, two distinctive cyclins have been described in Paramecium (PtCyc1 and PtCyc2,(Zhang et al., 1999). These cyclins contain the characteristic cyclin box and destruction domain, necessary for regulation of cyclins during the cell cycle. However, Paramecium cyclins show no further similarities with cyclins previously described in other eukaryotes suggesting that the control of cell cycle in ciliates is mediated by a divergent CDK-cyclin duo (Zhang et al., 1999). Nevertheless, it is known that small-CDK1 binds to

PtCyc1 and CDK2 forms complex with PtCyc2 and this binding correlates with the maximal activity of the respective CDKs during cell division (Zhang et al., 1999). This suggests that Paramecium cell cycle regulation better resembles the situation in higher eukaryotes where several CDKs exist and more than one cyclin is responsible for cell cycle regulation (Nurse, 2000; Tang et al., 1994).

After this detailed description it was expected that the regulation of cell cycle progression was similar for all the members of this class of protozoa. However, in *Tetrahymena* only one CDK has been identified (Zhang et al., 2002). *Tetrahymena* CDK is cell cycle regulated and accumulates in later stages of G2, which is one of the most remarkable characteristics of this CDK in comparison to other eukaryotes where CDKs are constantly expressed throughout the cell cycle (Zhang et al., 2002, Nurse, 2000). This argues that *Tetrahymena* cell cycle is regulated in a novel fashion.

Recently, the control of the cell cycle has been simplified to a basic component in fission yeast, Schizosaccharomyces pombe. Coudreuse and Nurse (Coudreuse & Nurse, 2010) were able to engineer a strain in which the mitotic cycle was modulated only by a single CDK-cyclin pair (Cdc2-L-Cdc13); under normal conditions the pair CDK-Cdc13 promotes mitosis in fission yeast. The abundance of the CDK-cyclin oscillated during the cell cycle, was accumulated at the end of G2 and eliminated at the end of mitosis. This study showed that a single oscillating CDK-cyclin pair provides the regulation necessary for cell cycle progression. Furthermore, the authors suggested that this system could resemble cell cycle regulation in primitive eukaryotes. Could *Tetrahymena* be an example of such eukaryotic system?

A further unusual characteristic in *Tetrahymena* is that no homolog for Cdc25 phosphatase family has been identified. Cdc25 is essential activator of CDK1 at the G2/M transition in other eukaryotes (Honda et al., 1993). It is worth to mention that plants also lack Cdc25. However, it has been postulated that the lack of Cdc25 has been substituted by a modified CDK during evolution (Boudolf et al., 2006). Plants-specific CDK (B-type CDK) accumulates at the end of the cell cycle, during G2/M transition where it shows a peak of activity (Porceddu et al., 2001). Furthermore, Coudreuse and Nurse (2010) with their model of minimal control network have shown that Cdc25 and other regulatory factors are dispensable for cell cycle progression. Also, members of the Cdc25 family are key components in the response to genotoxic stress, by modulating the activation of checkpoint pathways that ensure genetic stability. This suggests that the regulation of *Tetrahymena* cell cycles notably differ from other eukaryotes, but that the response to genotoxic stress may also differ.

In this chapter, I have used several strategies for the study of the activation of DNA damage response in *Tetrahymena*. In all studied eukaryotic systems the DNA damage response pathway triggers activation of a phosphorylation cascade. The intra-S phase checkpoint pathway maintains genome integrity by sensing replication stress. The main kinase responsible for these phosphorylation cascades are ATR and Chk1 kinases, which activate multiple strategies to slow down the cell cycle and allow time for DNA repair.

In Chapter II, I showed that the DNA damage response in *Tetrahymena* is mediate by an ATR-like pathway, basically defined by its inactivation in presence of

caffeine. To have a more clear view of the activation of the intra-S phase checkpoint, I subsequently induced a genotoxic response during early and late S phase. To directly link this response to progression of DNA synthesis I used flow cytometry to monitor DNA content. I also followed the fate of one subunit of the replicative helicase, Mcm6p. Cellular and macronuclear division, and the potential formation of macronuclear extrusion bodies were also assayed by microscopy. These studies revealed a novel response to DNA damage that is induced during S phase, in which the S phase DNA content is reset to a $G_1$/1N DNA level without the completion of DNA replication (formation of $G_2$/2N peak) and/or cell division. In an attempt to conclusively determine whether the generation of the new 1N peak was independent of cell cycle progression, a specific inhibitor of cytokinesis, W7, was used. W7 was previously tested in *Tetrahymena* (Numata et al., 1999). However, treatments with W7 itself activated the DNA damage response and cellular death in a concentration dependent manner. A further characterization of this new 1N peak generated in response to HU treatments revealed that HU-treated cells increase their size and this parameter is detectable by flow cytometry and by direct microscopic analysis.

These experiments also revealed that Mcm6p protein levels are differentially regulated in response to HU and MMS induced DNA damage, suggesting that more than one pathway is responsible for DNA damage response in *Tetrahymena*. This may be due to the origin of the damage; HU deplete the cells of endogenous precursor, while MMS induce DSB. The common point in both responses is that the regulation of Mcm6p is independent of the ATR pathway.

This contrasts with the situation in the budding yeast, *S. cerevisiae*, where the binding of Mrc1 to Mcm6p is essential for the activation of DNA damage response induced by MMS (Komata et al., 2009). Mrc1 is the homolog for claspin in metazoans and acts as a transducer of the phosphorylation signal from Mec1 to Rad53 (ATR to Chk1 in metazoans). The elimination of the interaction between Mcm6p to Mrc1 prevents activation of the DNA replication checkpoint after MMS treatment, but does not affect the response to DNA replication checkpoint induced by HU treatment (Komata et al., 2009). This placed MCMs as checkpoint sensor for MMS-induced damage and suggested an alternative pathway for HU activation of the DNA damage response. In *Tetrahymena*, previous studies in our lab have shown that Mcm6p is an intrinsic member of the pre-RC and binds specifically to origins of replication(Donti et al., 2009) (Donti et al., 2009). Furthermore, this work suggests that the role of Mcm6p in response to MMS is conserved, as well as the differential regulation in response to HU treatments.

Most interestingly, whereas HU induced the phosphorylation of Mcm4p in other eukaryotes (Ishimi et al., 2003), in *Tetrahymena* when added to either G1 or S phase synchronized cells. The decrease in the abundance of Mcm6p during HU treatment may be used as a strategy to inactivate or stabilize the progression of the MCM helicase during the treatments. This will suggest that degradation of the protein is favored over phosphorylation in *Tetrahymena*. In other eukaryotes systems, MCM-helicase activity is inactivated by ATR specific phosphorylation of Mcm4 in response to HU treatments (Forsburg, 2004; Ishimi et al., 2003). An alternative explanation for the gradual decrease

in the abundance of Mcm6p during HU treatment is that Mcm6p is averted from the macronuclei during replication stress and its cytoplasmic accumulation results in the degradation of the protein. In yeast, due to the closed mitosis character, peptide signal for nuclear localization are essential to regulate the nuclear abundance of proteins involved in replication. Nuclear signaling peptides have been described in *S. cerevisiae* for Mcm5p, Mcm2p and Mcm3p (Forsburg, 2004). As in yeast, in *Tetrahymena* the nuclear envelope of the micronucleus is maintained intact throughout the cell cycle (Davidson & LaFountain, 1975). Furthermore, studies in Paramecium showed that no fragmentation of the nuclear envelope occurs during macronuclear amitotic division (Jurand & Selmann, 1970). This suggests that a closed mitosis and amitosis might be a common feature between ciliates. Strongly basic peptides rich in arginines and lysines are widely recognized as nuclear localization signals among eukaryotes (Boulikas, 1994). However, no clear nuclear targeting peptide sequences have been described for (White et al., 1989). Also common for all eukaryotes is the regulation of nuclear pore complex that mediate the import and the export of proteins across the nuclear envelope (Strambio-De-Castillia et al., 2010). In *Tetrahymena*, specific peptides contained in components of the nuclear pore (nucleoporine, Nup98) precisely guide proteins to either macronucleus or micronucleus (Iwamoto et al., 2009). These determine a nuclear selective transport system for specific factors required in each nucleus. It is not clear whether Mcm6p requires a peptide signal for specific localization, but its high molecular mass and the fact that Mcm6p is cell cycle regulated in vegetatively growing *Tetrahymena* cultures suggest that some regulatory signal may be required.

A remarkable finding of my work is the indication of the plasticity of the amitotic macronucleus during the execution of the cell cycle immediately following HU-induced arrest. The doubling of DNA content and macronuclear division occur with no indication of replication stress. Yet, Mcm6p levels are not restored prior to the first S phase and cell division during the recovery. The absence of Mcm6p implies that an alternative helicase or MCM subunit is sufficient to unwind the parental DNA duplex and support DNA replication during recovery period. This alternative Mcm6p could be a protein encoded by an alternative gene that is expressed in response to replication stress and is responsible for helicase activity during the first cycle of recovery.

The Mcm2-7 proteins are each encoded by a single copy gene in all eukaryotes with the exception of a duplicated gene for Mcm6p and Mcm3p in Xenopus (Liu et al., 2009; Sible et al., 1998). During Xenopus development a switch from maternally synthesized Mcm6p to an Mcm6p form synthesized by the zygote occurs at the time of extensive cell cycle remodeling (midblastula transition) (Sible et al., 1998). This suggested that the replacement of Mcm6p contributes to the establishment of normal cell cycles in Xenopus. Here, since the recovery from HU arrest will include a re-setting of the normal cell cycle, the possibility of a replacement of Mcm6p will provide a nice model. However, in silico analysis of *Tetrahymena* macronuclear genome showed that, as in most of other eukaryotes, only a single ortholog sequence for Mcm6p can be found.

At this point it is not clear whether the decrease in the abundance of Mmc6p is common to all MCM subunits during HU treatments. If only the abundance of Mcm6p is affected during HU treatments, an alternative subunit might substitute for Mcm6p during

early recovery. In pea plants, a single Mcm6p subunit is able to form homohexamers that contain intrinsic helicase activity (Tran et al., 2010). This suggests that MCM-complex formation and helicase activity is not limited by the classical heterohexameric formation and opens the possibility that any other of the MCM subunits may substitute Mcm6p function during recovery from HU treatments in *Tetrahymena*.

The analysis of a hypomorphic ATR-mutant strain revealed that ATR, as in other eukaryotic systems, plays an important role DNA synthesis in unperturbed cell cycles. In order to determine downstream activation of the ATR pathway, I used an in situ assay previously characterized in yeast that measured the level of phosphorylation of Rad53/Chk1 (Pellicioli et al., 1999). The evaluation of kinase activity revealed that the response to DNA damage in *Tetrahymena* is completely different to most eukaryotic systems. While in yeast the autophosphorylation of Rad53 is promoted during DNA damage response, in *Tetrahymena* genotoxic stress induces a decrease in the phosphorylation state of the cell. A previous example of the lack of phosphorylation was shown in studies of CDK, which present no phosphorylation during the progression of cell cycle suggesting that phosphorylation is not one of the major mechanisms for regulatory pathways in ciliated protozoa (Tang et al., 1997). These findings situate *Tetrahymena* as one of the most intriguing models for the study of cell cycle regulation.

# CHAPTER V

## SUMMARY AND DISCUSSION

Maintenance of the genome integrity is essential for successful cell cycle progression. Genotoxic stress is constantly induced to the cell by endogenous or exogenous sources and the ability to repair the damage is vital for completion of cellular process like DNA replication and cell division. Following detection of the damage, the cell activates mechanisms that induce inhibition of the cell cycle progression and promotes the repair of damaged DNA. DNA damage responses include several pathways that are common to all eukaryotes studied to date.

In my dissertation research I set out to study how *Tetrahymena* acts in response to DNA damage. The work presented in Chapter II showed that induction of DNA damage with the alkylating agent (MMS) or depletion of DNA precursors with hydroxyurea (HU) triggers S phase arrest in *Tetrahymena*. This DNA damage response can be modulated by the addition of caffeine, suggesting that is most likely mediated by an ortholog of the human ATR/budding yeast Mec1 kinase. Furthermore, cellular depletion of a novel factor that regulates replication initiation, TIF1, activates this checkpoint response.

Further studies, described Chapter IV, revealed that the addition of HU to synchronized S phase cell cultures induces a decrease in the abundance of Mcm6p, a factor associated with the initiation of DNA replication and elongation of DNA

replication forks. However, the abundance of Mcm6p is stabile in MMS-treated S phase cultures, indicating that the modulation of this component of replicative helicase depends on two different pathways. Furthermore, this work revealed an unusual response to DNA damage induced during S phase, in which the S phase DNA content is reset to a $G_1$/1N DNA level without the completion of DNA replication (formation of $G_2$/2N peak) and/or cell division. Furthermore, the formation of the new $G_1$/1N peak was not associated with the elimination of macronuclear DNA through the formation of extrusion bodies a known pathway for adjusting DNA content following asymmetric macronuclear division. Analysis for the recovery from genotoxic stress showed that cells were competent to initiate a normal cell cycle as soon as the HU was removed from the culture. However, in the first S phase DNA replication occurred in absence of Mcm6p, which is an essential subunit of the heterohexameric MCM2-7 complex in all organisms studied to date. This data suggests that *Tetrahymena* uses novel mechanisms to repress DNA replication forks during genotoxic stress, deal with stalled forks, avert cellular catastrophe due a failure to complete DNA replication and replicate their genome when genotoxic stress is removed.

Also, in Chapter III, I designed a peptide antibody that recognizes specifically Tif1p and allowed its detection in normal cell cycles. Further analysis of the Tif1p binding showed that Tif1p association with the rDNA minichromosome extends beyond the replication origin. Tif1p binding was observed throughout the rDNA coding region. However, Tif1p was largely excluded from non-rDNA chromosomes. These findings

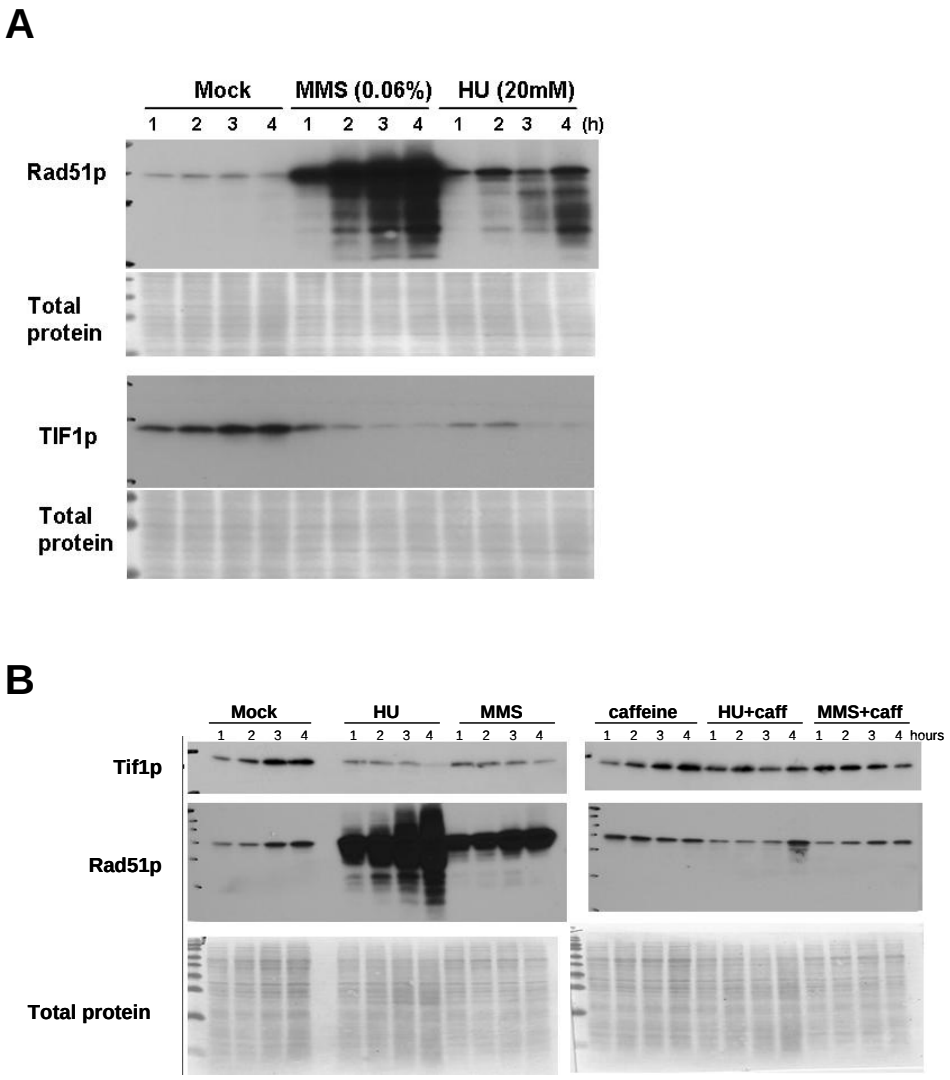


Figure 5.1 Regulation of Tif1p during genotoxic stress revealed by Tif1-peptide antibody in wild type strain. (A) $G_1$ synchronized cultures were treated with mock, MMS or HU and samples collected every hour post treatment. The abundance of Tif1p and Mcm6p where compared by western blot. (B) S phase synchronized cultures were treated with mock, HU, MMS, caffeine, caffeine and HU or caffeine and MMS. The abundance of Tif1p and Rad51p where compared by western blot. Rad51p showed as a marker for the activation of the DNA damage response.

suggest that mechanism for targeting Tif1p to rDNA and non-rDNA minichromosomes is fundamentally different.

In addition, I generated data that indicate that the fate of Tif1p parallels Mcm6p abundance when cells are exposed to HU-induced genotoxic stress (Figure 5.1A). The abundance of Tif1p decreases after 2h in HU-treated cells suggesting that this genotoxic stress affect factors involved in replication in a similar fashion. This decrease in Tif1p levels was also observed in treatment with MMS, this did not correlate with the Mcm6p levels, which are maintained during DNA damage induced by MMS. A further difference between Tif1p and Mcm6p abundance during genotoxic stress was their modulation in the presence of caffeine. While the addition of caffeine was not able to reverse the effect of HU or MMS in Mcm6p (Chapter IV, Figure 4.3C) a complete release of down regulation imposed to Tif1p was observed (Figure 5.1B). This data further supports evidence provided in Chapter II, which suggests that Tif1p and ATR kinase function in the same epistatic pathway. Additionally, they further promote the idea that Mcm6p is specially modulated by two different pathways depending of the origin of the induced damage.

In order to expand the lines of this study and further characterize DNA damage response in *Tetrahymena* several approaches can be use. One of the few orthologs of Tif1p in plants, Why2, was recently described as playing a primary role in organellar DNA repair in Arabidopsis (Cappadocia et al., 2010). Why2 was preferentially bound to single-stranded DNA in a sequence-independent manner during genotoxic treatments suggesting a role in the maintenance of genome integrity. The global defect present in

TIF1-hypomorphic strain (Morrison et al., 2005) and the strong binding of Tif1p to rDNA segments other than replication origins like coding regions in unstressed cells, supports the idea of Tif1p being responsible for the protection of rDNA minichromosomes.

Since TIF1-deficiet strain is hypersensitive to genotoxic stress (Morrison et al., 2005) and Tif1p appeared to be part of the ATR pathway (this work) is crucial to determine how the binding of Tif1p to rDNA is modulated under genotoxic stress and whether the preference of Tif1p for non-rDNA sequences increases during the induction of DNA damage. Furthermore, determine if there is any variation in the specificity of Tif1p binding to rDNA related with the time at which damage is induced. At the G1/S border vs. middle S phase, and its correlation to the generation of the new 1N peak. In addition, since caffeine suppresses the modulation of Tif1p abundance in presence of genotoxic stress, give us the opportunity to determine whether caffeine treatment alter as well the binding of Tif1p. Taking advantage of the Tif1p peptide antibody, ChIP assay can be used to determine how the induction of DNA damage alters the binding of Tif1p to macronuclear minichromosomes. This analysis must be done within 2h of genotoxic treatment since cells treated longer present a decrease in the abundance of Tif1p.

A cloning strategy is currently in progress to generate an overexpression transgene for Tif1p. In this overexpression construct, Tif1p will be placed under the control of an inducible promoter allowing modulation of Tif1p levels at any phase of the cell cycle and will provide an elegant tool to better understand the role of Tif1p in *Tetrahymena* during normal cell cycles and in response to genotoxic stress. Since the main role

described so far for Tif1p is as inhibitor of the initiation of rDNA replication, the increase in the cellular levels of Tif1p should further prevent initiation of replication and lead to late recruitment of pre-RC components (Orc1p and Mcm6p). Two dimensional electophoretic analysis of replication intermediates could be use to determine how the timing of rDNA replication is affected by an excess of Tif1p in the cell. Recruitment of Orc1p and Mcm6p will be assayed by ChIP and compared between strains (wild type, TIF1-hypomorphic, TIF1-overexpression and TIF1-overexpression in a TIF1-hypomorphic background).

Also, with this system will be possible determine whether the Tif1p macronuclear overexpression is able to rescue micronuclear chromosome instability induced in the TIF1-hypomorphic strain. In Chapter II, I showed by PCR analysis that 10 different clonal lines of the TIF1-hypomorphic strain presented genome instability and that these progressive loss occurred during vegetative cell divisions (250 fissions). The transformation of TIF1-hypomorphic strains with the overexpression construct will allow us to assay by conventional PCR whether Tif1p can rescue the defect by comparing clonal lines over time.

Given that Tif1p is downregulated during treatment with genotoxic agents, the overexpression of Tif1p offers the opportunity of better characterize the role of Tif1p in the DNA damage response. Since Tif1p acts as a repressor of replication initiation, this may as well decrease the ability to respond genotoxic stress and induce aberrant phenotypes or affect the viability of the cell. The analysis of the activation of DNA damage response and its modulation by caffeine in presence of an excess of Tif1p can be

analyzed by the approaches used in this work. Flow cytometry to examine cell cycle progression, abundance of Rad51p to monitor activation of genotoxic response and microscopic examination to determine abnormal phenotypes.

Another relevant result in my dissertation was the unexpected finding that the first S phase following the recovery from HU treatment occurs in the absence of Mcm6p. It is not clear how these cells are able to recover and complete S phase. Furthermore, it is unknown how other proteins involved in replication initiation (Orc1p and Tif1p) are modulated during recovery periods. Also a major question is how arrested replication forks are elongated during recovery in absence of Mcm6p or whether new origins of replication are activated. In order to begin answering this question, ChIP assay could be used to study how the origins are being populated by Mcm6p, Orc1p and Tif1p during recovery. This will allow us to determine whether alternative origins are activated or if halt forks are been re-activated during this period. As alternative approach, molecular combing technique is being developed in our lab to determine the distance between activated origins of replication and this could also be used to address the fate of origin firing in recovery periods. In this approach, DNA molecules are stretched and bound to a silanized coverslip, the posterior detection of base analogs incorporated in the DNA allow to measure significant features of chromosome replication as inter-origin distance, fork velocity and fork pausing. By taking advance of this technique the inter-origin distance during recovery time can be determined and compared to normal cell cycle of wild type, Tif1p-hypomorphic and partially-depleted-Orc1p strains are already available

in our lab. This will allow us to determine whether alternative origins are activated or if the halted forks are been re-activated during recovery period.

Also, it will be possible to examine protein binding by molecular combing. A modified protocol where chromatinized and fully proteinated fibers are stretched in a coverslip has been recently developed (Bailis et al., 2008). This allows distinguishing the direct binding of proteins to DNA combined with the direct visualization of DNA synthesis monitored by incorporation of base analogs. It has been shown that in cells where intra-S checkpoint is activated components of the MCM helicase are stabilized at halted replication forks (Cobb et al., 2005). We have raised antibodies that specifically recognize Mcm6p, Orc1p and TIF1p and strains deficient in Tif1p and Orc1p are available. With all these tools we will be able to determine whether replication factors follow the same fate during recovery or whether their association is different in comparison to normal cell cycles. This approach will allow monitoring the binding of Mcm6p and other components of the MCM helicase during recovery and follow they participation in DNA synthesis. Since Tif1p is an inhibitor of replication initiation, determine how an increase in Tif1p levels affect replication during recovery periods.

Since DNA repair act as a background signal of genomic DNA synthesis during recovery periods, different strategies can be follow to decrease the contribution of DNA repair. First, in case that newly activated origins can be fired during recovery the need of short RNA primers for replication of the lagging strand can be used as a technical advantage. Here, the identification of newly fired origins can be done by using RNA probes for FISH analysis combined with molecular combing. On another hand,

polymerases involved in repair (beta and gamma) are more sensitive to dideoxythymidine phosphate (ddTP) (Dresler & Kimbro, 1987). Treatments with ddTP can be added during recovery periods in order to decrease the background DNA synthesis induced by repair. These experiments will give us the opportunity for a further understanding of DNA damage response in *Tetrahymena*.

## REFERENCES

Abraham RT (2001) Cell cycle checkpoint signaling through the ATM and ATR kinases. *Genes Dev* **15:** 2177-2196

Aggarwal BD, Calvi BR (2004) Chromatin regulates origin activity in Drosophila follicle cells. *Nature* **430:** 372-376

Alberghina L, Rossi RL, Querin L, Wanke V, Vanoni M (2004) A cell sizer network involving Cln3 and Far1 controls entrance into S phase in the mitotic cycle of budding yeast. *J Cell Biol* **167:** 433-443

Allen SL (1967) Genomic exclusion: a rapid means for inducing homozygous diploid lines inTetrahymena pyriformis syngen I. *Science* **155**: 575–577

Allewell NM, Oles J, Wolfe J (1976) A physicochemical analysis of conjugation in Tetrahymena pyriformis. *Exp Cell Res* **97:** 394-405

Allis CD, Glover CV, Bowen JK, Gorovsky MA (1980) Histone variants specific to the transcriptionally active, amitotically dividing macronucleus of the unicellular eucaryote, Tetrahymena thermophila. *Cell* **20:** 609-617

Altman AL, Fanning E (2001) The Chinese hamster dihydrofolate reductase replication origin beta is active at multiple ectopic chromosomal locations and requires specific DNA sequence elements for activity. *Mol Cell Biol* **21:** 1098-1110

Altman AL, Fanning E (2004) Defined sequence modules and an architectural element cooperate to promote initiation at an ectopic mammalian chromosomal replication origin. *Mol Cell Biol* **24:** 4138-4150

Amon A, Irniger S, Nasmyth K (1994) Closing the cell cycle circle in yeast: G2 cyclin proteolysis initiated at mitosis persists until the activation of G1 cyclins in the next cycle. *Cell* **77:** 1037-1050

Bailis JM, Luche DD, Hunter T, Forsburg SL (2008) Minichromosome maintenance proteins interact with checkpoint and recombination proteins to promote S phase genome stability. *Mol Cell Biol* **28:** 1724-1738

Barlow SM, Finan DS, Lee J, Chu S (2008) Synthetic orocutaneous stimulation entrains preterm infants with feeding difficulties to suck. *J Perinatol* **28:** 541-548

Beall EL, Manak JR, Zhou S, Bell M, Lipsick JS, Botchan MR (2002) Role for a Drosophila Myb-containing protein complex in site-specific DNA replication. *Nature* **420:** 833-837

Beckerman R, Donner AJ, Mattia M, Peart MJ, Manley JL, Espinosa JM, Prives C (2009) A role for Chk1 in blocking transcriptional elongation of p21 RNA during the S phase checkpoint. *Genes Dev* **23:** 1364-1377

Beinoraviciute-Kellner R, Lipps G, Krauss G (2005) In vitro selection of DNA binding sites for ABF1 protein from Saccharomyces cerevisiae. *FEBS Lett* **579:** 4535-4540

Bell SP, Stillman B (1992) ATP-dependent recognition of eukaryotic origins of DNA replication by a multiprotein complex. *Nature* **357:** 128-134

Blow JJ, Dutta A (2005) Preventing re-replication of chromosomal DNA. *Nat Rev Mol Cell Biol* **6:** 476-486

Blow JJ, Ge XQ (2008) Replication forks, chromatin loops and dormant replication origins. *Genome Biol* **9:** 244

Bodenbender J, Prohaska A, Jauker F, Hipke H, Cleffmann G (1992) DNA elimination and its relation to quantities in the macronucleus of Tetrahymena. *Dev Genet* **13**: 103–110

Bolderson E, Richard DJ, Edelmann W, Khanna KK (2009a) Involvement of Exo1b in DNA damage-induced apoptosis. *Nucleic Acids Res* **37:** 3452-3463

Bolderson E, Richard DJ, Zhou BB, Khanna KK (2009b) Recent advances in cancer therapy targeting proteins involved in DNA double-strand break repair. *Clin Cancer Res* **15:** 6314-6320

Boudolf V, Inze D, De Veylder L (2006) What if higher plants lack a CDC25 phosphatase? *Trends Plant Sci* **11:** 474-479

Boulikas T (1994) Putative nuclear localization signals (NLS) in protein transcription factors. *J Cell Biochem* **55:** 32-58

Brown EJ, Baltimore D (2000) ATR disruption leads to chromosomal fragmentation and early embryonic lethality. *Genes Dev* **14:** 397-402

Brown JM, Marsala C, Kosoy R, Gaertig J (1999). Kinesin-II is preferentially targeted to assembling cilia and is required for ciliogenesis and normal cytokinesis in Tetrahymena. *Mol. Biol. Cell* **10**: 3081–3096

Bruns PJ, Brussard TB (1974) Pair formation in tetrahymena pyriformis, an inducible developmental system. *J Exp Zool* **188:** 337-344

Burma S, Chen BP, Murphy M, Kurimasa A, Chen DJ (2001) ATM phosphorylates histone H2AX in response to DNA double-strand breaks. *J Biol Chem* **276:** 42462-42467

Byun TS, Pacek M, Yee MC, Walter JC, Cimprich KA (2005) Functional uncoupling of MCM helicase and DNA polymerase activities activates the ATR-dependent checkpoint. *Genes Dev* **19:** 1040-1052

Caddle MS, Lussier RH, Heintz NH (1990) Intramolecular DNA triplexes, bent DNA and DNA unwinding elements in the initiation region of an amplified dihydrofolate reductase replicon. *J Mol Biol* **211:** 19-33

Cadoret JC, Meisch F, Hassan-Zadeh V, Luyten I, Guillet C, Duret L, Quesneville H, Prioleau MN (2008) Genome-wide studies highlight indirect links between human replication origins and gene regulation. *Proc Natl Acad Sci U S A* **105:** 15837-15842

Campbell C, Romero DP (1998). Identification and characterization of the RAD51 gene from the ciliate Tetrahymena thermophila. *Nucleic Acids Res* **26**: 3165–3172

Cappadocia L, Marechal A, Parent JS, Lepage E, Sygusch J, Brisson N (2010) Crystal structures of DNA-Whirly complexes and their role in Arabidopsis organelle genome repair. *Plant Cell* **22:** 1849-1867

Carreira A, Hilario J, Amitani I, Baskin RJ, Shivji MK, Venkitaraman AR, Kowalczykowski SC (2009) The BRC repeats of BRCA2 modulate the DNA-binding selectivity of RAD51. *Cell* **136:** 1032-1043

Cassidy-Hanley D, Bowen J, Lee JH, Cole E, VerPlank LA, Gaertig J, Gorovsky MA, Bruns PJ (1997) Germline and somatic transformation of mating Tetrahymena thermophila by particle bombardment. *Genetics* **146:** 135-147

Cervantes MD, Coyne RS, Xi X, Yao MC (2006) The condensin complex is essential for amitotic segregation of bulk chromosomes, but not nucleoli, in the ciliate Tetrahymena thermophila. *Mol Cell Biol* **26:** 4690-4700

Chalker DL (2008) Dynamic nuclear reorganization during genome remodeling of Tetrahymena. *Biochim Biophys Acta* **1783:** 2130-2136

Challoner PB, Amin AA, Pearlman RE, Blackburn EH (1985) Conserved arrangements of repeated DNA sequences in nontranscribed spacers of ciliate ribosomal RNA genes: evidence for molecular coevolution. *Nucleic Acids Res* **13:** 2661-2680

Chang M, Bellaoui M, Boone C, Brown GW (2002) A genome-wide screen for methyl methanesulfonate-sensitive mutants reveals genes required for S phase progression in the presence of DNA damage. *Proc Nat Acad Sci USA* **99:** 16934–16939

Chehab NH, Malikzay A, Stavridi ES, Halazonetis TD (1999) Phosphorylation of Ser-20 mediates stabilization of human p53 in response to DNA damage. *Proc Natl Acad Sci U S A* **96:** 13777-13782

Chen S, de Vries MA, Bell SP (2007) Orc6 is required for dynamic recruitment of Cdt1 during repeated Mcm2-7 loading. *Genes Dev* **21:** 2897-2907

Cherry JM, Blackburn EH (1985) The internally located telomeric sequences in the germ-line chromosomes of Tetrahymena are at the ends of transposon-like elements. *Cell* **43:** 747-758

Chesnokov I, Gossen M, Remus D, Botchan M (1999) Assembly of functionally active Drosophila origin recognition complex from recombinant proteins. *Genes Dev* **13:** 1289-1296

Chini CC, Chen J (2006) Repeated phosphopeptide motifs in human Claspin are phosphorylated by Chk1 and mediate Claspin function. *J Biol Chem* **281:** 33276-33282

Choi JH, Lindsey-Boltz LA, Sancar A (2007) Reconstitution of a human ATR-mediated checkpoint response to damaged DNA. *Proc Natl Acad Sci U S A* **104:** 13301-13306

Chuang RY, Kelly TJ (1999) The fission yeast homologue of Orc4p binds to replication origin DNA via multiple AT-hooks. *Proc Natl Acad Sci U S A* **96:** 2656-2661

Cleffmann G (1980) Chromatin elimination and the genetic organisation of the macronucleus in Tetrahymena thermophila. *Chromosoma* **78:** 313-325

Cleffmann G (1968) Regulation of the amount of DNA in the macronucleus of Tetrahymena. *Exp Cell Res* **50:** 193–207

Cobb JA, Schleker T, Rojas V, Bjergbaek L, Tercero JA, Gasser SM (2005) Replisome instability, fork collapse, and gross chromosomal rearrangements arise synergistically from Mec1 kinase and RecQ helicase mutations. *Genes Dev* **19:** 3055-3069

Cook JG, Chasse DA, Nevins JR (2004) The regulated association of Cdt1 with minichromosome maintenance proteins and Cdc6 in mammalian cells. *J Biol Chem* **279:** 9625-9633

Cortez D (2003) Caffeine inhibits checkpoint responses without inhibiting the ataxia-telangiectasia-mutated (ATM) and ATM- and Rad3-related (ATR) protein kinases. *J Biol Chem* **278:** 37139-37145

Cortez D (2005) Unwind and slow down: checkpoint activation by helicase and polymerase uncoupling. *Genes Dev* **19:** 1007-1012

Cortez D, Glick G, Elledge SJ (2004) Minichromosome maintenance proteins are direct targets of the ATM and ATR checkpoint kinases. *Proc Natl Acad Sci U S A* **101:** 10078-10083

Cortez D, Guntuku S, Qin J, Elledge SJ (2001) ATR and ATRIP: partners in checkpoint signaling. *Science* **294:** 1713-1716

Coudreuse D, Nurse P (2010) Driving the cell cycle with a minimal CDK control network. *Nature* **468:** 1074-1079

Coyne RS, Chalker DL, Yao MC (1996) Genome downsizing during ciliate development: nuclear division of labor through chromosome restructuring. *Annu Rev Genet* **30:** 557-578

Davidson L, LaFountain JR, Jr. (1975) Mitosis and early meiosis in Tetrahymena pyriformis and the evolution of mitosis in the phylum Ciliophora. *Biosystems* **7:** 326-336

Davoli T, Denchi EL, de Lange T (2010) Persistent telomere damage induces bypass of mitosis and tetraploidy. *Cell* **141:** 81-93

Delacroix S, Wagner JM, Kobayashi M, Yamamoto K, Karnitz LM (2007) The Rad9-Hus1-Rad1 (9-1-1) clamp activates checkpoint signaling via TopBP1. *Genes Dev* **21:** 1472-1477

DePamphilis ML (2005) Cell cycle dependent regulation of the origin recognition complex. *Cell Cycle* **4:** 70-79

Desveaux D, Allard J, Brisson N, Sygusch J (2002) Crystallization and preliminary X-ray crystallographic analysis of p24, a component of the potato nuclear factor PBF-2. *Acta Crystallogr D Bio. Crystallogr* **58:** 296–298

Desveaux D, Despres C, Joyeux A, Subramaniam R, Brisson N (2000) PBF-2 is a novel single-stranded DNA binding factor implicated in PR-10a gene activation in potato. *Plant Cell* **12:** 1477–1489

Desveaux D, Subramaniam R, Despres C, Mess JN, Levesque C, Fobert PR, Dangl JL, Brisson N (2004) A "Whirly" transcription factor is required for salicylic acid-dependent disease resistance in Arabidopsis. *Dev Cell* **6:** 229-240

Diffley JF (2004) Regulation of early events in chromosome replication. *Curr Biol* **14:** R778-786

Diffley JF (1998) Replication conrol: choreographing replication origins. *Curr Biol* **8:** R771-773

Diffley JF, Cocker JH, Dowell SJ, Rowley A (1994) Two steps in the assembly of complexes at yeast replication origins in vivo. *Cell* **78:** 303-316

Diffley JF, Stillman B (1988) Purification of a yeast protein that binds to origins of DNA replication and a transcriptional silencer. *Proc Natl Acad Sci U S A* **85:** 2120-2124

Dillin A, Rine J (1998) Roles for ORC in M phase and S phase. *Science* **279:** 1733-1737

Ding Q, MacAlpine DM (2010) Preferential re-replication of Drosophila heterochromatin in the absence of geminin. *PLoS Genet* **6:** 1001-1012

Dirick L, Bohm T, Nasmyth K (1995) Roles and regulation of Cln-Cdc28 kinases at the start of the cell cycle of Saccharomyces cerevisiae. *EMBO J* **14:** 4803-4813

Dobbs DL, Shaiu WL, Benbow RM (1994) Modular sequence elements associated with origin regions in eukaryotic chromosomal DNA. *Nucleic Acids Res* **22:** 2479–2489

Doerder FP, Debault LE (1975) Cytofluorimetric analysis of nuclear DNA during meiosis, fertilization and macronuclear development in the ciliate Tetrahymena pyriformis, syngen 1. *J Cell Sci* **17**: 471–493

Doksani Y, Bermejo R, Fiorani S, Haber JE, Foiani M (2009) Replicon dynamics, dormant origin firing, and terminal fork integrity after double-strand break formation. *Cell* **137:** 247-258

Donti TR, Datta S, Sandoval PY, Kapler GM (2009) Differential targeting of Tetrahymena ORC to ribosomal DNA and non-rDNA replication origins. *EMBO J* **28:** 223-233

Dorn ES, Chastain PD, 2nd, Hall JR, Cook JG (2009) Analysis of re-replication from deregulated origin licensing by DNA fiber spreading. *Nucleic Acids Res* **37:** 60-69

Dresler SL, Kimbro KS (1987) 2',3'-Dideoxythymidine 5'-triphosphate inhibition of DNA replication and ultraviolet-induced DNA repair synthesis in human cells: evidence for involvement of DNA polymerase delta. *Biochemistry* **26:** 2664-2668

Ellison V, Stillman B (2003) Biochemical characterization of DNA damage checkpoint complexes: clamp loader and clamp complexes with specificity for 5' recessed DNA. *PLoS Biol* **1:** 231-243

Enserink JM, Kolodner RD (2010) An overview of Cdk1-controlled targets and processes. *Cell Div* **5:** 11-52

Falck J, Mailand N, Syljuasen RG, Bartek J, Lukas J (2001) The ATM-Chk2-Cdc25A checkpoint pathway guards against radioresistant DNA synthesis. *Nature* **410:** 842-847

Fan Q, Yao M (1996) New telomere formation coupled with site-specific chromosome breakage in Tetrahymena thermophila. *Mol Cell Biol* **16:** 1267-1274

Feijoo C, Hall-Jackson C, Wu R, Jenkins D, Leitch J, Gilbert DM, Smythe C (2001) Activation of mammalian Chk1 during DNA replication arrest: a role for Chk1 in the intra-S phase checkpoint monitoring replication origin firing. *J Cell Biol* **154:** 913-923

Feng L, Wang B, Jong A (1998) Saccharomyces cerevisiae Cdc6 stimulates Abf1 DNA binding activity. *J Biol Chem* **273:** 1298-1302

Forsburg SL (2004) Eukaryotic MCM proteins: beyond replication initiation. *Microbiol Mol Biol Rev* **68:** 109-131

Foss E (2001) Tof1p regulates DNA damage responses during S phase in Saccharomyces cerevisiae. *Genetics* **157:** 567–577

Gaertig J, Gorovsky MA (1992) Efficient mass transformation of Tetrahymena thermophila by electroporation of conjugants. *Proc Natl Acad Sci U S A* **89:** 9196-9200

Gall JG (1974) Free ribosomal RNA genes in the macronucleus of Tetrahymena. *Proc Natl Acad Sci U S A* **71:** 3078-3081

Gallagher RC, Blackburn EH (1998) A promoter region mutation affecting replication of the Tetrahymena ribosomal DNA minichromosome. *Mol Cell Biol* **18:** 3021-3033

Gambus A, Jones RC, Sanchez-Diaz A, Kanemaki M, van Deursen F, Edmondson RD, Labib K (2006) GINS maintains association of Cdc45 with MCM in replisome progression complexes at eukaryotic DNA replication forks. *Nat Cell Biol* **8:** 358-366

Ganem NJ, Storchova Z, Pellman D (2007) Tetraploidy, aneuploidy and cancer. *Curr Opin Genet Dev* **17:** 157-162

Gavin KA, Hidaka M, Stillman B (1995) Conserved initiator proteins in eukaryotes. *Science* **270:** 1667-1671

Ge XQ, Jackson DA, Blow JJ (2007) Dormant origins licensed by excess Mcm2-7 are required for human cells to survive replicative stress. *Genes Dev* **21:** 3331-3341

Gilbert CS, Green CM, Lowndes NF (2001) Budding yeast Rad9 is an ATP-dependent Rad53 activating machine. *Mol Cell* **8:** 129–136

Gomez M, Antequera F (2008) Overreplication of short DNA regions during S phase in human cells. *Genes Dev* **22:** 375-385

Gorovsky MA, Woodard J (1969) Studies on nuclear structure and function in Tetrahymena pyriformis: RNA synthesis in macro- and micronuclei. *J Cell Biol* **42:** 673-682

Grallert B, Boye E (2008) The multiple facets of the intra-S checkpoint. *Cell Cycle* **7:** 2315-2320

Gregan J, Lindner K, Brimage L, Franklin R, Namdar M, Hart EA, Aves SJ, Kearsey SE (2003) Fission yeast Cdc23/Mcm10 functions after pre-replicative complex formation to promote Cdc45 chromatin binding. *Mol Biol Cell* **14:** 3876-3887

Guetg C, Lienemann P, Sirri V, Grummt I, Hernandez-Verdun D, Hottiger MO, Fussenegger M, Santoro R (2010) The NoRC complex mediates the heterochromatin formation and stability of silent rRNA genes and centromeric repeats. *EMBO J* **29:** 2135-2146

Hamilton EP, Bruns PJ, Lin C, Merriam V, Orias E, Vong L, Cassidy-Hanley D (2005) Genome-wide characterization ofTetrahymena thermophila chromosome breakage sites. I. Cloning and identification of functional sites. *Genetics* **170:** 1611–1621

Harper JW, Elledge SJ (2007) The DNA damage response: ten years after. *Mol Cell* **28:** 739-745

Hartwell LH, Weinert TA (1989) Checkpoints: controls that ensure the order of cell cycle events. *Science* **246:** 629-634

Hayashi MT, Takahashi TS, Nakagawa T, Nakayama J, Masukata H (2009) The heterochromatin protein Swi6/HP1 activates replication origins at the pericentromeric region and silent mating-type locus. *Nat Cell Biol* **11:** 357-362

Heichinger C, Penkett CJ, Bahler J, Nurse P (2006) Genome-wide characterization of fission yeast DNA replication origins. *EMBO J* **25:** 5171-5179

Heintz NH, Hamlin JL (1982) An amplified chromosomal sequence that includes the gene for dihydrofolate reductase initiates replication within specific restriction fragments. *Proc Natl Acad Sci U S A* **79:** 4083-4087

Hekmat-Nejad M, You Z, Yee MC, Newport JW, Cimprich KA (2000) Xenopus ATR is a replication-dependent chromatin-binding protein required for the DNA replication checkpoint. *Curr Biol* **10:** 1565-1573

Hinchcliffe EH, Sluder G (2002) Two for two: Cdk2 and its role in centrosome doubling. *Oncogene* **21:** 6154-6160

Hirao A, Kong YY, Matsuoka S, Wakeham A, Ruland J, Yoshida H, Liu D, Elledge SJ, Mak TW (2000) DNA damage-induced activation of p53 by the checkpoint kinase Chk2. *Science* **287:** 1824-1827

Honda R, Ohba Y, Nagata A, Okayama H, Yasuda H (1993) Dephosphorylation of human p34cdc2 kinase on both Thr-14 and Tyr-15 by human cdc25B phosphatase. *FEBS Lett* **318:** 331-334

Hook SS, Lin JJ, Dutta A (2007) Mechanisms to control rereplication and implications for cancer. *Curr Opin Cell Biol* **19:** 663-671

Hou Z, Umthun AR, Dobbs DL (1995) A single-stranded DNA binding protein that specifically recognizes cis-acting sequences in the replication origin and transcriptional promoter region of Tetrahymena rDNA. *Biochemistry* **34:** 4583-4592

Huang Y, Kowalski D (2003) WEB-THERMODYN: Sequence analysis software for profiling DNA helical stability. *Nucleic Acids Res* **31:** 3819-3821

Hwang HC, Clurman BE (2005) Cyclin E in normal and neoplastic cell cycles. *Oncogene* **24:** 2776-2786

Ilves I, Petojevic T, Pesavento JJ, Botchan MR (2010) Activation of the MCM2-7 helicase by association with Cdc45 and GINS proteins. *Mol Cell* **37:** 247-258

Ishimi Y, Komamura-Kohno Y, Kwon HJ, Yamada K, Nakanishi M (2003) Identification of MCM4 as a target of the DNA replication block checkpoint system. *J Biol Chem* **278:** 24644-24650

Iwamoto M, Mori C, Kojidani T, Bunai F, Hori T, Fukagawa T, Hiraoka Y, Haraguchi T (2009) Two distinct repeat sequences of Nup98 nucleoporins characterize dual nuclei in the binucleated ciliate tetrahymena. *Curr Biol* **19:** 843-847

Jackman M, Lindon C, Nigg EA, Pines J (2003) Active cyclin B1-Cdk1 first appears on centrosomes in prophase. *Nat Cell Biol* **5:** 143-148

Jacob F, Brenner S (1963) On the regulation of DNA synthesis in bacteria: the hypothesis of the replicon. *C R Hebd Seances Acad Sci* **256:** 298-300

Jahn CL, Klobutcher LA (2002) Genome remodeling in ciliated protozoa. *Annu Rev Microbiol* **56:** 489-520

Jazayeri A, Falck J, Lukas C, Bartek J, Smith GC, Lukas J, Jackson SP (2006) ATM- and cell cycle-dependent regulation of ATR in response to DNA double-strand breaks. *Nat Cell Biol* **8:** 37-45

Kaczanowski A, Ramel M, Kaczanowska J, Wheatley D (1991) Macronuclear differentiation in conjugating pairs of Tetrahymena treated with the antitubulin drug nocodazole. *Exp Cell Res* **195:** 330-337

Kanemaki M, Labib K (2006) Distinct roles for Sld3 and GINS during establishment and progression of eukaryotic DNA replication forks. *EMBO J* **25:** 1753-1763

Kapler GM, Blackburn EH (1994) A weak germ-line excision mutation blocks developmentally controlled amplification of the rDNA minichromosome of Tetrahymena thermophila. *Genes Dev* **8:** 84-95

Karlsson-Rosenthal C, Millar JB (2006) Cdc25: mechanisms of checkpoint inhibition and recovery. *Trends Cell Biol* **16:** 285-292

Karrer KM (2000) Tetrahymena genetics: two nuclei are better than one. *Methods Cell Biol* **62:** 127-186

Karrer KM, VanNuland TA (1999) Nucleosome positioning is independent of histone H1 in vivo. *J Biol Chem* **274:** 33020-33024

Kato H, Matsunaga F, Miyazaki S, Yin L, D'Urso G, Tanaka K, Murakami Y (2008) Schizosaccharomyces pombe Orc5 plays multiple roles in the maintenance of genome stability throughout the cell cycle. *Cell Cycle* **7:** 1085-1096

Katou Y, Kanoh Y, Bando M, Noguchi H, Tanaka H, Ashikari T, Sugimoto K, Shirahige K (2003) S phase checkpoint proteins Tof1 and Mrc1 form a stable replication-pausing complex. *Nature* **424:** 1078-1083

Katz LA (2001) Evolution of nuclear dualism in ciliates: a reanalysis in light of recent molecular data. *Int J Syst Evol Microbiol* **51:** 1587-1592

Kim SM, Dubey DD, Huberman JA (2003) Early-replicating heterochromatin. *Genes Dev* **17:** 330-335

Kim SM, Huberman JA (1998) Multiple orientation-dependent, synergistically interacting, similar domains in the ribosomal DNA replication origin of the fission yeast, Schizosaccharomyces pombe. *Mol Cell Biol* **18:** 7294-7303

Kobayashi T, Rein T, DePamphilis ML (1998) Identification of primary initiation sites for DNA replication in the hamster dihydrofolate reductase gene initiation zone. *Mol Cell Biol* **18:** 3266-3277

Komata M, Bando M, Araki H, Shirahige K (2009) The direct binding of Mrc1, a checkpoint mediator, to Mcm6, a replication helicase, is essential for the replication checkpoint against methyl methanesulfonate-induced stress. *Mol Cell Biol* **29:** 5008-5019

Kong D, DePamphilis ML (2001) Site-specific DNA binding of the Schizosaccharomyces pombe origin recognition complex is determined by the Orc4 subunit. *Mol Cell Biol* **21:** 8095-8103

Kozar K, Sicinski P (2005) Cell cycle progression without cyclin D-CDK4 and cyclin D-CDK6 complexes. *Cell Cycle* **4:** 388-391

Krause K, Kilbienski I, Mulisch M, Rodiger A, Schafer A, Krupinska K (2005) DNA-binding proteins of the Whirly family in Arabidopsis thaliana are targeted to the organelles. *FEBS Lett* **579:** 3707-3712

Kumagai A, Kim SM, Dunphy WG (2004) Claspin and the activated form of ATR-ATRIP collaborate in the activation of Chk1. *J Biol Chem* **279:** 49599-49608

Kumagai A, Lee J, Yoo HY, Dunphy WG (2006) TopBP1 activates the ATR-ATRIP complex. *Cell* **124:** 943-955

Lam MH, Liu Q, Elledge SJ, Rosen JM (2004) Chk1 is haploinsufficient for multiple functions critical to tumor suppression. *Cancer Cell* **6:** 45-59

Lambert S, Carr AM (2005) Checkpoint responses to replication fork barriers. *Biochimie* **87:** 591–602

Larson DD, Blackburn EH, Yaeger PC, Orias E (1986) Control of rDNA replication in Tetrahymena involves a cis-acting upstream repeat of a promoter element. *Cell* **47:** 229-240

Lee CH, Chung JH (2001) The hCds1 (Chk2)-FHA domain is essential for a chain of phosphorylation events on hCds1 that is induced by ionizing radiation. *J Biol Chem* **276:** 30537-30541

Lee DG, Bell SP (1997) Architecture of the yeast origin recognition complex bound to origins of DNA replication. *Mol Cell Biol* **17:** 7159-7168

Lee HO, Davidson JM, Duronio RJ (2009) Endoreplication: polyploidy with purpose. *Genes Dev* **23:** 2461-2477

Lee JK, Moon KY, Jiang Y, Hurwitz J (2001) The Schizosaccharomyces pombe origin recognition complex interacts with multiple AT-rich regions of the replication origin DNA by means of the AT-hook domains of the spOrc4 protein. *Proc Natl Acad Sci U S A* **98:** 13589-13594

Li R, Yu DS, Tanaka M, Zheng L, Berger SL, Stillman B (1998) Activation of chromosomal DNA replication in Saccharomyces cerevisiae by acidic transcriptional activation domains. *Mol Cell Biol* **18:** 1296-1302

Liang C, Weinreich M, Stillman B (1995) ORC and Cdc6p interact and determine the frequency of initiation of DNA replication in the genome. *Cell* **81:** 667-676

Liberi G, Foiani M (2010) The double life of Holliday junctions. *Cell Res* **20:** 611-613

Lin R, Cook RG, Allis CD (1991) Proteolytic removal of core histone amino termini and dephosphorylation of histone H1 correlate with the formation of condensed chromatin and transcriptional silencing during Tetrahymena macronuclear development. *Genes Dev* **5:** 1601-1610

Lin S, Kowalski D (1997) Functional equivalency and diversity of cis-acting elements among yeast replication origins. *Mol Cell Biol* **17:** 5473-5484

Lipford JR, Bell SP (2001) Nucleosomes positioned by ORC facilitate the initiation of DNA replication. *Mol Cell* **7:** 21-30

Liu P, Barkley LR, Day T, Bi X, Slater DM, Alexandrow MG, Nasheuer HP, Vaziri C (2006) The Chk1-mediated S phase checkpoint targets initiation factor Cdc45 via a Cdc25A/Cdk2-independent mechanism. *J Biol Chem* **281:** 30631-30644

Liu Q, Guntuku S, Cui XS, Matsuoka S, Cortez D, Tamai K, Luo G, Carattini-Rivera S, DeMayo F, Bradley A, Donehower LA, Elledge SJ (2000) Chk1 is an essential kinase that is regulated by Atr and required for the G(2)/M DNA damage checkpoint. *Genes Dev* **14:** 1448-1459

Liu JS, Kuo SR, Melendy T (2003) Comparison of checkpoint responses triggered by DNA polymerase inhibition versus DNA damaging agents. *Mutat Res* **532:** 215–226

Liu Y, Richards TA, Aves SJ (2009) Ancient diversification of eukaryotic MCM DNA replication proteins. *BMC Evol Biol* **9:** 60

Loidl J, Mochizuki K (2009) Tetrahymena meiotic nuclear reorganization is induced by a checkpoint kinase-dependent response to DNA damage. *Mol Biol Cell* **20:** 2428-2437

Loidl J, Scherthan H (2004) Organization and pairing of meiotic chromosomes in the ciliate Tetrahymena thermophila. *J Cell Sci* **117:** 5791–5801

Lopez-Mosqueda J, Maas NL, Jonsson ZO, Defazio-Eli LG, Wohlschlegel J, Toczyski DP (2010) Damage-induced phosphorylation of Sld3 is important to block late origin firing. *Nature* **467:** 479-483

Lou H, Komata M, Katou Y, Guan Z, Reis CC, Budd M, Shirahige K, Campbell JL (2008) Mrc1 and DNA polymerase epsilon function together in linking DNA replication and the S phase checkpoint. *Mol Cell* **32:** 106-117

Lupardus PJ, Byun T, Yee MC, Hekmat-Nejad M, Cimprich KA (2002) A requirement for replication in activation of the ATR-dependent DNA damage checkpoint. *Genes Dev* **16:** 2327–2332

Lutzmann M, Maiorano D, Mechali M (2006) A Cdt1-geminin complex licenses chromatin for DNA replication and prevents rereplication during S phase in Xenopus. *EMBO J* **25:** 5764-5774

Ma C, Leu TH, Hamlin JL (1990) Multiple origins of replication in the dihydrofolate reductase amplicons of a methotrexate-resistant chinese hamster cell line. *Mol Cell Biol* **10:** 1338-1346

MacAlpine DM, Bell SP (2005) A genomic view of eukaryotic DNA replication. *Chromosome Res* **13:** 309-326

MacAlpine DM, Zhang Z, Kapler GM (1997) Type I elements mediate replication fork pausing at conserved upstream sites in the Tetrahymena thermophila ribosomal DNA minichromosome. *Mol Cell Biol* **17:** 4517-4525

MacAlpine HK, Gordan R, Powell SK, Hartemink AJ, MacAlpine DM (2010) Drosophila ORC localizes to open chromatin and marks sites of cohesin complex loading. *Genome Res* **20:** 201-211

Machida YJ, Dutta A (2005) Cellular checkpoint mechanisms monitoring proper initiation of DNA replication. *J Biol Chem* **280:** 6253-6256

Machida YJ, Teer JK, Dutta A (2005) Acute reduction of an origin recognition complex (ORC) subunit in human cells reveals a requirement of ORC for Cdk2 activation. *J Biol Chem* **280:** 27624-27630

Mailand N, Bekker-Jensen S, Faustrup H, Melander F, Bartek J, Lukas C, Lukas J (2007) RNF8 ubiquitylates histones at DNA double-strand breaks and promotes assembly of repair proteins. *Cell* **131:** 887-900

Mailand N, Falck J, Lukas C, Syljuasen RG, Welcker M, Bartek J, Lukas J (2000) Rapid destruction of human Cdc25A in response to DNA damage. *Science* **288:** 1425-1429

Mailand N, Podtelejnikov AV, Groth A, Mann M, Bartek J, Lukas J (2002) Regulation of G(2)/M events by Cdc25A through phosphorylation-dependent modulation of its stability. *EMBO J* **21:** 5911-5920

Maiorano D, Lemaitre JM, Mechali M (2000) Stepwise regulated chromatin assembly of MCM2-7 proteins. *J Biol Chem* **275:** 8426-8431

Malone CD, Anderson AM, Motl JA, Rexer CH, Chalker DL (2005) Germ line transcripts are processed by a Dicer-like protein that is essential for developmentally programmed genome rearrangements of Tetrahymena thermophila. *Mol Cell Biol* **25:** 9151-9164

Malumbres M (2005) Revisiting the "Cdk-centric" view of the mammalian cell cycle. *Cell Cycle* **4:** 206-210

Mandal M, Bandyopadhyay D, Goepfert TM, Kumar R (1998) Interferon-induces expression of cyclin-dependent kinase-inhibitors p21WAF1 and p27Kip1 that prevent activation of cyclin-dependent kinase by CDK-activating kinase (CAK). *Oncogene* **16:** 217-225

Marahrens Y, Stillman B (1992) A yeast chromosomal origin of DNA replication defined by multiple functional elements. *Science* **255:** 817-823

Marechal A, Parent JS, Veronneau-Lafortune F, Joyeux A, Lang BF, Brisson N (2009) Whirly proteins maintain plastid genome stability in Arabidopsis. *Proc Natl Acad Sci U S A* **106:** 14693-14698

Martindale DW, Allis CD, Bruns PJ (1982) Conjugation in Tetrahymena thermophila. A temporal analysis of cytological stages. *Exp Cell Res* **140:** 227-236

Masumoto H, Muramatsu S, Kamimura Y, Araki H (2002) S-Cdk-dependent phosphorylation of Sld2 essential for chromosomal DNA replication in budding yeast. *Nature* **415:** 651-655

Masumoto H, Sugino A, Araki H (2000) Dpb11 controls the association between DNA polymerases alpha and epsilon and the autonomously replicating sequence region of budding yeast. *Mol Cell Biol* **20:** 2809-2817

Matsuoka S, Rotman G, Ogawa A, Shiloh Y, Tamai K, Elledge SJ (2000) Ataxia telangiectasia-mutated phosphorylates Chk2 in vivo and in vitro. *Proc Natl Acad Sci U S A* **97:** 10389-10394

Maya-Mendoza A, Petermann E, Gillespie DA, Caldecott KW, Jackson DA (2007) Chk1 regulates the density of active replication origins during the vertebrate S phase. *EMBO J* **26:** 2719-2731

Mayo KA, Orias E (1981) Further evidence for lack of gene expression in the Tetrahymena micronucleus. *Genetics* **98:** 747-762

McBroom LD, Sadowski PD (1995) Functional analysis of the ABF1-binding sites within the Ya regions of the MATa and HMRa loci of Saccharomyces cerevisiae. *Curr Genet* **28:** 1-11

McGarry TJ, Kirschner MW (1998) Geminin, an inhibitor of DNA replication, is degraded during mitosis. *Cell* **93:** 1043-1053

Melchionna R, Chen XB, Blasina A, McGowan CH (2000) Threonine 68 is required for radiation-induced phosphorylation and activation of Cds1. *Nat Cell Biol* **2:** 762-765

Mendenhall MD, Hodge AE (1998) Regulation of Cdc28 cyclin-dependent protein kinase activity during the cell cycle of the yeast Saccharomyces cerevisiae. *Microbiol Mol Biol Rev* **62:** 1191-1243

Merriam EV, Bruns PJ (1988) Phenotypic assortment in Tetrahymena thermophila: assortment kinetics of antibiotic-resistance markers, tsA, death, and the highly amplified rDNA locus. *Genetics* **120:** 389-395

Mimitou EP, Symington LS (2008) Sae2, Exo1 and Sgs1 collaborate in DNA double-strand break processing. *Nature* **455:** 770-774

Minami H, Takahashi J, Suto A, Saitoh Y, Tsutsumi K (2006) Binding of AlF-C, an Orc1-binding transcriptional regulator, enhances replicator activity of the rat aldolase B origin. *Mol Cell Biol* **26:** 8770-8780

Miyahara K, Hashimoto N, Higashinakagawa T, Pearlman RE (1993) Common sequence elements are important for transcription and replication of the extrachromosomal rRNA-encoding genes of Tetrahymena. *Gene* **127:** 209-213

Mizzen CA, Dou Y, Liu Y, Cook RG, Gorovsky MA, Allis CD (1999) Identification and mutation of phosphorylation sites in a linker histone. Phosphorylation of macronuclear H1 is not essential for viability in tetrahymena. *J Biol Chem* **274:** 14533-14536

Mochizuki K, Gorovsky MA (2004) Small RNAs in genome rearrangement in Tetrahymena. *Curr Opin Genet Dev* **14:** 181-187

Mochizuki K, Gorovsky MA (2005) A Dicer-like protein in Tetrahymena has distinct functions in genome rearrangement, chromosome segregation, and meiotic prophase. *Genes Dev* **19:** 77-89

Mohammad M, Saha S, Kapler GM (2000) Three different proteins recognize a multifunctional determinant that controls replication initiation, fork arrest and transcription in Tetrahymena. *Nucleic Acids Res* **28:** 843-851

Mohammad M, York RD, Hommel J, Kapler GM (2003) Characterization of a novel origin recognition complex-like complex: implications for DNA recognition, cell cycle control, and locus-specific gene amplification. *Mol Cell Biol* **23:** 5005-5017

Mohammad MM, Donti TR, Sebastian Yakisich J, Smith AG, Kapler GM (2007) Tetrahymena ORC contains a ribosomal RNA fragment that participates in rDNA origin recognition. *EMBO J* **26:** 5048-5060

Molinari M, Mercurio C, Dominguez J, Goubin F, Draetta GF (2000) Human Cdc25 A inactivation in response to S phase inhibition and its role in preventing premature mitosis. *EMBO Rep* **1:** 71-79

Morrison TL, Yakisich JS, Cassidy-Hanley D, Kapler GM (2005) TIF1 Represses rDNA replication initiation, but promotes normal S phase progression and chromosome transmission in Tetrahymena. *Mol Biol Cell* **16:** 2624-2635

Moynahan ME, Jasin M (2010) Mitotic homologous recombination maintains genomic stability and suppresses tumorigenesis. *Nat Rev Mol Cell Biol* **11:** 196-207

Mpoke S, Wolfe J (1996) DNA digestion and chromatin condensation during nuclear death in Tetrahymena. *Exp Cell Res* **225:** 357-365

Mucenski ML, McLain K, Kier AB, Swerdlow SH, Schreiner CM, Miller TA, Pietryga DW, Scott WJ, Jr., Potter SS (1991) A functional c-myb gene is required for normal murine fetal hepatic hematopoiesis. *Cell* **65:** 677-689

Muramatsu S, Hirai K, Tak YS, Kamimura Y, Araki H (2010) CDK-dependent complex formation between replication proteins Dpb11, Sld2, Pol (epsilon}, and GINS in budding yeast. *Genes Dev* **24:** 602-612

Newlon CS, Theis JF (1993) The structure and function of yeast ARS elements. *Curr Opin Genet Dev* **3:** 752-758

Nilsson JR, Leick V (1970) Nucleolar organization and ribosome formation in Tetrahymena pyriformis GL. *Exp Cell Res* **60:** 361-372

Nitani N, Yadani C, Yabuuchi H, Masukata H, Nakagawa T (2008) Mcm4 C-terminal domain of MCM helicase prevents excessive formation of single-stranded DNA at stalled replication forks. *Proc Natl Acad Sci U S A* **105:** 12973-12978

Numata O, Fujiu K, Gonda K (1999) Macronuclear division and cytokinesis in Tetrahymena. *Cell Biol Int* **23:** 849-857

Nurse P (2000) A long twentieth century of the cell cycle and beyond. *Cell* **100:** 71-78

Ogawa Y, Takahashi T, Masukata H (1999) Association of fission yeast Orp1 and Mcm6 proteins with chromosomal replication origins. *Mol Cell Biol* **19:** 7228-7236

Okuno Y, McNairn AJ, den Elzen N, Pines J, Gilbert DM (2001) Stability, chromatin association and functional activity of mammalian pre-replication complex proteins during the cell cycle. *EMBO J* **20:** 4263-4277

Okuno Y, Okazaki T, Masukata H (1997) Identification of a predominant replication origin in fission yeast. *Nucleic Acids Res* **25:** 530-537

Okuno Y, Satoh H, Sekiguchi M, Masukata H (1999) Clustered adenine/thymine stretches are essential for function of a fission yeast replication origin. *Mol Cell Biol* **19:** 6699-6709

Orias E, Bruns PJ (1976) Induction and isolation of mutants in Tetrahymena. *Methods Cell Biol* **13:** 247–282

Orias E, Hashimoto N, Chau MF, Higashinakagawa T (1991) PCR amplification of Tetrahymena rDNA segments starting with individual cells. *J Protozool* **38:** 306-311

Osborn AJ, Elledge SJ (2003) Mrc1 is a replication fork component whose phosphorylation in response to DNA replication stress activates Rad53. *Genes Dev* **17:** 1755-1767

Palen TE, Cech TR (1984) Chromatin structure at the replication origins and transcription-initiation regions of the ribosomal RNA genes of Tetrahymena. *Cell* **36:** 933-942

Pan J, Woodson SA (1998) Folding intermediates of a self-splicing RNA: mispairing of the catalytic core. *J Mol Biol* **280:** 597-609

Paredes S, Maggert KA (2009) Ribosomal DNA contributes to global chromatin regulation. *Proc Natl Acad Sci U S A* **106:** 17829-17834

Park SY, Asano M (2008) The origin recognition complex is dispensable for endoreplication in Drosophila. *Proc Natl Acad Sci U S A* **105:** 12343-12348

Patil NS, Hempen PM, Udani RA, Karrer KM (1997) Alternate junctions and microheterogeneity of Tlr1, a developmentally regulated DNA rearrangement in Tetrahymena thermophila. *J Eukaryot Microbiol* **44:** 518-522

Pellicioli A, Lucca C, Liberi G, Marini F, Lopes M, Plevani P, Romano A, Di Fiore PP, Foiani M (1999) Activation of Rad53 kinase in response to DNA damage and its effect in modulating phosphorylation of the lagging strand DNA polymerase. *EMBO J* **18:** 6561-6572

Peng CY, Graves PR, Thoma RS, Wu Z, Shaw AS, Piwnica-Worms H (1997) Mitotic and G2 checkpoint control: regulation of 14-3-3 protein binding by phosphorylation of Cdc25C on serine-216. *Science* **277:** 1501-1505

Peng JC, Karpen GH (2008) Epigenetic regulation of heterochromatic DNA stability. *Curr Opin Genet Dev* **18:** 204-211

Petermann E, Helleday T (2010) Pathways of mammalian replication fork restart. *Nat Rev Mol Cell Biol* **11:** 683-687

Petermann E, Helleday T, Caldecott KW (2008) Claspin promotes normal replication fork rates in human cells. *Mol Biol Cell* **19:** 2373-2378

Petermann E, Maya-Mendoza A, Zachos G, Gillespie DA, Jackson DA, Caldecott KW (2006) Chk1 requirement for high global rates of replication fork progression during normal vertebrate S phase. *Mol Cell Biol* **26:** 3319-3326

Petermann E, Woodcock M, Helleday T (2010) Chk1 promotes replication fork progression by controlling replication initiation. *Proc Natl Acad Sci U S A* **107:** 16090-16095

Peters JM (2006) The anaphase promoting complex/cyclosome: a machine designed to destroy. *Nat Rev Mol Cell Biol* **7:** 644-656

Pflumm MF, Botchan MR (2001) Orc mutants arrest in metaphase with abnormally condensed chromosomes. *Development* **128:** 1697-1707

Pinato S, Scandiuzzi C, Arnaudo N, Citterio E, Gaudino G, Penengo L (2009) RNF168, a new RING finger, MIU-containing protein that modifies chromatin by ubiquitination of histones H2A and H2AX. *BMC Mol Biol* **10:** 55-69

Porceddu A, Stals H, Reichheld JP, Segers G, De Veylder L, Barroco RP, Casteels P, Van Montagu M, Inze D, Mironov V (2001) A plant-specific cyclin-dependent kinase is involved in the control of G2/M progression in plants. *J Biol Chem* **276:** 36354-36360

Prescott DM (1994) The DNA of ciliated protozoa. *Microbiol Rev* **58:** 233-267

Prescott DM (1994) The DNA of ciliated protozoa. *Microbiol Rev* **58:** 233-267

Rao PN, Johnson RT (1970) Mammalian cell fusion: studies on the regulation of DNA synthesis and mitosis. *Nature* **225:** 159-164

Reed SH, Akiyama M, Stillman B, Friedberg EC (1999) Yeast autonomously replicating sequence binding factor is involved in nucleotide excision repair. *Genes Dev* **13:** 3052-3058

Reischmann KP, Zhang Z, Kapler GM (1999) Long range cooperative interactions regulate the initiation of replication in the Tetrahymena thermophila rDNA minichromosome. *Nucleic Acids Res* **27:** 3079-3089

Remus D, Beall EL, Botchan MR (2004) DNA topology, not DNA sequence, is a critical determinant for Drosophila ORC-DNA binding. *EMBO J* **23:** 897-907

Rhode PR, Elsasser S, Campbell JL (1992) Role of multifunctional autonomously replicating sequence binding factor 1 in the initiation of DNA replication and transcriptional control in Saccharomyces cerevisiae. *Mol Cell Biol* **12:** 1064-1077

Richardson H, Lew DJ, Henze M, Sugimoto K, Reed SI (1992) Cyclin-B homologs in Saccharomyces cerevisiae function in S phase and in G2. *Genes Dev* **6:** 2021-2034

Ricke RM, Bielinsky AK (2004) Mcm10 regulates the stability and chromatin association of DNA polymerase-alpha. *Mol Cell* **16:** 173-185

Rogakou EP, Pilch DR, Orr AH, Ivanova VS, Bonner WM (1998) DNA double-stranded breaks induce histone H2AX phosphorylation on serine 139. *J Biol Chem* **273:** 5858-5868

Roos-Mattjus P, Hopkins KM, Oestreich AJ, Vroman BT, Johnson KL, Naylor S, Lieberman HB, Karnitz LM (2003) Phosphorylation of human Rad9 is required for genotoxin-activated checkpoint signaling. *J Biol Chem* **278:** 24428-24437

Russell P, Moreno S, Reed SI (1989) Conservation of mitotic controls in fission and budding yeasts. *Cell* **57:** 295-303

Saha S, Kapler GM (2000) Allele-specific protein-DNA interactions between the single-stranded DNA-binding protein, ssA-TIBF, and DNA replication determinants in Tetrahymena. *J Mol Biol* **295:** 423-439

Saha S, Nicholson A, Kapler GM (2001) Cloning and biochemical analysis of the tetrahymena origin binding protein TIF1: competitive DNA binding in vitro and in vivo to critical rDNA replication determinants. *J Biol Chem* **276:** 45417-45426

Sanchez Y, Wong C, Thoma RS, Richman R, Wu Z, Piwnica-Worms H, Elledge SJ (1997) Conservation of the Chk1 checkpoint pathway in mammals: linkage of DNA damage to Cdk regulation through Cdc25. *Science* **277:** 1497-1501

Santamaria D, Barriere C, Cerqueira A, Hunt S, Tardy C, Newton K, Caceres JF, Dubus P, Malumbres M, Barbacid M (2007) Cdk1 is sufficient to drive the mammalian cell cycle. *Nature* **448:** 811-815

Santocanale C, Diffley JF (1998) A Mec1- and Rad53-dependent checkpoint controls late-firing origins of DNA replication. *Nature* **395:** 615-618

Santocanale C, Sharma K, Diffley JF (1999) Activation of dormant origins of DNA replication in budding yeast. *Genes Dev* **13:** 2360-2364

Sarkaria JN, Busby EC, Tibbetts RS, Roos P, Taya Y, Karnitz LM, Abraham RT (1999) Inhibition of ATM and ATR kinase activities by the radiosensitizing agent, caffeine. *Cancer Res* **59:** 4375-4382

Saxena S, Dutta A (2005) Geminin-Cdt1 balance is critical for genetic stability. *Mutat Res* **569:** 111-121

Schlecht U, Erb I, Demougin P, Robine N, Borde V, Nimwegen E, Nicolas A, Primig M (2008) Genome-wide expression profiling, in vivo DNA binding analysis, and probabilistic motif prediction reveal novel Abf1 target genes during fermentation, respiration, and sporulation in yeast. *Mol Biol Cell* **19:** 2193-2207

Schwob E, Bohm T, Mendenhall MD, Nasmyth K (1994) The B-type cyclin kinase inhibitor p40SIC1 controls the G1 to S transition in S. cerevisiae. *Cell* **79:** 233-244

Schwob E, Nasmyth K (1993) CLB5 and CLB6, a new pair of B cyclins involved in DNA replication in Saccharomyces cerevisiae. *Genes Dev* **7:** 1160-1175

Sclafani RA (2000) Cdc7p-Dbf4p becomes famous in the cell cycle. *J Cell Sci* **113 ( Pt 12):** 2111-2117

Sclafani RA, Holzen TM (2007) Cell cycle regulation of DNA replication. *Annu Rev Genet* **41:** 237-280

Segurado M, de Luis A, Antequera F (2003) Genome-wide distribution of DNA replication origins at A+T-rich islands in Schizosaccharomyces pombe. *EMBO Rep* **4:** 1048-1053

Shechter D, Costanzo V, Gautier J (2004) ATR and ATM regulate the timing of DNA replication origin firing. *Nat Cell Biol* **6:** 648-655

Shen X, Yu L, Weir JW, Gorovsky MA (1995) Linker histones are not essential and affect chromatin condensation in vivo. *Cell* **82:** 47-56

Sheu YJ, Stillman B (2010) The Dbf4-Cdc7 kinase promotes S phase by alleviating an inhibitory activity in Mcm4. *Nature* **463:** 113-117

Shieh SY, Ahn J, Tamai K, Taya Y, Prives C (2000) The human homologs of checkpoint kinases Chk1 and Cds1 (Chk2) phosphorylate p53 at multiple DNA damage-inducible sites. *Genes Dev* **14:** 289-300

Shimada K, Pasero P, Gasser SM (2002) ORC and the intra-S phase checkpoint: a threshold regulates Rad53p activation in S phase. *Genes Dev* **16:** 3236-3252

Shimada M, Niida H, Zineldeen DH, Tagami H, Tanaka M, Saito H, Nakanishi M (2008) Chk1 is a histone H3 threonine 11 kinase that regulates DNA damage-induced transcriptional repression. *Cell* **132:** 221-232

Shirahige K, Hori Y, Shiraishi K, Yamashita M, Takahashi K, Obuse C, Tsurimoto T, Yoshikawa H (1998) Regulation of DNA-replication origins during cell-cycle progression. *Nature* **395:** 618-621

Sible JC, Erikson E, Hendrickson M, Maller JL, Gautier J (1998) Developmental regulation of MCM replication factors in Xenopus laevis. *Curr Biol* **8:** 347-350

Sleeth KM, Sorensen CS, Issaeva N, Dziegielewski J, Bartek J, Helleday T (2007) RPA mediates recombination repair during replication stress and is displaced from DNA by checkpoint signalling in human cells. *J Mol Biol* **373:** 38-47

Smith JJ, Cole ES, Romero DP (2004a) Transcriptional control of RAD51 expression in the ciliate Tetrahymena thermophila. *Nucleic Acids Res* **32:** 4313–4321

Smith JJ, Yakisich JS, Kapler GM, Cole ES, Romero DP (2004b) A β-tubulin mutation selectively uncouples nuclear division and cytokinesis in Tetrahymena thermophila. *Eukaryotic Cell* **3:** 1217–1226

Sonneborn TM (1974) [Ciliate morphogenesis and its bearing on general cellular morphogenesis]. *Tsitologiia* **16:** 1063-1088

Sorensen CS, Hansen LT, Dziegielewski J, Syljuasen RG, Lundin C, Bartek J, Helleday T (2005) The cell-cycle checkpoint kinase Chk1 is required for mammalian homologous recombination repair. *Nat Cell Biol* **7:** 195-201

Sorensen CS, Syljuasen RG, Lukas J, Bartek J (2004) ATR, Claspin and the Rad9-Rad1-Hus1 complex regulate Chk1 and Cdc25A in the absence of DNA damage. *Cell Cycle* **3:** 941-945

Spellman PT, Sherlock G, Zhang MQ, Iyer VR, Anders K, Eisen MB, Brown PO, Botstein D, Futcher B (1998) Comprehensive identification of cell cycle-regulated genes of the yeast Saccharomyces cerevisiae by microarray hybridization. *Mol Biol Cell* **9:** 3273-3297

Stargell LA, Bowen J, Dadd CA, Dedon PC, Davis M, Cook RG, Allis CD, Gorovsky MA (1993) Temporal and spatial association of histone H2A variant hv1 with transcriptionally competent chromatin during nuclear development in Tetrahymena thermophila. *Genes Dev* **7:** 2641-2651

Strahl BD, Ohba R, Cook RG, Allis CD (1999) Methylation of histone H3 at lysine 4 is highly conserved and correlates with transcriptionally active nuclei in Tetrahymena. *Proc Natl Acad Sci U S A* **96:** 14967-14972

Strambio-De-Castillia C, Niepel M, Rout MP (2010) The nuclear pore complex: bridging nuclear transport and gene regulation. *Nat Rev Mol Cell Biol* **11:** 490-501

Struhl K, Stinchcomb DT, Scherer S, Davis RW (1979) High-frequency transformation of yeast: autonomous replication of hybrid DNA molecules. *Proc Natl Acad Sci U S A* **76:** 1035-1039

Stucki M, Clapperton JA, Mohammad D, Yaffe MB, Smerdon SJ, Jackson SP (2005) MDC1 directly binds phosphorylated histone H2AX to regulate cellular responses to DNA double-strand breaks. *Cell* **123:** 1213-1226

Suryadinata R, Sadowski M, Sarcevic B (2010) Control of cell cycle progression by phosphorylation of cyclin-dependent kinase (CDK) substrates. *Biosci Rep* **30:** 243-255

Suter B, Tong A, Chang M, Yu L, Brown GW, Boone C, Rine J (2004) The origin recognition complex links replication, sister chromatid cohesion and transcriptional silencing in Saccharomyces cerevisiae. *Genetics* **167:** 579-591

Sweeney FD, Yang F, Chi A, Shabanowitz J, Hunt DF, Durocher D (2005) Saccharomyces cerevisiae Rad9 acts as a Mec1 adaptor to allow Rad53 activation. *Curr Biol* **15:** 1364-1375

Szyjka SJ, Viggiani CJ, Aparicio OM (2005) Mrc1 is required for normal progression of replication forks throughout chromatin in *S. cerevisiae*. *Mol. Cell* **19:** 691–697

Takai H, Tominaga K, Motoyama N, Minamishima YA, Nagahama H, Tsukiyama T, Ikeda K, Nakayama K, Nakanishi M (2000) Aberrant cell cycle checkpoint function and early embryonic death in Chk1(-/-) mice. *Genes Dev* **14:** 1439-1447

Tanaka S, Araki H (2010) Regulation of the initiation step of DNA replication by cyclin-dependent kinases. *Chromosoma* **119:** 565-574

Tanaka K, Russell P (2001) Mrc1 channels the DNA replication arrest signal to checkpoint kinase Cds1. *Nat Cell Biol* **3:** 966–972

Tanaka S, Umemori T, Hirai K, Muramatsu S, Kamimura Y, Araki H (2007) CDK-dependent phosphorylation of Sld2 and Sld3 initiates DNA replication in budding yeast. *Nature* **445:** 328-332

Tang L, Pelech SL, Berger JD (1994) A cdc2-like kinase associated with commitment to division in Paramecium tetraurelia. *J Eukaryot Microbiol* **41:** 381-387

Tapia-Alveal C, Calonge TM, O'Connell MJ (2009) Regulation of chk1. *Cell Div* **4:** 8-15

Tercero JA, Diffley JF (2001) Regulation of DNA replication fork progression through damaged DNA by the Mec1/Rad53 checkpoint. *Nature* **412:** 553-557

Tourriere H, Versini G, Cordon-Preciado V, Alabert C, Pasero P (2005) Mrc1 and Tof1 promote replication fork progression and recovery independently of Rad53. *Mol Cell* **19:** 699-706

Tower J (2004) Developmental gene amplification and origin regulation. *Annu Rev Genet* **38:** 273-304

Tran NQ, Dang HQ, Tuteja R, Tuteja N (2010) A single subunit MCM6 from pea forms homohexamer and functions as DNA helicase. *Plant Mol Biol* **74:** 327-336

Traven A, Heierhorst J (2005) SQ/TQ cluster domains: concentrated ATM/ATR kinase phosphorylation site regions in DNA-damage-response proteins. *Bioessays* **27:** 397–407

Trawick JD, Kraut N, Simon FR, Poyton RO (1992) Regulation of yeast COX6 by the general transcription factor ABF1 and separate HAP2- and heme-responsive elements. *Mol Cell Biol* **12:** 2302-2314

Tyers M, Futcher B (1993) Far1 and Fus3 link the mating pheromone signal transduction pathway to three G1-phase Cdc28 kinase complexes. *Mol Cell Biol* **13:** 5659-5669

Umthun AR, Hou Z, Sibenaller ZA, Shaiu WL, Dobbs DL (1994) Identification of DNA-binding proteins that recognize a conserved type I repeat sequence in the replication origin region of Tetrahymena rDNA. *Nucleic Acids Res* **22:** 4432-4440

Uziel T, Lerenthal Y, Moyal L, Andegeko Y, Mittelman L, Shiloh Y (2003) Requirement of the MRN complex for ATM activation by DNA damage. *EMBO J* **22:** 5612-5621

Vavra KJ, Allis CD, Gorovsky MA (1982a) Regulation of histone acetylation in Tetrahymena macro- and micronuclei. *J Biol Chem* **257:** 2591-2598

Vavra KJ, Colavito-Shepanski M, Gorovsky MA (1982b) Histone acetylation and the deoxyribonuclease I sensitivity of the Tetrahymena ribosomal gene. *Biochemistry* **21:** 1772-1781

Venditti P, Costanzo G, Negri R, Camilloni G (1994) ABFI contributes to the chromatin organization of Saccharomyces cerevisiae ARS1 B-domain. *Biochim Biophys Acta* **1219:** 677-689

Wakabayashi M, Ishii C, Hatakeyama S, Inoue H, Tanaka S (2010) ATM and ATR homologes of Neurospora crassa are essential for normal cell growth and maintenance of chromosome integrity. *Fungal Genet Biol* **47:** 809-817

Walter J, Newport J (2000) Initiation of eukaryotic DNA replication: origin unwinding and sequential chromatin association of Cdc45, RPA, and DNA polymerase alpha. *Mol Cell* **5:** 617-627

Walter JC (2000) Evidence for sequential action of cdc7 and cdk2 protein kinases during initiation of DNA replication in Xenopus egg extracts. *J Biol Chem* **275:** 39773-39778

Walworth NC, Bernards R (1996) rad-dependent response of the chk1-encoded protein kinase at the DNA damage checkpoint. *Science* **271:** 353-356

White EM, Allis CD, Goldfarb DS, Srivastva A, Weir JW, Gorovsky MA (1989) Nucleus-specific and temporally restricted localization of proteins in Tetrahymena macronuclei and micronuclei. *J Cell Biol* **109:** 1983-1992

Wiley EA, Myers T, Parker K, Braun T, Yao MC (2005) Class I histone deacetylase Thd1p affects nuclear integrity in Tetrahymena thermophila. *Eukaryot Cell* **4:** 981-990

Williams RS, Moncalian G, Williams JS, Yamada Y, Limbo O, Shin DS, Groocock LM, Cahill D, Hitomi C, Guenther G, Moiani D, Carney JP, Russell P, Tainer JA (2008) Mre11 dimers coordinate DNA end bridging and nuclease processing in double-strand-break repair. *Cell* **135:** 97-109

Wilson KA, Stern DF (2008) NFBD1/MDC1, 53BP1 and BRCA1 have both redundant and unique roles in the ATM pathway. *Cell Cycle* **7:** 3584-3594

Wohlschlegel JA, Dhar SK, Prokhorova TA, Dutta A, Walter JC (2002) Xenopus Mcm10 binds to origins of DNA replication after Mcm2-7 and stimulates origin binding of Cdc45. *Mol Cell* **9:** 233-240

Wohlschlegel JA, Dwyer BT, Dhar SK, Cvetic C, Walter JC, Dutta A (2000) Inhibition of eukaryotic DNA replication by geminin binding to Cdt1. *Science* **290:** 2309-2312

Wolfe J, Hunter B, Adair WS (1976) A cytological study of micronuclear elongation during conjugation in Tetrahymena. *Chromosoma* **55:** 289-308

Woodard J, Kaneshiro E, Gorovsky MA (1972) Cytochemical studies on the problem of macronuclear subnuclei in tetrahymena. *Genetics* **70:** 251-260

Wu PY, Nurse P (2009) Establishing the program of origin firing during S phase in fission Yeast. *Cell* **136:** 852-864

Xiong JY, Lai CX, Qu Z, Yang XY, Qin XH, Liu GQ (2009) Recruitment of AtWHY1 and AtWHY3 by a distal element upstream of the kinesin gene AtKP1 to mediate transcriptional repression. *Plant Mol Biol* **71:** 437-449

Yaeger PC, Orias E, Shaiu WL, Larson DD, Blackburn EH (1989) The replication advantage of a free linear rRNA gene is restored by somatic recombination in Tetrahymena thermophila. *Mol Cell Biol* **9:** 452-460

Yakisich JS, Kapler GM (2004) The effect of phosphoinositide 3-kinase inhibitors on programmed nuclear degradation inTetrahymena and fate of surviving nuclei. *Cell Death Differ* **11:** 1146–1149

Yakisich JS, Kapler GM (2006) Deletion of the Tetrahymena thermophila rDNA replication fork barrier region disrupts macronuclear rDNA excision and creates a fragile site in the micronuclear genome. *Nucleic Acids Res* **34:** 620–634

Yang H, Li Q, Fan J, Holloman WK, Pavletich NP (2005) The BRCA2 homologue Brh2 nucleates RAD51 filament formation at a dsDNA-ssDNA junction. *Nature* **433:** 653-657

Yao MC (1982) Elimination of specific DNA sequences from the somatic nucleus of the ciliate Tetrahymena. *J Cell Biol* **92:** 783-789

Yao MC, Chao JL (2005) RNA-guided DNA deletion in Tetrahymena: an RNAi-based mechanism for programmed genome rearrangements. *Annu Rev Genet* **39:** 537-559

Yao MC, Gorovsky MA (1974) Comparison of the sequences of macro- and micronuclear DNA of Tetrahymena pyriformis. *Chromosoma* **48:** 1-18

Yao MC, Zheng K, Yao CH (1987) A conserved nucleotide sequence at the sites of developmentally regulated chromosomal breakage in Tetrahymena. *Cell* **48:** 779-788

Yasuda LF, Yao MC (1991) Short inverted repeats at a free end signal large palindromic DNA formation in Tetrahymena. *Cell* **67:** 505-516

Yoo HH, Kwon C, Lee MM, Chung IK (2007) Single-stranded DNA binding factor AtWHY1 modulates telomere length homeostasis in Arabidopsis. *Plant J* **49:** 442-451

You Z, Chahwan C, Bailis J, Hunter T, Russell P (2005) ATM activation and its recruitment to damaged DNA require binding to the C terminus of Nbs1. *Mol Cell Biol* **25:** 5363-5379

You Z, Kong L, Newport J (2002) The role of single-stranded DNA and polymerase alpha in establishing the ATR, Hus1 DNA replication checkpoint. *J Biol Chem* **277:** 27088-27093

Zegerman P, Diffley JF (2007) Phosphorylation of Sld2 and Sld3 by cyclin-dependent kinases promotes DNA replication in budding yeast. *Nature* **445:** 281-285

Zegerman P, Diffley JF (2010) Checkpoint-dependent inhibition of DNA replication initiation by Sld3 and Dbf4 phosphorylation. *Nature* **467:** 474-478

Zeng Y, Piwnica-Worms H (1999) DNA damage and replication checkpoints in fission yeast require nuclear exclusion of the Cdc25 phosphatase via 14-3-3 binding. *Mol Cell Biol* **19:** 7410-7419

Zhang H, Adl SM, Berger JD (1999) Two distinct classes of mitotic cyclin homologues, Cyc1 and Cyc2, are involved in cell cycle regulation in the ciliate Paramecium tetraurelia. *J Eukaryot Microbiol* **46:** 585-596

Zhang H, Berger JD (1999) A novel member of the cyclin-dependent kinase family in Paramecium tetraurelia. *J Eukaryot Microbiol* **46:** 482-491

Zhang H, Huang X, Tang L, Zhang QJ, Frankel J, Berger JD (2002) A cyclin-dependent protein kinase homologue associated with the basal body domains in the ciliate Tetrahymena thermophila. *Biochim Biophys Acta* **1591:** 119-128

Zhang Z, Macalpine DM, Kapler GM (1997) Developmental regulation of DNA replication: replication fork barriers and programmed gene amplification in Tetrahymena thermophila. *Mol Cell Biol* **17:** 6147-6156

Zhu Z, Chung WH, Shim EY, Lee SE, Ira G (2008) Sgs1 helicase and two nucleases Dna2 and Exo1 resect DNA double-strand break ends. *Cell* **134:** 981-994

Zou L, Cortez D, Elledge SJ (2002) Regulation of ATR substrate selection by Rad17-dependent loading of Rad9 complexes onto chromatin. *Genes Dev* **16:** 198-208

Zou L, Elledge SJ (2003) Sensing DNA damage through ATRIP recognition of RPA-ssDNA complexes. *Science* **300:** 1542-1548

Zou L, Liu D, Elledge SJ (2003) Replication protein A-mediated recruitment and activation of Rad17 complexes. *Proc Natl Acad Sci U S A* **100:** 13827-13832

Zou L, Stillman B (2000) Assembly of a complex containing Cdc45p, replication protein A, and Mcm2p at replication origins controlled by S phase cyclin-dependent kinases and Cdc7p-Dbf4p kinase. *Mol Cell Biol* **20:** 3086-3096

# VITA


| | |
|---|---|
| Name: | Pamela Yohanna de Lourdes Sandoval Oporto |
| Address: | Department of Molecular and Cellular Medicine, HSC, 440 Reynolds Medical Building, College Station TX 77840-1114 |
| Email Address: | psandovalo@tamu.edu |
| Education: | B.S., Biochemistry, Universidad Austral de Chile, 2001<br>Ph.D., Genetics, Texas A&M University, 2011 |